NUMERICAL AND OBSERVATIONAL METHODS OF DETERMINING THE BEHAVIOUR OF ROCK SLOPES IN OPENCAST MINES

A Thesis submitted to the University of London
(Imperial College of Science and Technology)
for the Degree of Doctor of Philosophy
in the Faculty of Engineering

by

Christopher Michael St. John, B.Sc.(Eng.), A.R.S.M.

January 1972

This thesis is intended to be a study of methods of determining the behaviour of rock slopes, particularly as resulting from opencast mining excavations. Numerical and observational methods are discussed and are shown to be linked via displacement studies on model and prototype.

The majority of numerical work was carried out using the Finite Element Method. As far as is relevant to the main theme of the thesis, attention is given to this method. The exposition, given primarily in Chapter 2, provides sufficient information to follow the computer programs given in Appendices B and D for the analysis of two and three dimensional structures respectively.

Chapters 3, 4 and 5 deal with studies carried out using the Finite Element Method to explore its application in slope stability investigations. For simple examples sufficient cases have been studied to permit general conclusion to be drawn. In many situations, in particular the jointed three dimensional problem, only simple models were amenable to solution. Where possible comparison is made with limiting equilibrium models.

Chapter 6 deals exclusively with observational methods and gives some current examples of their use. Field trials designed to measure displacements around a small opencast mining operation are described and general proposals for monitoring systems are outlined.

Finally, in Chapter 7, an attempt is made to apply the methods discussed in Chapters 3 and 4 to a simulation of a physical model of a systematically jointed rock slope.

The author would like to express his gratitude to all those who made this work possible. In particular, thanks are due to:

All the members of the Rock Mechanics Project at Imperial College over the years 1967 - 1971, and especially to the author's supervisor, Professor E. Hoek.

The Rio Tinto Zinc Corporation Ltd, for generous financial support, together with Anglo American International (U.K.) Ltd, Bougainville Copper Pty Ltd, Consolidated Gold Fields Ltd, English China Clays Ltd, Iranian Selection Trust Ltd, National Coal Board Opencast Executive, Palabora Mining Co. Ltd, and seven member companies of the Australian Mineral Industries Research Association Ltd.

Professor R.E. Goodman, of the University of California, for his interest and for computer programmes that provided a basis for the author's research.

Dr. J.W. Bray for his valuable comments and critical study of this manuscript.

Dr. T.L. Thomas for anything connected with surveying.

Mr. L.D. Wilson for arranging everything from transport to optical reflectors.

Gortdrum Mines (Ireland) Ltd, and their staff for permission to carry out field measurements and assistance whilst doing so.

The Mining Department, Imperial College, for leaving the author almost uninterrupted during the final stages of the preparation of this thesis.

Those involved in the production of the thesis, and especially to Mrs. R. Smith who typed the manuscript.

The author's wife for patience.

		Page
ABSTRACT		2
ACKNOWLEDGEMENTS		3
GENERAL INDEX		4
CHAPTER 1 -	Introduction	5
CHAPTER 2 -	The Finite Element Method	23
Part I -	Continuum Mechanics	
Part II -	Special Considerations for Jointed Materials	41
CHAPTER 3 -	The Elastic Analysis of Rock Slopes - Plain Strain Conditions	69
CHAPTER 4 -	Two Dimensional Analysis of Jointed Rock Slopes	108
CHAPTER 5 -	Three Dimensional Analysis of Rock Slopes	159
CHAPTER 6 -	Observational Methods	198
CHAPTER 7 -	A Study of a Physical Model and the Modelling Material	231
APPENDIX A -	Plotting Input and Output of Two Dimensional Finite Element Studies	261
APPENDIX B -	Two Dimensional Simulation of Jointed Rock Structures by Finite Elements	274
APPENDIX C -	Wedge Stability Analysis by Vector Methods	300
APPENDIX D -	Three Dimensional Analysis of Jointed Rock Masses by Finite Elements	307

CHAPTER

1

INTRODUCTION

	Page
Chapter Index	5
Synopsis	6
1.1 Object and Outline	7
1.2 Description of the Problem	8
1.3 Existing Methods of Analysis - An Outline	9
1.4 Conclusion	20
References	21

SYNOPSIS

An outline of the aim and nature of this thesis is followed by a brief description of the rock slope problem to be studied.

An attempt is made to review methods used to estimate the behaviour of rock slopes. These methods range from simple limiting equilibrium calculations, through numerical techniques to observational studies. The aim of this discussion is to place the remainder of the work reported in this thesis in the context of current slope stability research and practice.

1.1 OBJECT AND OUTLINE

A rock slope may be designed prior to excavation, or it may be designed by observation and experience during the early stages of the work. In the context of opencast mining the latter approach is relatively common but initial estimates may be essential since the viability of a project can be closely related to the angle at which the rock slopes are mined (Ref. 1). Estimates of bench behaviour may also govern the choice of heavy mining machinery.

The primary purpose of this thesis is to draw together the body of knowledge concerning the application of numerical methods in rock slope design and to place these in context with other current methods. It further aims to show how such work may be coupled with field measurements and how these may be carried out in a real situation. Comments on the latter are based on field trials carried out at a small open pit mine and on relevant technical literature.

The majority of work in this thesis is based upon the Finite Element Method of structural analysis. The method has been widely reported in scattered literature and this thesis to some extent reviews its current uses in estimating rock slope behaviour. When this study began relatively little work in this field had been reported. Since then there has been very rapid development, much of which will be referenced where relevant. Instead of reporting other researcher's work the author has attempted to cover the whole range of possible approaches himself. Where computer programs were already available in the literature they have been used, modified and extended where necessary. In some cases, new approaches required the writing of completely new programs. Although some of this work may have been repetitive, it is believed that it should all be included in order to cover the whole of this relatively new field, and to make informed criticism where necessary. Since the object of this thesis is not a study of Numerical Methods themselves, discussion of the Finite Element Method is restricted almost entirely to a single chapter. Only when the method itself,

or the computer programming, have a direct bearing on the assumptions inherent in the analysis, are these discussed within the main body of the text. The mathematical content of even the chapter on the Finite Element Method is extremely limited since the emphasis is on a user tool rather than a research topic. In order to be consistent with this aim, computer programs, with input instructions, are given in the appendices. The collection is fairly comprehensive, but avoids duplication with other publications.

1.2 DESCRIPTION OF THE PROBLEM

The behaviour of a rock mass when an excavation is made in it will depend upon the characteristics of the rock material itself and its state prior to disturbance. The geological history will have determined both the initial conditions and the rock characteristics, but the latter may be considerably modified by the process of excavation if it involves heavy blasting.

1.2.1 Initial Conditions

A considerable amount of effort has been given to the study of the state of stress in the earth's crust. It is usually accepted that the vertical stresses in undisturbed material may be deduced from self weight alone. Horizontal stresses vary considerably, according to the environment. Measurements by Hast (Ref. 2) in the Fennoscandian mountain ranges showed considerable horizontal stresses even at the surface, and a much higher rate of increase with depth than normally is assumed. Where possible measurements of initial stress conditions should be made since they are an important parameter that may be included in the numerical design techniques.

1.2.2 Rock Mass Classification

In most cases, the material constituting a rock slope is a discontinuum. The spatial orientation and frequency of fractures, together with the relative strength and deformability of the rock material and the discontinuities, are the major factors that control

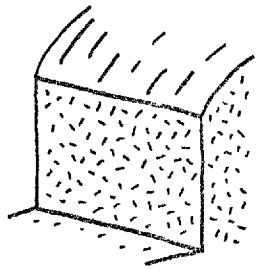
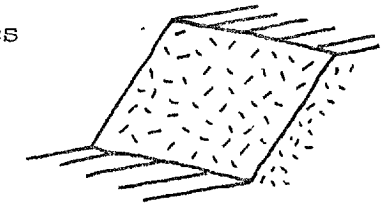
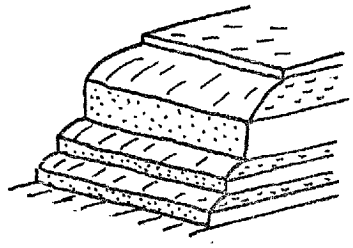
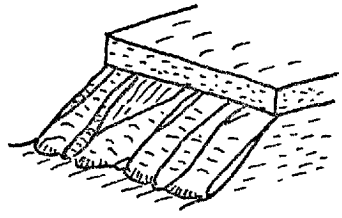
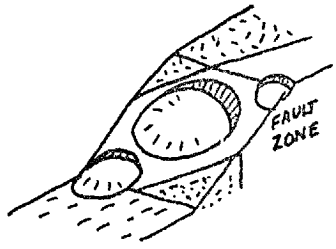
the behaviour of the rock mass during and after excavation. The method of analysis required will depend on the above considerations, since these control the mode of failure.

A number of classifications of rock masses relating to surface excavations, have been presented. Müller and Hoffmann (Ref. 3) drew the distinction between quasi-monolithic, jointed, cracked, and shattered rock. Duncan and Goodman (Ref. 4) have given a more comprehensive classification that is reproduced (Table 1.1) together with comments on the pertinent method of analysis.

1.3 EXISTING METHODS OF ANALYSIS - AN OUTLINE

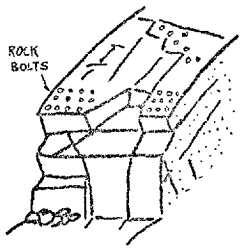
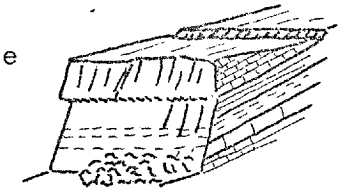
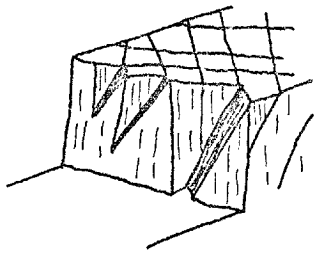
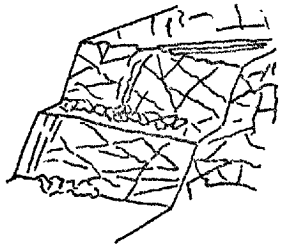
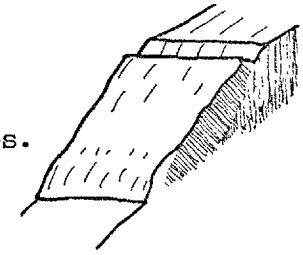
There are three basic methods of estimating the behaviour of a rock slope. The first of these is Limit Equilibrium. This finds extensive use since it provides a simple method of calculating a Factor of Safety and, hence, the required YES/NO answer. In addition, the calculations, in some cases, may be done on'the back of an envelope' or reduced to a graphical or tabular presentation. The second alternative is stress analysis. This has, until recently, been restricted almost exclusively to the study of rock as a continuum. The Factor of Safety is difficult to deduce without resorting to a limiting equilibrium calculation, but considerable data regarding slope stresses and displacements may be obtained. Although the latter may not have a bearing on Mining Practice, other than as a reference for physical observations, they may be important when the slope acts as a foundation for an artificial structure. The third method, the empirical and observational approach, involves the study of models and the performance of the prototype itself. Physical models may be replaced by numerical simulations which fulfill precisely the same purpose but are not subject to some of the limitations inherent in the former. It is advisable that such simulations should be checked against a comprehensive physical model.

Each of these three methods will be discussed briefly below. In doing so the usual, but rather arbitrary, division into two or three dimensional cases will be avoided as far as possible. All

TYPE	DESCRIPTION	ANALYSIS	FIGURE
1) Strong Homogeneous Rock	As strong as concrete. Free from discontinuities.	Elastic Continuum. Stress Analysis.	
2) Weak Homogeneous Rock	Much weaker than concrete. Free from discontinuities.	Soil Mechanics techniques. Plastic Analysis.	
3) Terraced Rock	Horizontal beds of varying strength.	Check behaviour of soft zones by Soil Mechanics techniques.	
4) Ravelling Rock	Rock continuous but breaks upon weathering.	Analyse as a cohesionless soil.	
5) Slumping Rock	Altered or clay rich rock with very low strength.	Soil Mechanics techniques.	

CLASSIFICATION OF ROCK MASSES FOR SURFACE EXCAVATION
- CONTINUOUS ROCK MASSES - (After Duncan & Goodman 1968)

TABLE 1.1 (Part 1)

TYPE	DESCRIPTION	ANALYSIS	FIGURE
6) Sheeted Rock	Hard strong rock with planar weakness roughly parallel to natural slopes.	2-dimensional analysis. Limiting Equilibrium Calculations Check for toppling failure.	
7) Slabby Rock	Hard rock with one strongly developed set of discontinuities which control the strength.	2-dimensional analysis. Finite Element may be used. Also Limiting Equilibrium.	
8) Buttressed Rock	Hard rock with two sets of weaknesses which dominate the rock mass strength.	3-dimensional analysis. Limiting Equilibrium by Vector/Stereographic Projection methods. Also Finite Elements.	
9) Blocky Rock	Hard rock with three or more sets of weaknesses which dominate behaviour.	Soil Mechanics if very heavily fractured. Search for dominant features and then as (8).	
10) Schistose Rock	Schistocity planes, usually steeply dipping, control mass behaviour.	2-dimensional analysis by Soil Mechanics techniques. May also consider toppling failure.	

CLASSIFICATION OF ROCK MASSES FOR SURFACE EXCAVATION

- DISCONTINUOUS ROCK MASSES -

(After Duncan & Goodman 1968)

TABLE 1.1 (Part 2)

practical problems are three dimensional, but both the growth of Rock Mechanics from Soil Mechanics and the relative simplicity of calculations for cross-sections have resulted in attention being placed on the two-dimensional subcase.

1.3.1 Limit Equilibrium Methods

The condition of limiting equilibrium occurs when the disturbing forces are exactly matched by the resisting forces. Analyses based on the calculation of this limiting condition are referred to as Limit Equilibrium Methods. These methods all assume that rock behaves in a rigid/perfectly plastic manner, and that failure occurs on a predetermined surface. If the material of the rock slope is considered to be homogeneous then the Soil Mechanics approach of assuming an arbitrary failure surface is adopted. The Rock Mechanics approach takes into account the structural control on the possible shape of the sliding mass.

Structurally determined behaviour must be analysed as a three dimensional problem, unless the critical features strike parallel to the slope face. Vector and graphical methods for analysis of the more general case have been discussed at length elsewhere (Ref. 5) and these will be referred to in a later chapter of this thesis.

The two-dimensional sub-case:

When the rock is either truly homogeneous or sufficiently discontinuous to be considered isotropic, the usual slip circle and non-circular arc analyses of the Soil Mechanics approach may be used. The degree of fissuration which justifies the assumption that a rock mass is isotropic is highly debatable. Bray (Ref. 6) showed that rock with ten radially spaced joints approximated to a granular soil, for the case of an angle of internal friction of 30 degrees. Few rock masses can meet this specification so the criterion is modified to whether the rock is sufficiently discontinuous for any chosen slip surface to be possible without necessitating fracture of the solid material.

In many situations, the stability of a slope is likely to be governed by relatively planar discontinuities with large lateral extent, and shear strength considerably below that of solid rock. These features are faults, fault zones, bedding planes and joint sets.

The simplest case that can be considered is a single discontinuity dipping into the excavation and striking parallel to the slope surface. The wedge of material above the surface is assumed to behave as a monolithic block and the only forces involved are the resolved components of the weight of the potentially sliding wedge. For the simple case of frictional behaviour alone, the angle of friction necessary for stability is equal to the dip of the slip surface. (Fig. 1.1) That it is independent of the slope height is contrary to observed behaviour.

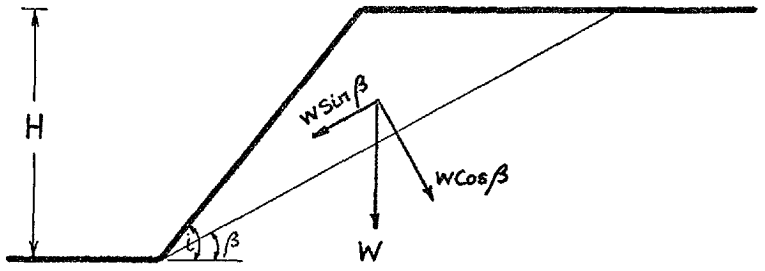


Figure 1.1

Normal Force (F_n)	$= W \cos\beta$
Shear Strength (T)	$= F_n \tan\phi$
Sliding Force	$= W \sin\beta$
Resisting Force	$= W \cos\beta \tan\phi$
Angle of Friction for Stability (ϕ_r)	$= \beta$

The further possible variables for this simple model are (Fig. 1.2):-

γ, γ_w	=	Unit weights of Rock and Water respectively	
H	=	Slope Height	
c	=	Cohesion	Coulomb Law
ϕ	=	Friction Angle	

i = Slope Angle

z_o = Depth of Tension Crack

H_w = Height of Water Table (assumed to be horizontal)

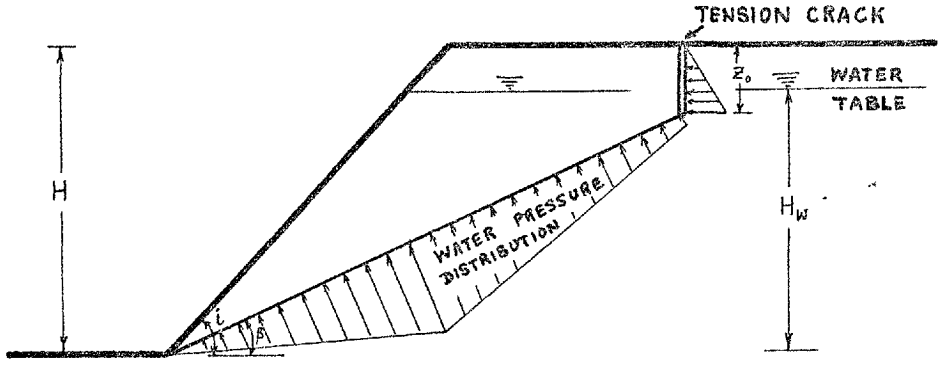


Figure 1.2

From the geometry of the slope the Factor of Safety now becomes

$$F = \frac{\text{Total Resisting Force}}{\text{Total Disturbing Force}} = \frac{cA + (W\cos\beta - U - V\sin\beta)\tan\phi}{W\sin\beta + V\cos\beta} \quad 1(1)$$

where

$$W = \tfrac{1}{2}\gamma H^2\left\{(\cot\beta - \cot i) - \left(\frac{z_o}{H}\right)^2 \cot\beta\right\}$$

$$U = \frac{\gamma_w}{2\sin\beta}\left\{H_w^2\left(1. - \cot i \tan\beta\right) - \left(z_o + H_w - H\right)^2\right\}$$

$$V = \tfrac{1}{2}\gamma_w z_o^2$$

$$A = \frac{H - z_o}{\sin\beta}$$

These formulae are tedious to calculate manually, if all the terms are included, so Hoek (Ref. 7) has devised slope design charts requiring only the calculation of simple slope functions. These charts entail approximations not apparent to the user, and the author has produced design tables as an alternative (Table 1.II). This requires interpolation between tabulated values of the variables given above, but the approximations involved in this process are quite evident without further investigation.

SLOPE ANGLE= 40.00 COHESION FACTOR= 60.00 JOINT ANGLES ACROSS PAGE, FRICTION DOWN TENSION CRACK EMPTY AND FULL

WATER TABLE RATIO= 0.00

THI	TENSION CRACK RATIO= 0.00								TENSION CRACK RATIO= .30								TENSION CRACK RATIO= .60							
	10	20	30	40	50	60	70	80	10	20	30	40	50	60	70	80	10	20	30	40	50	60	70	80
10	1.25	.67	.55	0.00	0.00	0.00	0.00	0.00	1.20	.64	.55	0.00	0.00	0.00	0.00	0.00	1.18	0.00	0.00	0.00	0.00	0.00	0.00	0.00
10	1.25	.67	.55	0.00	0.00	0.00	0.00	0.00	1.14	.59	.46	0.00	0.00	0.00	0.00	0.00	.88	0.00	0.00	0.00	0.00	0.00	0.00	0.00
20	2.31	1.18	.88	0.00	0.00	0.00	0.00	0.00	2.26	1.15	.87	0.00	0.00	0.00	0.00	0.00	2.25	0.00	0.00	0.00	0.00	0.00	0.00	0.00
20	2.31	1.18	.88	0.00	0.00	0.00	0.00	0.00	2.15	1.06	.72	0.00	0.00	0.00	0.00	0.00	1.67	0.00	0.00	0.00	0.00	0.00	0.00	0.00
30	3.52	1.77	1.25	0.00	0.00	0.00	0.00	0.00	3.47	1.74	1.24	0.00	0.00	0.00	0.00	0.00	3.45	0.00	0.00	0.00	0.00	0.00	0.00	0.00
30	3.52	1.77	1.25	0.00	0.00	0.00	0.00	0.00	3.29	1.60	1.02	0.00	0.00	0.00	0.00	0.00	2.56	0.00	0.00	0.00	0.00	0.00	0.00	0.00
40	5.00	2.49	1.70	0.00	0.00	0.00	0.00	0.00	4.95	2.46	1.70	0.00	0.00	0.00	0.00	0.00	4.94	0.00	0.00	0.00	0.00	0.00	0.00	0.00
40	5.00	2.49	1.70	0.00	0.00	0.00	0.00	0.00	4.70	2.26	1.39	0.00	0.00	0.00	0.00	0.00	3.66	0.00	0.00	0.00	0.00	0.00	0.00	0.00

WATER TABLE RATIO= .33

THI	TENSION CRACK RATIO= 0.00								TENSION CRACK RATIO= .30								TENSION CRACK RATIO= .60							
	10	20	30	40	50	60	70	80	10	20	30	40	50	60	70	80	10	20	30	40	50	60	70	80
10	1.20	.64	.53	0.00	0.00	0.00	0.00	0.00	1.14	.61	.52	0.00	0.00	0.00	0.00	0.00	1.10	0.00	0.00	0.00	0.00	0.00	0.00	0.00
10	1.20	.64	.53	0.00	0.00	0.00	0.00	0.00	1.09	.56	.44	0.00	0.00	0.00	0.00	0.00	.81	0.00	0.00	0.00	0.00	0.00	0.00	0.00
20	2.22	1.13	.84	0.00	0.00	0.00	0.00	0.00	2.15	1.09	.82	0.00	0.00	0.00	0.00	0.00	2.07	0.00	0.00	0.00	0.00	0.00	0.00	0.00
20	2.22	1.13	.84	0.00	0.00	0.00	0.00	0.00	2.04	1.01	.68	0.00	0.00	0.00	0.00	0.00	1.54	0.00	0.00	0.00	0.00	0.00	0.00	0.00
30	3.37	1.69	1.19	0.00	0.00	0.00	0.00	0.00	3.30	1.64	1.16	0.00	0.00	0.00	0.00	0.00	3.18	0.00	0.00	0.00	0.00	0.00	0.00	0.00
30	3.37	1.69	1.19	0.00	0.00	0.00	0.00	0.00	3.13	1.51	.95	0.00	0.00	0.00	0.00	0.00	2.36	0.00	0.00	0.00	0.00	0.00	0.00	0.00
40	4.79	2.37	1.61	0.00	0.00	0.00	0.00	0.00	4.71	2.32	1.58	0.00	0.00	0.00	0.00	0.00	4.54	0.00	0.00	0.00	0.00	0.00	0.00	0.00
40	4.79	2.37	1.61	0.00	0.00	0.00	0.00	0.00	4.47	2.13	1.29	0.00	0.00	0.00	0.00	0.00	3.36	0.00	0.00	0.00	0.00	0.00	0.00	0.00

WATER TABLE RATIO= .67

THI	TENSION CRACK RATIO= 0.00								TENSION CRACK RATIO= .30								TENSION CRACK RATIO= .60							
	10	20	30	40	50	60	70	80	10	20	30	40	50	60	70	80	10	20	30	40	50	60	70	80
10	1.06	.57	.48	0.00	0.00	0.00	0.00	0.00	.99	.52	.45	0.00	0.00	0.00	0.00	0.00	.86	0.00	0.00	0.00	0.00	0.00	0.00	0.00
10	1.06	.57	.48	0.00	0.00	0.00	0.00	0.00	.94	.48	.37	0.00	0.00	0.00	0.00	0.00	.68	0.00	0.00	0.00	0.00	0.00	0.00	0.00
20	1.93	.98	.73	0.00	0.00	0.00	0.00	0.00	1.83	.91	.66	0.00	0.00	0.00	0.00	0.00	1.58	0.00	0.00	0.00	0.00	0.00	0.00	0.00
20	1.93	.98	.73	0.00	0.00	0.00	0.00	0.00	1.74	.84	.54	0.00	0.00	0.00	0.00	0.00	1.25	0.00	0.00	0.00	0.00	0.00	0.00	0.00
30	2.92	1.45	1.01	0.00	0.00	0.00	0.00	0.00	2.79	1.36	.91	0.00	0.00	0.00	0.00	0.00	2.41	0.00	0.00	0.00	0.00	0.00	0.00	0.00
30	2.92	1.45	1.01	0.00	0.00	0.00	0.00	0.00	2.65	1.25	.74	0.00	0.00	0.00	0.00	0.00	1.90	0.00	0.00	0.00	0.00	0.00	0.00	0.00
40	4.13	2.02	1.36	0.00	0.00	0.00	0.00	0.00	3.97	1.91	1.21	0.00	0.00	0.00	0.00	0.00	3.43	0.00	0.00	0.00	0.00	0.00	0.00	0.00
40	4.13	2.02	1.36	0.00	0.00	0.00	0.00	0.00	3.77	1.75	.98	0.00	0.00	0.00	0.00	0.00	2.71	0.00	0.00	0.00	0.00	0.00	0.00	0.00

WATER TABLE RATIO= 1.00

THI	TENSION CRACK RATIO= 0.00								TENSION CRACK RATIO= .30								TENSION CRACK RATIO= .60							
	10	20	30	40	50	60	70	80	10	20	30	40	50	60	70	80	10	20	30	40	50	60	70	80
10	.83	.45	.39	0.00	0.00	0.00	0.00	0.00	.74	.38	.32	0.00	0.00	0.00	0.00	0.00	.57	0.00	0.00	0.00	0.00	0.00	0.00	0.00
10	.83	.45	.39	0.00	0.00	0.00	0.00	0.00	.74	.38	.32	0.00	0.00	0.00	0.00	0.00	.57	0.00	0.00	0.00	0.00	0.00	0.00	0.00
20	1.46	.73	.54	0.00	0.00	0.00	0.00	0.00	1.34	.64	.43	0.00	0.00	0.00	0.00	0.00	1.03	0.00	0.00	0.00	0.00	0.00	0.00	0.00
20	1.46	.73	.54	0.00	0.00	0.00	0.00	0.00	1.34	.64	.43	0.00	0.00	0.00	0.00	0.00	1.03	0.00	0.00	0.00	0.00	0.00	0.00	0.00
30	2.17	1.05	.71	0.00	0.00	0.00	0.00	0.00	2.01	.93	.56	0.00	0.00	0.00	0.00	0.00	1.55	0.00	0.00	0.00	0.00	0.00	0.00	0.00
30	2.17	1.05	.71	0.00	0.00	0.00	0.00	0.00	2.01	.93	.56	0.00	0.00	0.00	0.00	0.00	1.55	0.00	0.00	0.00	0.00	0.00	0.00	0.00
40	3.04	1.44	.93	0.00	0.00	0.00	0.00	0.00	2.84	1.29	.73	0.00	0.00	0.00	0.00	0.00	2.19	0.00	0.00	0.00	0.00	0.00	0.00	0.00
40	3.04	1.44	.93	0.00	0.00	0.00	0.00	0.00	2.84	1.29	.73	0.00	0.00	0.00	0.00	0.00	2.19	0.00	0.00	0.00	0.00	0.00	0.00	0.00

TABLE 1.II

The models described above, have assumed a single continuous discontinuity, perhaps delimited by a tension crack. Any lack of continuity will result in an increase in the strength of the failure surface, or the formation of a surface that steps between discontinuities possibly belonging to the same joint set.

The case of complex surfaces has been discussed in detail by Jennings (Ref. 8). He considers the case of a mean plane defined by two joint sets and partial fracture of the solid (Fig. 1.3).

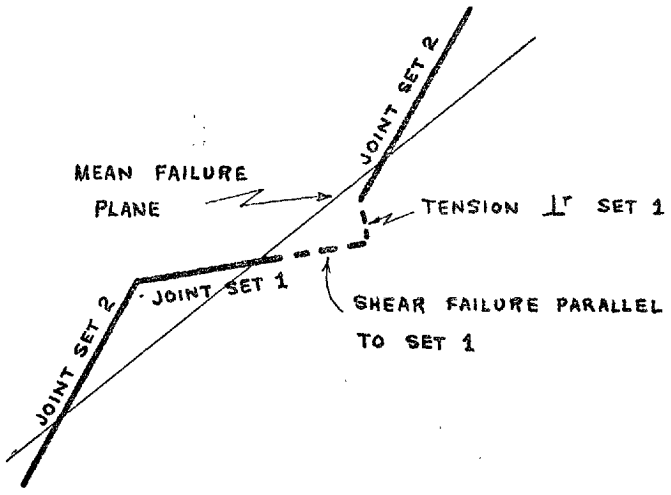


Figure 1.3

The assumption of sliding on joint set 2, opening on set 1, shear failure parallel to set 2 through the solid, and tensile fracture normal to set 2 makes the model relatively complex. Resort to computer methods must be essential, in view of the large number of possible combinations, unless very extensive structural data can be gathered.

Barton (Ref. 9) examined limit equilibrium methods in some detail and developed a method of slices taking into account inter-slice forces. This was used to study the case of sliding on a stepped surface, defined by successive overstressing of joints of a single set during slope deepening. This is an interesting approach to progressive failure, but, in the author's opinion, is rather too simple to model such a complex phenomenon.

1.3.2 Stress Analysis

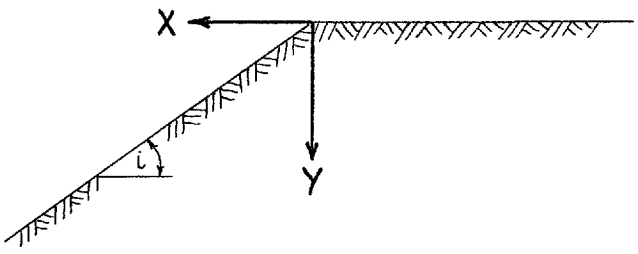
Photoelastic methods have been used to study the gravity stresses induced by excavation of a slope. These have been reported, notably by La Rochelle (Ref. 10), Yu, Gyenge and Coates (Ref. 11) and Long (Ref. 12). The method is not particularly convenient for gravity structures since centrifugal loading is necessary except for high sensitivity materials such as Gelatine (which demonstrates unwanted time-dependent effects). There is an additional problem of the effect of Poissons ratio, which in the case of gelatine is approximately 0·5. Using the normal restraint boundary conditions it is only possible to achieve initial horizontal to vertical stress ratios of 0·5 or 1·0 in Plane Stress or Plane Strain models respectively.

An attempt to calculate the stresses in an infinite elastic slope, by assuming the stresses to be a linear function of the co-ordinates (Fig. 1.4), yields the following expressions:-

$$\sigma_{xx} = -\gamma \cot i \,.\, X + 2\gamma \cot^2 i \,.\, Y$$

$$\sigma_{yy} = \gamma \,.\, Y \qquad 1(2)$$

$$\tau_{xy} = \gamma \cot i \,.\, Y$$



Unit Weight = γ

Infinite Elastic Wedge
Figure 1.4

Since the horizontal stress (σ_{xx}) becomes increasingly large with Y and no account is taken of toe effects, this does not seem a reasonable approximation except at the crest. Richards and Schmid

(Ref. 13) obtained analytical solutions for body-force stresses in earth dams, but concluded they were invalid for top wedge angles greater than 90^{o}. It was therefore impossible to give an analytical solution for a vertical cut or sloping embankment.

By a process of elimination, it is necessary to use numerical methods, even for the simple case of modelling an isotropic slope exhibiting linear, elastic behaviour. Finite Difference and Finite Element techniques have been used extensively. The Finite Difference methods (Refs. 14 and 15) are generally harder to use because special arrangements must be made for boundaries and different material types (Ref. 5). The Finite Element method has the advantage of being ideally suited to the consideration of arbitrary boundary conditions, inhomogeneity, and any initial stress conditions. It may be modified to treat in-elastic and non-linear behaviour. In fact, it is probably true to say that any material behaviour may be simulated providing it can be adequately defined. Discussion of this work forms the major part of this thesis and literature will be referred to where relevant.

These methods may all be considered as numerical models and may be designed to reproduce closely the properties of the prototype. They have a great advantage over physical models in that they are quasi-indestructable. The tedious part of model preparation is reduced to definition of the geometry, whilst other changes become trivial.

1.3.3 Model Studies and Observation Methods

Observational methods range from simple records of visual inspection of an excavation, in its early stages, to complex instrumentation of the whole rock mass. These provide qualitative data on the slope behaviour on which to evaluate current practice and base future design.

Physical models may be designed to demonstrate a mechanism or to provide a simulation of a real situation. In both cases there may be difficulty in matching the stress levels and the

material strength, in order that the physical problem may be reasonably reproduced. The problem may be easily resolved for the case of weak granular materials, but not so readily when modelling a discontinuum.

The 'Base Friction' model discussed by Hoek and Boyd (Ref. 16) is an excellent example of a quantitative simulation of a discon tinuum. They demonstrated the importance of toppling as a mode of failure and showed that the final configuration could easily be confused with one of the more familiar sliding modes. This is in agreement with the far more sophisticated Plane Strain models reported by Müller and Hofmann (Ref. 3).

Probably the most elaborate model of a rock slope was constructed and tested by Barton (Ref. 9). He reproduced the strength and behaviour of rough joints by the creation of sets of tensile fractures in a weak brittle material. This study provides an excellent test case for numerical analysis since it is extremely well documented.

An interesting three dimensional model was reported by Heuzé and Goodman (Ref. 17). They used a remouldable material which was cut according to the measured orientation of discontinuities in the field. Water was then introduced to promote sliding or toppling of the three dimensional blocks so defined.

It appears that complex models simulating real situations are restricted to slope stability in the context of Civil Engineering. In connection with dam construction, several models in which the abutments were included have been reported. Undertaking such formidable work has been justified by lack of any alternative. The interaction between dam and abutments may be vital to the dam stability and has, until recently, not been amenable to numerical analysis.

The demarcation between stress analysis and modelling becomes blurred as more complex behaviour is studied using computer simulations. Cundall has reported (Ref. 15) on the analysis of

granular materials comprising packings of either cylindrical or prismatic units. This method is particularly applicable to slope studies, where the assumption of rigid units is realistic. It has been checked with considerable success against the toppling model referred to above (Ref. 16). An increase in computer capacity will enable developments of such methods to be used as design tools. These will be of much greater power than the small displacement methods that are discussed in this thesis.

1.4 CONCLUSION

The aim of this introduction was to review the whole spectrum of methods of estimating the behaviour of rock slopes. The referenced material is deliberately not extensive and is aimed chiefly, to support the author's opinion that the numerical techniques based on the Finite Element Method are likely to make a continuing and important contribution to slope design.

(1) Hoek, E. & Pentz, D.L. Review of the Role of Rock Mechanics in the Design of Opencast Mines. 9th Comm. Min & Met. Congress. London 1969.

(2) Hast, N. The State of Stress in the Upper Part of the Earth's Crust. Eng. Geol. 2(1) 1967.

(3) Müller, L. & Hofmann, H. Selection, Compilation and Assessment of Geological Data for the Slope Problem. Symposium on Open Pit Mine Planning. Johannesburg 1970.

(4) Duncan, J.M. & Goodman, R.E. Finite Element Analyses of Slopes in Jointed Rock. Report to the U.S. Army Corps of Engineers, Vicksburg, Miss. Contract No. DACW39-67-C-0091 by Geotechnical Engineering, University of California, Berkeley.

(5) Goodman, R.E. & Taylor, R.L. Methods of Analysis for Rock Slopes and Abutments: A Review of Recent Developments. 8th Symposium on Rock Mechanics, Minnesota 1966.

(6) Bray, J.W. A Study of Jointed and Fractured Rock. Rock Mech. & Eng. Geol. Vol. V/2-3, 1967.

(7) Hoek, E. Estimating the stability of excavated slopes in opencast mines. Transactions I.M.M. Vol. 79 Bul. 767, 1970.

(8) Jennings, J.E. A Mathematical Theory of Calculation of the Stability of Slopes in Opencast Mines. Symposium on Open Pit Mine Planning. Johannesburg 1970.

(9) Barton, N.R. A Model Study of the Behaviour of Steep Excavated Rock Slopes. Ph.D.Thesis London 1971.

(10) La Rochelle, P. The Short Term Stability of Slopes in London Clay. Ph.D.Thesis London 1960.

(11) Yu, Y.S., Gyenge, M., & Coates, D.F. Comparison of Stress and Displacement in a Gravity-Loaded 60 Degree Slope by Photoelasticity and Finite Element Analysis. Canada Department of Energy, Mines and Resources. Mining Research Centre Internal Report MR 68/24-ID.

(12) Long, A.E. Problems in Designing Stable Open-Pit Mine Slopes. Canada. Min. & Met. Bull. 1964, Vol. 57, No. 627.

(13) Richards, R., & Schmid, W.E. Body Force Stresses in Gravity Structures. A.S.C.E. Soil Mech and Found Div SM 1 January 1968.

(14) Tamuly Phukan, A.L. Non-Linear Deformation of Rocks. Ph.D.Thesis, London 1968.

(15) Cundall, P.A. The Measurement and Analysis of Acceleration in Rock Slopes. Ph.D.Thesis, London 1971.

(16) Hoek, E., & Boyd, J.M. Stability of Slopes in Jointed Rock. Symposium on Rock Mechanics in Highway Construction. Newcastle University, 1971.

(17) Heuzé, F.E., & Goodman, R.E. A Design Procedure for High Cuts in Jointed Hard Rock - Three Dimensional Solutions. Report to the U.S. Bureau of Reclamation, Denver, Colorado. Contract 14-06-D-6990 by Geotechnical Engineering, University of California, Berkeley.

CHAPTER

2

THE FINITE ELEMENT METHOD

	Page
Chapter Index	23
Synopsis	24
PART I - CONTINUUM MECHANICS	
2.1 Introduction	25
2.2 The Method	25
2.3 Solution of Equations	39
PART II - SPECIAL CONSIDERATIONS FOR JOINTED MATERIALS	
2.4 Introduction	41
2.5 Continuum Approach	41
2.6 Discrete Discontinuities - Special Joint Elements	46
2.7 The Linkage Elements	49
2.8 Treatment of Non-Linear Problems	63
2.9 Conclusions	66
References	67

SYNOPSIS

The chapter is divided into two parts. The first part gives a general introduction to the Finite Element Method of structural analysis. From this the properties of some of the plane and solid elements used in this study are derived. The second part of the chapter presents the special methods used for modelling jointed materials. Most attention is given to the derivation of the properties of one and two dimensional joint elements for inclusion in two and three dimensional models respectively.

The contents of this chapter provides the basis of much of the work reported in this thesis. It also describes the formulation of the computer programs given in Appendices B and D.

PART I - CONTINUUM MECHANICS

2.1 INTRODUCTION

The Finite Element Method of analysis has been widely discussed both from a fundamental standpoint and in its application to the solution of engineering problems. The purpose of this thesis is to apply this method to rock slopes in particular, rather than to pursue developments.

2.2 THE METHOD

The following description of the method of finite elements in continuum mechanics has been given in the text by Zienkiewicz and Cheung (Ref. 1):

(a) The continuum is separated by imaginary lines or surfaces into a number of finite elements.

(b) The elements are assumed to be interconnected at a discrete number of points on their boundaries. It is assumed that the displacements of these nodal points are the unknown parameters.

(c) A function is chosen to define uniquely the state of displacement within each 'element' in terms of the nodal displacements.

(d) The state of strain may be defined uniquely from the displacement functions. The state of stress may be determined if the elastic properties of the material are known, together with any initial stresses or strains.

(e) A system of forces concentrated at the nodes and equilibrating the boundary stresses and any distributed loads is determined.

(f) The stiffness of the whole model may be written down as the sum of the contributions of individual elements. The response of the structure to the loading of (e) may be calculated and the stresses and strains throughout the model thereby determined.

The above description places no limitation on either the model or the elements utilized in its construction.

2.2.1 A General Formulation

The first step is to choose how the displacement varies throughout each element. (In fact there is no reason why this variation is restricted to displacements. The method has been applied to many physical phenomenon including temperature and seepage flow.) If $\{\ \}$ and $[\ ]$ are taken to signify a column vector and a matrix respectively, then the variation of displacement may be written as:-

$$\{\phi\} = [N]\{\delta\}^e \qquad 2(1)$$

where $\{\phi\}$ is the displacement at any point within the element due to nodal displacements $\{\delta\}^e$. $[N]$ is the relationship between $\{\phi\}$ and $\{\delta\}^e$ and is known as the shape function, as it is dependent upon the spacial co-ordinates.

Since the displacement at any point is known from 2(1) the strain $\{\varepsilon\}$ may be calculated.

$$\{\varepsilon\} = [B]\{\delta\}^e \qquad 2(2)$$

where $[B]$ may be deduced from the element shape function.

Also assuming linear elastic behaviour, the relationship between the stresses $\{\sigma\}$ and strains $\{\varepsilon\}$ is:-

$$\{\sigma\} = [D]\left(\{\varepsilon\} - \{\varepsilon_o\}\right) + \{\sigma_o\} \qquad 2(3)$$

where $[D]$ is the material stiffness matrix, $\{\varepsilon_o\}$ initial strains in the material of the element and $\{\sigma_o\}$ the initial stresses. ($[D]$ is usually, and non-rigorously, referred to as elasticity matrix.)

Each element is subject to nodal forces $\{F\}^e$ and distributed loads $\{p\}$ acting per unit volume. If the structure is now subjected to a virtual displacement $\{\delta^*\}^e$ at the nodes, the resulting element displacements $\{f^*\}$ and strains $\{\varepsilon^*\}$ are:

$$\{f^*\} = [N]\{\delta^*\}^e \qquad 2(4)$$

and $$\{\varepsilon^*\} = [B]\{\delta^*\}^e \qquad 2(5)$$

The work done by the nodal forces is:-

$$\left(\{\delta^*\}^e\right)^T \{F\}^e \qquad 2(6)$$

The internal work per unit volume by the stresses and distributed forces:-

$$\left(\{\varepsilon^*\}^e\right)^T \{\sigma\} - \{f^*\}^T \{p\} \qquad 2(7)$$

Substituting equations 2(4) and 2(5) equation 2(7) becomes:-

$$\left(\{\delta^*\}^e\right)^T \left([B]^T \{\sigma\} - [N]\{p\}\right) \qquad 2(8)$$

Equating external work (Equation 2(6)) with the total internal work by integrating over the volume of the element:

$$\left(\{\delta^*\}^e\right)^T\{F\}^e = \left(\{\delta^*\}^e\right)^T\left(\int [B]^T\{\sigma\}\, d(vol) - \int [N]^T\{p\}\, d(vol)\right) \qquad 2(9)$$

Since this is valid for any virtual displacement, equation 2(9) can be written with substitution, as:

$$\{F\}^e = \left(\int [B]^T[D]\,[B]\, d(vol)\{\delta\}^e - \int [B]^T\{\sigma_0\}\, d(vol)\right.$$
$$\left. - \int [B]^T[D]\{\varepsilon_0\}\, d(vol) - \int [N]^T\{p\}\, d(vol)\right) \qquad 2(10)$$

The right hand side of this equation is in four parts. The first refers to the stiffness of the element. The stiffness matrix $[k]^e$ of the element may therefore be written down by inspection as:

$$[k]^e = \int [B]^T[D]\,[B]\, d(vol) \qquad 2(11)$$

The equivalent nodal forces due to initial stress, initial strain and distributed loads comprise the remaining three terms respectively.

2.2.2 Natural Co-Ordinates

Formulation of the properties of arbitrary shaped elements is facilitated if special local co-ordinate systems are used. These are chosen so that the co-ordinates only have the range $(0 \rightarrow +1)$ or $(-1 \rightarrow +1)$. (Refs. 2 and 3) and they are therefore particularly convenient when considering curvilinear elements (Fig. 2.1).

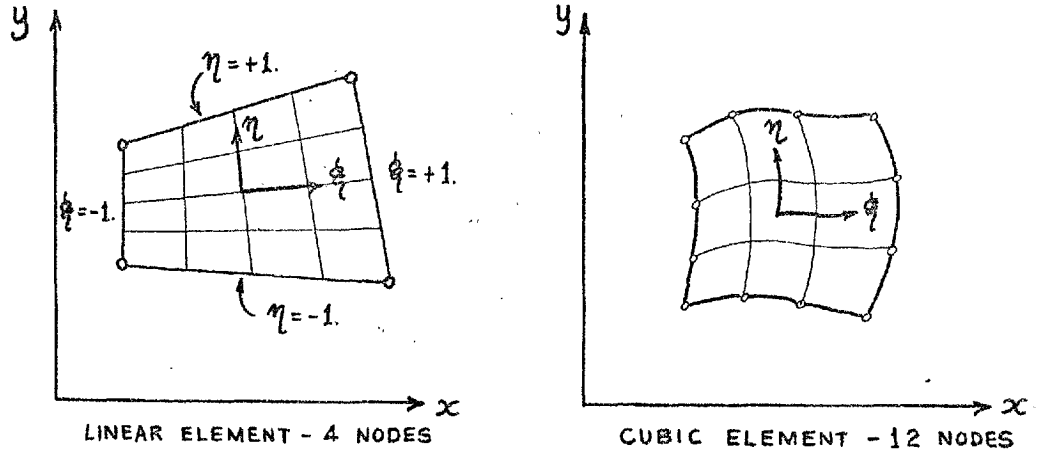


Figure 2.1

In order to use the co-ordinate systems some relationship with the original cartesian co-ordinates must be established. Equation 2(1) defined a relationship between the displacement at any point and the nodal point displacements. Similarly a relationship between the cartesian co-ordinates at any point and the cartesian co-ordinates of the nodes may be defined. If these two relationships are the same the element is said to be isoparametric (Ref. 3).

2.2.3 The Plane Triangular Element

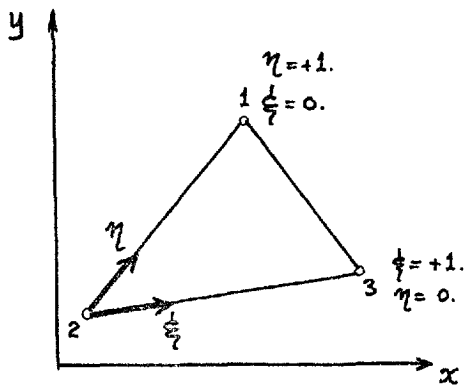


Figure 2.2

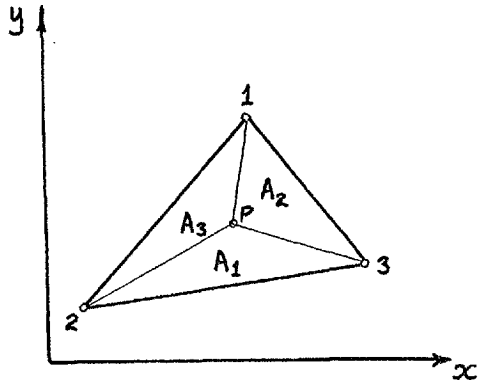


Figure 2.3

For a plane triangular element, defined by nodes 1, 2, 3, the co-ordinates of the point P (Fig. 2.3) inside the element are given in area co-ordinates as (L_1, L_2, L_3) where:-

$$L_1 = \frac{A_1}{A} \qquad L_2 = \frac{A_2}{A} \qquad L_3 = \frac{A_3}{A} \tag{2(13)}$$

A is the area of the triangle 123. From the equation 2(13), if P lies within the triangle:

$$L_1 + L_2 + L_3 = 1. \tag{2(14)}$$

Then the relationship between the natural co-ordinates of Fig. 2.2 and the area co-ordinates of Figure 2.3 is:

$$\begin{aligned} L_1 &= \eta \qquad L_3 = \xi \\ L_2 &= 1. - L_1 - L_3 = 1. - \eta - \xi \end{aligned} \tag{2(15)}$$

If it is assumed that the displacement (u) of any point within the element is a linear function only of its co-ordinates then:

$$u = L_1 u_1 + L_2 u_2 + L_3 u_3 \tag{2(16)}$$

where u_1, u_2, u_3 are the nodal point displacements. This relationship has the property that at node 1 the displacement is u_1, etc., as required. The physical interpretation of the element shape functions is that they represent the contribution each particular node makes to the displacement throughout the element. Hence, generally it is written that:

$$u = N_1 u_1 + N_2 u_2 \ . \ . \ . + N_i u_i \ . \ . \ . + N_n u_n \tag{2(17)}$$

where N_i is the shape function for node i.

For the case of the plane three node triangle the shape functions can be given as:

$$N_i = L_i \qquad 2(18)$$

For the isoparametric elements the shape function also relates the cartesian and local natural co-ordinates (η , ξ). Thus:

$$\begin{aligned} x &= L_1 x_1 + L_2 x_2 + L_3 x_3 = \eta x_1 + (1.-\eta-\xi) x_2 + \xi x_3 \\ y &= L_1 y_1 + L_2 y_2 + L_3 y_3 = \eta y_1 + (1.-\eta-\xi) y_2 + \xi y_3 \end{aligned} \qquad 2(19)$$

from equations 2(15) and 2(16).

For the bi-axial cases the state of strain is:

$$\{\varepsilon\} = \begin{Bmatrix} \varepsilon_x \\ \varepsilon_y \\ \gamma_{xy} \end{Bmatrix} = \begin{Bmatrix} \frac{\partial u}{\partial x} \\ \frac{\partial v}{\partial y} \\ \frac{\partial u}{\partial y} + \frac{\partial v}{\partial x} \end{Bmatrix} = [B]\{\delta\}^e \qquad 2(20)$$

where $\{\delta\}^e$ is a vector of nodal point displacements in cartesian co-ordinates (Equation 2(1)).

From elementary mathematics

$$\begin{aligned} \frac{\partial u}{\partial \xi} &= \frac{\partial u}{\partial x} \cdot \frac{\partial x}{\partial \xi} + \frac{\partial u}{\partial y} \cdot \frac{\partial y}{\partial \xi} \\ \frac{\partial u}{\partial \eta} &= \frac{\partial u}{\partial x} \cdot \frac{\partial x}{\partial \eta} + \frac{\partial u}{\partial y} \cdot \frac{\partial y}{\partial \eta} \end{aligned} \qquad 2(21)$$

or

$$\begin{Bmatrix} \frac{\partial u}{\partial \xi} \\ \frac{\partial u}{\partial \eta} \end{Bmatrix} = \begin{bmatrix} \frac{\partial x}{\partial \xi} & \frac{\partial y}{\partial \xi} \\ \frac{\partial x}{\partial \eta} & \frac{\partial y}{\partial \eta} \end{bmatrix} \begin{Bmatrix} \frac{\partial u}{\partial x} \\ \frac{\partial u}{\partial y} \end{Bmatrix} = [J] \begin{Bmatrix} \frac{\partial u}{\partial x} \\ \frac{\partial u}{\partial y} \end{Bmatrix} \qquad 2(22)$$

$[J]$ being the Jacobian Matrix

From equation 2(19) the Jacobian Matrix can be written down by substituting in 2(22) for the partial differentials.

$$[J] = \begin{bmatrix} -x_2 + x_3 & -y_2 + y_3 \\ x_1 - x_2 & y_1 - y_2 \end{bmatrix} \qquad 2(23)$$

Also from the shape functions

$$\begin{aligned} \frac{\partial u}{\partial \xi} &= -u_2 + u_3 & \frac{\partial v}{\partial \xi} &= -v_2 + v_3 \\ \frac{\partial u}{\partial \eta} &= u_1 - u_2 & \frac{\partial v}{\partial \eta} &= v_1 - v_2 \end{aligned} \qquad 2(24)$$

But

$$\begin{Bmatrix} \frac{\partial u}{\partial x} \\ \frac{\partial u}{\partial y} \end{Bmatrix} = [J]^{-1} \begin{Bmatrix} \frac{\partial u}{\partial \xi} \\ \frac{\partial u}{\partial \eta} \end{Bmatrix} = [\mathcal{J}] \begin{Bmatrix} \frac{\partial u}{\partial \xi} \\ \frac{\partial u}{\partial \eta} \end{Bmatrix} \qquad 2(25)$$

and similarly

$$\begin{Bmatrix} \frac{\partial v}{\partial x} \\ \frac{\partial v}{\partial y} \end{Bmatrix} = [\mathcal{J}] \begin{Bmatrix} \frac{\partial v}{\partial \xi} \\ \frac{\partial v}{\partial \eta} \end{Bmatrix} \qquad 2(26)$$

From equation 2(23)

$$[\mathcal{J}] = \frac{1}{|J|} \begin{bmatrix} y_1 - y_2 & y_2 - y_3 \\ x_2 - x_1 & x_3 - x_2 \end{bmatrix} \qquad 2(27)$$

$[B]$ may be deduced from the equations 2(20), 2(24), 2(25) and 2(26).

$$[B] = \left[\begin{array}{cc|cc|cc} y_2 - y_3 & 0 & y_3 - y_1 & 0 & y_1 - y_2 & 0 \\ 0 & x_3 - x_2 & 0 & x_1 - x_3 & 0 & x_2 - x_1 \\ x_3 - x_2 & y_2 - y_3 & x_1 - x_3 & y_3 - y_1 & x_2 - x_1 & y_1 - y_2 \end{array}\right] \qquad 2(28)$$

The element stiffness matrix can be determined by substitution in equation 2(11).

$$[k]^e = \iint [B]^T [D][B]\, dx\, dy = \int_{L_1=0}^{1} \int_{L_3=0}^{1-L_1} [B]^T [D][B] |J|\, d\xi\, d\eta \qquad 2(29)$$

$$= [B]^T [D][B] \cdot \frac{|J|}{2} = [B]^T [D][B] \cdot A$$

since $dx\, dy = |J|\, d\xi\, d\eta = 2A\, d\xi\, d\eta$

2.2.4 Other Plane Elements

The integration of equation 2(29) was performed explicitly as $[B]$ is a constant. For many other shaped elements this is not possible and it becomes necessary to resort to numerical integration. The arbitrary quadrilaterals illustrated in Fig. 2.1

are examples.

Division of a model into triangular elements is often unnecessarily tedious, so arbitrary quadilateral elements are commonly used. In order to avoid numerical integration the quadrilateral may be automatically divided, within the computer program, into either two or four triangles. The second alternative involves the creation of a fictitious node at the centroid. The element now has two additional degrees of freedom which must be suppressed before the contribution of the element to the whole structure can be determined. This element, which is now a sub-structure, is more efficient than its alternative and is the one used for plane stress/strain studies in this thesis. It was originally used by Wilson (Ref. 4).

2.2.5 The Four-Node Tetrahedron Element

Since the original properties of an element were derived making no assumption regarding the type of element there is no difficulty in treating the three dimensional case. The simplest element is now the tetrahedron. As for the plane stress triangle it is assumed that stress and strain are constant within the element and the element shape functions can be written down by considering a local co-ordinate scheme.

If the local co-ordinates of point p are:-

$$\frac{V_1}{V}, \quad \frac{V_2}{V}, \quad \frac{V_3}{V}, \quad \frac{V_4}{V}$$

V is the volume of the tetrahedron and these volume co-ordinates are defined so that:-

$$\frac{V_1}{V} + \frac{V_2}{V} + \frac{V_3}{V} + \frac{V_4}{V} = 1. \qquad 2(29)$$

Clearly this is directly analagous to the plane triangle case.

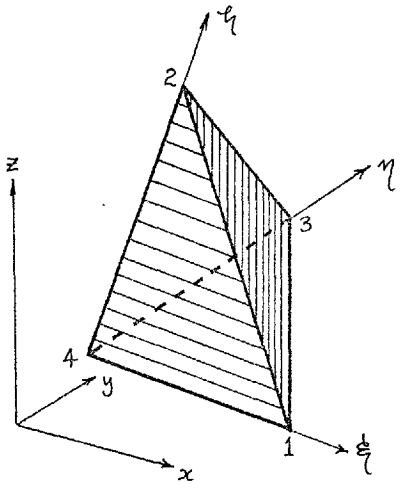


Figure 2.4

If

$$V_1 = \xi$$
$$V_2 = \zeta \qquad 2(30)$$
$$V_3 = \eta$$

Then from 2(29)

$$V_4 = 1. - \xi - \eta - \zeta$$

The natural and cartesian co-ordinates are related by the shape functions.

$$\text{e.g.} \quad x = V_1 x_1 + V_2 x_2 + V_3 x_3 + V_4 x_4 \qquad 2(31)$$
$$= \xi x_1 + \zeta x_2 + \eta x_3 + (1 - \xi - \zeta - \eta) x_4$$

For the three dimensional case the Jacobian matrix is:-

$$[J] = \begin{bmatrix} \frac{\partial x}{\partial \xi} & \frac{\partial y}{\partial \xi} & \frac{\partial z}{\partial \xi} \\ \frac{\partial x}{\partial \eta} & \frac{\partial y}{\partial \eta} & \frac{\partial z}{\partial \eta} \\ \frac{\partial x}{\partial \zeta} & \frac{\partial y}{\partial \zeta} & \frac{\partial z}{\partial \zeta} \end{bmatrix} \qquad 2(32)$$

which, for the tetrahedron, becomes by substitution

$$[J] = \begin{bmatrix} x_1 - x_4 & y_1 - y_4 & z_1 - z_4 \\ x_3 - x_4 & y_3 - y_4 & z_3 - z_4 \\ x_2 - x_4 & y_2 - y_4 & z_2 - z_4 \end{bmatrix} \qquad 2(33)$$

The strain vector is now:-

$$\{\varepsilon\} = \begin{Bmatrix} \varepsilon_x \\ \varepsilon_y \\ \varepsilon_z \\ \gamma_{xy} \\ \gamma_{yz} \\ \gamma_{zx} \end{Bmatrix} = \begin{Bmatrix} \frac{\partial u}{\partial x} \\ \frac{\partial v}{\partial y} \\ \frac{\partial w}{\partial z} \\ \frac{\partial u}{\partial y} + \frac{\partial v}{\partial x} \\ \frac{\partial v}{\partial z} + \frac{\partial w}{\partial y} \\ \frac{\partial w}{\partial x} + \frac{\partial y}{\partial z} \end{Bmatrix} \qquad 2(34)$$

And:-

$$\begin{Bmatrix} \frac{\partial u}{\partial x} \\ \frac{\partial u}{\partial y} \\ \frac{\partial u}{\partial z} \end{Bmatrix} = [\mathcal{J}] = \begin{Bmatrix} \frac{\partial u}{\partial \xi} \\ \frac{\partial u}{\partial \eta} \\ \frac{\partial u}{\partial \zeta} \end{Bmatrix} = \begin{bmatrix} 1. & 0. & 0. & -1. \\ 0. & 0. & 1. & -1. \\ 0. & 1. & 0. & -1. \end{bmatrix} \begin{Bmatrix} u_1 \\ u_2 \\ u_3 \\ u_4 \end{Bmatrix} \qquad 2(35)$$

Using equation 2(35) and the similar expressions for the other terms of equation 2(34) the B matrix may be calculated. This is again constant and the element stiffness matrix becomes:

$$[k]^e = \int [B]^T [D][B] \, d(vol) = [B]^T [D][B] \frac{|J|}{6} = [B]^T [D][B].V \qquad 2(36)$$

2.2.6 Other Simple Three Dimensional Solid Elements

It is not usually convenient to work entirely with tetrahedral

elements since data preparation is then excessively tedious. Hexahedral bricks and wedge shaped elements are useful. Both these elements may be either assembled from tetrahedra or formulated directly.

A hexahedron may be divided into five tetrahedra in two possible ways. Both of these constructions may be envisaged as a small tetrahedron on each of the four faces of a central and larger tetrahedron. One construction is shown in Figure 2.5.

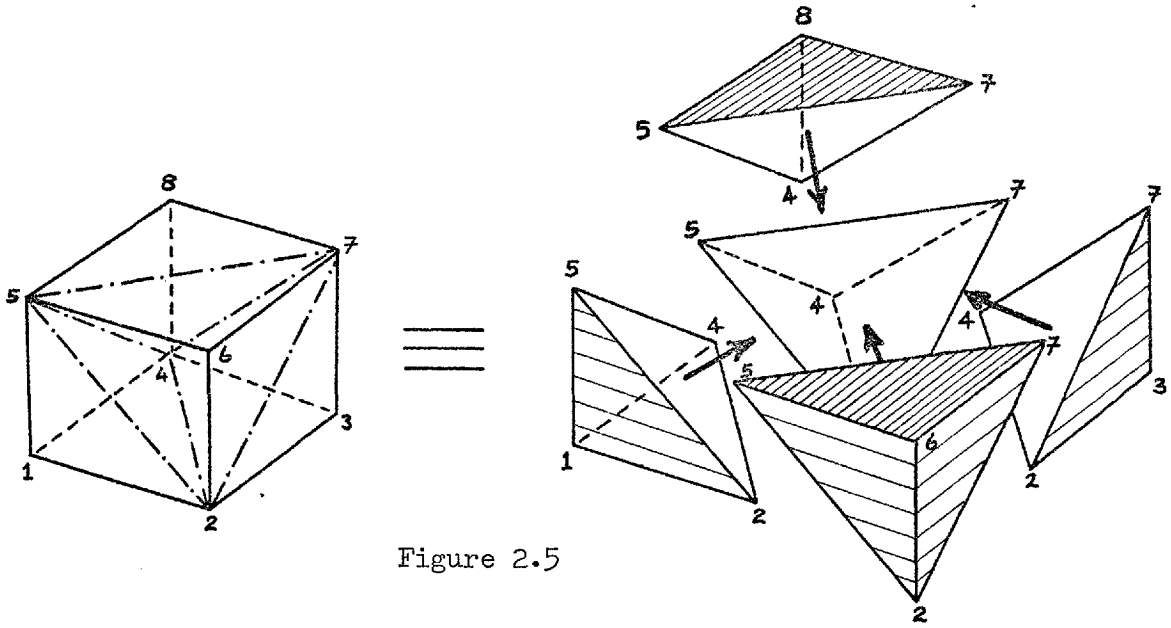


Figure 2.5

In order to overcome the assymmetry of this sub-division a mean stiffness matrix is obtained by formulating the properties of the two possible assemblies.

The tetrahedron derived hexahedral element can only have plane faces. This is not a limitation if an isoparametric hexahedron is formulated directly. (Fig. 2.6) The elements may be curvilinear.

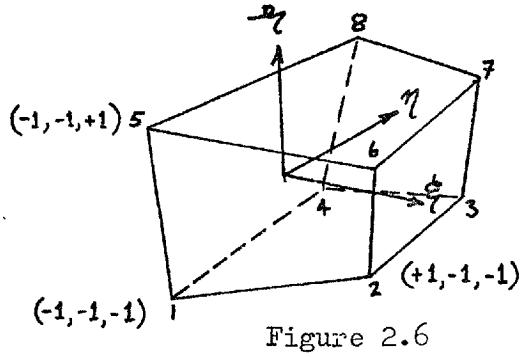


Figure 2.6

The shape functions for this element are:-

$$N_i = \frac{1}{8}\left(1+\xi_0\right)\left(1+\eta_0\right)\left(1+\zeta_0\right) \qquad 2(36)$$

where $\xi_0 = \xi\xi_i$ etc.

From the equations 2(36) the element stiffness matrix may be derived in exactly the same manner as described above.

$$[K]^e = \int [B]^T [D] [B] \, d(vol)$$

$$= \int_{-1}^{+1}\int_{-1}^{+1}\int_{-1}^{+1} [B(\xi,\eta,\zeta)]^T [D] [B(\xi,\eta,\zeta)] |J| \, d\xi \, d\eta \, d\zeta \qquad 2(37)$$

Resort must now be made to numerical integration.

If $G(\xi,\eta,\zeta)$ is the value of $[B(\xi,\eta,\zeta)]^T [D] [B(\xi,\eta,\zeta)] |J|$ at the sample point ξ, η, ζ then

$$[K]^e = \sum_{k=1}^{n}\sum_{j=1}^{n}\sum_{i=1}^{n} H_k H_j H_i \, G(a_i b_j c_k) \qquad 2(38)$$

where $H_{i,j,k}$ are constants of integration and a_i, b_j, c_k the sample points for an n point Gauss Rule. (For this simple case the two point rule is quite adequate.)

A pentahedron may also be subdivided into tetrahedra. In this case the division may be carried out in four possible ways. The author derived a mean stiffness matrix by using all four possibilities but took account of repetitious terms to economize on computer time.

The direct formulation of the six node pentahedral element Fig. 2.7 is based on the following shape functions:-

$$N_1, N_4 = \zeta(1+\xi_0)/2.$$
$$N_3, N_6 = \eta(1+\xi_0)/2. \qquad 2(39)$$
$$N_2, N_5 = (1-\eta-\zeta)(1+\xi_0)/2.$$

where

$$\xi_0 = \xi\xi_i$$

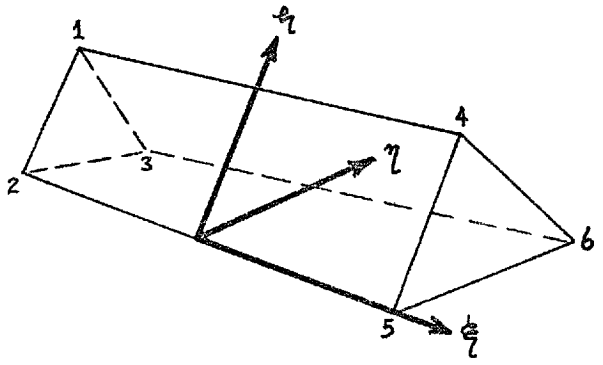


Figure 2.7

Formulation of the stiffness matrix shows that only the terms containing ξ need to be integrated numerically, so using a two-point rule the stiffness can be evaluated from

$$[k]^e = \sum_{i=1}^{2} H(i)\, G\left(a_i, \tfrac{1}{3}, \tfrac{1}{3}\right) \qquad 2(40)$$

using the same terminology as above.

2.3 SOLUTION OF EQUATIONS

The equation 2(10) derived by equating internal and external work gives the contribution of a single element to the whole structure. This may be rewritten as:-

$$\{F\}^e + \int [B]^T \{\sigma_0\}\, d(vol) + \int [B]^T [D] \{\varepsilon_0\}\, d(vol) + \int [N]^T \{P\}\, d(vol)$$
$$= [k]^e \{\delta\}^e \qquad 2(40)$$

The left hand side of this equation is simply a list of nodal point loads and may be evaluated if the initial stresses and strains, distributed loads and concentrated nodal forces are known. The contribution of an individual element with n degrees of freedom has therefore been reduced to n simultaneous equations. Summation of all such contributions gives an overall stiffness matrix $[K]$ and load vector $\{R\}$. The solution of this set of equations may be written as:

$$\{\delta\} = [K]^{-1}\{R\} \qquad 2(41)$$

where $\{\delta\}$ is the vector of all nodal displacements. The overall stiffness matrix is modified to take account of any nodal constraints before solution is obtained by either direct inversion, an elimination procedure, or relaxation.

In this study the subroutine BANSOL written by Wilson (Ref. 5) has been used in all computer programs. This equation solver is based on Gaussian Elimination and exploits the properties of the symmetric, narrow banded stiffness matrix. The Frontal Solution program presented by Irons (Ref. 6) was investigated later in this study, but appeared to offer little advantage for the very small and simple models discussed in this thesis.

PART II - SPECIAL CONSIDERATIONS FOR JOINTED MATERIALS

2.4 INTRODUCTION

On the scale considered in open pit mining the rock is usually highly discontinuous. The presence of these discontinuities has a considerable influence on the behaviour of the rock mass, so special methods have to be used to take them into account. Two approaches, using Finite Elements, may be adopted. In the first the rock is assumed to behave macroscopically as a continuum. Alternatively, the behaviour of discrete discontinuities within the solid may be considered. This involves modelling phenomenon such as slip, separation under tensile loading and dilatancy.

2.5 CONTINUUM APPROACH

2.5.1 Anisotropic Material Properties

If the discontinuities are sufficiently close together, with respect to the size of the model, the mass may be ascribed anisotropic elastic properties. The deformability of the discontinuities will determine the mass anisotropic elastic constants.

The simplest case is when the discontinuities are parallel. (Ref. 7) This is analagous to a stratiform body in which the material is transversely isotropic (Figure 2.7). There are only five independent elastic constants for this material and the stress-strain equations are:-

$$\begin{aligned}
\varepsilon_x &= \frac{\sigma_x}{E_1} - \frac{\nu_2 \sigma_y}{E_2} - \frac{\nu_1 \sigma_z} {E_1} & \gamma_{xz} &= \left\{2(1+\nu_1)/E_1\right\} \tau_{xz} \\
\varepsilon_y &= -\frac{\nu_2 \sigma_x}{E_2} + \frac{\sigma_y}{E_2} - \frac{\nu_2 \sigma_z}{E_2} & \gamma_{xy} &= \frac{1}{G_2} \tau_{xy} \\
\varepsilon_z &= -\frac{\nu_1 \sigma_x}{E_1} - \frac{\nu_2 \sigma_y}{E_2} + \frac{\sigma_z}{E_1} & \gamma_{yz} &= \frac{1}{G_2} \tau_{yz}
\end{aligned} \qquad 2(42)$$

with the constants E_2, G_2, ν_2 associated with behaviour normal to

the plane of the strata and the constant E_1 , ν_1 with the plane of the strata.

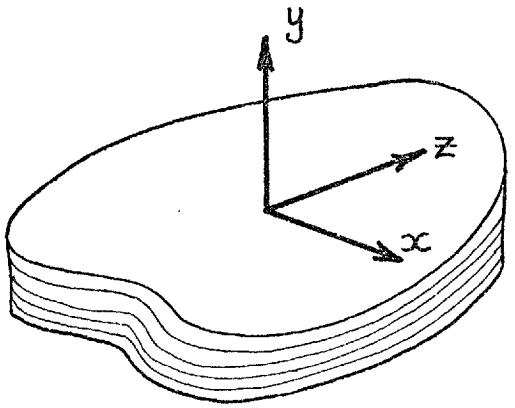


Figure 2.7

2.5.2 Calculation of Equivalent Elastic Properties

It is required to take account of joint deformability. In order to do this it is necessary to assume that the joint behaves linearly both with respect to shear and normal stresses (Fig. 2.8).

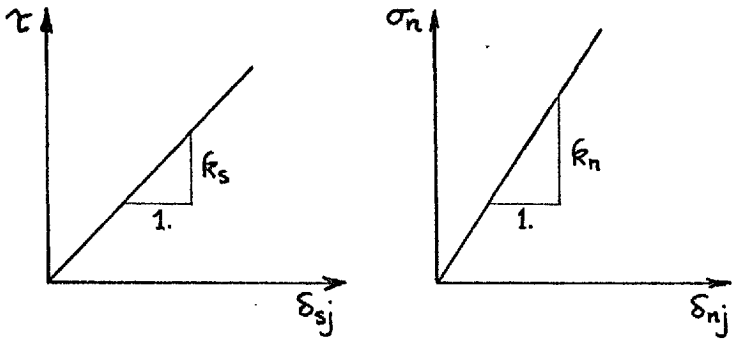


Figure 2.8

If the shear and normal displacements δ_{sj} and δ_{nj} result from shear and normal forces per unit area of τ and σ_n then the stiffnesses of the discontinuity are defined as:-

$$\text{Shear Stiffness } (k_s) = \frac{\tau}{\delta_{sj}} \qquad 2(43)$$

$$\text{Normal Stiffness } (k_n) = \frac{\sigma_n}{\delta_{nj}}$$

When a joint does not behave linearly this definition may be generalised to the rate of change of displacement with force per unit area.

Duncan and Goodman (Ref. 8) discussed the case of deformability of a rock containing a single joint set (Fig. 2.9).

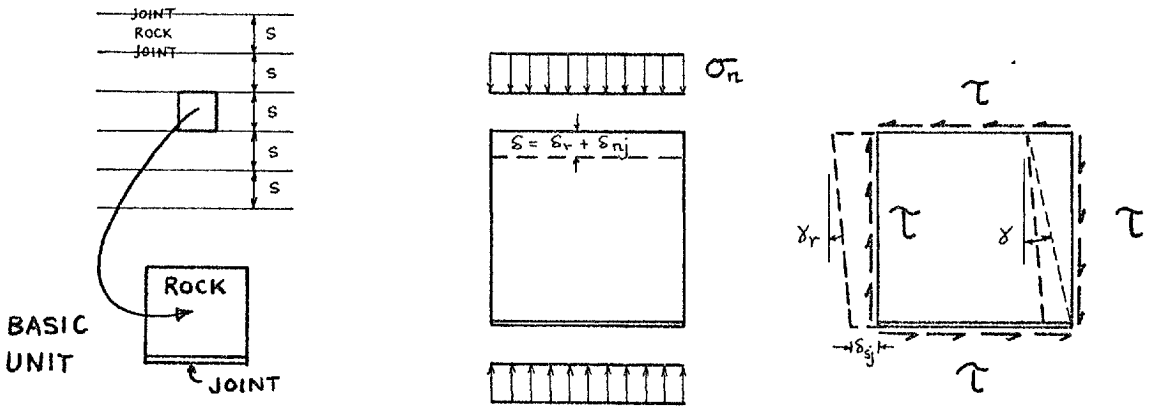


Figure 2.9 Deformation of Jointed Rock
(After Duncan & Goodman (8))

The total response (δ) of the rock to normal loading comprises contributions of the solid rock (δ_r) and the discontinuities (δ_{nj}).

$$\delta = \delta_r + \delta_{nj} = \frac{\sigma_n S}{E_r} + \frac{\sigma_n}{k_n} \qquad 2(44)$$

The equivalent modulus in the direction normal to the joints is thus:-

$$E_n = \frac{1.}{\left(\frac{1.}{E_r} + \frac{1.}{S.k_n}\right)} \qquad 2(45)$$

The equivalent shear modulus (G_{ns}) may be similarly derived:

$$G_{ns} = \frac{1.}{\left(\frac{1.}{G_r} + \frac{1.}{S k_s}\right)} \qquad 2(46)$$

Duncan and Goodman used this approach to establish the relationships for Othotropic Continua with three mutually perpendicular joints sets.

In general, the co-ordinate system to which the material properties are referred will not coincide with the global system used to define the model. Transformation equations are therefore necessary.

These may be written (Ref. 8) as:-

$$\{\sigma\}_{1,2,3} = [A]\{\sigma\}_{x,y,z}$$
$$\{\varepsilon\}_{1,2,3} = [B]\{\varepsilon\}_{x,y,z} \qquad 2(47)$$

If $[C]$ is the inverse of the material stiffness matrix $[D]$ (Equation 2(3)) i.e. the elasticity matrix:

$$\{\varepsilon\}_{1,2,3} = [C]_{1,2,3}\{\sigma\}_{1,2,3} \qquad 2(48)$$

1, 2 ,3 being the local co-ordinate scheme in which the material properties were evaluated.

From 2(47) and 2(48)

$$[B]\{\varepsilon\}_{x,y,z} = [C]_{1,2,3}[A]\{\sigma\}_{x,y,z}$$

Therefore $$\{\varepsilon\}_{x,y,z} = [B]^{-1}[C]_{1,2,3}[A]\{\sigma\}_{x,y,z}$$

Hence

$$[C]_{x,y,z} = [B]^{-1}[C]_{1,2,3}[A] \qquad 2(49)$$

It can be shown that $[A]$ and $[B]$ are orthogonal matrices, i.e.

$$[A]^{-1} = [B]^{T} \quad \text{and} \quad [A]^{T} = [B]^{-1} \qquad 2(50)$$

Equation 2(49) therefore can be rewritten:

$$[C]_{x,y,z} = [A]^{T} [C]_{1,2,3} [A] \qquad 2(51)$$

Similarly the transformation for the material stiffness matrix is:-

$$[D]_{x,y,z} = [B]^{T} [D]_{1,2,3} [B] \qquad 2(52)$$

The transformations for the biaxial cases are given by Jaeger (Ref. 9) as:-

$$[A] = \begin{bmatrix} \cos^2\beta & \sin^2\beta & 2.\sin\beta\cos\beta \\ \sin^2\beta & \cos^2\beta & -2.\sin\beta\cos\beta \\ -\sin\beta\cos\beta & \sin\beta\cos\beta & \cos^2\beta - \sin^2\beta \end{bmatrix} \qquad 2(53)$$

$$[B] = \begin{bmatrix} \cos^2\beta & \sin^2\beta & \sin\beta\cos\beta \\ \sin^2\beta & \cos^2\beta & -\sin\beta\cos\beta \\ -2.\sin\beta\cos\beta & 2.\sin\beta\cos\beta & \cos^2\beta - \sin^2\beta \end{bmatrix} \qquad 2(54)$$

where β is the angle between the x-axis and the X_1-axis measured counterclockwise from x to X_1. These equations hold for the case where rotation is about the X_3-axis.

The way is now open to determine the global material stiffness or elasticity matrix for any single joint set of arbitrary orientation. The global material elasticity matrix may now be obtained by linear superposition of the contributions of both the solid material and the discontinuities.

For the plane stress case the relationship for an isotropic solid is:-

$$\begin{Bmatrix} \varepsilon_x \\ \varepsilon_y \\ \gamma_{xy} \end{Bmatrix}_r = \begin{bmatrix} \frac{1}{E_r} & -\frac{\nu}{E_r} & 0. \\ \frac{\nu}{E_r} & \frac{1}{E_r} & 0. \\ 0. & 0. & \frac{2(1+\nu)}{E} \end{bmatrix} \begin{Bmatrix} \sigma_x \\ \sigma_y \\ \tau_{xy} \end{Bmatrix} \qquad 2(55)$$

That for a joint set parallel to the x-axis:-

$$\begin{Bmatrix} \varepsilon_x \\ \varepsilon_y \\ \gamma_{xy} \end{Bmatrix}_j = \begin{bmatrix} 0. & 0. & 0. \\ 0. & \frac{1}{S\bar{k}_n} & 0. \\ 0. & 0. & \frac{1}{S\bar{k}_s} \end{bmatrix} \begin{Bmatrix} \sigma_x \\ \sigma_y \\ \tau_{xy} \end{Bmatrix} \qquad 2(56)$$

By linear superposition exactly the same relationship is obtained as before (Equation 2(45),

$$\text{i.e. } \frac{1}{E_n} = \frac{1}{E_r} + \frac{1}{S.k_n}$$

In this manner any number of joint systems may be superimposed upon the original rock material, providing the reference axes for each system are identical.

2.6 DISCRETE DISCONTINUITIES - SPECIAL JOINT ELEMENTS

Three different methods have been used to model specific discontinuities where the spacing is no longer small with respect to the total scale. The different methods will be summarised briefly before that used in this study is developed in greater detail.

2.6.1 Discontinuity Representations

Pin-jointed linkage elements

Anderson and Dodd (Ref. 10) proposed that a fault be represented by linking elements on either side of the discontinuity by pin ended straight members (Fig. 2.10). These are able to transmit only longitudinal compressive forces. Tension in the member is not permitted and no resistance is offered to shear as it is free to rotate. This procedure is not physically very satisfactory since discontinuities are observed to transmit shear forces.

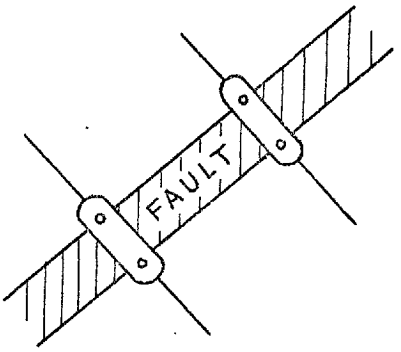


Figure 2.10

Modified continuum elements

The simplest approach is to model a discontinuity using rectangular elements with a high aspect ratio (In fact a length to width ratio of about 1:5 is a reasonable maximum). Isotropic or anisotropic material properties may be used to simulate the deformability of the joint.

In order to model joints using elements with an aspect ratio greater than about 5 a modification to the usual rectangular elements is required. (Ref. 11). A plane rectangular element with eight nodes (Fig. 2.11) may be satisfactorily reduced in one direction by suppressing the relevant nodes.

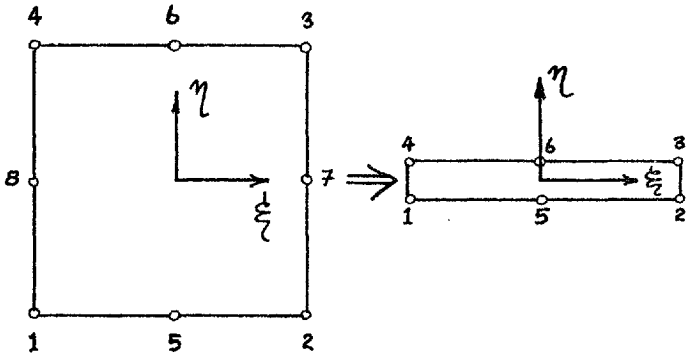


Figure 2.11

Displacement variation may now be linear in the short direction and parabolic in the long. Under these conditions the shape functions for this, and similar elements, can be deduced using the Lagrange interpolation formula.

They are:-

For Corner Nodes 1, 2, 3, 4 $$N_i = \frac{\xi_0}{2}(1 + \xi_{i_0})$$

For Mid Nodes 5, 6 $$N_i = (1 - \xi^2)$$ 2(57)

where $$\xi_0 = \xi_i \xi$$

From these the element properties can be derived as in Section 2.2.

Similar elements may be used to model discontinuities in three dimensional structures. These are discussed by Ahmad et al (Ref. 12) in the context of shell structures. There is, of course, no reason why such elements should be plane. Using the isoparametric concept, the shape functions provide all the information necessary to form elements which simply conform to the defined nodal points. The stiffness matrix of these elements must be obtained by using numerical integration.

The main short-coming of these continuum elements is that the measurable properties of joints are shear and normal stiffness. For lack of any information to the contrary, it is assumed that these two parameters are independent. The apparent shear and normal stiffness of the continuum elements are interrelated by virtue of the elastic laws assumed during their formulation (Ref. 8). The normal stiffness is also dependent on the element thickness, and becomes infinite as the thickness approaches zero. This can give rise to numerical problems (Ref. 11).

Stiff Linkage Elements

Discontinuities can be ascribed shear and normal stiffness if they are considered to behave elastically. Physically the discontinuity may be thought of as the interface between two solid units. The stiffness terms refer to this interface, which may be replaced by an element consisting of two coincident faces whose interaction has already been defined.

The above model was developed By Goodman, Taylor and Brekke (Ref. 13) from the idea, investigated by Ngo and Scordelis (Ref. 14), of adding linkage element stiffness to total structural stiffness. This method has the advantages that elements have no thickness - a physically observable fact except when gouge is present - and the shear and normal stiffnesses are independent.

2.7 THE LINKAGE ELEMENTS

2.7.1 A General Formulation

Goodman, Taylor and Brekke originally developed a one-dimensional joint element to simulate plane discontinuities in biaxial stress problems. The derivation may be given in a completely general way, in a manner consistent with that used above (Section 2.2.1) for continuum elements.

Equation 2(4) related the virtual displacement $\{f^*\}$ at any point within any element to the virtual displacements $\{\delta^*\}^e$ of the nodes. In this case only the relative displacements of the two faces are of concern. Hence if $\{f^*\}_{rel}$ is now the virtual relative displacement and $[N]$ is the shape function of each face then:-

$$\{f^*\}_{rel} = [-N, N]\{\delta^*\}^e \qquad 2(58)$$

If $\{p\}$ are the forces per unit area on the joint then these are related to the relative displacements by a joint material stiffness matrix

$$\{p\} = [k][-N, N]\{\delta\}^e \qquad 2(59)$$

The internal work done by these distributed forces due to the virtual displacement $\{\delta^*\}^e$ is:-

$$\{f^*\}^T\{p\} = [-N, N]^T[k][-N, N]\{\delta^*\}^{eT} \qquad 2(60)$$

Equating internal and external work by integrating over the surface are of the element.

$$[\{\delta^*\}^e]^T\{F\}^e = [\{\delta^*\}^e]^T\left(\int [-N,N]^T[\bar{k}][-N,N]\,d(\text{Area})\right) \qquad 2(61)$$

For convenience, initial distributed loads and relative displacements have been left out of equation 2(61). If they are included the final expression becomes:-

$$\{F\}^e = \int [-N,N]^T[\bar{k}][-N,N]\,d(\text{Area})\{\delta\}^e - \int [-N,N]^T\{p_o\}\,d(\text{Area}) - \int [\bar{k}][-N,N]\{\delta_o\}\,d(\text{Area}) \qquad 2(62)$$

where $\{p_o\}$ and $\{\delta_o\}$ are the initial loads and relative displacements respectively.

The stiffness matrix will not, in general, have been formed in global coordinates. Transformations, as discussed for the anisotropic case (Section 2.5.2) will be necessary. Thus:-

$$[\bar{k}]^e = \int [A]^T[-N,N]^T[\bar{k}][-N,N][A]\,d(\text{Area}) \qquad 2(63)$$

where the original material stiffnesses $[\bar{k}]$ were given in the local co-ordinates and $[\bar{k}]^e$ is the final element stiffness matrix.

2.7.2 One Dimensional Joint Elements

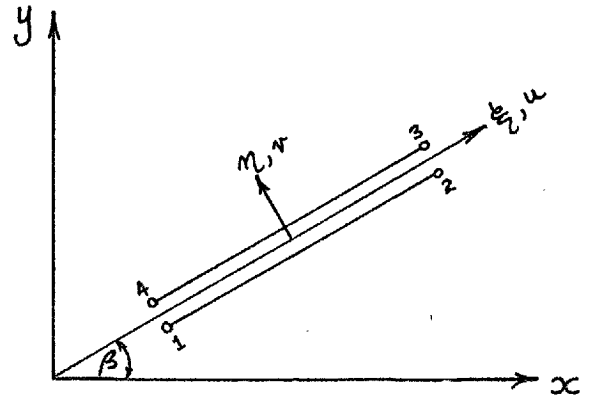


Figure 2.12

Equation 2(43) may be expressed in matrix form:-

$$\begin{Bmatrix} \tau \\ \sigma_n \end{Bmatrix} = \begin{bmatrix} k_s & 0. \\ 0. & k_n \end{bmatrix} \begin{Bmatrix} \delta_{sj} \\ \delta_{nj} \end{Bmatrix} = [k]\{f\}_{rel} \qquad 2(64)$$

In this context τ and σ_n are shear and normal forces per unit length. These are related to the relative displacement vector $\{f\}_{rel}$ by the material stiffness matrix $[k]$.

Using the Lagrange interpolation formula for each face of the four node element, the shape functions may be written down immediately.

$$N_i = \frac{1}{2}\left(1. + \xi\xi_i\right) \qquad 2(65)$$

For the top face (3, 4) the shear displacement (δ_s) and the normal displacement (δ_n) are, from the nodal displacements.

$$\begin{Bmatrix} \delta_{s\ top} \\ \delta_{n\ top} \end{Bmatrix} = \frac{1}{2}\begin{bmatrix} 1.+\xi & 0. & 1.-\xi & 0. \\ 0. & 1.+\xi & 0. & 1.-\xi \end{bmatrix} \begin{Bmatrix} u_3 \\ v_3 \\ u_4 \\ v_4 \end{Bmatrix} \qquad 2(66)$$

and for bottom face (1, 2)

$$\begin{Bmatrix} \delta_{s\ bottom} \\ \delta_{n\ bottom} \end{Bmatrix} = \frac{1}{2}\begin{bmatrix} 1.-\xi & 0. & 1.+\xi & 0. \\ 0. & 1.-\xi & 0. & 1.+\xi \end{bmatrix} \begin{Bmatrix} u_1 \\ v_1 \\ u_2 \\ v_2 \end{Bmatrix} \qquad 2(67)$$

The relative displacement of the two faces is

$$\{w\} = \begin{Bmatrix} \delta_{s\ top} - \delta_{s\ bottom} \\ \delta_{n\ top} - \delta_{n\ bottom} \end{Bmatrix} = \frac{1}{2}\begin{bmatrix} -A & 0. & -B & 0. & B & 0 & A & 0 \\ 0. & -A & 0. & -B & 0 & B & 0 & A \end{bmatrix}\{u\} \qquad 2(68)$$

where $A = 1.-\xi$, $B = 1.+\xi$, and $\{u\}$ is the nodal displacement vector.

The element stiffness matrix in local co-ordinates is given by equation 2(62) as:-

$$[k']^e = \int [-N, N]^T [k] [-N, N] \, d(\text{Area}) \qquad 2(69)$$

Substitution of 2(67) gives the terms of the stiffness matrix as:-

$$\int_{-1}^{+1} (1.+\xi)^2 \, d\xi = \frac{8}{3}$$

$$\int_{-1}^{+1} (1.-\xi)^2 \, d\xi = \frac{8}{3}$$

$$\int_{-1}^{+1} (1.+\xi)(1.-\xi) \, d\xi = \frac{4}{3}$$

Noting

$$\int_{-1}^{+1} (f) \, dx = \int_{-1}^{+1} (f) \frac{L}{2} \, d\xi$$

The joint stiffness matrix is:-

$$[k']^e = \frac{L}{6} \begin{bmatrix} +[\bar{K}] & -[\bar{K}] \\ -[K] & +[\bar{K}] \end{bmatrix} \qquad 2(70)$$

where

$$[\bar{K}] = \begin{bmatrix} 2. & 0. & 1. & 0. \\ 0. & 2. & 0. & 1. \\ 1. & 0. & 2. & 0. \\ 0. & 1. & 0. & 2. \end{bmatrix} \begin{Bmatrix} k_s \\ k_n \\ k_s \\ k_n \end{Bmatrix}$$

The contribution of the element to the global stiffness matrix may be determined by transformation from the local to global co-ordinates. In the general case, the forces and displacements of a node given in the local (x', y', z') system transform from the local system by a matrix $[L]$ giving

$$\{\delta_i'\} = [L]\{\delta_i\} \quad : \quad \{F_i'\} = [L]\{F_i\} \qquad 2(71)$$

in which $[L]$ is derived from the direction cosines of the angles formed between the sets of axes.

For the set of forces acting on the nodes of the element

$$\{\delta'\}^e = [T]\{\delta\}^e \quad : \quad \{F'\} = [T]\{F\}^e \qquad 2(72)$$

Following a parallel argument to section 2.5.2 the transformation for the stiffness matrix is

$$[k]^e = [T]^T[k']^e[T] \qquad 2(73)$$

For the two dimensional case the relationship between the axes may be written down by inspection (Fig. 2.12):-

$$\begin{Bmatrix} x' \\ y' \end{Bmatrix} = [\lambda]\begin{Bmatrix} x \\ y \end{Bmatrix} \qquad 2(74)$$

where

$$[\lambda] = \begin{bmatrix} \cos\beta & \sin\beta \\ -\sin\beta & \cos\beta \end{bmatrix} \qquad 2(75)$$

And

$$[T] = \begin{bmatrix} \lambda & 0. & 0. & 0. \\ 0. & \lambda & 0. & 0. \\ 0. & 0. & \lambda & 0. \\ 0. & 0. & 0. & \lambda \end{bmatrix}$$

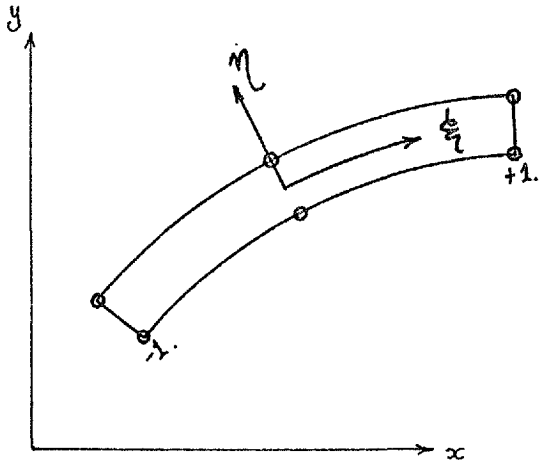


Figure 2.13

Extension of the above approach to non-plane one-dimensional elements, with more than two nodes per face (Fig. 2.13), is easily accomplished using the Langrange polynomials. These give a value of unity at any point of the division and zero at all the others, and are, in fact, the necessary shape functions (Ref. 3).

$$N_i = \frac{(\xi-\xi_1)(\xi-\xi_2)\cdots(\xi-\xi_{i-1})(\xi-\xi_{i+1})\cdots(\xi-\xi_n)}{(\xi_i-\xi_1)(\xi_i-\xi_2)\cdots(\xi_i-\xi_{i-1})(\xi_i-\xi_{i+1})\cdots(\xi_i-\xi_n)} \qquad 2(76)$$

For the non-plane case the necessary co-ordinate transformations will vary along the length of the element. The stiffness contribution of each node must be evaluated and a locally othogonal co-ordinate set derived to obtain the required transformations. Alternatively, a numerical integration procedure can be adopted, in which case a local orthogonal set must be determined for each integration point.

Finally it is noted that there will be continuity between the one dimensional joint elements and the two dimensional plate elements providing there are a matching number of nodal points for each type. As the co-ordinates of the nodal points must have the

same values for adjacent elements, continuity is automatically satisfied.

2.7.3 Two Dimensional Linkage Elements

The derivation of the stiffness matrix of a linkage element was given (Section 2.7.1) in a general manner. The treatment of two dimensional linkage elements, for modelling discontinuities in three dimensional structures, therefore presents no particular problem. All that is necessary is a choice of element shape functions for the top and bottom faces. This presentation follows the lines of Mahtab and Goodman (Ref. 15) although the publication of their work post-dated the author's original formulation.

The transformation equations for this case are a little more complex since local orthogonal axes have to be constructed with respect to a planar, rather than a linear, feature. In this study the discontinuities are considered to be flat, over any one element, and the transformations may be derived quite simply.

A Triangular Joint Element

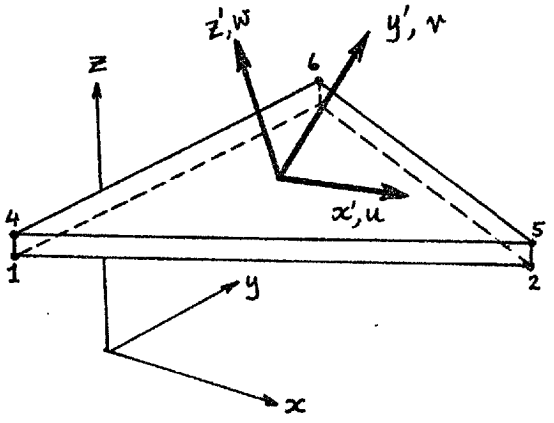


Figure 2.14

The shape functions of the two faces have already been given in connection with the triangular plate element (Section 2.2.3). If the three components of displacement are given in the local orthogonal co-ordinate system (x', y', z') then the relative displacement of the two faces, at any point within the element is:-

$$\{f\}_{rel} = \{f\}_{Top} - \{f\}_{Bottom}$$

$$= \left[\begin{array}{ccc|ccc|ccc|ccc|ccc|ccc} -N_1 & 0. & 0. & -N_2 & 0. & 0. & -N_3 & 0. & 0. & +N_4 & 0. & 0. & +N_5 & 0. & 0. & +N_6 & 0. & 0. \\ 0. & -N_1 & 0. & 0. & -N_2 & 0. & 0. & -N_3 & 0. & 0. & +N_4 & 0. & 0. & +N_5 & 0. & 0. & +N_6 & 0. \\ 0. & 0 & -N_1 & 0. & 0 & -N_1 & 0. & 0. & -N_3 & 0. & 0 & +N_4 & 0. & 0. & +N_5 & 0. & 0. & +N_6 \end{array}\right] \quad 2(78)$$

where $\{f\}_{Top}$ and $\{f\}_{Bottom}$ are the displacements of the top and bottom faces and $\begin{Bmatrix} u \\ v \\ w \end{Bmatrix}$ the vector of nodal displacements.

Since the two faces (123 and 456) are coincident, the shape functions for each are identical. i.e. $N_1 = N_4$ etc.

Equation 2(77) may therefore be rewritten as:-

$$\{f\}_{rel} = [-N, N]^T \begin{Bmatrix} u \\ v \\ w \end{Bmatrix} \qquad 2(78)$$

The element stiffness matrix is now:-

$$[k]^e = \int [-N, N]^T [k] [-N, N] \, d(Area) \qquad 2(79)$$

where

$$[k] = \begin{bmatrix} k_{x'} & 0. & 0. \\ & k_{y'} & 0. \\ \text{SYM} & & k_{z'} \end{bmatrix}$$

The joint stiffness matrix $[k]$ consists of the stiffness in the directions of the local orthogonal axes. It is assumed that these stiffnesses are independent of each other and that there are no off-diagonal terms in $[k]$. The latter would result in cross-coupling between shear and normal behaviour. Although this is a possible method of introducing dilatational behaviour for the joint the author considers the approach to be unsatisfactory.

The alternative method of modelling such phenomena will be discussed, later in this thesis, in connection with two dimensional studies.

Substitution in equation 2(79) results, upon multiplication, in the following expression:-

$$[\bar{k}]^e = \int \begin{bmatrix} +[\tilde{N}] & -[\tilde{N}] \\ -[\tilde{N}] & +[\tilde{N}] \end{bmatrix} d(\text{Area}) \qquad 2(80)$$

where

$$[\tilde{N}] = \begin{bmatrix} N_1^2 k_x & 0. & 0. & N_1N_2 k_x & 0. & 0. & N_1N_3 k_x & 0. & 0. \\ & N_1^2 k_y & 0. & 0. & N_1N_2 k_y & 0. & 0. & N_1N_3 k_y & 0. \\ & & N_1^2 k_z & 0. & 0. & N_1N_2 k_z & 0. & 0. & N_1N_3 k_z \\ & & & N_2^2 k_x & 0. & 0. & N_2N_3 k_x & 0. & 0. \\ & & & & N_2^2 k_y & 0. & 0. & N_2N_3 k_y & 0. \\ & & & & & N_2^2 k_z & 0. & 0. & N_2N_3 k_z \\ & & & & & & N_3^2 k_x & 0. & 0. \\ & & \text{SYM} & & & & & N_3^2 k_y & 0. \\ & & & & & & & & N_3^2 k_z \end{bmatrix}$$

The integration may be performed explicitly. This formulation was originally carried out in the local cartesian co-ordinate system to yield terms of the form:-

$$\int N_i N_j \, d(\text{Area}) = \frac{1}{48A}\left[12a_i a_j + b_i b_j\left(\Sigma x_i^2\right) + \left(b_i c_j + b_j c_i\right)\left(\Sigma x_i y_i\right) + c_i c_j\left(\Sigma y_i^2\right)\right] \qquad 2(81)$$

where a_i, b_i, c_i, etc. are constants depending on the nodal co-ordinates of the element. If instead, the shape functions obtained from the area co-ordinates are used, then the general rule for integrating over the triangle area can be applied. This is:-

$$\int\int L_1^a L_2^b L_3^c \, dx\, dy = \frac{\lfloor a \cdot \lfloor b \cdot \lfloor c}{\lfloor (a+b+c+2)} \cdot 2A \qquad 2(82)$$

where L_1 , L_2 , L_3 are the area co-ordinates.

Hence

$$\iint L_i^2 \, dx \, dy = \frac{\lfloor 2}{\lfloor 4} \cdot 2A = \frac{A}{6}$$

and

$$\iint L_i L_j \, dx \, dy = \frac{\lfloor 1 \, \lfloor 1}{\lfloor 4} \cdot 2A = \frac{A}{12}$$

For this case $N_i = L_i$ so $[\bar{N}]$ becomes:-

$$[\bar{N}] = \frac{A}{12} \begin{bmatrix} 2k_x & 0. & 0. & k_x & 0. & 0. & k_x & 0 & 0. \\ & 2k_y & 0. & k_y & 0. & 0. & k_y & 0. & \\ & & 2k_z & 0. & 0. & k_z & 0 & 0. & k_z \\ & & & 2k_x & 0. & 0. & k_x & 0. & 0. \\ & & & & 2k_y & 0. & 0. & k_y & 0. \\ & & & & & 2k_z & 0. & 0. & k_z \\ & & & \text{SYM} & & & 2k_x & 0. & 0. \\ & & & & & & & 2k_y & 0. \\ & & & & & & & & 2k_z \end{bmatrix} \qquad 2(83)$$

The original version of the computer programme used for the work reported in this thesis evaluated the expression above (Equation 2(81)). The author failed to find any simplification.

Quadrilateral Joint Elements

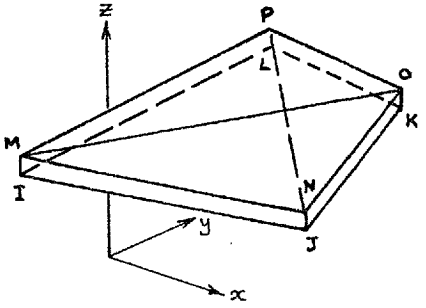


Figure 2.15

A quadrilateral joint element may be divided into two triangles (Fig. 2.15) in two different ways. Consideration of both divisions will yield a mean stiffness matrix with improved characteristics.

Alternatively, an arbitrary shaped quadrilateral element based on the isoparametric quadrilateral plate element may be used. This has the advantage that it need not be flat and is compatible with the arbitrary hexahedral and pentahedral elements discussed earlier (In this study only flat elements are considered).

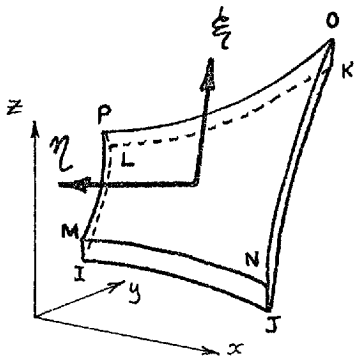


Figure 2.16

The shape functions for each face are now:-

$$N_i = \frac{1}{4}(1.+\xi_o)(1.+\eta_o) \qquad 2(84)$$

where $\xi_o = \xi\xi_i$ and $\eta_o = \eta\eta_i$

Proceeding in an identical manner as for the triangular case, the stiffness matrix can be obtained.

$$[K]^e = \int_{-1}^{+1}\int_{-1}^{+1} [-N,N]^T[K][-N,N]|J|\, d\xi\, d\eta \qquad 2(85)$$

Numerical integration must be resorted to for this case

$$[k]^e = \sum_{j=1}^{n}\sum_{i=1}^{n} H_j H_i \left[-N,N(\xi,\eta)\right]^T [k] \left[-N,N(\xi,\eta)\right] |J|$$

where H_i, H_j are constants of integration.

2.7.4 Transformation Equations for Planar Joint Elements

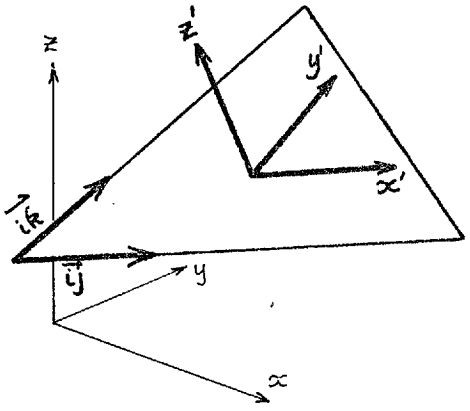


Figure 2.17

Since the plane ijk is flat it is completely defined by any two vectors lying within it. e.g. $\vec{ik}$ and $\vec{ij}$.

These two vectors can be written down as the co-ordinates of i, j, k are known

$$\vec{ik} = \left\{ x_i - x_k \; ; \; y_i - y_k \; ; \; z_i - z_k \right\}^T$$

$$\vec{ij} = \left\{ x_i - x_j \; ; \; y_i - y_j \; ; \; z_i - z_j \right\}^T \qquad 2(86)$$

The vector product of these two is normal to the plane and therefore parallel to z'. That is, the vector of z' can be given by the normalised product of $\vec{ij}$ and $\vec{ik}$.

$$\vec{z} = \frac{\vec{ij} \times \vec{ik}}{|\vec{ij} \times \vec{ik}|} \qquad 2(87)$$

$$= \left\{ \frac{A}{\sqrt{(A^2+B^2+C^2)}} ; \frac{B}{\sqrt{(A^2+B^2+C^2)}} ; \frac{C}{\sqrt{(A^2+B^2+C^2)}} \right\}^T$$

where

$$A = (y_i - y_j)(z_i - z_k) - (y_i - y_k)(z_i - z_j)$$

$$B = -(x_i - x_j)(z_i - z_k) + (x_i - x_k)(z_i - z_j)$$

$$C = (x_i - x_j)(y_i - y_k) - (x_i - x_k)(y_i - y_j)$$

The local x' axis is in the plane of the joint and is chosen to be parallel to the xy plane. It is therefore horizontal and corresponds to the geological strike of the joint.

$$\vec{z} \times \vec{z}' = \begin{Bmatrix} 0. \\ 0. \\ 1. \end{Bmatrix} \times \begin{Bmatrix} \frac{A}{\sqrt{(A^2+B^2+C^2)}} \\ \frac{B}{\sqrt{(A^2+B^2+C^2)}} \\ \frac{C}{\sqrt{(A^2+B^2+C^2)}} \end{Bmatrix} \qquad 2(88)$$

Hence

$$\vec{x}' = \begin{Bmatrix} \frac{-B}{\sqrt{(A^2+B^2)}} \\ \frac{A}{\sqrt{(A^2+B^2)}} \\ 0. \end{Bmatrix}$$

The local y' axis vector is simply the vector product of the other two axes. For a right handed co-ordinate system:

$$\vec{y}' = \frac{\vec{z}' \times \vec{x}'}{|\vec{z}' \times \vec{x}'|} = \begin{Bmatrix} \dfrac{-AC}{\sqrt{(A^2+B^2+C^2)(A^2+B^2)}} \\ \dfrac{-BC}{\sqrt{(A^2+B^2+C^2)(A^2+B^2)}} \\ \dfrac{A^2+B^2}{\sqrt{(A^2+B^2+C^2)(A^2+B^2)}} \end{Bmatrix} \qquad 2(89)$$

The relationship between the local and global axes can now be written as:

$$\begin{Bmatrix} x' \\ y' \\ z' \end{Bmatrix} = \begin{bmatrix} \vec{x}' \\ \vec{y}' \\ \vec{z}' \end{bmatrix} \begin{Bmatrix} x \\ y \\ z \end{Bmatrix} = [DC] \begin{Bmatrix} x \\ y \\ z \end{Bmatrix} \qquad 2(90)$$

For the triangular joint element the transformation equation is now:

$$[T] = \begin{bmatrix} [DC] & & & & & \\ & [DC] & & 0. & & \\ & & [DC] & & & \\ & & & [DC] & & \\ & 0. & & & [DC] & \\ & & & & & [DC] \end{bmatrix} \qquad 2(91)$$

(c.f. Equations 2(73), 2(74), 2(75))

Since the quadrilateral elements are all flat, the transformation equations may be determined from any three of the nodal point co-ordinates of one face.

2.7.5 Output from Joint Elements

Equation 2(59) enables the forces per unit area to be calculated when the nodal displacements, in local co-ordinates, are known. Since all of the elements in this study are based on the assumption of a linear displacement variation, the forces per unit area will be constant right across their surface. Their values will therefore be given at the centroid of the element.

For the one dimensional joint element equation 2(59) becomes:-

$$\begin{Bmatrix} \tau \\ \sigma_n \end{Bmatrix} = \frac{1}{2} \begin{bmatrix} k_s & 0. \\ 0. & k_n \end{bmatrix} \begin{bmatrix} -1. & 0. & -1. & 0. & 1. & 0. & 1. & 0. \\ 0. & -1. & 0. & -1. & 0. & 1. & 0. & 1. \end{bmatrix} \{\delta\}^e \qquad 2(92)$$

And for the two dimensional triangular element:

$$\begin{Bmatrix} \tau_x \\ \tau_y \\ \sigma_n \end{Bmatrix} = \frac{1}{3} \begin{bmatrix} k_x & 0. & 0. \\ 0. & k_y & 0. \\ 0. & 0. & k_z \end{bmatrix} \begin{bmatrix} 0. & 0. & 0. & -1. & 0. & 0. & -1. & 0. & 0. & +1. & 0. & 0. & +1. & 0. & 0. & +1. & 0. & 0. \\ 0. & -1. & 0. & 0. & -1. & 0. & 0. & -1. & 0. & 0. & +1. & 0. & 0. & +1. & 0. & 0. & +1. & 0. \\ 0. & 0. & -1. & 0. & 0. & -1. & 0. & 0. & -1. & 0. & 0. & +1. & 0. & 0. & +1. & 0. & 0. & +1 \end{bmatrix} \{\delta\}^e \qquad 2(93)$$

In fact, these expressions are obvious from the original definition of the properties of the joint elements.

The displacements $\{\delta\}^e$ are given in the local co-ordinate scheme. These may be derived from the displacements in the global system using the transformation equations 2(91) and 2(75). The local displacements and forces per unit area for the two dimensional element, will therefore correspond with axes definition, Section 2.7.4

2.8 TREATMENT OF NON-LINEAR PROBLEMS

So far discussion has been restricted to the solution of problems where the material has been assumed to behave according to linear, elastic laws. In many cases the problem will not be amenable to a one step solution. Not only may the final situation be achieved after a complex history, but the material properties may be non-linear and history dependent. Also, the final displacements

may not be infinitesimal.

2.8.1 Large Displacements

In most large displacement problems the strains are, in fact, small and a direct iterative procedure may be adopted to provide a solution (Ref. 1). Linear elastic deformations are computed for the structure in the normal way. The original nodal co-ordinates are then adjusted to their displaced position and the problem resolved. The second step leads to an improved estimate of displacements by repeating the complete solution with the recalculated element stiffnesses. This process may be repeated until convergence is achieved. This process of modifying element nodal co-ordinates may also be used for cases of incremental loading, in which linear behaviour may indeed occur if the increments are sufficiently small. Argyris (Ref. 16) has discussed such cases at length.

No consideration has been given to large displacements in this study. It has been assumed that a reasonable approximation is obtained providing the geometry of individual elements remains substantially unaltered. This assumption enables the stiffness matrix of the whole structure to be assembled once only, unless there are geometrical alterations to the model during its simulated history. A number of different load cases may therefore be studied with economy of computer time.

2.8.2 Non-Linear Material Properties

The simplest method of treating materials that behave non-linearly is an iterative procedure in which the elastic properties are modified according to the total stress calculated for each element. In the same manner as discussed in connection with large displacements, a first solution provides revised values with which to form the stiffness matrix for the next solution (Fig. 2.18).

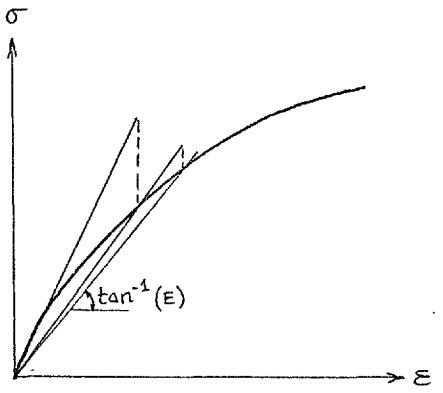


Figure 2.18

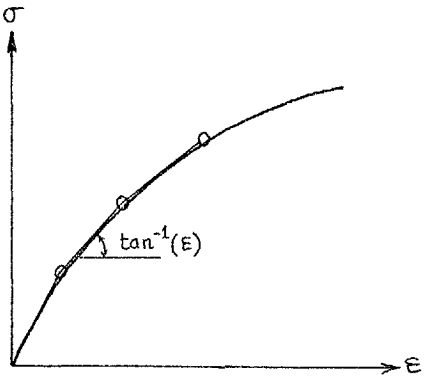


Figure 2.19

An alternative procedure applies to the loading in small increments and modifies the elastic constants according to the current stress level. For the first case, a secant value of Young's modulus is used and for the second a tangent value. The latter results in an actual stress/strain behaviour that lies above true curve (Fig. 2.19).

The above methods suffer from the disadvantages that it is impossible to model work softening materials - such as typical rock joint - and that the stiffness matrix must be reformed each cycle. These problems may be avoided using initial stress (Fig. 2.20) or initial strain (Fig. 2.21) procedures.

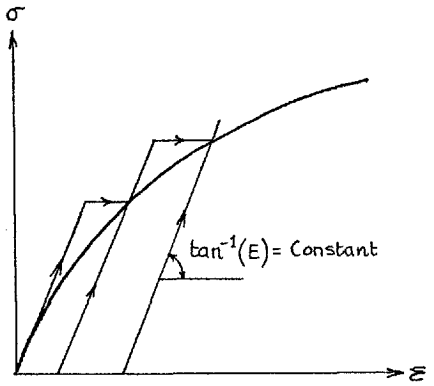


Figure 2.21

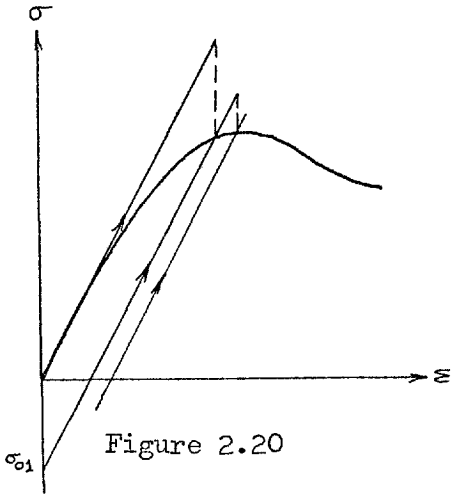


Figure 2.20

The equation 2(10) includes terms due to initial stresses and strains. These may be used to simulate non-linear behaviour

by introducing the departure from linearity as initial conditions for the linear model. This procedure has been discussed in detail in references 11, 17 and 18 and will be described as relevant to the main body of the text.

2.9 CONCLUSION

The outline of the Finite Element method given in this chapter provides the necessary knowledge for the generation of all the procedures that are discussed in this thesis. The exposition is by no means exhaustive, and the references represent only a small part of the total literature.

(1) Zienkiewicz, O.C. & Cheung, Y.K. The Finite Element Method in Structural and Continuum Mechanics. McGraw Hill 1967.

(2) Irons, B.M. Engineering Applications of Numerical Integration in Stiffness Method. A.I.A.A. Int. V.4. p. 2035 - 37.

(3) Zienkiewicz, O.C., Irons, B.M., Ergatoudis, J., Ahmad, S., & Scott, F.C. Iso-Parametric and Associated Element Families for Two- and Three-Dimensional Analysis. ed. I. Holand & K. Bell, Tapir Press, Trondheim 1969.

(4) Wilson, E.L. Structural Analysis of Axisymmetric Solids. A.I.A.A. Vol. 3 No. 12 1965 p. 2269 - 2274.

(5) Wilson, E.L. A Digital Computer Program for the Finite Element Analysis of Solids with Non-Linear Material Properties. Department of Civil Engineering, University of California, Berkeley 1965.

(6) Irons, B.M. A Frontal Solution Program for Finite Element Analysis. Int.J.Num.Meth.Eng. Vol. 2, 5-32, 1970.

(7) Zienkiewicz, O.C., Cheung, Y.K. & Stagg, K.G. Stresses in Anisotropic Media with Particular Reference to Problems in Rock Mechanics. J. Strain Anal. Vol. 1, No. 2, 1966.

(8) Duncan, J.M. & Goodman, R.E. Finite Element Analysis of Slopes in Jointed Rock. Report to the U.S. Army Corps of Engineers, Vicksburg, Miss. Contract No. DACW39-67-C-0091 by Geotechnical Engineering, University of California, Berkeley.

(9) Jaeger, J.C. Elasticity, Fracture and Flow. Pub. Methuen 1956.

(10) Anderson, H.W. & Dodd, J.S. Finite Element Method Applied to Rock Mechanics. 1st Cong. I.S.R.M. Lisbon, 1966. Paper 7.17.

(11) Zienkiewicz, O.C., Best, B., Dullage, C. & Stagg, K.G. Analysis of Non-Linear Problems in Rock Mechanics with Particular Reference to Jointed Rock Systems. 2nd Congress I.S.R.M. Belgrade 1970. Paper 8.14.

(12) Ahmad, S., Irons, B.M. & Zienkiewicz, O.C. Analysis of Thick and Thin Shell Structures by Curved Finite Elements. Int. J.Num.Meth.Eng. Vol. 2, 419-451, 1970.

(13) Goodman, R.E., Taylor, R.L. & Brekke, T.L. A Model for the Mechanics of Jointed Rock. A.S.C.E., S.M.3. May 1968.

(14) Ngo, D & Scordelis, A.C. Finite Element Analysis of Reinforced Concrete Beams. Journal of the American Concrete Institute Vol. 64, No. 3, March 1967.

(15) Mahtab, M.A. & Goodman, R.E. Three Dimensional Finite Element Analysis of Jointed Rock Slopes. 2nd Congress I.S.R.M. Belgrade 1970. Paper 7.12.

(16) Argyris, J.H. Matrix Analysis of Three-Dimensional Elastic Media Small and Large Displacements. A.I.A.A. Journal, Vol. 3, No. 1. January 1965.

(17) Zienkiewicz, O.C. & Valliappan. Analysis of Real Structures for Creep, Plasticity and Other Complex Constitutive Laws. Proc. Conf. on Structures Solid Mechanics and Engineering Design Civil Engineering Materials, Southampton University 1964 (J. Wiley 1970).

(18) Zienkiewicz, O.C., Valliappan, S. & King, I.P. Elasto-Plastic Solutions of Engineering Problems Initial Stress, Finite Element Approach. Int.J.Num.Methods in Engineering, Vol. 1 p. 75 - 100, 1969.

CHAPTER

3

THE ELASTIC ANALYSIS OF ROCK SLOPES - PLAIN STRAIN CONDITIONS

	Page
Chapter Index	69
Synopsis	70
3.1 Previous Work	71
3.2 Computer Program Verification	71
3.3 Some Observations on the Elastic Analysis of Slopes	72
3.4 Slope Study Variables	77
3.5 The Computer Model	78
3.6 Presentation of Results	79
3.7 Results of Analyses	80
3.8 Stability Analyses from Stress Distributions	91
3.9 The Stress on a Single Discontinuity through the Slope Toe	92
3.10 The Ubiquitous Joint Analysis	95
3.11 Conclusions	104
References	106

SYNOPSIS

A large number of elastic analyses of rock slopes, assuming plane strain conditions, were carried out by the author in an attempt to draw some conclusions regarding the use of stability calculations based on such work. Geometry and initial stress conditions were varied in order to make some observations on the influence of these parameters on the behaviour of rock slopes.

3.1 PREVIOUS WORK

Numerous studies of stresses in the vicinity of slopes subject to body forces have been reported in the literature. Numerical methods of obtaining solutions have been either Finite Difference or Finite Element techniques.

The application of Finite Difference methods to slope studies is relatively uncommon. Sturgul and Scheidegger (Ref. 1) used a standard relaxation method to solve for stresses around a vertical wall subject to tectonic loading alone. A solution for an open trench subject to gravity loading, by Dibiagio (Ref. 2), was later checked by Phukan (Ref. 3), who used a Lumped Parameter method. More recently Cundall (Ref. 4) obtained solutions for a gravity loaded vertical slope with and without additional tectonic stresses.

Examples of Finite Element Analyses of slopes are now too numerous to be mentioned individually. Nevertheless the papers by Yu et al (Ref. 5) and Phukan et al (Ref. 6) are noteworthy since they provide evidence of agreement between the numerical and photoelastic methods for analysis of continua subject to body forces.

A number of other publications have provided material, in addition to the author's, from which to make some general observations regarding stresses around slopes. The report by Duncan and Goodman (Ref. 7) contains a very thorough discussion of the case of a vertical slope subject to different initial stresses. Both Wang & Sun (Ref. 8) and Stacey (Ref. 9) have recently reported on studies, with a similar purpose to the author's, in which they analysed a large number of different slope geometries and initial conditions.

3.2 COMPUTER PROGRAM VERIFICATION

In order to verify the computer programs for biaxial cases that were used in this study, comparisons were made with available solutions by other workers in this field. The programming itself

required no verification since extensive use was made of the program given by Wilson (Ref. 10).

Agreement between solutions can only be expected providing the parameters defining the original model are identical. Wang & Sun (Ref. 8) gave a solution for a symmetrical excavation with vertical sides, a Poissons ratio of 0·2 and subject to gravitation loading only. Figure 3.1 gives some results from the above publication together with those due to the author. Wang & Sun used a model with boundaries as indicated in the figure. The finite element idealization used by the author is given in Figure 3.3. The closer boundaries of the former model have some influence on the stress distribution but the results of the analysis are essentially similar.

A second comparison was made with an unpublished analysis by Cundall (Ref. 11). In this case the models were identical, but the methods of analysis differed since Cundall used Dynamic Relaxation. Computer drawn contours, done to the same scale, showed no perceptable differences upon superposition so these have not been reproduced.

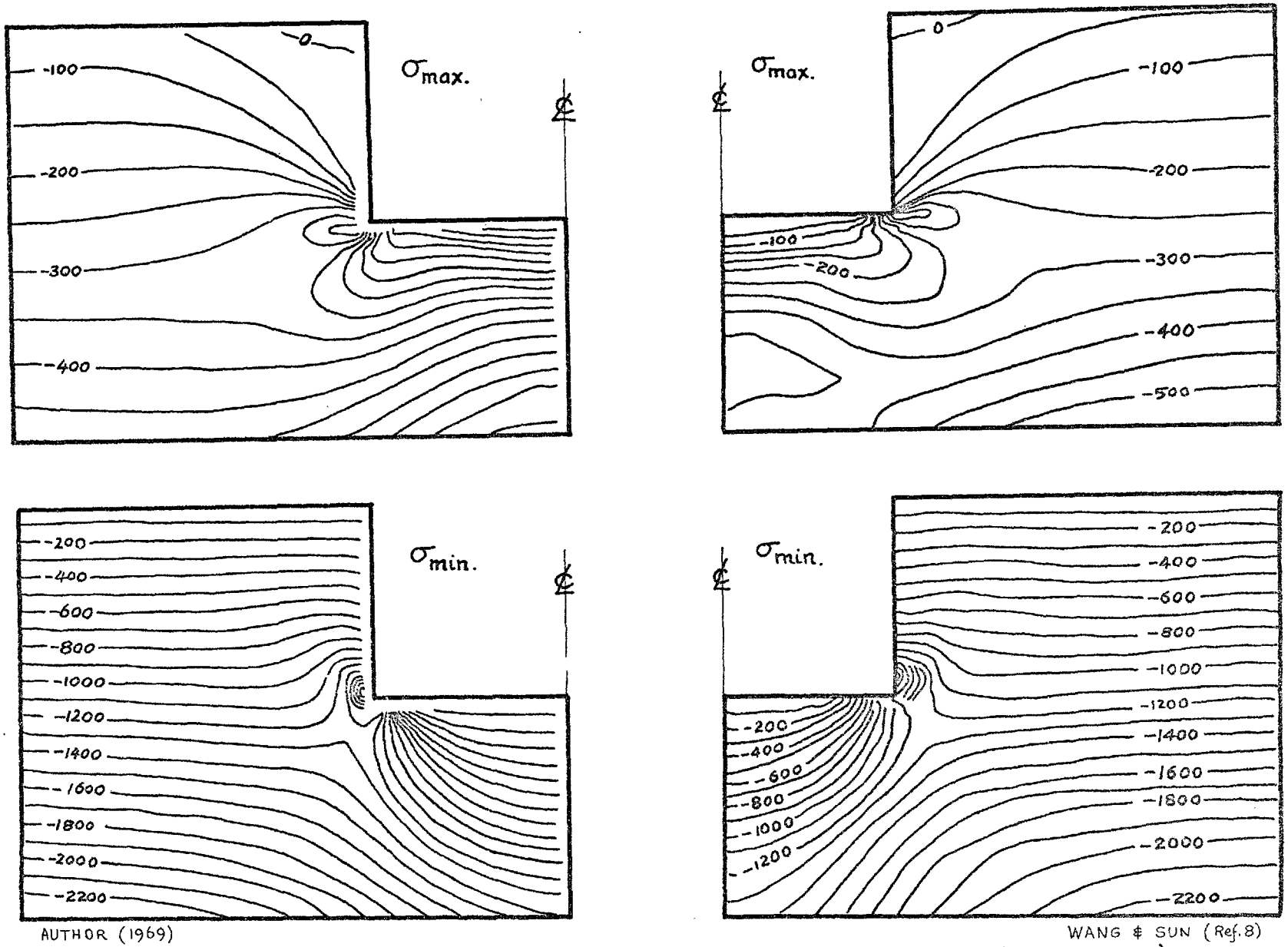
3.3 SOME OBSERVATIONS ON THE ELASTIC ANALYSIS OF SLOPES

For the purposes of this study the material of a slope has been considered to be homogeneous, isotropic, linearly elastic and time independent. These assumptions have some bearing on the method of analysis and the presentation.

3.3.1 Dimensionless Presentation

The stresses in a slope of the above material are linearly dependent upon the slope height (H) and the unit weight (γ). The stresses may therefore be normalised by dividing by the product of these two variables. The results may then be rescaled for geometrically similar situations.

In the same manner the displacements are proportional to the



AUTHOR (1969)

WANG & SUN (Ref. 8)

Stress Distribution for a 90° Slope ($\nu = 0.2$, $\gamma = 160$ lbf/ft^3, $H = 1036.8$ ft)

FIGURE 3.1

unit weight and the square of the slope height and inversely proportional to the elastic modulus. They may, therefore, be normalised by dividing by ($\gamma H^2/E$). (See equation 3(2))

3.3.2 Excavation Simulation

Two methods of conducting the analysis of an excavation are possible:

(a) Gravity may be applied instantaneously to an unstressed body.

(b) Excavation may be simulated in a prestressed body.

These two methods must result in exactly the same stress distribution providing the prestress in (b) is equal to the stresses that would exist in case (a) if no excavation were present. The equality of these two methods must also hold if the excavation is carried out in any number of arbitrary increments, since the model is a conservative system. References (12) and (13) provide recent evidence that numerical methods do not transgress this fundamental principle. In the author's opinion the only qualification to the above statements is that the final co-ordinates of the structure should be identical after, rather than before the analysis. This observation is really trivial since infinitesimal strain is assumed.

Although the stresses are identical the vertical displacements are different since case (a) contains the component due to pre-excavation response to gravity loading. The application of body force loading to a uniform layer with complete all round constraint will result in vertical strains:

$$\varepsilon_v = \frac{\sigma_v}{E}\left(1. - \frac{2.\nu^2}{(1.-\nu)}\right) \qquad 3(1)$$

where σ_v is the vertical stress, ν the Poissons ratio and E the Youngs modulus.

Integrating the expression 3(1) the total displacement (δ_v) at any depth D below the surface of a layer thickness T is:

$$\delta_v = \frac{\gamma}{2E}\left(D^2 - T^2\right)\left(1. - \frac{2.\nu^2}{(1.-\nu)}\right) \qquad 3(2)$$

The equation 3(2) provides all the information necessary to calculate the correct displacements due to excavation from results obtained by method (a).

The computer simulation of material removal from a pre-stressed model may be accomplished in two ways. The first method is illustrated by Figure 3.2. Nodal forces equivalent to the forces existing on the new free surface, due to stresses in the material to be removed, are calculated. Equal and opposite forces are now applied and the resulting stresses $(\Delta\sigma)$ added to those (σ_o) existing prior to the increment. (Ref. 14).

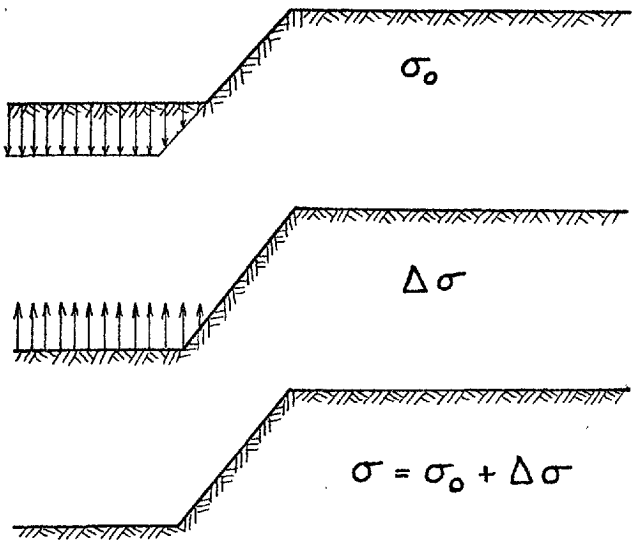


Figure 3.2

Alternatively, material may simply be excavated by completely removing elements from the stressed model. Equilibrium will no

longer exist and readjustments will occur so that it is re-established.

Consideration of the computational procedure for the above methods shows them to be basically identical. Differences should therefore only arise from variations in the calculated values of the nodal forces along the free surface. For both these methods previous workers have chosen to ascribe a very low modulus value to material that had been excavated. This procedure does not appear to influence the results, but the author preferred to use a simple by-pass statement that resulted in zero contribution to the overall stiffness matrix. An advantage of presentation is achieved since excavated elements appear stress free in computer output.

3.3.3 Influence of Initial Stresses and Poisson's Ratio

Consideration of the method of simulating the excavation of a slope in initially stressed material makes it obvious that, all other things being equal, the resulting stresses will be directly proportional to the initial stresses. Calculation of two extreme conditions of initial stress will therefore, in principle, provide all necessary data for the solution for other cases, without resort to further stress analysis.

Poisson's ratio will not influence the results of an analysis if constant stress boundary conditions are used. If a model is subject to lateral constraint in its own plane, then Poisson's ratio will determine the stresses that would exist if no excavation were present. For a horizontal surface these are:-

$$\begin{aligned} &\text{Vertical stress} && = \gamma . D && && \\ &\text{Horizontal stress} && = \nu . \gamma . D && \text{Plane Stress} && 3(3) \\ &\text{Horizontal stress} && = \frac{\nu}{1-\nu} . \gamma . D && \text{Plane Strain} && \end{aligned}$$

using the same symbols as in the previous section.

Hence, for these displacement boundary conditions, the stresses

will be linearly dependent upon (ν) or $(\nu/(1-\nu))$, for plane stress or plane strain cases respectively. A series of plane strain analyses for Poisson's ratios 0·0, 0·2, 0·3, 0·47, conducted by the author, verified this linear dependence. Such analyses enable the stresses for the case of a Poisson's ratio of 0·5 to be determined by linear extrapolation, when this cannot be done using existing computer program (Bray (Ref. 15)).

3.4 SLOPE STUDY VARIABLES

In order to reduce the amount of computation necessary in this study, it was essential to limit the variation of the individual parameters defining the slopes to be analysed. These parameters will be discussed briefly below.

3.4.1 Material Properties

As has been stated above (Section 3.4) the material was assumed to be homogeneous, isotropic, linearly elastic and time independent. In view of this assumption the only material property that need be considered is the Poisson's ratio. The author chose to use a value of 0·2 for all the analyses that will be discussed below. This means that the initial stress conditions that may be deduced assuming all round constraint are exactly equivalent to a ratio of 1:4 between the horizontal and vertical stresses on the boundaries. For high initial horizontal stresses the influence of Poisson's ratio on the in plane stresses was shown to be minimal.

3.4.2 Slope Geometry

Open pit excavations are assumed to be symmetrical and made in a half space so that the original surface geometry is not a variable. The excavation itself has the two variables; the slope angle and the ratio of toe width (half the base width) to slope height. (Since the results may be expressed in a dimensionless form the physical dimensions of the model are arbitrary.) In order to study the influence of the toe width the case of a

vertical slope with height to toe width ratios (for the half model) of 0·3, 0·5, 1·0 were considered. For further cases the ratio was standardised as 0·3, this being considered a typical value for an open pit mine.

3.4.3 Residual Stress State

It is widely assumed that vertical stresses prior to excavation are due to self weight only. If plane stress or plane strain conditions pertain then the vertical and horizontal stresses prior to excavation are given by Equations 3(3). The latter neglect the possibility of any horizontal residual stresses that may be present, although there is increasing evidence (Refs. 16, 17, 18) that this is often not the case. Despite this departure from ideal conditions the horizontal stresses still appear to increase linearly with depth, according to an expression of the form:

$$\sigma_{xx} = C + K.\gamma.H \qquad 3(4)$$

where C is the horizontal stress ~~and~~ *at* the surface and K a constant. Hast (Ref. 16) found evidence of quite considerable horizontal stresses at the surface, but more usually C is deleted from the above expression. K then becomes simply the ratio of the initial horizontal and vertical stresses.

In this study the influence of initial stresses was considered only for the case of a 45° slope. Several cases are illustrated, although there is a linear relationship between the stresses and the K value for each model.

3.5 THE COMPUTER MODEL

Yu et al (Ref. 5) judged that the overall vertical dimensions of a slope model should be three times the slope height, in order for the effect of the boundaries to be minimal. This ratio was used for most cases reported in this study. The horizontal extent was greater than the vertical and dependent upon the slope angle.

The main features of a typical model are given in Fig. 3.3. The meshes used for other slope angles were topologically equivalent to that illustrated.

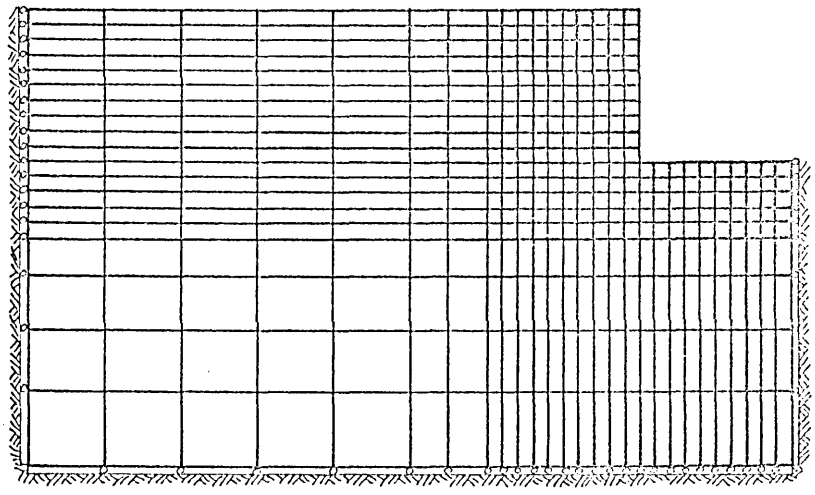


Figure 3.3

Model dimensions:

3000 x 5000 units ≡ 19 x 27 elements

Excavation depth:

1000 units ≡ 10 elements

Toe width:

1000 units ≡ 10 elements

3.6 PRESENTATION OF RESULTS

Evidence, to support observations on the influence of various parameters on the stresses around an open pit excavation, is given in the form of computer drawn contours of stresses. These were produced using the plotting program, for a regular mesh, that is given in Appendix A. All options in this plotting package were exploited in order to give as complete a representation as possible.

The following cases are illustrated:

Figure 3.4. Horizontal stresses for a vertical slope with various toe widths.

Figures 3.5, 3.6, 3.7. All contours :- $\sigma_{xx}, \sigma_{yy}, \tau_{xy}, \sigma_1, \sigma_2, \frac{\sigma_1+\sigma_3}{2}, \frac{\sigma_1-\sigma_3}{2}$ and relevant vectors are given for slope angles 30°, 60° and 90° for the case of gravity loading only on a plane strain model with a Poisson's ratio of 0·2.

Figures 3.8, 3.9, 3.10, 3.11. All contours and vectors for a slope angle of 45° with initial stress ratios (K) of 0·25, 0·5, 1·0 and 2·0 respectively.

On examination of these contour diagrams it should be noted that the outline of each unit does not correspond to the total model dimensions. Additionally, it should be noted that the vectors have the correct direction but an arbitrary magnitude, chosen to facilitate visual interpretation.

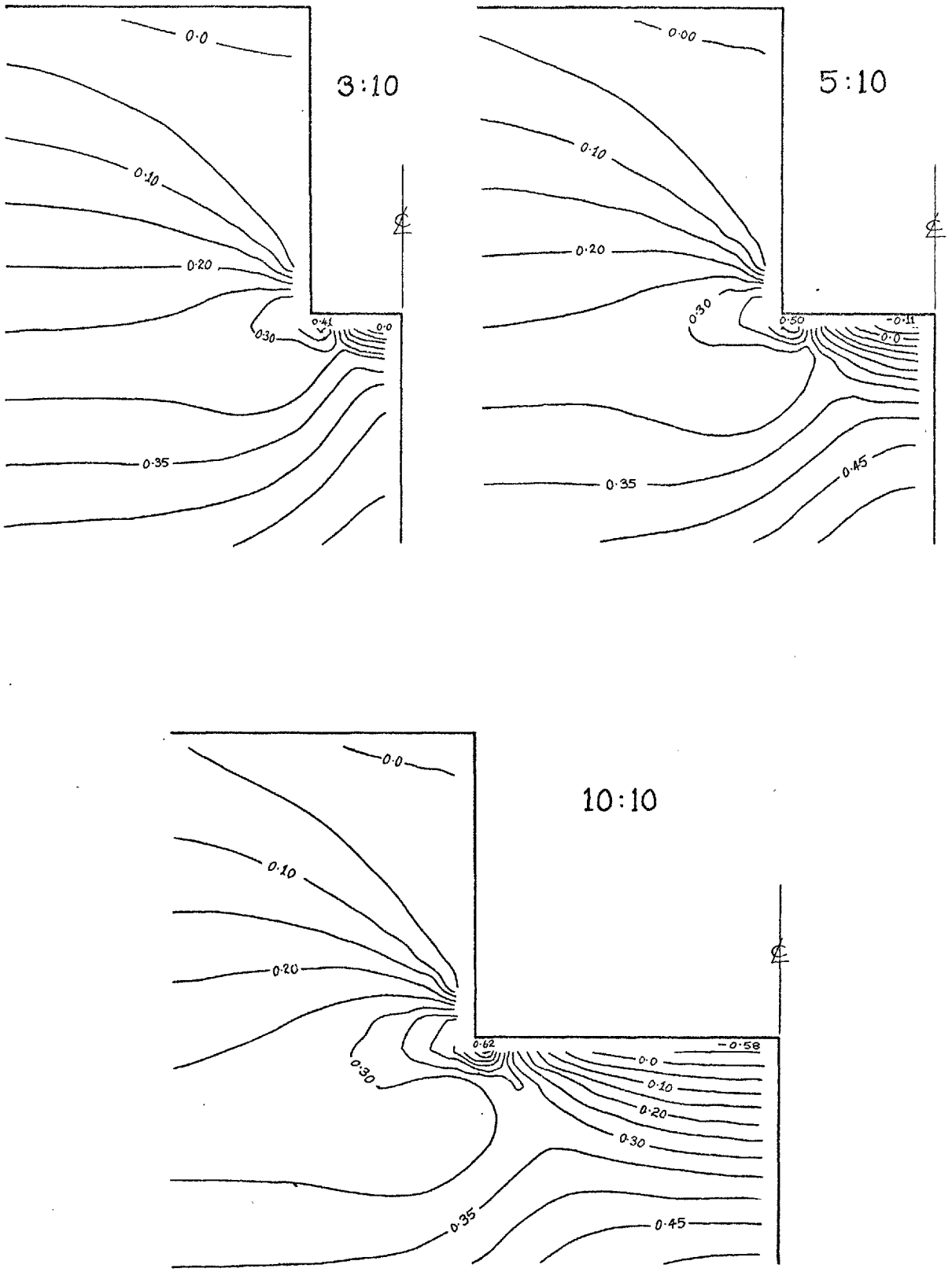
3.7 RESULTS OF ANALYSES

General conclusions concerning the importance of each parameter defining the slope are given below. These are based on the results obtained by the author, some of which are illustrated in Figures 3.4 to 3.11, and also other published data.

3.7.1 Influence of Toe Width

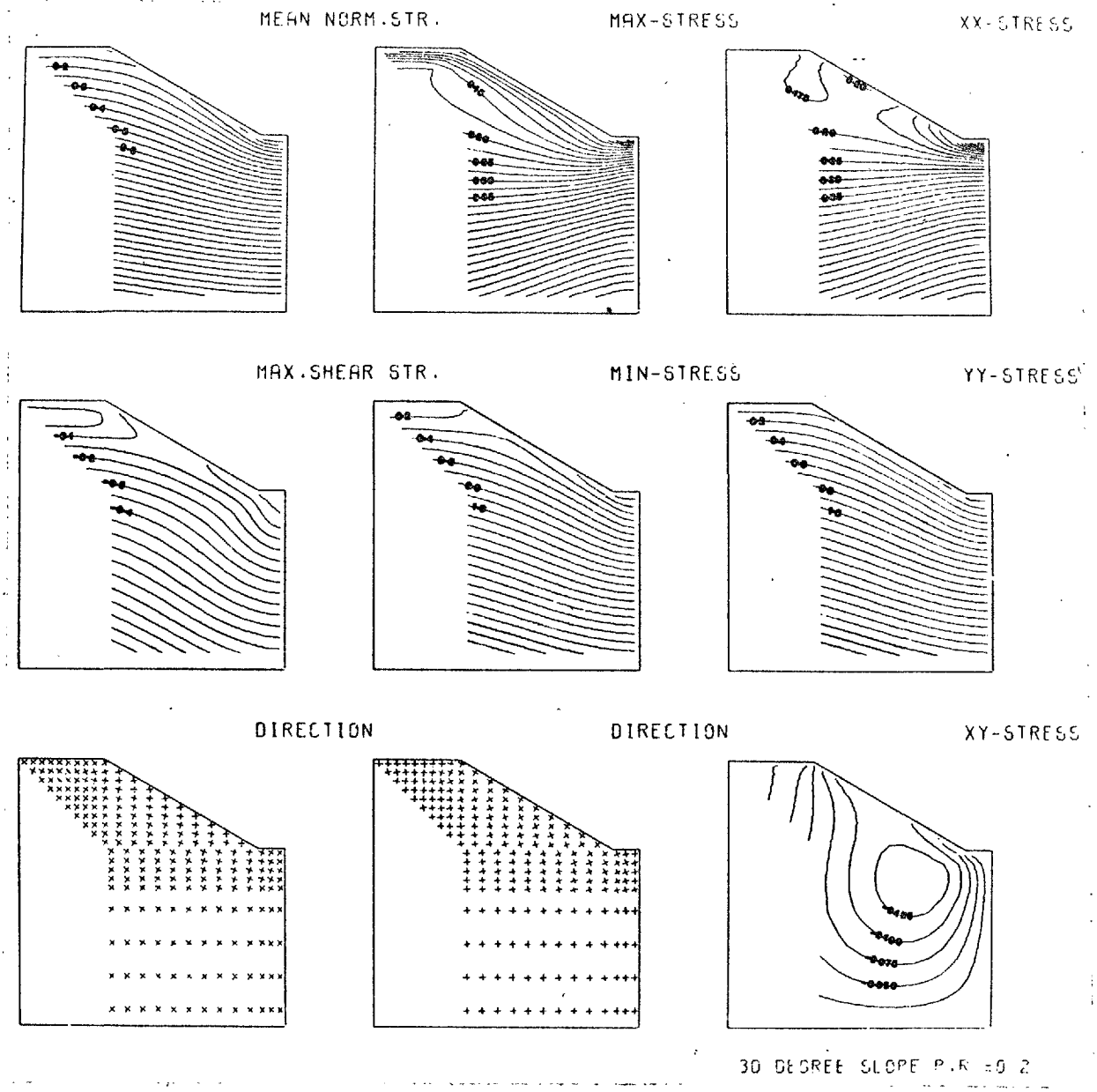
The influence of toe width was found to be minimal except in the region of the toe itself (Fig. 3.2). For the wider toe widths there is increased floor heave and corresponding tensile horizontal stresses. These would be manifested, in a real situation, by cracking in the base of the excavation.

It is noted that the stress concentrations in the toe region increase with toe width. This is in agreement with the more recent findings of Wang and Sun (Ref. 8).



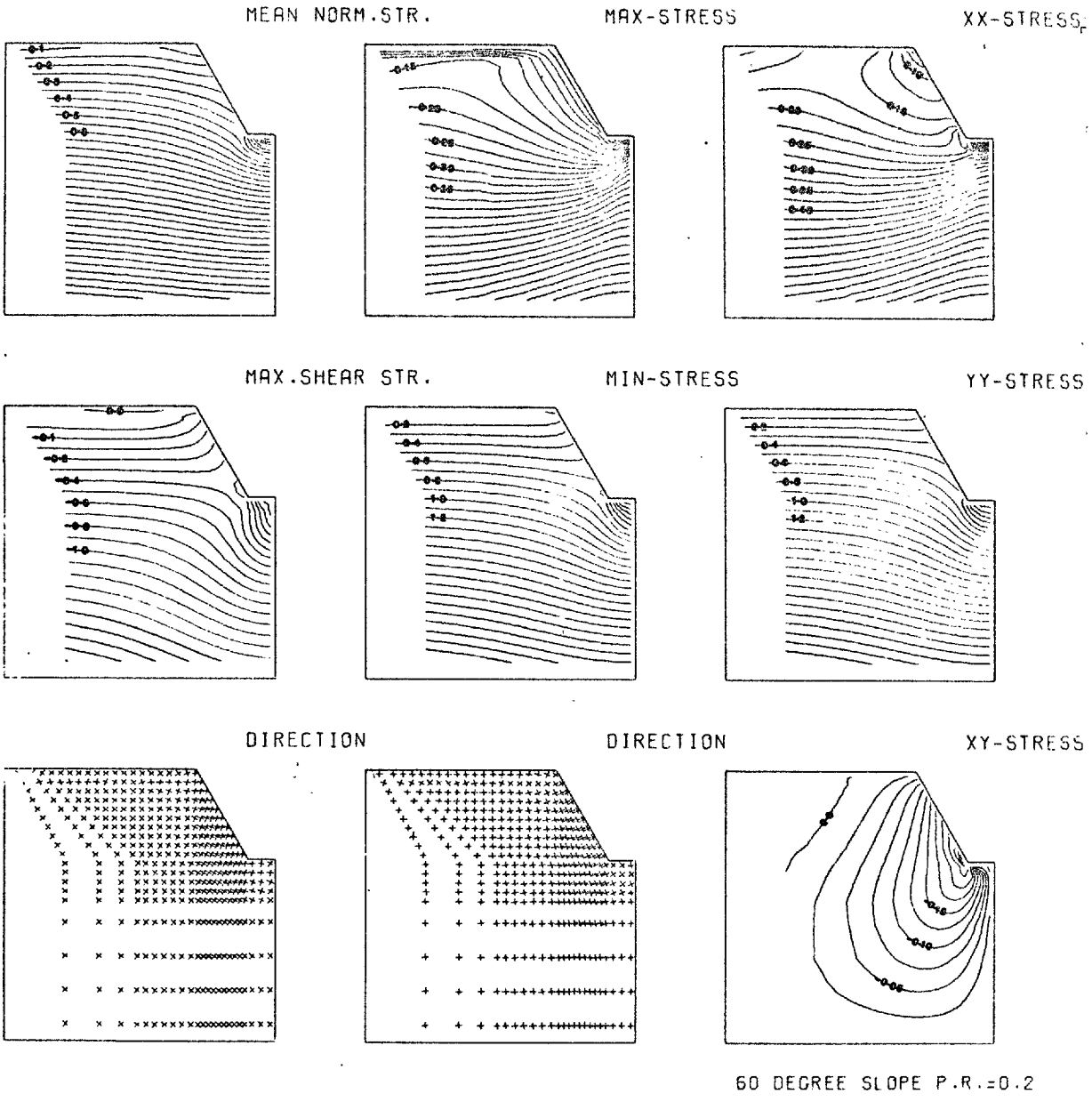
HORIZONTAL STRESSES (σ_{xx}) FOR VARIOUS TOE TO SLOPE HEIGHT RATIOS

FIGURE 3.4



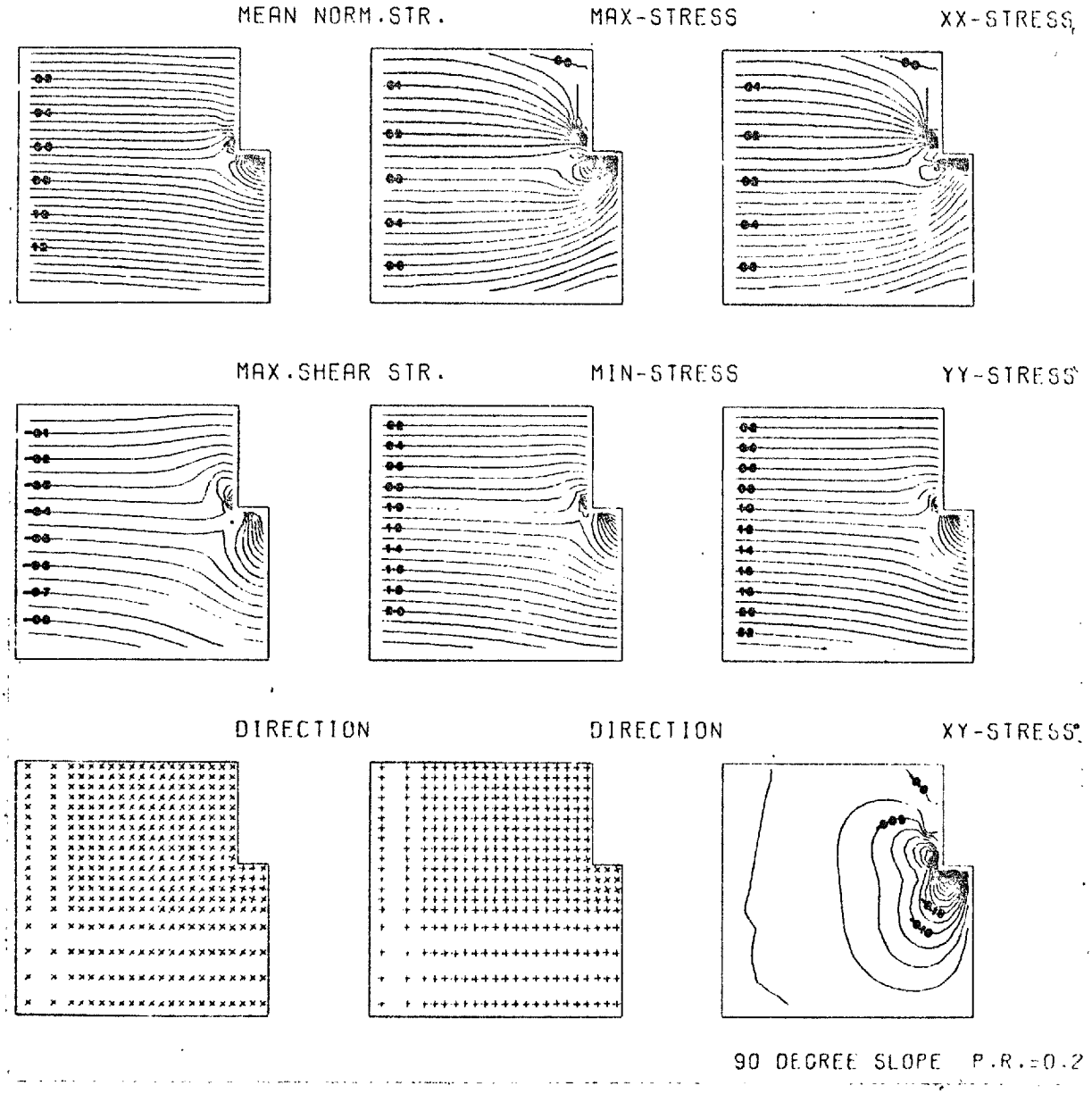
30° SLOPE

FIGURE 3.5



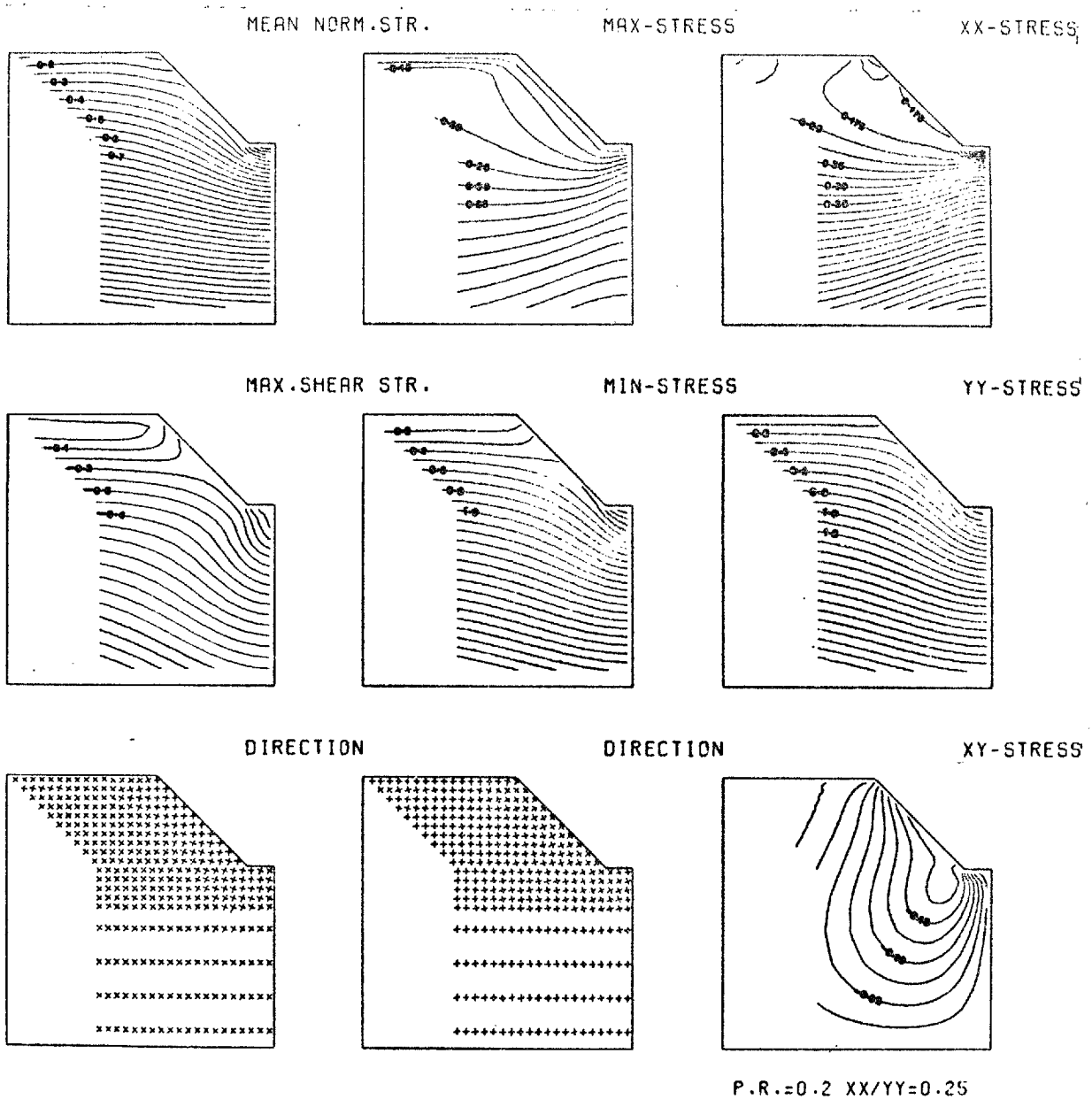
60° SLOPE

FIGURE 3.6



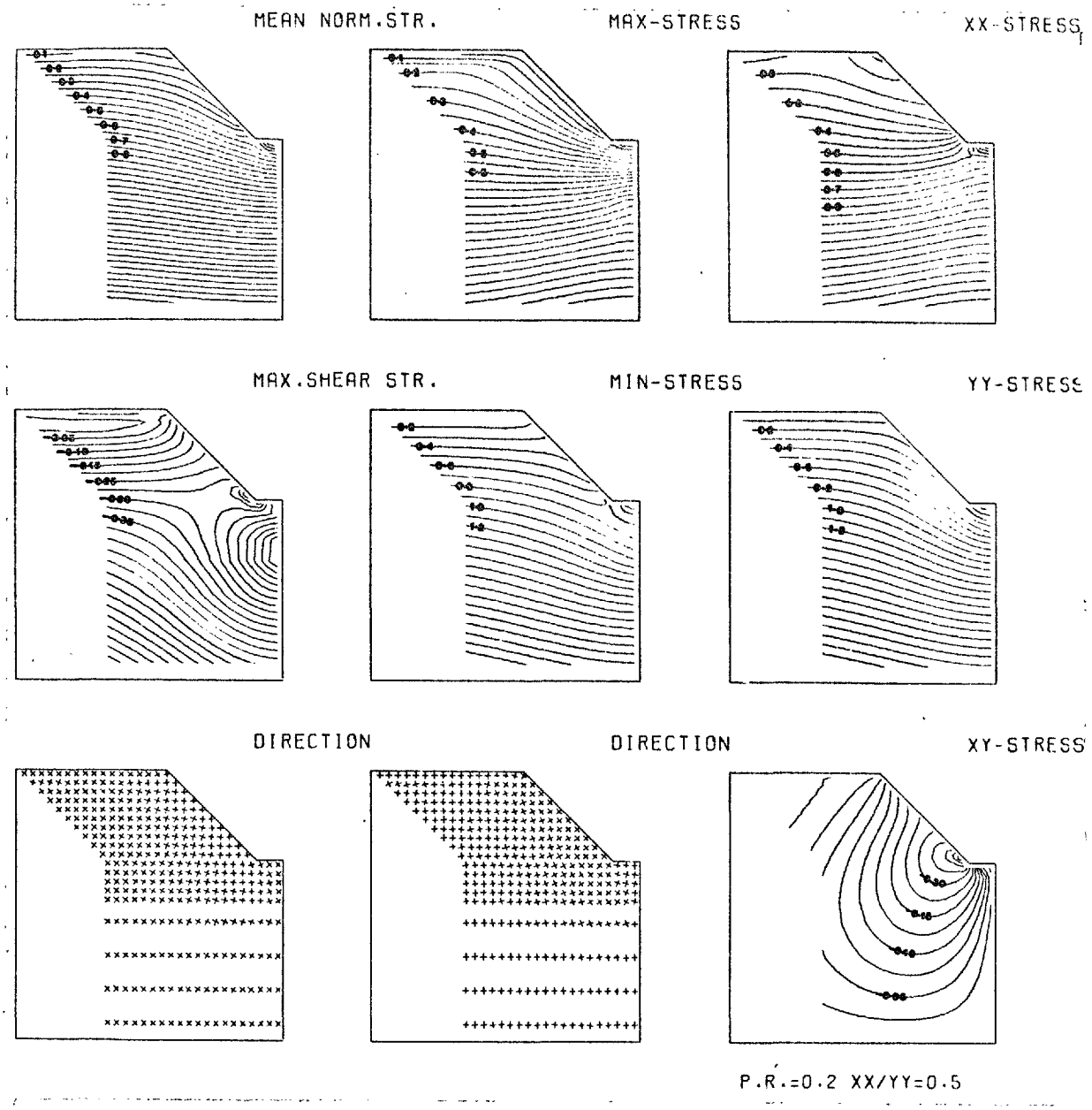
90° SLOPE

FIGURE 3.7



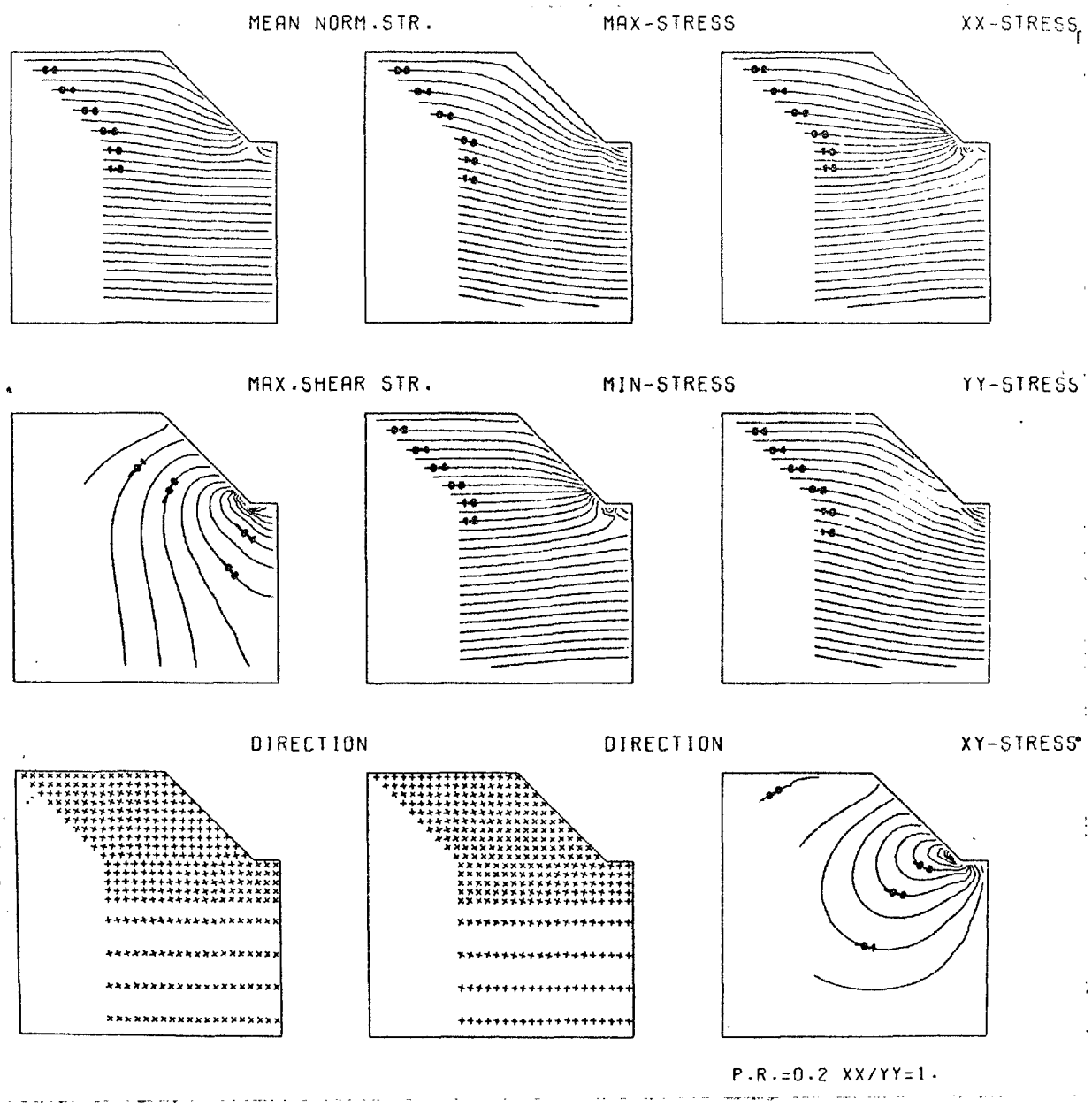
45° SLOPE $\sigma_{xx} : \sigma_{yy} :: 1. : 4.$

FIGURE 3.8



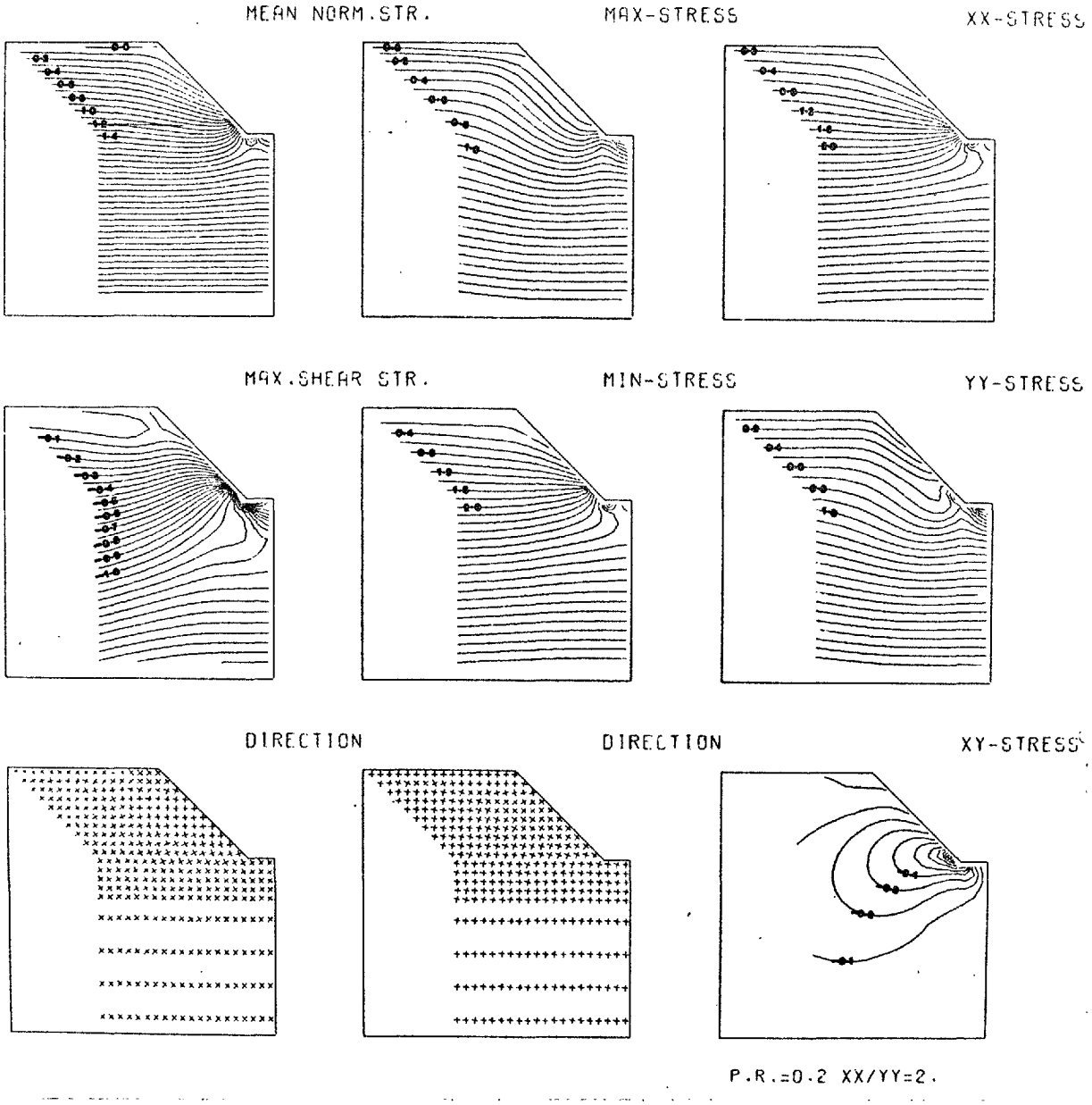
45° SLOPE $\sigma_{xx} : \sigma_{yy} :: 1. : 2.$

FIGURE 3.9



45° SLOPE $\sigma_{xx} : \sigma_{yy}$ :: 1. : 1.

FIGURE 3.10



45° SLOPE $\sigma_{xx} : \sigma_{yy} :: 2. : 1.$

FIGURE 3.11

3.7.2 Influence of Slope Angle

A number of general observations can be made on the results of analysis in which the slope angle was varied.

(a) Horizontal stresses in the slope tend to decrease as the slope angle increases. This is apparently due to a buttressing effect that becomes increasingly important as the slope flattens.

(b) Vertical stresses in the main body of the slope increase with an increase in slope angle to an upper limit for the case of a vertical cut. For the latter case there is little modification to the pre-excavation stresses except in the toe region.

(c) There is a considerable increase in the shear stresses, in the toe region, with the slope angle.

(d) The magnitudes of the principal stresses are similar for different slope angles, except in the toe region. The orientations are strongly influenced by the slope angle, as the principal stress directions must correspond to zero stress normal to the free surface.

(e) The magnitude of the maximum shear stresses increases with slope angle, particularly in the toe region.

Wang and Sun (Ref. 8) deduced relationships between the slope angle and the stresses after excavation. Although the author generated sufficient data to have done likewise it was felt at the time that such results would be dependent upon the chosen mesh size, particularly in the toe region. In addition it neither did nor does appear that such quantitative results are of any direct use in estimating the stability of rock slopes.

3.7.3 Influence of Initial Stresses

In view of the publication of results for vertical slopes subject to various initial stresses (Ref. 7), only the case of a 45° slope was studied. This also represents a more typical condition in the field of open pit mining.

Firstly, it should be noted that the minor principal stresses are vertical for the low residual stress conditions and horizontal for the high. (The sign convention is tensile stresses positive, but the stresses are normalised by dividing by the virgin vertical stress at full depth.) For the case K = 1, the principal stress direction is originally indeterminate.

The presence of high horizontal stresses prior to excavation results in concentrations in the toe region. The most significant increase is probably in the maximum shear stresses, though the importance of this is somewhat offset by an increase in the corresponding mean normal stresses.

A very interesting feature of this analysis is the presence of a tensile zone for the case of high residual stresses. This feature is extremely slope dependent, due to the buttressing effect in flatter slopes, and is therefore considerably more marked for the vertical slopes studied by Duncan and Goodman (Ref. 7). Based on this observation it seems reasonable to suggest that tension cracks at the crest of a pit are unlikely to be due to 'tension zones' unless the slope is either near vertical, or subject to very high initial stresses.

For the condition K = 1 an additional case with a Poisson's ratio of 0·475 was studied. The influence of this parameter was found to be minimal, as expected. The lesson that can be learnt from such studies is that considerable attention should be devoted to determining the initial state of stress rather than the elastic properties of the solid.

3.8 STABILITY ANALYSES FROM STRESS DISTRIBUTIONS

From the stress analyses discussed above, it is clear that the stress concentrations in the region of an open pit will not cause the failure of competent rock. In the context of Soil Mechanics, however, analysis may be conducted in terms of the shear strength of unruptured material.

Brown & King (Ref. 19) produced stress distributions for embankments and predicted failure surfaces by working backwards from specific exit points, calculating the most critical direction for slip at each sample point. Calculation of the average cohesion required to prevent sliding along this surface provided a stability indicator.

Wang and Sun (Ref. 20) used stress distributions to calculate the stresses on predefined circular surfaces. They claimed that the method was 'a much more nearly exact solution than any method of slices because the elastic stress analysis by the finite element method is used in the analysis'. Although this technique may be easier to use for more complex geometries and non-homogeneous materials, the author is of the opinion that this statement is meaningless. If the main body is elastic then the entire slip surface cannot yield plastically without influencing the original stress distribution.

The above approaches may be applied in rock slope design if the rock may be considered as a cohesionless soil. However, attention will be directed towards slopes with systems of parallel discontinuities since these pose a more truly rock mechanics problem.

In his discussion on displacement and strain, Bray (Ref. 21) considers four cases for the analysis of strain of a rock element traversed by parallel joints. These cases are:-

(a) Where the displacement due to slip is so large that elastic components of strain may be ignored, and

the concepts of finite strain must be employed.

(b) Where displacement due to slip is large compared with the elastic component, but the strain is infinitesimal.

(c) Where the displacement due to slip is of the same order of magnitude as the elastic displacements.

(d) Where no slip occurs on any of the joint planes and the strain is purely elastic.

If only case (d) is considered, then the elastic stress distributions will be valid. If, however, an analysis shows that joint slip would occur under the existing stresses, then the distribution is no longer valid. Resort must then be made to some other technique or the simulation of inelastic behaviour. Calculations based on ignoring this 'no-slip' criterion will be discussed in the knowledge that they are only valid within certain limits. Note should be taken that the results of all such analyses are only as good as the numerical approximation, and in this case, will be mesh dependent.

3.9 THE STRESS ON A SINGLE DISCONTINUITY THROUGH THE SLOPE TOE

The simple model, described in Section 1.3.1, of a single discontinuity dipping into an excavation may be re-studied using the elastic stress distributions obtained.

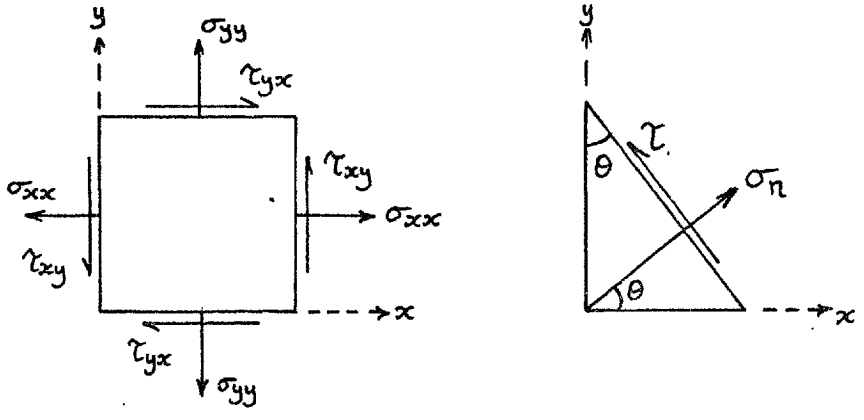


Figure 3.12

Following the sign convention of Figure 3.12 the shear stresses (τ) and normal stresses (σ_n) may be given by the following expressions:-

$$\sigma_n = \sigma_{xx} \cos^2\theta + 2.\tau_{xy} \sin\theta \cos\theta + \sigma_{yy} \sin^2\theta$$

$$\tau = (\sigma_{yy} - \sigma_{xx}) \sin\theta \cos\theta + \tau_{xy} (\cos^2\theta - \sin^2\theta) \qquad 3(4)$$

where θ is the angle, measured clockwise, between the X axis and the normal to the plane.

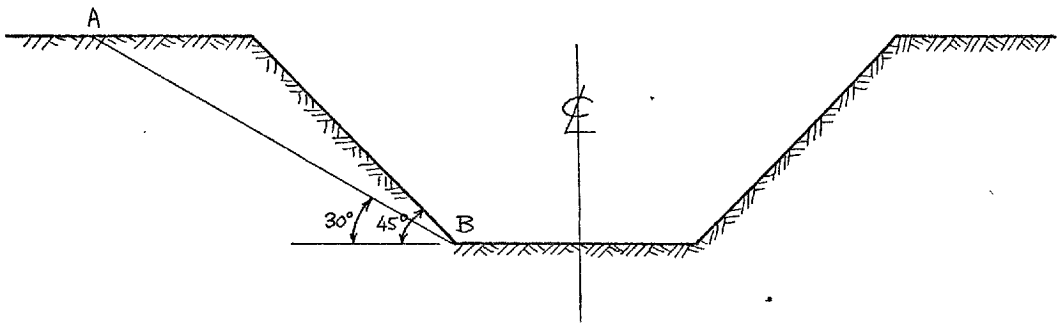
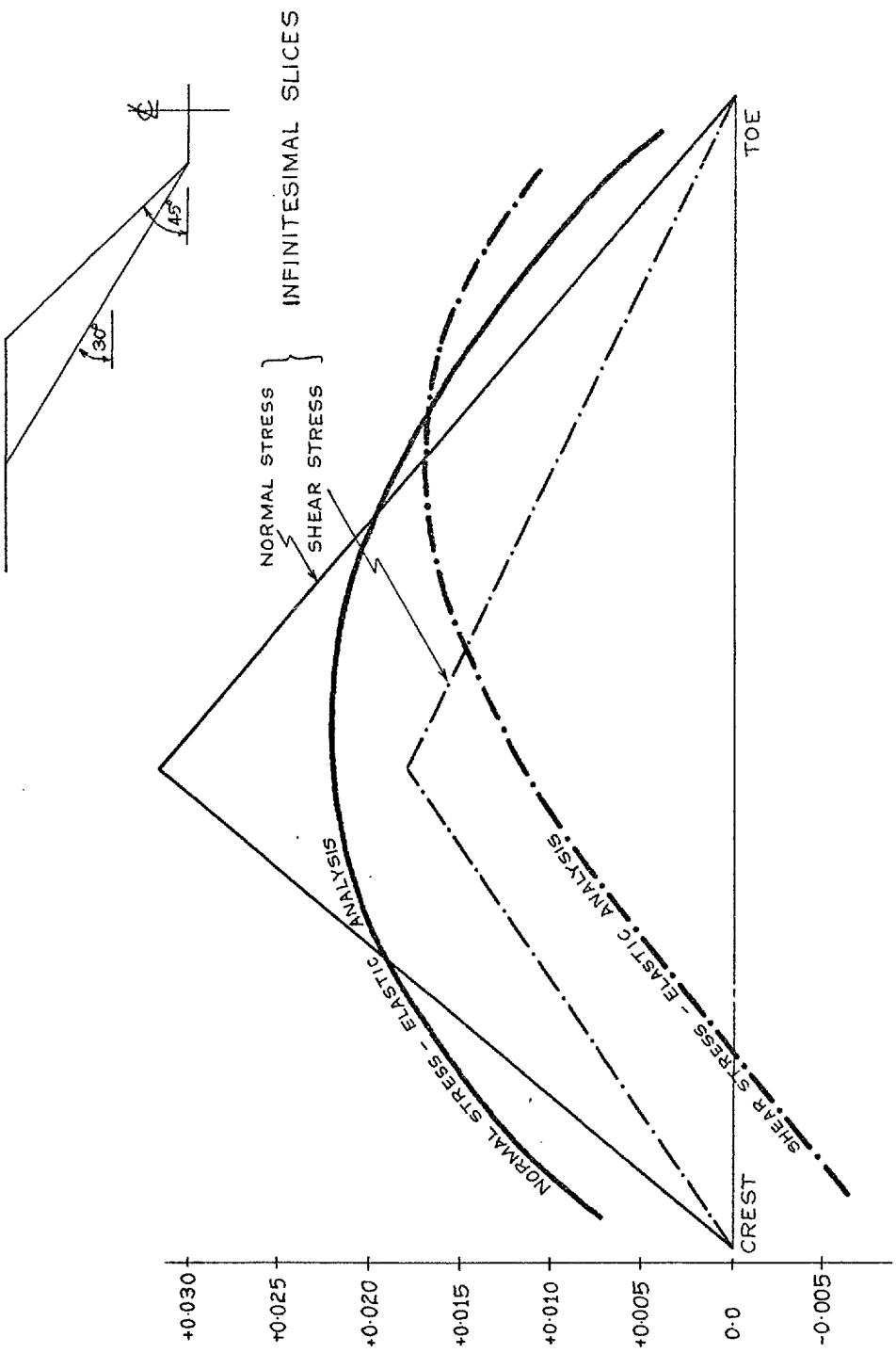


Figure 3.13

Working from the stress distribution given in Fig. 3.8 for a 45° slope, the shear and normal stresses on the surface AB (Fig. 3.13) may be calculated using equations 3(4). As there is no merit in rescaling the results, the non-dimensional presentation is retained in Figure 3.14.

The results show that the stress distribution on the surface is far from uniform and also dissimilar to that deduced by an infinite number of slices method. (i.e. assuming the stress is dependent upon the vertical height of material above the point of consideration.) The most significant feature is the occurrence of very low normal stresses at the toe region, where the shear stresses are relatively high.



STRESS DISTRIBUTION ON PLANE DIPPING AT 30° INTO AN EXCAVATION WITH 45° SLOPE ANGLE

FIGURE 3.14

It is worth noting at this point that whatever stress distribution on the surface is assumed, equilibrium cannot be violated. The sum of all the shear and normal forces on the surface must be exactly equal to the respective resolved components of the weight of the material above. This means that, if a linear failure criterion is used, limit equilibrium analyses based on plane slip surfaces must give the same answer irrespective of the assumed stress distribution in the slope. This observation does not apply to curved failure surfaces, since under these circumstances there may be a considerable variation of stresses on the surface without violating equilibrium considerations.

3.10 THE UBIQUITOUS JOINT ANALYSIS

If a rock mass is traversed by a large number of parallel joints it may be assumed, for the purpose of computation, that such discontinuities exist at all points - i.e. they are ubiquitous. Duncan and Goodman (Ref. 7) applied this concept to the analysis of a vertical slope by consideration of the three dimensional state of stress, which they calculated from Plane Strain analysis. The stresses on ubiquitous joint systems with specified orientations with respect to the slope were determined and used to calculate whether slip or tensile fracture was expected for prescribed joint properties. A similar procedure was adopted by the author, although only the case of joints striking normal to the plane of the section was considered.

The stresses on the selected discontinuities may be transformed (Equation 3(4)) to determine the relevant shear (τ) and normal stresses (σ_n). If the strength of a joint is given by a Coulomb law (Fig. 3.5), then slip is expected if:

$$|\tau| > c - \sigma_n \tan\phi \qquad 3(5)$$

where c is the cohesion intercept and ϕ the angle of friction.

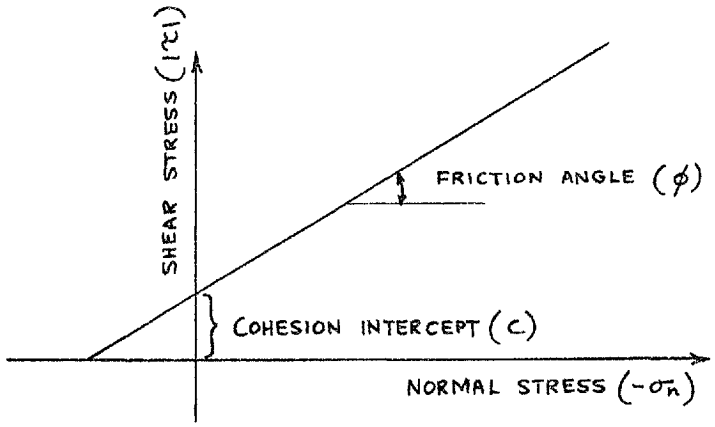


Figure 3.15

The results of such analysis may be presented in the form of maps of zones of potential slip for particular material properties. The method is, however, open to criticism since it is not valid if a zone of potential slip exists. Despite this, the method provides a lower bound for the acceptable material properties. A further criticism that joints do not behave according to a simple Coulomb law may be overcome by inclusion of a realistic stress dependent relationship between shear strength and normal stress.

For the purpose of presenting the results of a ubiquitous joint analysis it is useful to define a Shearing Ratio that may be calculated for each sample point.

$$S.R. = \frac{\tau_{av}}{|\tau|} > 1.0 \quad \text{for no slip} \qquad 3(6)$$

where τ_{av} is the available shear strength corresponding to the normal stress (σ_n).

The output from the elastic stress analyses discussed above had been stored on punched cards to facilitate further computations. Since the stresses were all in a dimensionless form it is convenient to rewrite the expression for the shearing ratio by using the dimensionless grouping ($c/\gamma H$) to replace the cohesion term:

$$S.R. = \frac{\left|\frac{c}{\gamma H} + \sigma_n \tan\phi\right|}{|\tau|} \qquad 3(6)$$

From this expression it is noted that the Shearing Ratio is directly proportional to the dimensionless cohesion group value for the slope. Since the model used (Fig. 3.3) was topologically equivalent to a regular mesh the results of this type of analysis may be printed out in matrix form. Typical output is given in Figure 3.16, which demonstrates the simple visual interpretation of results possible with this method of presentation.

The results given in Figure 3.16 are transformed to true slope geometry in Figure 3.17. This is, in fact, the case discussed in Section 3.9. It is clear that a proportion of this slope is overstressed in view of the material properties assumed. In practice gross failure is not likely to occur since the factor of safety deduced from a simple sliding wedge calculation is 1·66. From this simple example it is apparent that the presence of zones of potential slip means that stress redistribution must occur, and can occur, without total slope failure.

3.10.1 Variable Joint Orientation

It is interesting to study the importance of joint orientation by varying this parameter while maintaining all others unchanged. The lowest shear ratios determined for each selected orientation may be presented as a polar diagram (Fig. 3.18).

These diagrams display two high points associated with joints either normal or parallel to the slope face. The low points are obtained for low and steep angle joints, the latter representing toppling rather than sliding mode of slip. (Fig. 3.19)

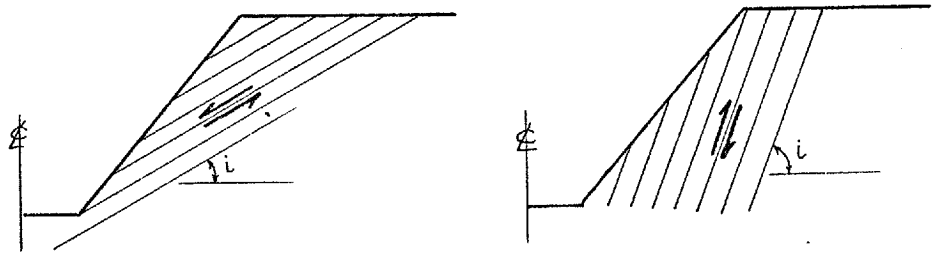


Figure 3.19

```
UBIQUITOUS JOINT ANALYSIS OF 45 DEGREE SLOPE

     STRESSES ON PLANES INCLINED AT    60.00TO THE VERTICAL

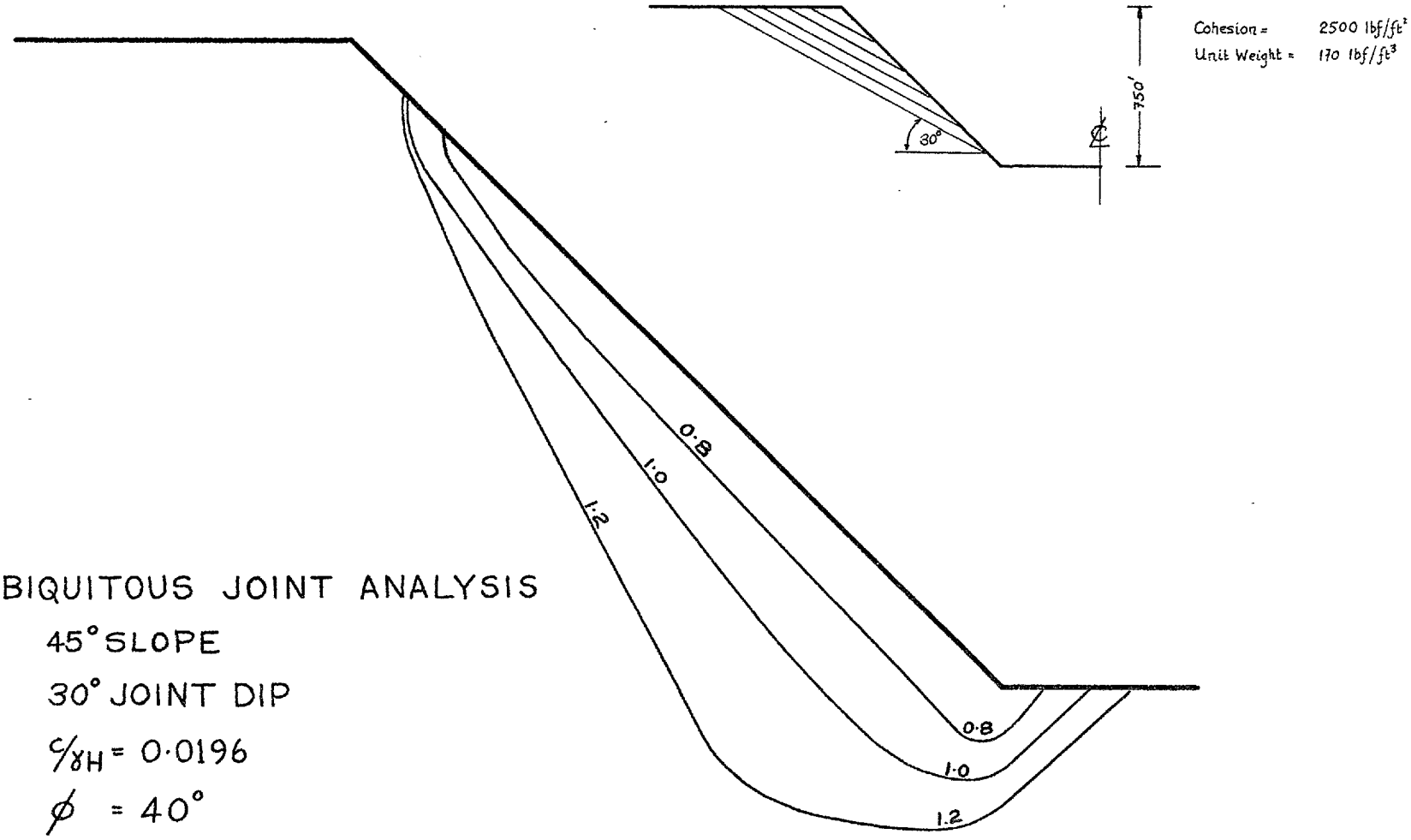
STRESSES NORMAL TO PLANE
*0.000*0.000*0.000   .031   .044   .062   .074   .081   .085   .087
*0.000*0.000*0.000   .035   .070   .091   .113   .130   .142   .151
*0.000*0.000*0.000   .048   .090   .122   .147   .170   .189   .204
*0.000*0.000*0.000   .055   .107   .147   .180   .207   .230   .250
*0.000*0.000*0.000   .059   .117   .167   .207   .240   .268   .292
*0.000*0.000*0.000   .062   .125   .180   .228   .267   .301   .330
*0.000*0.000*0.000   .064   .131   .191   .243   .289   .329   .363
*0.000*0.000*0.000   .065   .135   .199   .256   .307   .352   .391
*0.000*0.000*0.000   .066   .139   .206   .266   .321   .370   .414
*0.000*0.000*0.000   .064   .144   .213   .276   .334   .387   .435
  .032   .027   .036   .085   .183   .253   .317   .375   .429   .478
  .160   .141   .145   .189   .260   .329   .390   .446   .498   .546
  .296   .271   .272   .303   .354   .412   .468   .521   .570   .617
  .430   .404   .401   .420   .457   .503   .552   .600   .647   .690
  .559   .533   .527   .538   .565   .601   .642   .685   .728   .768

SHEAR STRESSES ON PLANE
*0.000*0.000*0.000   .009  -.030  -.046  -.055  -.060  -.063  -.064
*0.000*0.000*0.000   .057   .033   .015   .003  -.004  -.010  -.014
*0.000*0.000*0.000   .081   .073   .062   .052   .045   .040   .035
*0.000*0.000*0.000   .097   .100   .098   .093   .089   .085   .081
*0.000*0.000*0.000   .108   .121   .127   .128   .127   .126   .124
*0.000*0.000*0.000   .114   .136   .150   .158   .162   .163   .163
*0.000*0.000*0.000   .118   .148   .169   .183   .192   .197   .199
*0.000*0.000*0.000   .119   .155   .183   .204   .218   .227   .232
*0.000*0.000*0.000   .117   .161   .195   .220   .239   .252   .261
*0.000*0.000*0.000   .112   .163   .203   .233   .256   .274   .287
  .036   .035   .051   .123   .186   .225   .256   .280   .299   .313
  .027   .056   .106   .170   .223   .260   .288   .311   .329   .343
  .048   .088   .140   .197   .247   .285   .315   .338   .356   .371
  .084   .123   .171   .221   .267   .306   .336   .360   .380   .395
  .126   .161   .203   .247   .289   .325   .356   .381   .401   .418

 C/(H*GAMMA) =    .1960E-01
ANGLE OF FRICTION ON JOINT =      40.0000
*0.000*0.000*0.000  4.781-1.909-1.572-1.488-1.455-1.444-1.450
*0.000*0.000*0.000   .863 2.344 6.60133.271*8.629*3.500*0.250
*0.000*0.000*0.000   .740 1.307 1.983 2.739 3.569 4.473 5.440
*0.000*0.000*0.000   .675 1.086 1.460 1.827 2.172 2.504 2.826
*0.000*0.000*0.000   .642  .975 1.253 1.503 1.733 1.944 2.141
*0.000*0.000*0.000   .626  .914 1.136 1.331 1.508 1.670 1.820
*0.000*0.000*0.000   .621  .878 1.064 1.223 1.368 1.502 1.627
*0.000*0.000*0.000   .626  .857 1.017 1.152 1.273 1.388 1.497
*0.000*0.000*0.000   .640  .850  .989 1.104 1.209 1.309 1.405
*0.000*0.000*0.000   .650  .860  .977 1.077 1.169 1.256 1.342
 1.302 1.195  .968   .736  .935 1.031 1.114 1.192 1.268 1.343
 5.676 2.475 1.340 1.045 1.069 1.138 1.202 1.265 1.328 1.391
 5.524 2.805 1.772 1.389 1.282 1.280 1.311 1.352 1.399 1.449
 4.535 2.914 2.083 1.682 1.508 1.446 1.436 1.452 1.480 1.515
 3.888 2.905 2.276 1.909 1.710 1.612 1.570 1.561 1.570 1.589
```

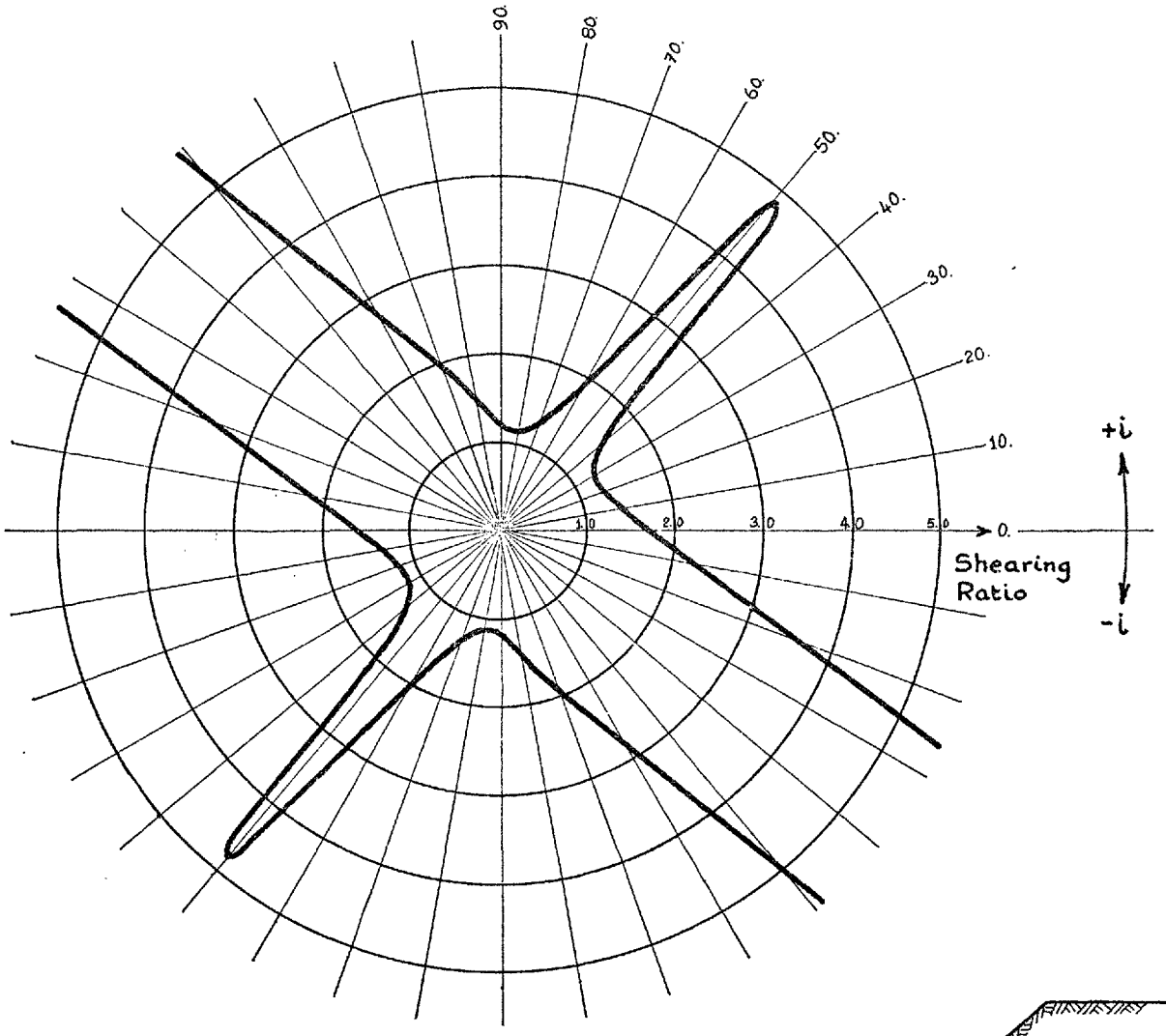
Computer Output . Ubiquitous Joint Analysis

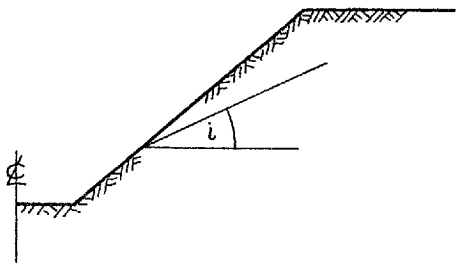
FIGURE 3.16



Transposed from Figure 3.16

FIGURE 3.17





POLAR DIAGRAM OF MINIMUM SHEARING RATIO

50° SLOPE

Slope Height = 300.ft

Unit Weight = 170. lbf/ft^3

Cohesion = 5000. lbf/ft^2

Angle of Friction = 40.°

FIGURE 3.18

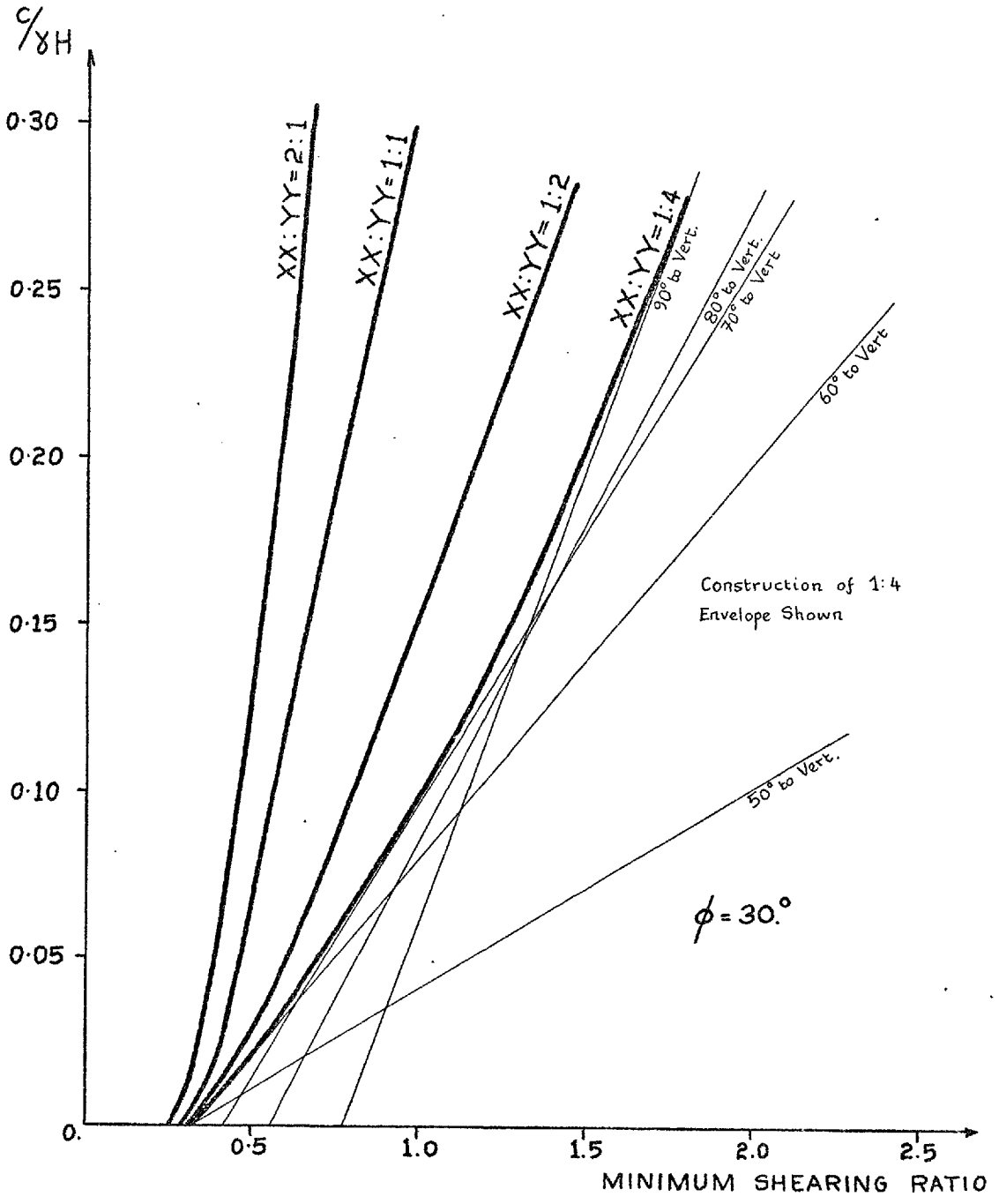
If the results are plotted on a 'cohesion term' versus minimum Shearing Ratio basis the influence of the former is apparent. Taking note only of situations where the joints dip into the excavation, an envelope for the lines due to different joint orientations may be drawn. This corresponds to a plot of the minimum possible value of Shearing Ratio against the dimensionless cohesion grouping, and, as such, constitutes a design criterion for the slope. It is, however, dependent on the accuracy of the original stress analysis and is therefore valueless in reality. Ignoring this possible criticism the method may still be used to give a qualitative assessment of the influence of various parameters.

3.10.2 Influence of Initial Stress

The calculations for 45° slopes with various initial stress conditions provided data with which to carry out ubiquitous joint studies. The resulting ~~maximum~~ minimum shearing ratio envelopes for an angle of friction of 30° are given in Figure 3.20. These curves indicate that, for the same material properties, high initial stresses will result in worse stress conditions in some parts of the slope. Perhaps greater redistribution of stress may be necessary but equilibrium still cannot be violated so, in the final analysis, gross failure is not initial stress dependent if these simple models hold true in reality. Consideration of non-linear failure criteria and progressive failure will lead to a different conclusion.

3.10.3 General Design Curves

If the ~~maximum~~ minimum Shearing Ratio envelopes are plotted for a number of possible slope angles then the value of the cohesion grouping necessary to ensure no slip within the slope can be plotted against slope angle. (Fig. 3.21). This constitutes a general design curve that may be tested against a real situation. Figure 3.22 superimposes results obtained, using this design criterion, on observed slope height/slope angle data gathered from the Atalaya open pit in Spain (Ref. 22). As expected, the no-slip design criterion is extremely conservative.



MINIMUM SHEARING RATIO v 'COHESION GROUP' ENVELOPES FOR VARIOUS INITIAL STRESS RATIOS

FIGURE 3.20

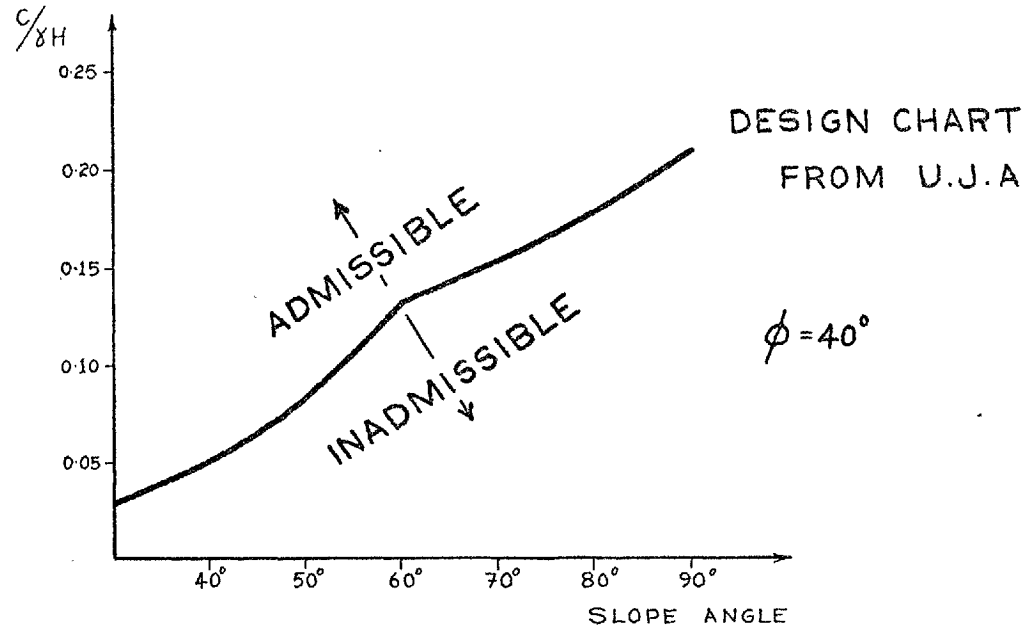


FIGURE 3.21

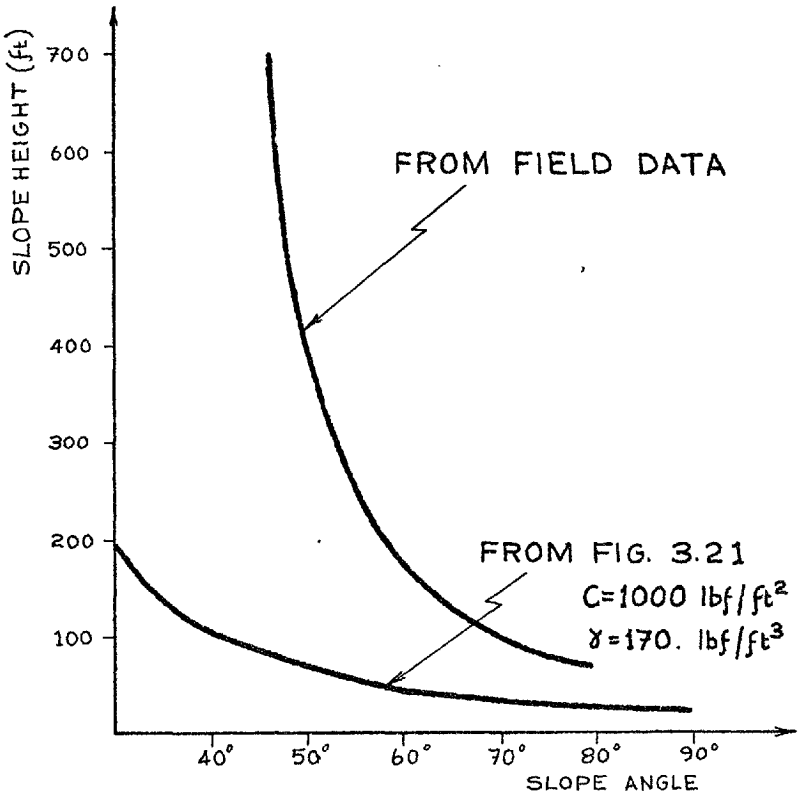


FIGURE 3.22

It is noted that the discontinuity in Figure 3.21 is due to a shift in location of the locally overstressed region. For high angle slopes the minimum shearing ratio occurs at the toe, whilst for lower angle slopes it may occur at mid-height.

3.11 CONCLUSIONS

Stress analyses were conducted assuming rock slopes to behave as homogeneous, isotropic, linearly elastic, time independent solids. The results of these analyses were used to estimate the stability of rock slopes containing parallel joint systems, making the assumption that these have no influence on the stress distribution if no slip or separation occurs. The following conclusions are drawn from this study.

(1) Stress concentrations in the region of open pit excavations are generally low, although more pronounced for steep slopes and high initial stress conditions. Reports by other workers (Refs. 8, 23) show that detailed slope geometry has little influence on the stress distribution in the main body of the slope.

(2) The initial stress conditions can be deduced from the Poisson's Ratio of the material of the slope by assuming boundary restraints only. In practice it is vital to measure the in situ stresses. If the original horizontal stresses are high then the influence of Poisson's Ratio is minimal.

(3) Tension zones around excavations may occur both at the toe and the crest of a slope. The former are more pronounced for wide toe widths and the latter for steeper slopes and high initial stresses.

(4) For plane failure surfaces, the overall factor of safety of a slope cannot be influenced by the stress distribution since equilibrium must be satisfied.

(Ignoring Peak/Residual behaviour for joints.)

(5) The stresses within a slope may be transformed to determine the shear and normal stresses on a ubiquitous joint set. The Shearing Ratio, defined as the ratio of available shear strength to actual shear stress, provides a quantitative assessment of slope stability.

(6) Adoption of design based on the ubiquitous joint analysis results in extreme conservatism since only a 'no-slip' condition can be accepted. In a real situation stress redistribution must occur for locally overstressed regions.

(1) Sturgul, J.R. & Scheidegger, A.E. Tectonic Stresses in the Vicinity of a Wall. Rock Mechanics and Eng. Geol. Vol. V/2-3.

(2) Dibiagio, E.L. Stresses and Displacements around an Unbraced Rectangular Excavation in an Elastic Medium. Ph.D. Thesis, University of Illinois, 1966.

(3) Tamuly Phukan, A.L. Non-Linear Deformation of Rock. Ph.D. Thesis, London, 1968.

(4) Cundall, P.A. The Measurement and Analysis of Accelerations in Rock Slopes. Ph.D. Thesis, London, 1971.

(5) Yu, Y.S., Gyenge, M. & Coates, D.F. Comparison of Stress and Displacement in a Gravity-Loaded 60 Degree Slope by Photoelasticity and Finite Element Analysis. Canada Dept. Energy, Mines and Resources, Mines Branch. Rep. MR68/24-ID.

(6) Tamuly Phukan, A.L., Lo, K.Y. & La Rochelle, P. Stresses and Deformations of Vertical Slopes in Elasto-Plastic Rocks. 11th Symp. Rock Mechanics 1969, Berkeley, California.

(7) Duncan, J.M. & Goodman, R.E. Finite Element Analysis of Slopes in Jointed Rock. Report to the U.S. Army Corps of Engineers, Vicksburg, Miss. Contract No. DACW39-67-C-0091 by Geotechnical Engineering, University of California, Berkeley.

(8) Wang, F-D. & Sun, M-C. A Systematic Analysis of Pit Slope Structures by the Stiffness Matrix Method. U.S.B.M. R.I. 7343.

(9) Stacey, T.R. The Stresses Surrounding Open-Pit Mine Slopes. Open Pit Planning Symposium. Johannesburg, 1970.

(10) Wilson, E.L. A Digital Computer Program for the Finite Element Analysis of Solids with non-linear Material Properties. Department of Civil Engineering, University of California, Berkeley, 1965.

(11) Cundall, P.A. Personal Communication 1969.

(12) Ishihara, K. Discussion of 'Failure Around Excavated Slopes' A.S.C.E. Vol. 96, SM6, November 1970.

(13) Duncan, J.M. & Dunlop, P. Reply to Discussion of 'Slopes in Stiff-Fissured Clays and Shales. A.S.C.E. Vol. 96, S.M.5. September 1970.

(14) Duncan, J.M. & Dunlop, P. Slopes in Stiff-Fissured Clays and Shales. A.S.C.E. S.M.2. March 1969.

(15) Bray, J.W. Personal Communication 1969.

(16) Hast, N. The State of Stress in the Upper Part of the Earth's Crust. Eng. Geol. 2(1) 1967.

(17) Pallister, G.F., Gay, N.C. & Cook, N.G.W. Measurement of the Virgin State of Stress in Rock at Depth. 2nd Congress I.S.R.M. Belgrade 1971. Paper 1.5.

(18) Li, B. Natural Stress Values obtained in Different Parts of the Fennoscandian Rock Masses. 2nd Congress I.S.R.M. Belgrade 1971. Paper 1.28.

(19) Brown, C.B. & King, I.P. Automatic Embankment Analysis: Equilibrium and Instability Conditions. Geotechnique Vol. 16, No. 3, 1966.

(20) Wang, F-D. & Sun, M-C. Slope Stability Analysis by the Finite Element Stress Analysis and Limiting Equilibrium Method. U.S.B.M. R.I. 7341.

(21) Bray, J.W. A Study of Jointed and Fractured Rock. Part II Rock Mechanics Eng. Geol. Vol. V/4 1967.

(22) Hoek, E. Approximate Design of Rock Slopes Utilizing Field Observations. Rock Mechanics Progress Report No. 2. July 1969. Imperial College, London (Restricted).

(23) Blake, W. Stresses and Displacement Surrounding an Open Pit in a Gravity-Loaded Rock. U.S.B.M. R.I. 7002.

CHAPTER

4

THE TWO DIMENSIONAL ANALYSIS OF JOINTED ROCK SLOPES

		Page
	Chapter Index	108
	Synopsis	109
4.1	Introduction	110
4.2	Continuum Approaches to Modelling Jointed Rock Masses	110
4.3	Modelling a Discontinuum	126
4.4	Properties and Simulation of Discontinuities in Rock Masses	127
4.5	Extension to More Complex Joint Behaviour	142
4.6	Conclusions	156
	References	157

SYNOPSIS

The elastic analyses discussed in the previous chapter are extended to take account of material anisotropy and inelastic behaviour. This includes no-tension analysis and progressive slip on a ubiquitous joint set.

The use of discrete joint elements to model discontinuities, after the method proposed by Goodman et al (Ref. 1), is discussed. The results of analyses of jointed rock slopes are presented.

Finally consideration is given to the general behaviour of discontinuities under load and to a method of simulation. A computer program which enables complex joint properties to be modelled by initial stress and strain methods is described.

4.1 INTRODUCTION

The methods of stress analysis based on the treatment of rock as a linearly elastic isotropic material have been discussed in the previous chapter. These did not appear to offer a satisfactory approach to the design of rock slopes. Methods of taking into account the existence of discontinuities, or planes of weakness, must therefore be considered. However, before attention is given to treatment including discrete discontinuities, it seems justifiable to consider situations where such planes are sufficiently close together to ascribe bulk properties to the rock mass.

4.2 CONTINUUM APPROACHES TO MODELLING JOINTED ROCK MASSES

Measurable characteristics of a discontinuity in rock are its shear strength and its resistance to normal and shear deformation. The latter properties have been defined in Section 2.5.2 as the normal and shear stiffnesses. For the present it will be assumed that force displacement laws for discontinuities are linear provided the strength is not exceeded.

A simple approach to jointed rock, possible when the discontinuities are closely spaced and in parallel sets, is to assume that the joints contribute only to the elastic deformability of the rock mass. The material is still elastic but is anisotropic, with the anisotropy controlled by the jointing. This approach was discussed at some length in Section 2.5 so it suffices to state that the elastic properties of the discontinuities and the solid are superimposed to determine a bulk deformability. An example of the use of this method is given in Chapter 7 in connection with an analysis of a physical model study.

Duncan and Goodman (Ref. 2) performed a series of analyses for a rectangular slope excavated in orthotropic material. They concluded that the stress conditions around the slope were not greatly different from the isotropic case. The displacements, however, were strongly influenced by the anisotropy.

It is concluded that the above approach is reasonable when discontinuities are parallel and closely spaced with respect to the scale of the excavation. The stress changes during excavation must, of course, be sufficiently small to justify the assumption that the joints deform linearly and that no slip occurs.

A second possible approach to jointed rock masses is to assume they behave in an elasto-plastic manner. The yield point is defined either by the shear strength of the discontinuities, or the rock mass as a whole if it is highly and randomly fractured. The latter type of material more closely corresponds to a soil than a jointed rock and has been widely studied in the context of soil mechanics.

Phukan and La Rochelle (Ref. 3) reported on a comparison of stresses and deformations around vertical slopes using a finite element method and a lumped parameter finite difference technique. Similar results for both methods showed a growth of a plastic zone in the toe region. They suggested that this might coalesce with a tension zone in the slope crest.

Duncan and Dunlop (Ref. 4) simulated elastic-perfectly plastic behaviour by reducing the elastic modulus in regions where yield was predicted. The authors recognised the importance of the loading history and performed the excavation in a series of increments. Baker et al used an elasto-plastic analysis to obtain a stress distribution which was studied to determine the most critical slip surface. The results compared favourably with those obtained by the Morgenstern-Price method although the predicted surfaces were different. Their approach is, of course, subject to an earlier criticism made in Section 3.8 in connection with the assumption that slip on the selected surface will not alter the stress distribution in the body.

Perloff et al (Refs. 5 and 6) reported on a study of the use of elasto-plastic analysis of underground excavations. Field studies showed no correlation between computer and measured results,

even in cases where instrumentation was installed well in advance of the excavation. Quite clearly the rock did not behave as a granular material and should have been treated as a true discontinuum, with attention being given to structural data.

The approaches referred to above consider rock either as an anisotropic elastic solid or a material exhibiting elasto-plastic behaviour and obeying a plastic yield criterion. No account is taken of the observed importance of slip upon pre-existing discontinuities or the inability of the rock mass to sustain tension. These conditions may both be simulated with relative ease when the inelastic and elastic components of displacements are of the same order of magnitude.

4.2.1 No-Tension Analysis of Rock Materials

The simplest approach to the analysis of materials unable to sustain tension is by direct iteration. This involves modification of the elastic properties of the portions in which tension occurs. The procedure has been described by Zienkiewicz et al (Ref. 7) as follows:

(a) Analyse the problem as an isotropic elastic one and check where tensile principal stresses are developed.

(b) Where principal tensions are shown assume the material to be highly anisotropic with zero (or very small) elastic modulus in the direction indicated by the tension.

(c) Re-analyse the original problem on the basis of new, now anisotropic, properties and repeat (b) and (c) until a no-tension state is reached.

Unfortunately this process is slow from the computational standpoint. The stiffness matrix of the model must be reformed each iteration if the finite element method is used. Additionally

it has been observed by Zienkiewicz et al (Ref. 7) that convergence cannot be guaranteed. These authors therefore devised an alternative procedure which may usefully be described in terms of the stress transfer process they presented:

(a) Analyse the problem as an elastic one.

(b) At the end of (a) tensile stresses may have been developed. Since the material cannot sustain tension these are eliminated without permitting any point in the structure to displace. In order to maintain equilibrium 'restraining' forces have to be applied to the structure.

(c) The restraining forces do not exist in fact so their influence has to be removed by superposition of equal but opposite nodal forces. The structure is now re-analysed for the effect of such forces and the stresses computed are added to those pertaining at the end of (b) (when tensions have been eliminated).

(d) If at the end of (c) principal tensions are still in existence steps (b) and (c) are repeated until all tensile stresses are reduced to a negligible figure.

(e) Repeat the whole process for the next load increment.

This procedure may be accompanied by a variation in the elastic properties as for the direct iteration method, either every iteration or at selected intervals. The computer programming may be accomplished with relatively few modifications to standard linear elastic versions. In order to make full use of the economy of a constant stiffness matrix some adjustments to the equation solver must be made so that only a partial inversion is required for each new load condition. It was also found convenient

to store on tape the element properties necessary for evaluating the forces referred to in (b) and (c) above.

In the author's general two-dimensional program, listed in Appendix B, the rock may be ascribed a limited tensile strength that is set to zero once the rock is cracked (Figure 4.1). Also the program has been written so that a final analysis using anisotropic elastic properties may be performed when load perturbations have led to an irreducible area of tension. (Of course, elastic analysis may be performed by setting the tensile strength to an arbitrarily high value.)

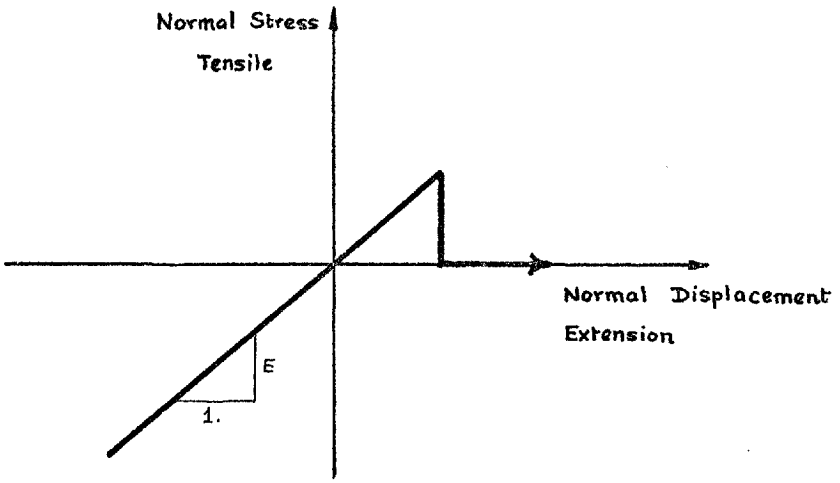


Figure 4.1

In order to test the computer program, and by way of illustration of its use, the small model given in Figure 4.2 was studied. The rigid inclusion in the centre of the model is subject to horizontal loading that results in a large area of tension. After ten cycles of readjustment the differences between the results of cycles were small and the zone of tension was considered to be effectively irreducible. The important influence of the cracking is shown in Figure 4.3, which illustrates the difference in horizontal displacements, at or near the free surface, for the elastic and no-tension situations.

In the author's opinion no-tension analysis is most applicable to slope analysis when used in conjunction with the discrete joints

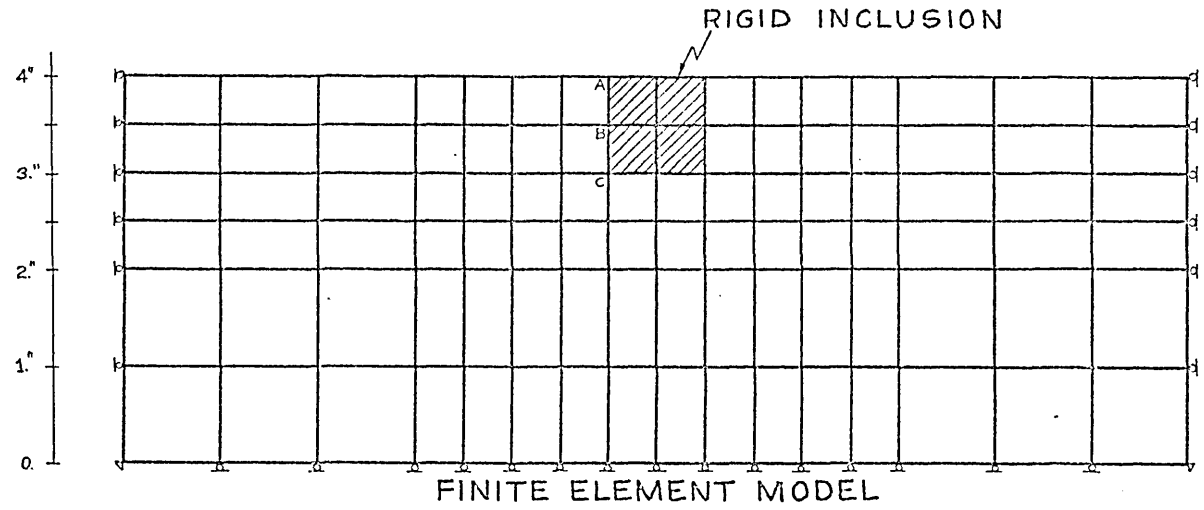
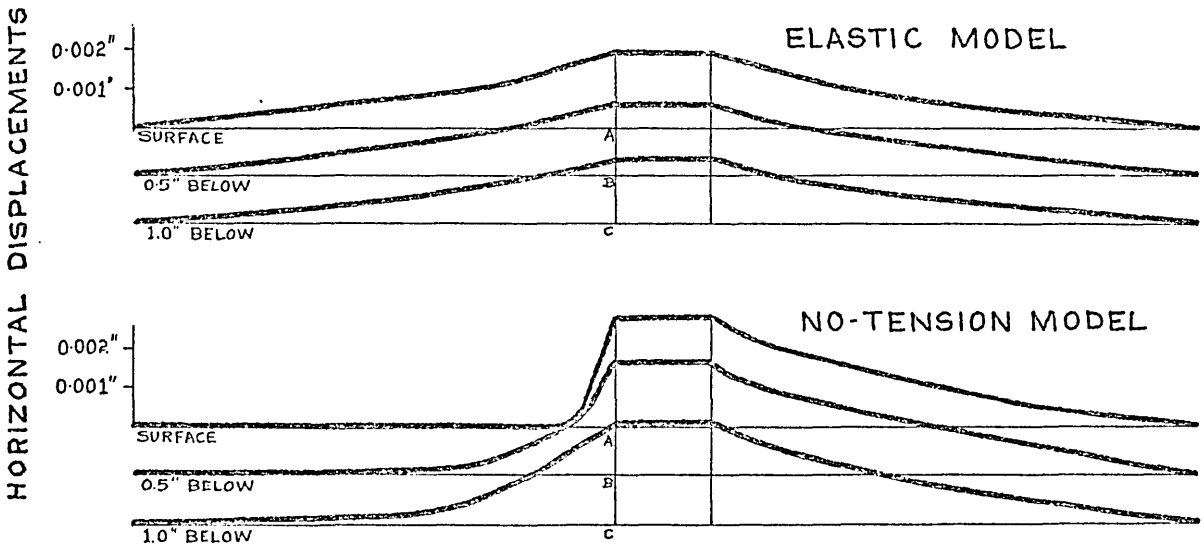


FIGURE 4.2



MODEL PARAMETERS

$E = 1500.\ lbf/in^2$

$\nu = 0.2$

$\gamma = 1.0\ lbf/in^3$

1.0 lbf at Nodes A, B, C

HORIZONTAL DISPLACEMENTS
ELASTIC AND NO-TENSION ANALYSES

FIGURE 4.3

that are discussed below. Tension cracking at the crest of the slope may be adequately catered for without including specially orientated joint elements in the model. In these circumstances a considerable saving on the total number of elements might be achieved.

4.2.2 Joint Controlled Plasticity

The ubiquitous joint analysis described in Chapter 3 referred to studies made on elastic solutions for stresses in rock slopes. It was stated that these solutions were only valid if the assumed failure criterion was not violated in any part of the slope. The logical extension of this method is to consider elasto-plastic behaviour which permits slip to occur, parallel to the ubiquitous joint set, in the overstressed regions.

The program written by the author assumes that the rock mass behaves elastically unless overstressed. The latter condition is defined either by a no-tension, or limited tension, criterion or a Coulomb law for the joint set. Depending on which criterion is violated the program will simulate either tensile cracking or slip in the defined direction.

The overall failure criterion for the solid material is defined by the following parameters:

(1) Tensile Strength.
(2) Direction of the Ubiquitous Joint Set.
(3) Cohesion of the Joints.
(4) Friction Angle for the Joints.

Although the tension criterion takes precedence over the slip criterion it may be overwritten by ascribing the material an arbitrarily high tensile strength.

To put the above into practice it is necessary to generalize the stress transfer process discussed above. The latter is clearly

none other than the initial stress method for modelling non-linear material behaviour, as discussed in Chapter 2. There is, in fact, a difference as the initial stress method has been used where there is a given relationship defining the state of stress at any computed strain. In the author's program there is simply a stress transfer from the overstressed regions to the surrounding material (Fig. 4.4).

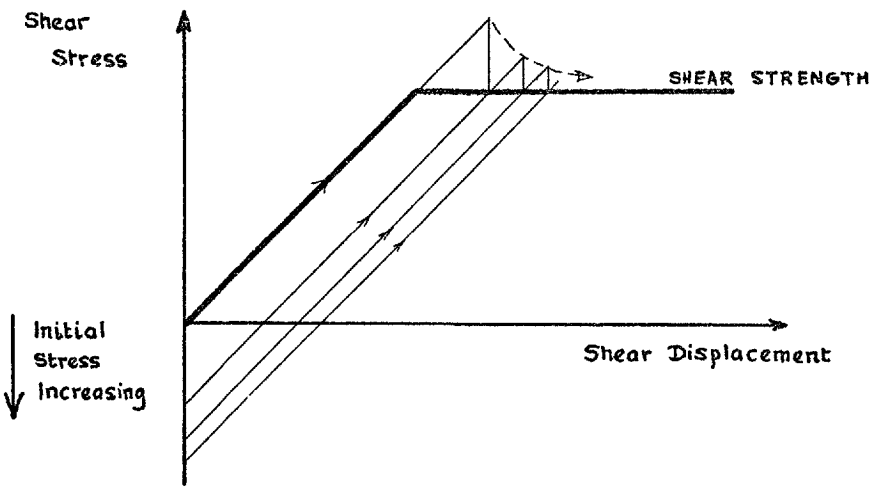


Figure 4.4

4.2.3 Ubiquitous Joint Slip by the Initial Stress Method

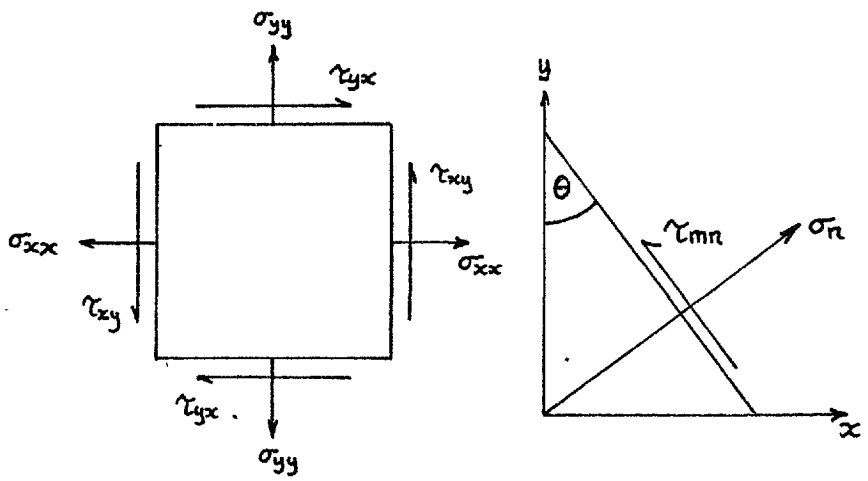


Figure 4.5

The shear and normal stresses on any plane, as shown in Figure 4.5 may be determined from the xy stresses by the following transformation equations (3.9):

$$\sigma_n = \tfrac{1}{2}\left(\sigma_{xx}+\sigma_{yy}\right) + \tfrac{1}{2}\left(\sigma_{xx}-\sigma_{yy}\right)\cos 2\theta + \tau_{xy}\sin 2\theta$$

$$\tau_{mn} = \left(\sigma_{yy}-\sigma_{xx}\right)\sin\theta\cos\theta + \left(\cos^2\theta - \sin^2\theta\right)\tau_{xy} \qquad 4(5)$$

If the permissible shear stress (τ_p) at a particular normal stress (σ_n) is given by a Coulomb strength criterion:

$$\left|\tau_p\right| = c - \sigma_n \tan\phi \qquad 4(6)$$

where c and ϕ are the joint cohesion and friction angle respectively. The shear stress to be shed is therefore:

$$\tau' = \left|\tau_{mn}\right| - \left|\tau_p\right| \qquad 4(7)$$

Since all the computations in the program are done in terms of stresses in the global co-ordinate system, it is necessary to transform this excess shear stress to give the initial stresses for the next increment. This transformation yields the following expressions:

$$\sigma_{xx}' = -2\tau'\sin\theta\cos\theta$$

$$\sigma_{yy}' = +2\tau'\sin\theta\cos\theta \qquad 4(8)$$

$$\tau_{xy}' = \tau'\left(\cos^2\theta - \sin^2\theta\right)$$

Substituting these expressions back into equations 4(5) shows that there is no change in the normal stress and that the required decrease in the shear stress is achieved.

Using the algorithm given in Figure 4.6 in the form of a flow chart, the computer simulation of slip on a ubiquitous joint set may be achieved. Clearly a number of possible variations may be adopted. The most obvious is to start with anisotropic material properties, as described in Section 4.2, which could be modified according to the amount of slip that has occurred within particular elements. More complex stress strain relationships for the pre- and post-failure material could be selected. The author did not explore either of the above possibilities. In any case such modifications may be made with relatively few computer program adjustments.

4.2.4 Application of the Ubiquitous Joint Slip Program

The model shown in Figure 4.2 is used to illustrate the use of this approach to jointed materials. Assuming a vertical joint set, Figure 4.7 shows the vertical displacements due to vertical loading applied to the rigid inclusion. The influence of slip on the vertical displacements at the surface is quite clear. Accompanying this inelastic behaviour there is a general transfer of vertical stress down into the model. The phenomenon was noted to be less marked for higher Poisson ratios. A similar observation would be made if the joints were dilatant during shear, as both types of behaviour result in horizontal stress increases when under confinement. However, it is important not to confuse dilantancy and Poisson's ratio effects as they are completely different phenomena.

The computer program may also be used for slope behaviour studies. Figure 4.8 shows the results of the analysis of a 45° slope with joints dipping at 20° into the excavation. The initial slip zone corresponded closely with the results from the study discussed in Chapter 3, although the finite element mesh (Figure 4.8) was considerably more coarse. Subsequent iterations resulted in displacements into the excavation and a lowering of the crest, but not a very extensive growth of the slip zone.

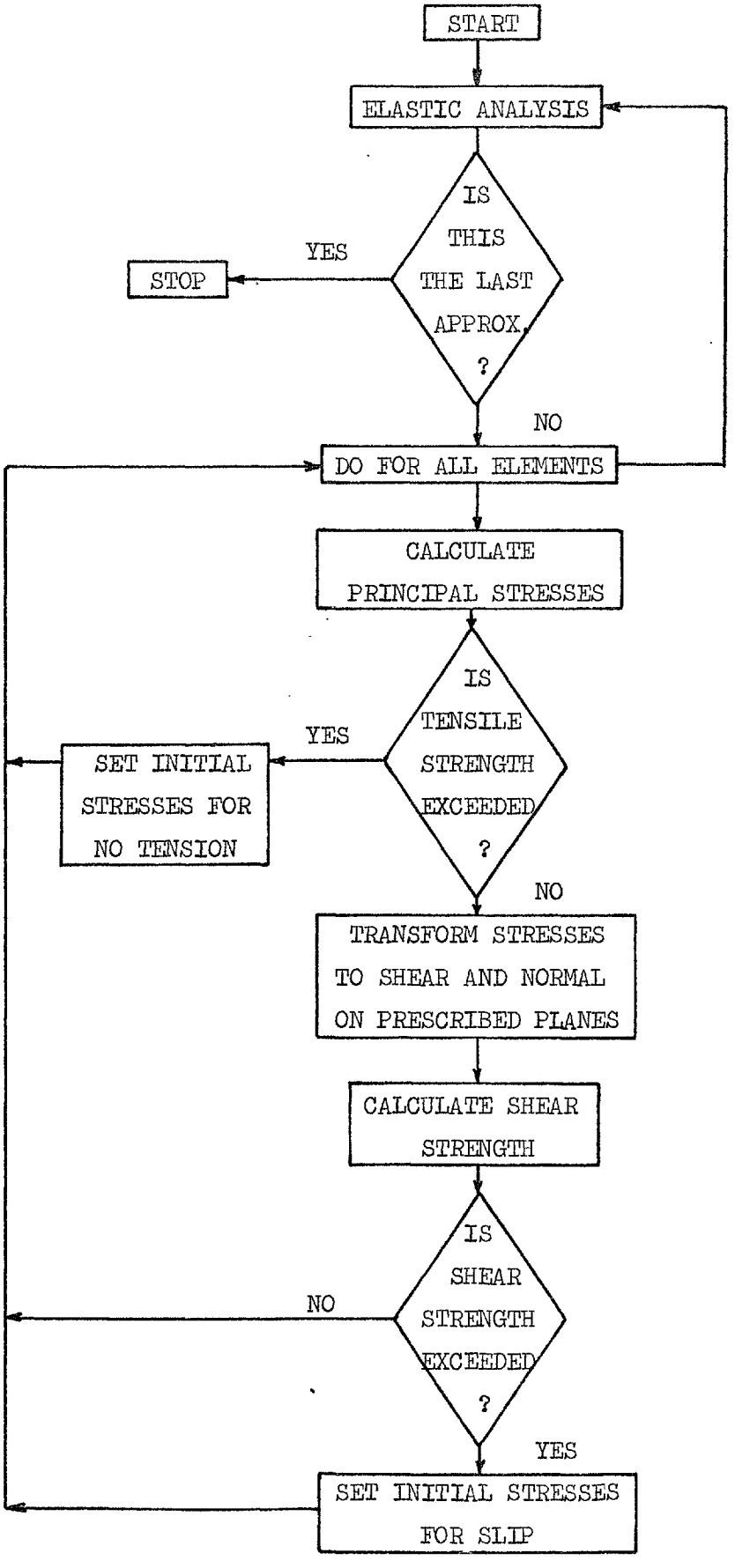
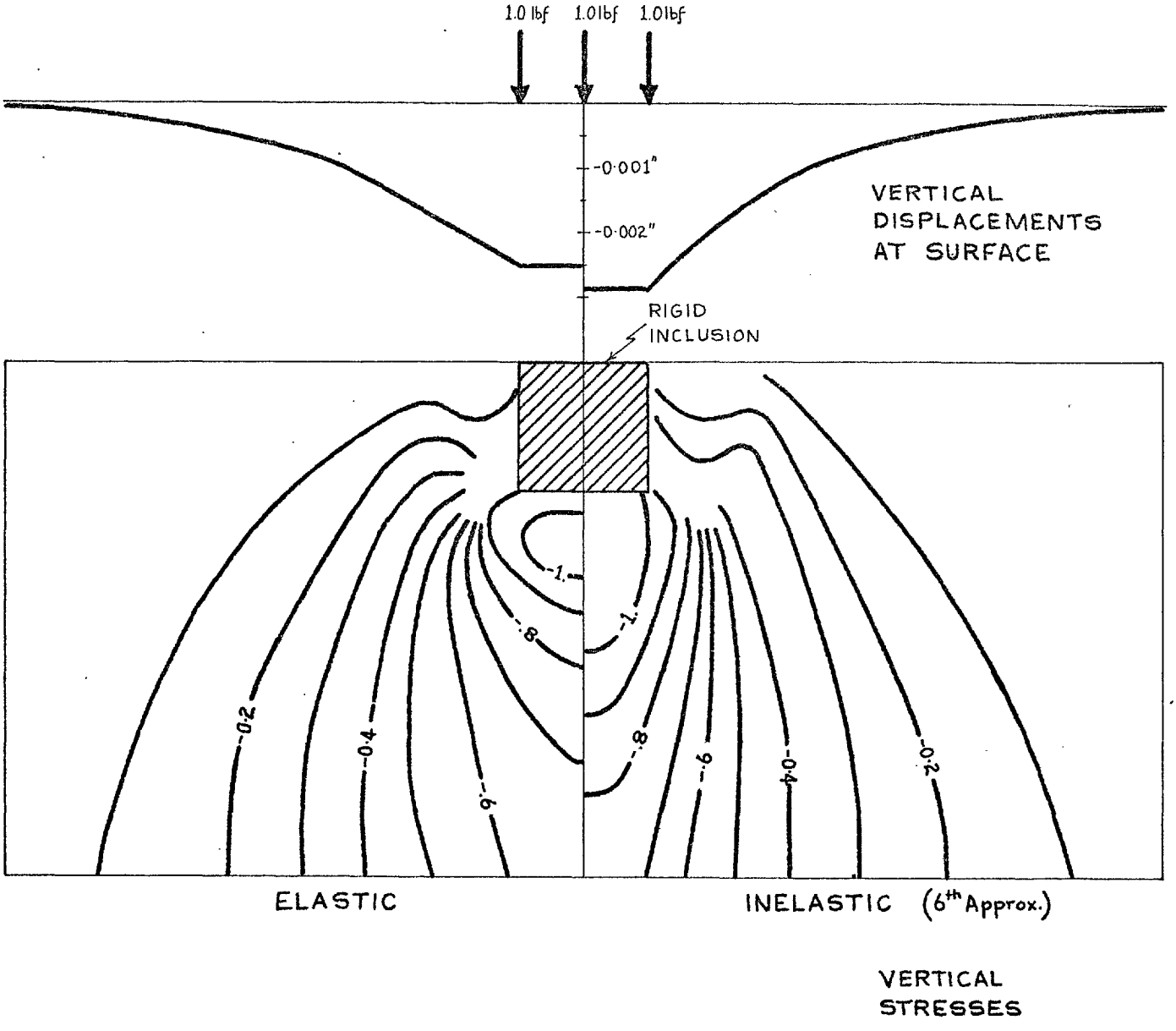


FIGURE 4.6

FLOW CHART FOR NO-TENSION AND UBIQUITOUS JOINT SLIP PROGRAM



Residual Horizontal Stress = −0·25 lbf/in²

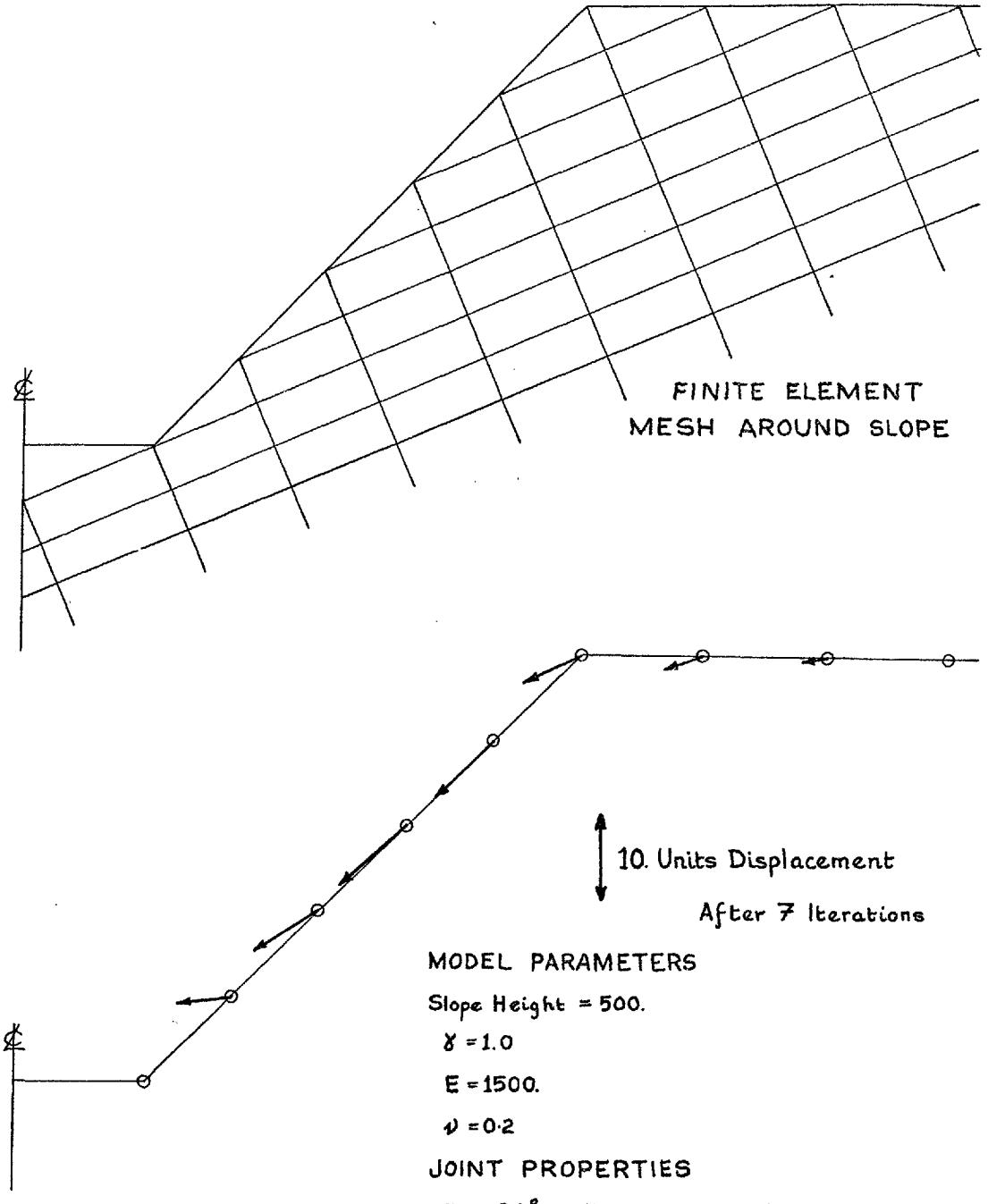
Vertical Joints

Cohesion = 0.0

Angle of Friction = 40.°

UBIQUITOUS JOINT SLIP MODEL

FIGURE 4.7



DISPLACEMENT DUE TO SLIP ON A UBIQUITOUS JOINT SET

FIGURE 4.8

Although the above behaviour is included in the computer program listed in Appendix B the author does not believe it has wide application in rock slope studies if used on its own. For foundation problems (Ref. 10) and in underground situations, where the stresses are generally higher and there are kinematic constraints on the displacements, the method may well prove useful.

4.2.5 A Further Application of the Initial Stress Method

The presence of water in a rock slope is observed to have a significant influence upon its stability. This influence is dependent upon the water pressure and hence upon the phreatic surface. In the context of a rock slope the latter is determined by the draw-down behind the face and, hence, the permeability of the rock mass.

The conductivity of a solid rock is several orders of magnitude less than that of the discontinuities, so the former may be ignored for most practical purposes. Since the conductivity of the discontinuities is proportional to the third power of the aperture (Ref. 12) it is highly stress dependent if the discontinuities are deformable. Assuming a linear normal stress/displacement relationship the conductivity (C') may be written as:

$$C' = \left(1. + \frac{F_n}{k_n}\right)^3 . C \qquad 4(9)$$

where C is the conductivity of the joint with zero normal load. F_n and k_n are the normal force per unit area and stiffness respectively. (Note that F_n is negative if the joint is in compression.)

In order to study the influence of the stress distribution on the permeability and the location of the phreatic surface an elementary model of a vertical slope was considered. It was assumed that this was traversed by horizontal and vertical joints

and that each element of the model contained one joint intersection. The configuration is shown in Figure 4.9. Water pressure on the joints was deemed equivalent to an initial stress in the composite element.

The interaction between the stress and the water pressure was necessarily solved iteratively. As the finite element method was used to solve for the material stresses and a finite difference network analysis (Ref. 13) for the potential distribution a means of communication between the two parts had to be devised. This was achieved by systematic labelling of the nodes of the two systems and equivalencing which resulting in the node points of the finite difference network being located at the centroid of each finite element. It was therefore possible to use the results from the stress analysis to calculate the current effective stress and, therefore, the current joint conductivities. Each calculation after the stress analysis started with the initial hydraulic boundary conditions and the conductivities were iteratively revised until the phreatic surface and potential distribution corresponding to the stress state had been determined. This, in turn, provided the necessary data for the following stress calculation which took into account the influence of the water pressures. This procedure is expressed as a flow chart in Figure 4.10.

The author undertook the above investigation to show that simple programming methods could be used to study this extremely complex problem. However, the limited results that were obtained are of some considerable interest. Evidence was produced that the stress conditions around a slope may encourage drainage, rather than vice versa as has been assumed in the past. It was also shown that the presence of water may have a marked influence on slope deformations. At this stage of development the study was handed over to Maini who has reported the findings (Ref. 14) and intends to carry out further work on this interaction problem. The model studied to date is particularly simple and should be extended to take account of the presence of discrete discontinuities. Very recently the author has been informed of work of this type

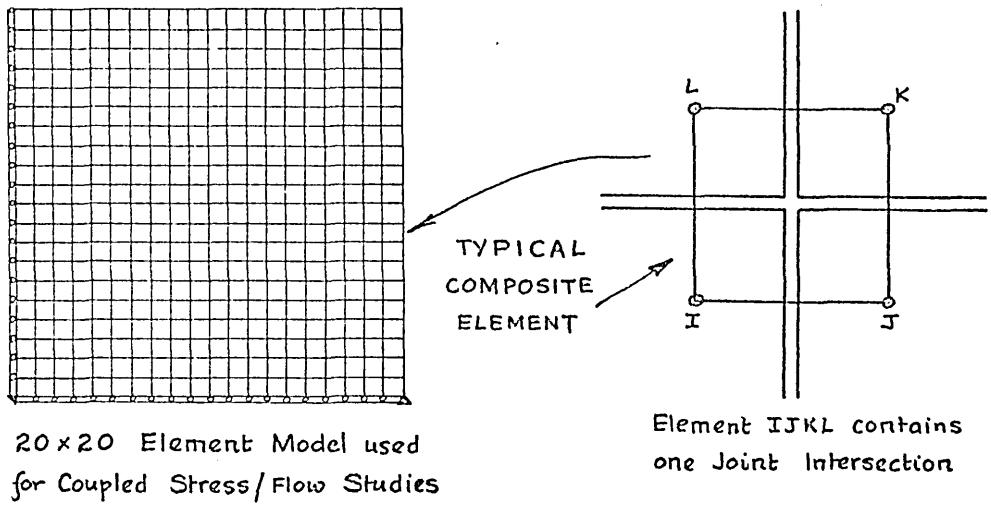


FIGURE 4.9

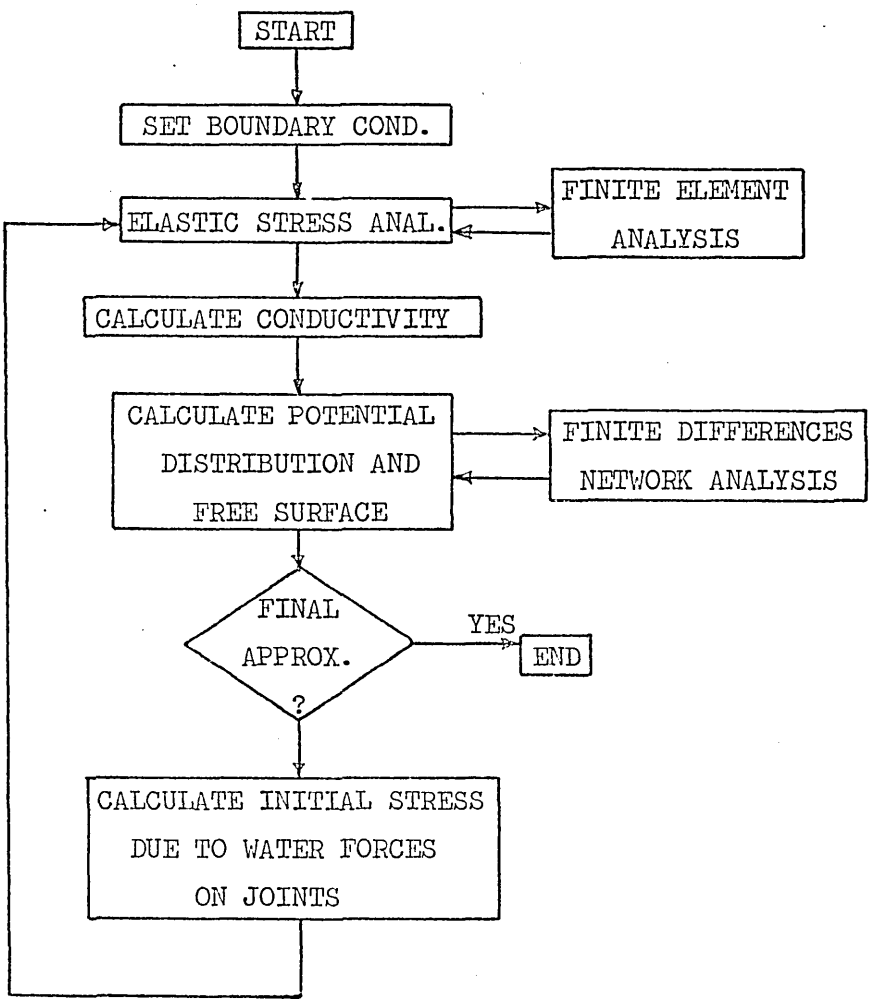


FIGURE 4.10

FLOW DIAGRAM FOR COUPLED STRESS/FLOW PROGRAM

that is being carried out at the University of California, Berkeley (Ref. 15).

4.3 MODELLING A DISCONTINUUM

There appear to be two possible approaches to modelling discontinua. One method is to include special joint elements in an otherwise elastic continuum. Such an approach restricts modelling to conditions of small displacements, even if finite strain theory is used. Elements initially in contact must remain in juxtaposition even if physically separated by tension across the interface. Alternatively a jointed rock mass may be treated as a granular material. The shape and size of each unit is then determined by the spacing and orientation of the relevant joint sets.

Trollope (Ref. 16) studied interparticle forces for a variety of particle shapes to determine stress distributions in wedges of granular material. This concept was applied to slope studies by Trollope and Burman (Ref. 17). The method is, however, essentially static even though the laws of continuum mechanics are no longer the basis of solution. What appeared to be required was a method that described the interaction of particles in such a manner that they could move freely with respect to each other.

After discussions with the author, Cundall devised a truly discontinuous model. Starting with the case of cylinders which could move independently according to interparticle force displacement laws, he extended his study to slopes constructed of rectangular blocks. For both these models the equations of motion were set up for each particle and solved in real time increments. The results of these analyses were mainly qualitative and served to draw attention to the important phenomenon of toppling failure (Ref. 18).

The chief limitation of the method devised by Cundall is that the particles are assumed rigid, although force displacement laws are defined for the points of contact in order to calculate inter-

particle forces. This means that the method is particularly suitable for studying low stress situations, but is likely to be in error if applied to relative high stress problems. The author attempted to overcome this limitation by using deformable particles based on arbitrary shaped twelve-node quadrilateral finite elements. Unfortunately unexpected computational problems were encountered and the attempt has been shelved for the present.

The first method of simulating a discontinuum, as mentioned above, necessitates the modelling of the individual joints, or interfaces, between blocks of solid rock. In terms of finite elements this means the special joint elements described in Section 2.6. As stated in Chapter 2 such elements are restricted to small relative displacement problems although the displacement of the whole model may be relatively large. In principle finite rather than infinitesimal strain theory should be applied but this was not done in this study.

4.4 PROPERTIES AND SIMULATION OF DISCONTINUITIES IN ROCK MASSES

Before considering more complex characteristics for discontinuities it is of interest to study previous work and the assumptions that were made. Goodman et al (Ref. 1) listed joint properties as:

(a) They are tabular.

(b) No resistance to tension normal to their surface.

(c) Joints offer a high resistance to normal compression. They may deform to some extent, particularly if there is detritus between the faces or they do not match exactly.

(d) At low normal stresses shear displacement results in dilational behaviour if the joint has moderate or low inclination asperities. The shear strength is then frictional unless there is

'cohesion' due to interlock of asperities, lack of continuity or joint infilling. At high normal stresses shear through the solid rock may be essential and the 'cohesion' may then be considerable.

(e) Small shear displacements may occur before the yield stress is reached.

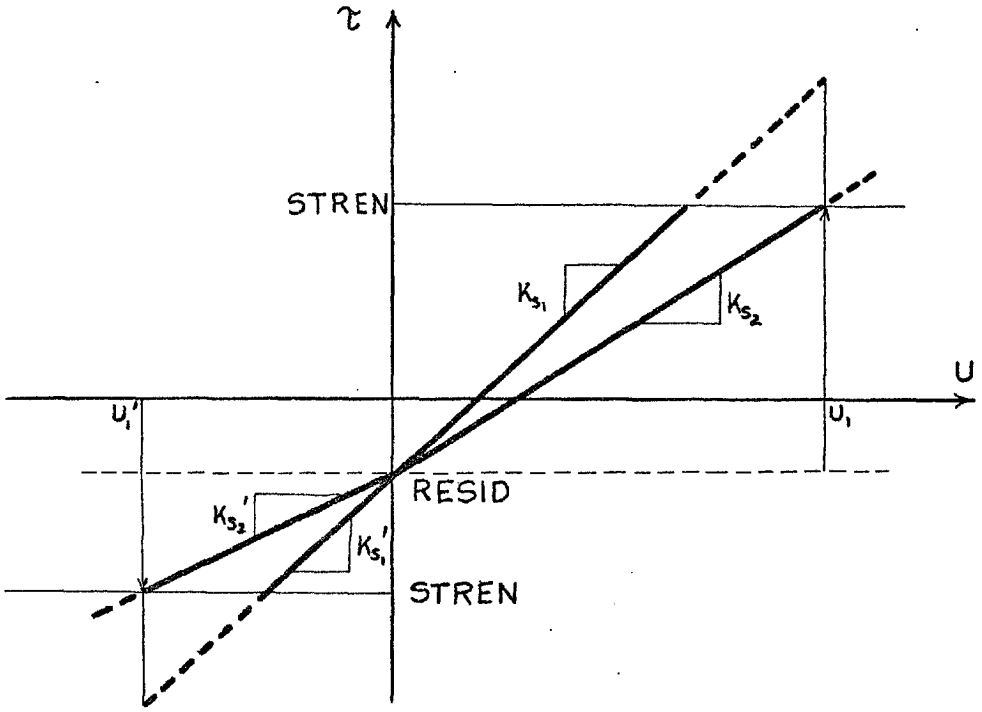
The above authors developed a model which assumed that a joint behaved linearly up to a yield shear stress defined by a linear Coulomb strength law. After the shear strength of the discontinuity was reached the shear stiffness was reduced to a residual to model slip. A limit was placed on the amount of normal closure permitted, the normal stiffness being increased if this were exceeded. The normal stiffness was set to zero if the joint was in tension. Each of these processes is a direct iterative approach based on variable elastic properties for elements. The program written by these authors was later modified by Heuzé to include the following features:

(a) An initial stress field.

(b) The shear stiffness was modified so that peak shear strength was maintained after yield. This is illustrated in Figure 4.11.

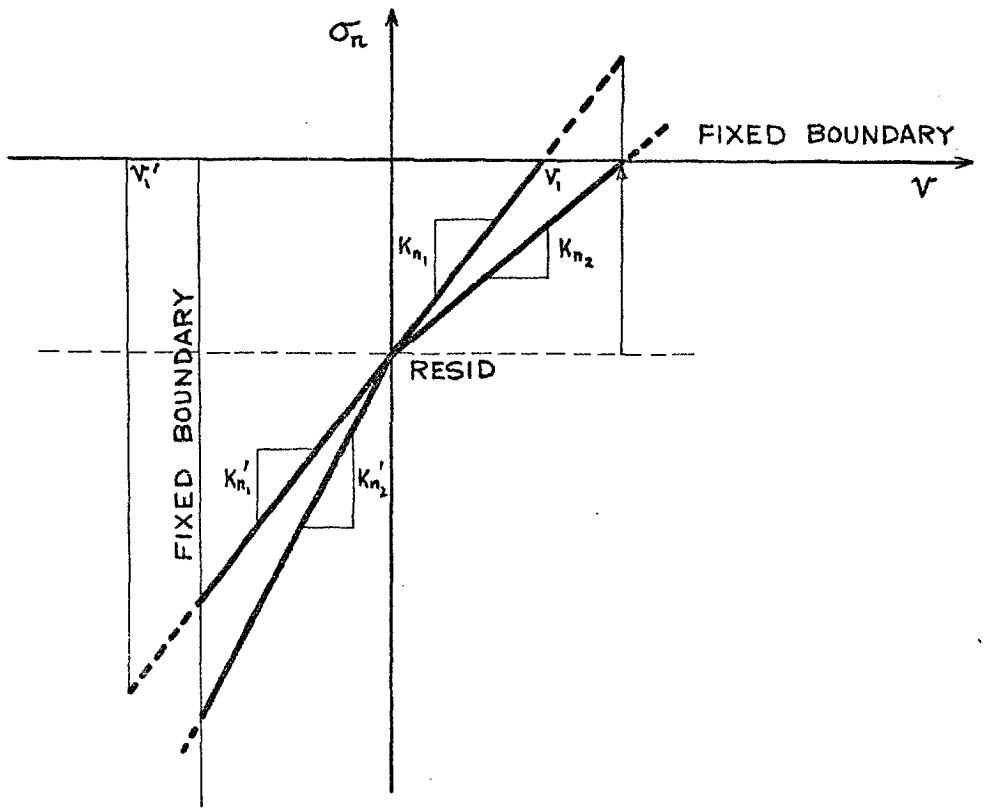
(c) The condition of maximum permitted normal closure and no-tension were remodelled by progressive alteration of the joint normal stiffness according to Figure 4.12.

A listing of the program, as modified by Heuzé, was made available to the author by Professor Goodman (Ref. 19). The author has made several modifications and corrections to the program and it is now particularly suitable for modelling multistage excavations in rock masses. This version has been used in the study of a jointed 45° slope described below. The sign conventions



SHEAR FORCE PER UNIT AREA v TANGENTIAL DISPLACEMENT

FIGURE 4.11



NORMAL FORCE PER UNIT AREA v NORMAL DISPLACEMENT

FIGURE 4.12

necessary to interpret this study are given in Figure 4.13.

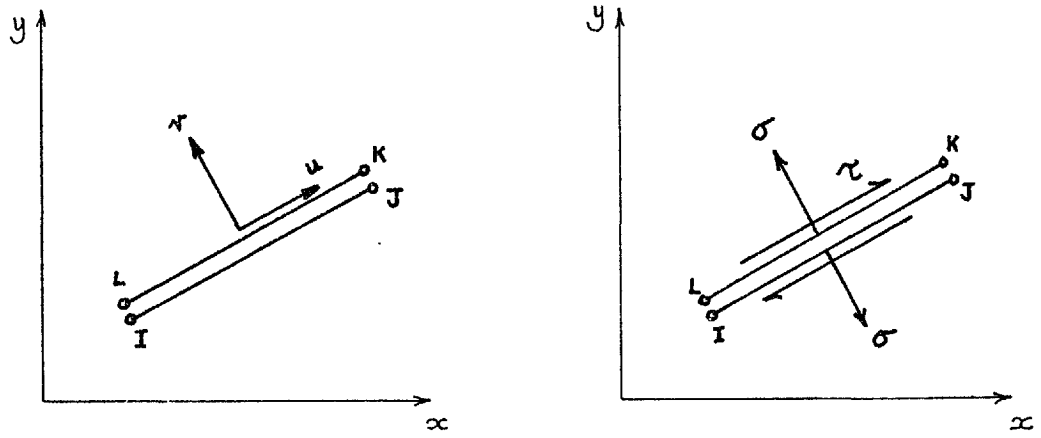


Figure 4.13 - Joint Sign Convention

4.4.1 Case Study of a 45° Slope

In order to test the simulation of jointed rock masses that is discussed above, several models of a 45° slope were studied. These were either a continuum or contained one, three or five joints down the slope face, as illustrated in Figure 4.14. Each of these models may be considered as a degeneration of the five joint model, of which Figure 4.15 is a computer drawing made using the first of the programs given in Appendix A. Clearly the element idealization is much coarser than used in the models studies of Chapter 3. The stress distribution for the continuum case, which is given in Figure 4.16, is therefore less accurate than that given in Figure 3.8. However, the model was considered satisfactory for the present purpose of studying the influence of parallel joints on slope behaviour.

Rather than giving consideration to all possible parameters, the cases of joints dipping into the excavation at $22\frac{1}{2}^{\circ}$ to the horizontal were studied. The stresses and deformations were then determined for a variety of material parameters. Namely: the elastic modulus of the solid, the shear and normal stiffnesses of the discontinuities and the stress conditions prior to excavation

of the slope. No joint strength parameters were included as the 'elastic' response was considered to be of most interest. In the absence of peak residual behaviour, the limiting conditions for equilibrium can be calculated without resort to numerical simulation (Chapter 1).

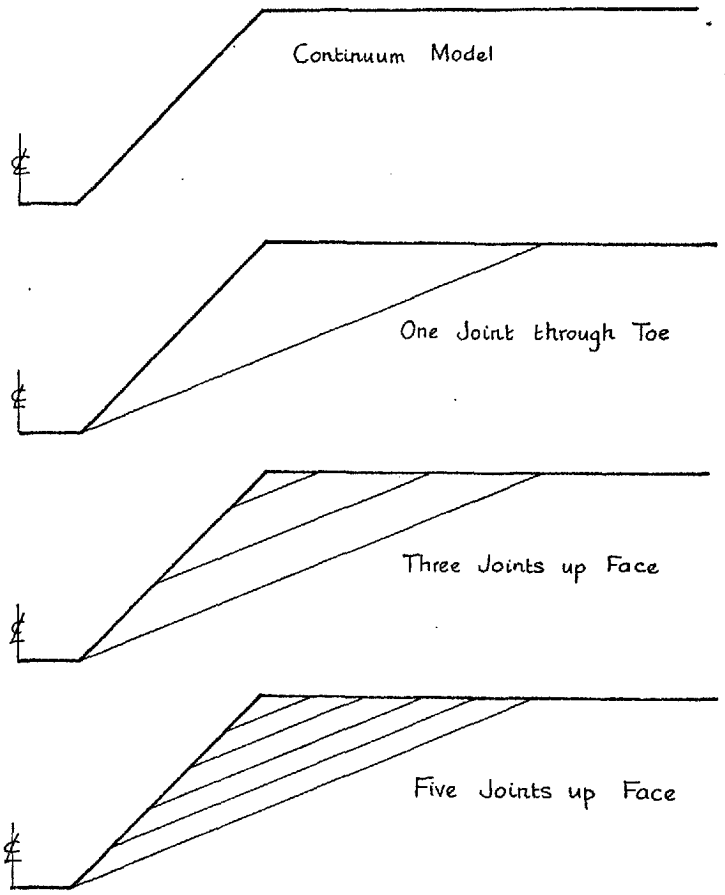


Figure 4.14 - Models of Rock Slope

Before drawing any conclusions from the results of the study it is perhaps worthwhile to give attention to the situation being considered. Figure 4.17 shows the stress conditions, on a joint passing through the toe, that exist before the residual stress state is disturbed by the excavation. The residual stress ratio (σ_{xx} : σ_{yy}) is varied in the range 0·25 to 2·0 but the normal stress on the joint is almost constant as the latter is flat lying.

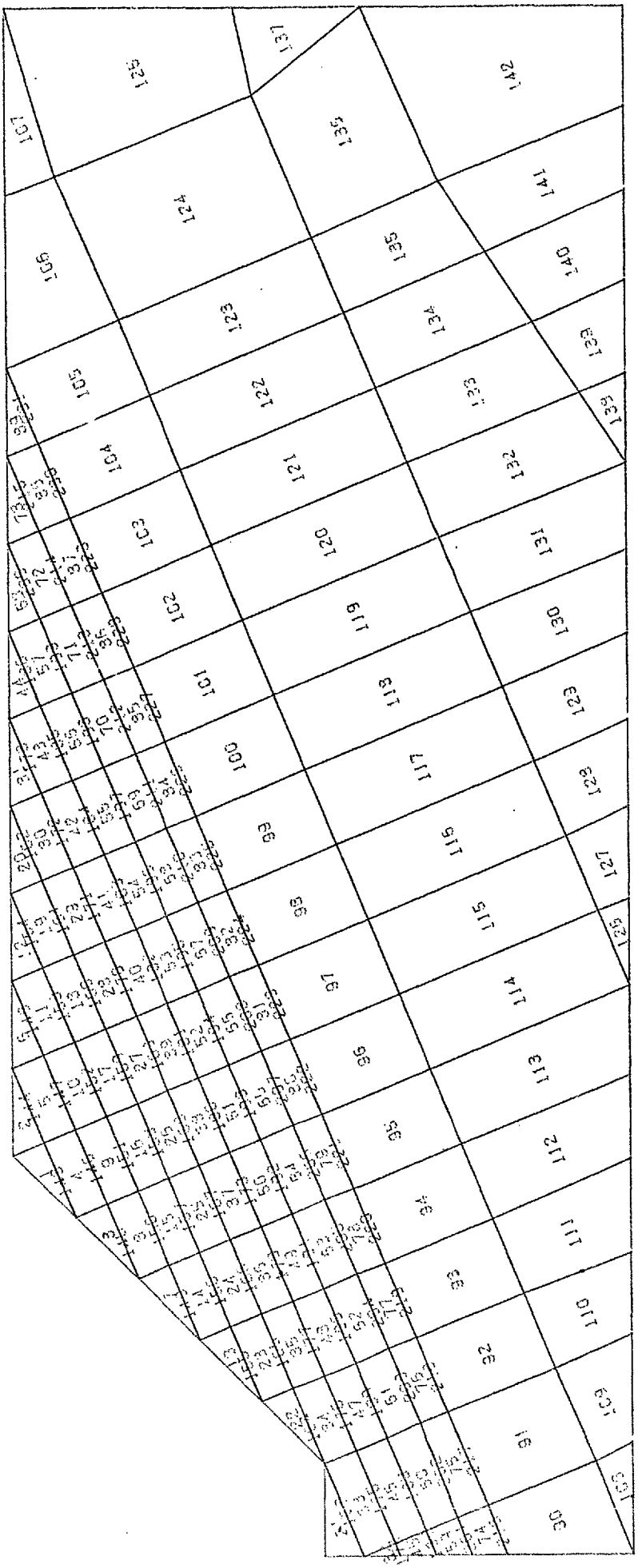
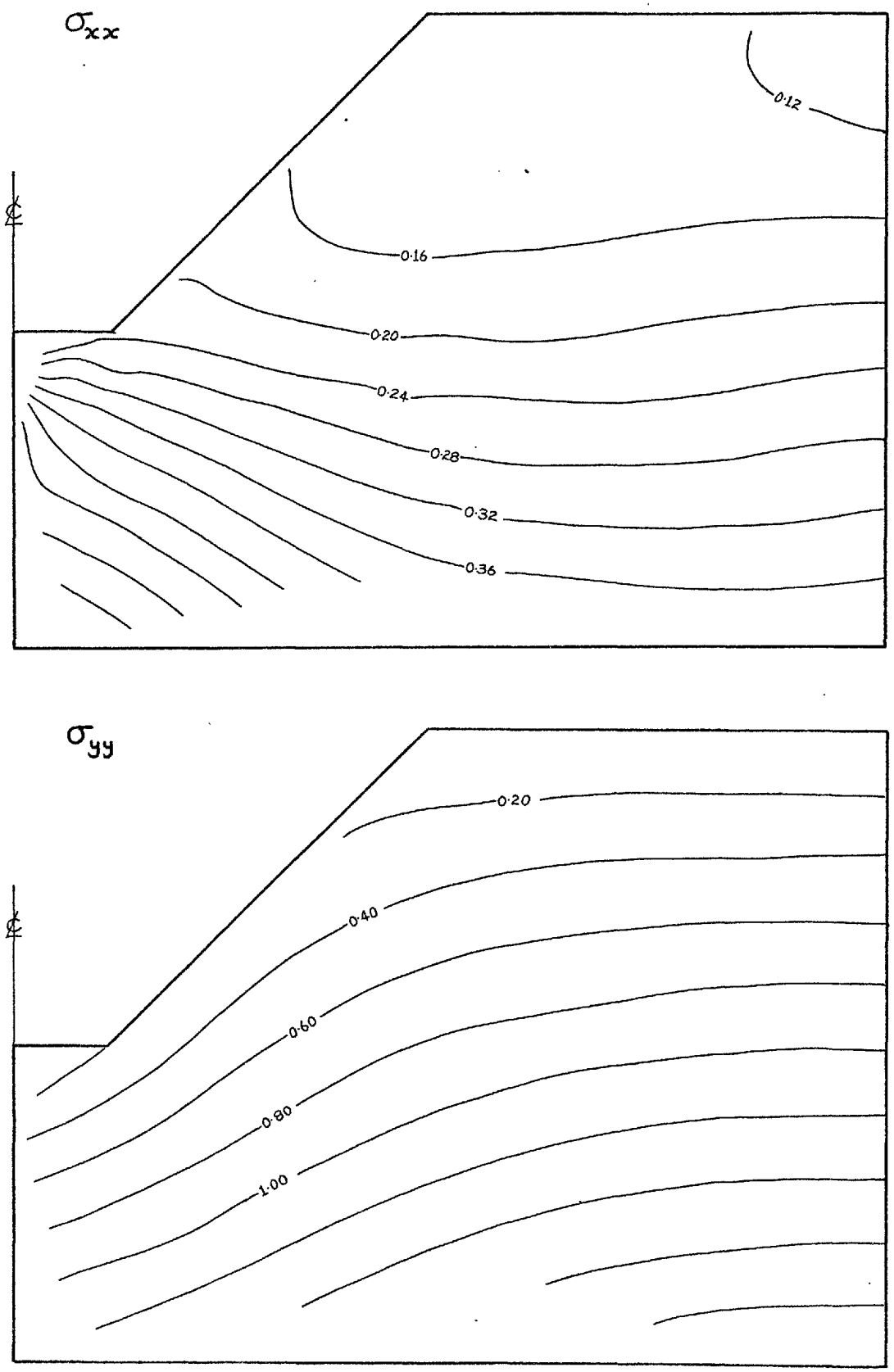

FINITE ELEMENT MESH
FIVE JOINTS DOWN FACE
SOLID ELEMENT
JOINT ELEMENT

FIGURE 4.15



STRESSES IN CONTINUUM MODEL $\sigma_{xx} : \sigma_{yy} = 0{\cdot}25 : 1{\cdot}0$

FIGURE 4.16

The shear stresses, however, vary considerably and are zero when the residual horizontal and vertical stresses are equal. Although the stresses prior to excavation may vary widely, the average stresses on a particular plane must be equal after excavation if the conditions of equilibrium are to be satisfied. Thus, if the joints behave in the elastic manner described above, the response of the rock to the excavation will be strongly influenced by the residual stress condition.

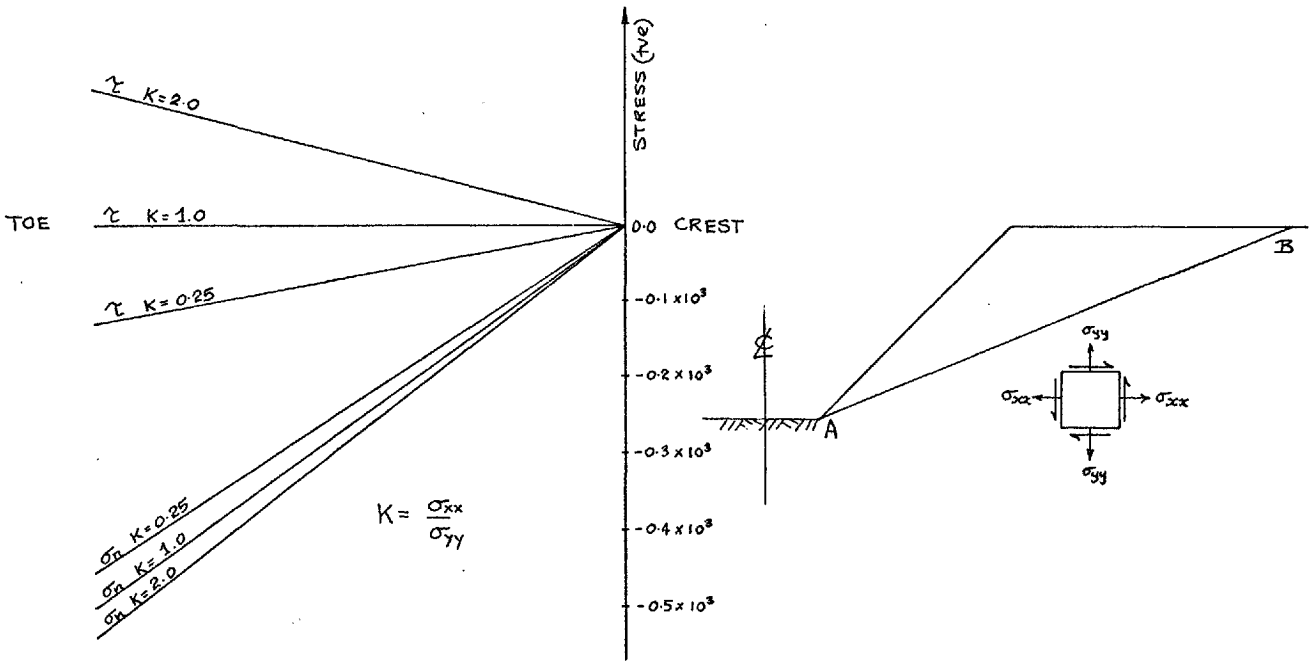
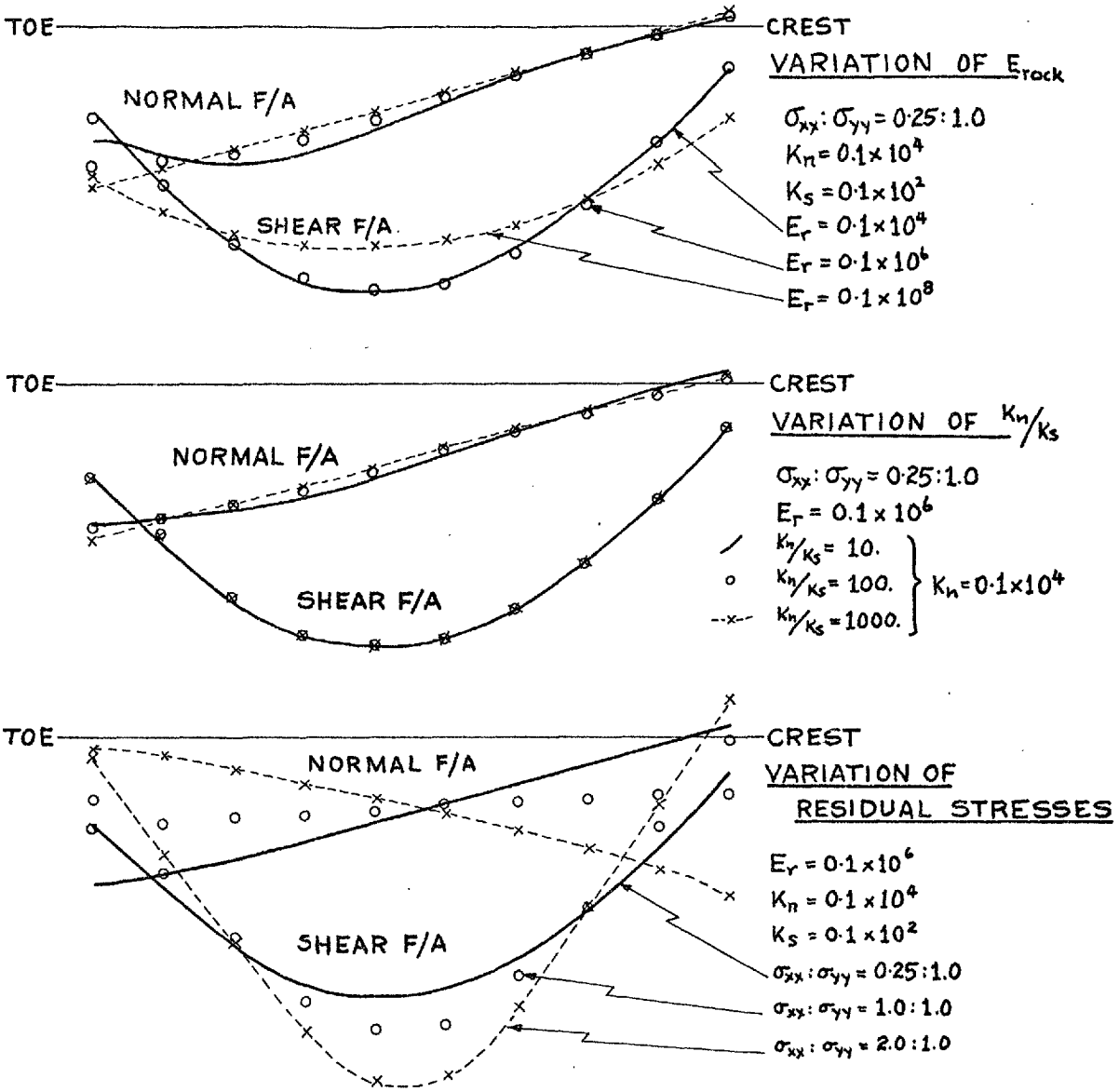


Figure 4.17

The results of the study are given in Figures 4.18 to 4.23. These all refer to a slope 500 units in depth constructed in a material of unit weight. Dimensions may therefore be chosen at will, providing they are consistent.

Figure 4.19 shows the displacements due to excavation in a continuum model. Unless the solid rock is very much more rigid than the joints these displacements will be a significant proportion of the total displacements of the jointed system.

Figure 4.18 combines the results of parameter variations for the case of a single joint model. The stress distributions given are so similar to those from the multi-joint cases, that the



STRESS DISTRIBUTION ON A DISCONTINUITY FROM CREST TO TOE

FIGURE 4.18

latter have not been reproduced. The conclusions given below are therefore common for all cases.

(a) The elastic modulus has some influence. For a rigid material the joint displacement due to excavation and the resulting stress distribution on the joint will vary linearly with depth.

(b) The variation of the ratio of joint shear to normal stiffness has no appreciable influence on the stresses, all other things being equal. This is a consequence of the two dimensional nature of the model.

(c) Variation of the initial, or residual, stress field has a marked influence. Shear stresses at the toe tend to be lower for the higher initial horizontal stresses. In such cases progressive failure should start at the crest rather than the toe of the slope.

Figures 4.20 to 4.23 attempt to indicate the influence of the various parameters on the slope displacement. This is relatively simple for the single joint case as only the displacements of the wedge are shown. For the five joint case the displacements refer to the nodes above the joint. These will obviously be different from those of the nodes below the joint if the joint is considered to be deformable. The following observations may be made on these figures.

(a) The joint deformation becomes dominant as the elastic modulus of the solid rock increases (Figures 4.18, 4.20).

(b) The softer the joint in shear the more the displacements will be controlled by their orientation (Figure 4.21).

(c) Displacements into the excavation, rather than out of it, will occur except when the initial horizontal stresses are low (Figures 4.21 - 4.23). As discussed above, their direction will largely depend upon the initial shear stress on the joints.

(d) Displacements are greater for the multi-joint systems, particularly if the joints are significantly more deformable than the solid.

Obviously this case study is by no means exhaustive and the conclusions apply to the particular models that are described. However, the results do give qualitative impressions of the influence of some of the parameters defining a rock slope situation. Clearly all these must be measured with some precision if meaningful simulation of jointed rock slopes is to be accomplished.

4.4.2 Toppling Modes of Failure

The studies reported by Cundall (Refs. 9, 18) and Hofmann (Ref. 11) have drawn attention to the importance of toppling as a mode of failure of jointed rock slopes. Figure 4.24 shows two stages in a model study by Ashby (Ref. 20). The slope model, which was constructed from plaster of paris blocks, was slowly rotated until failure by toppling occurred. The model itself may be reproduced using a finite element idealization but the mechanism of failure cannot.

The first limitation of the finite element model discussed in this thesis is that only infinitesimal strain can be considered. This means that only pre slip conditions can be modelled. The second limitation is the assumption of uniform stress across any joint element. The transition from line contact to point contact between two blocks is therefore precluded, unless every discontinuity is represented by a very large number of elements. This last course is clearly impractical except for trivial cases.

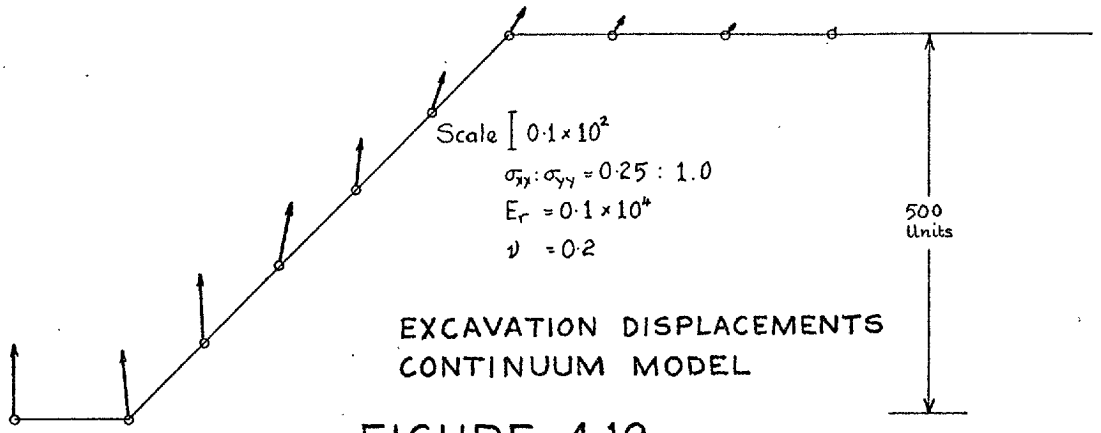


FIGURE 4.19

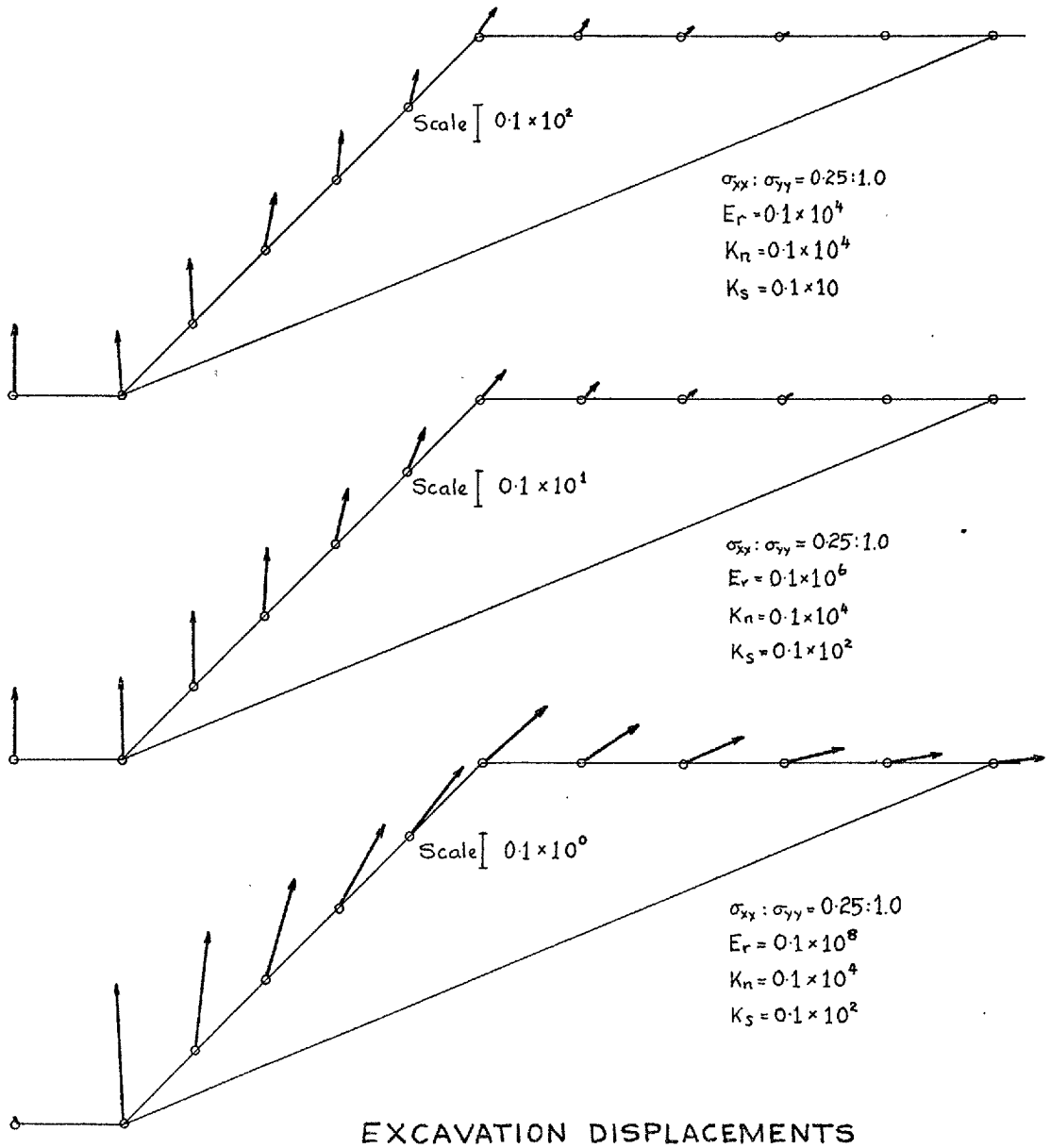
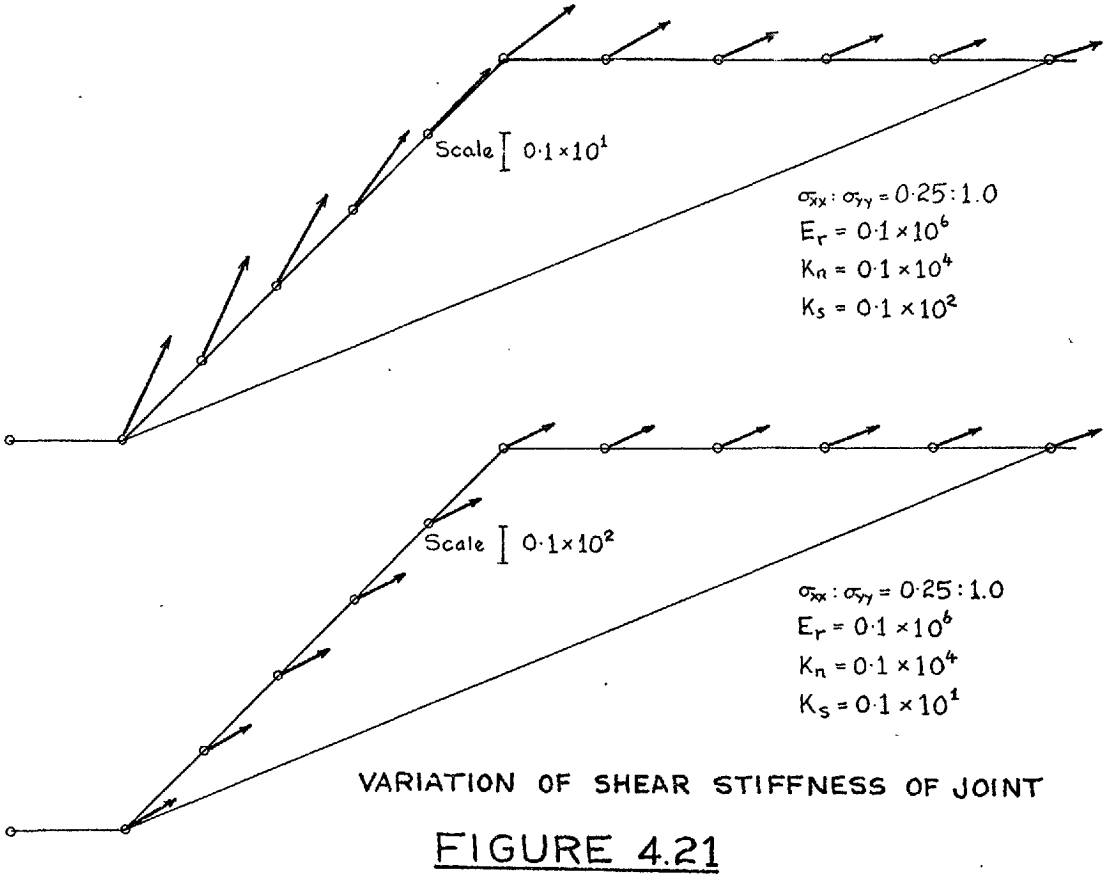
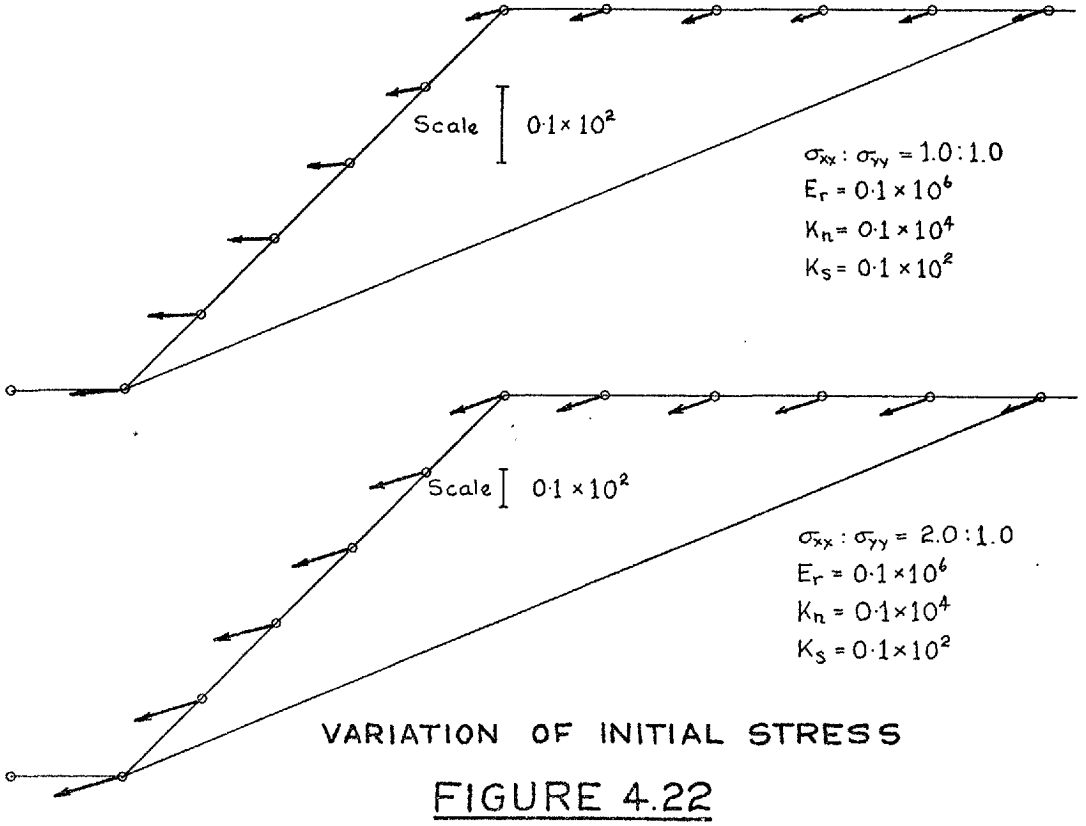


FIGURE 4.20



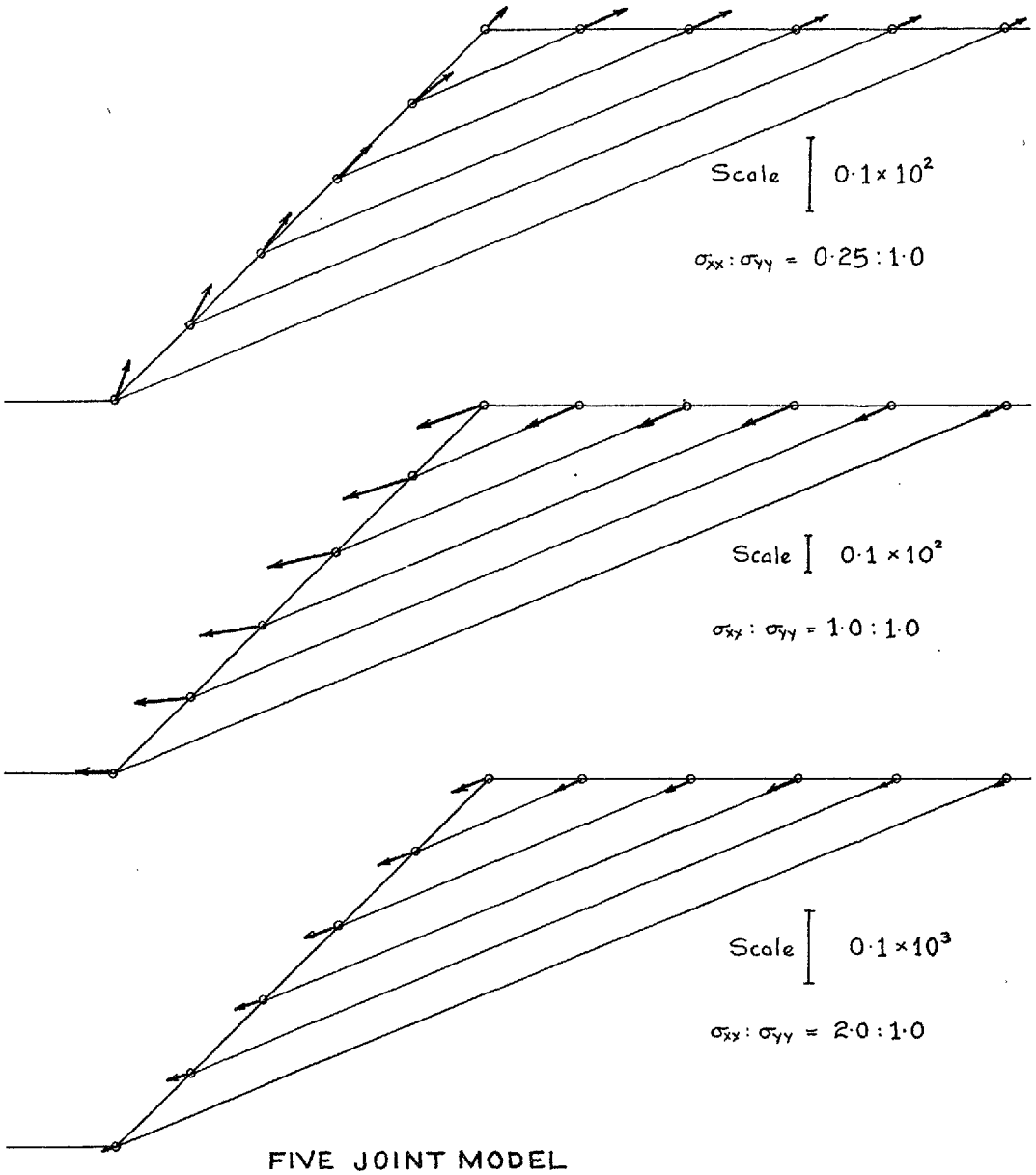
VARIATION OF SHEAR STIFFNESS OF JOINT

FIGURE 4.21



VARIATION OF INITIAL STRESS

FIGURE 4.22



FIVE JOINT MODEL
VARIATION OF RESIDUAL STRESS STATE

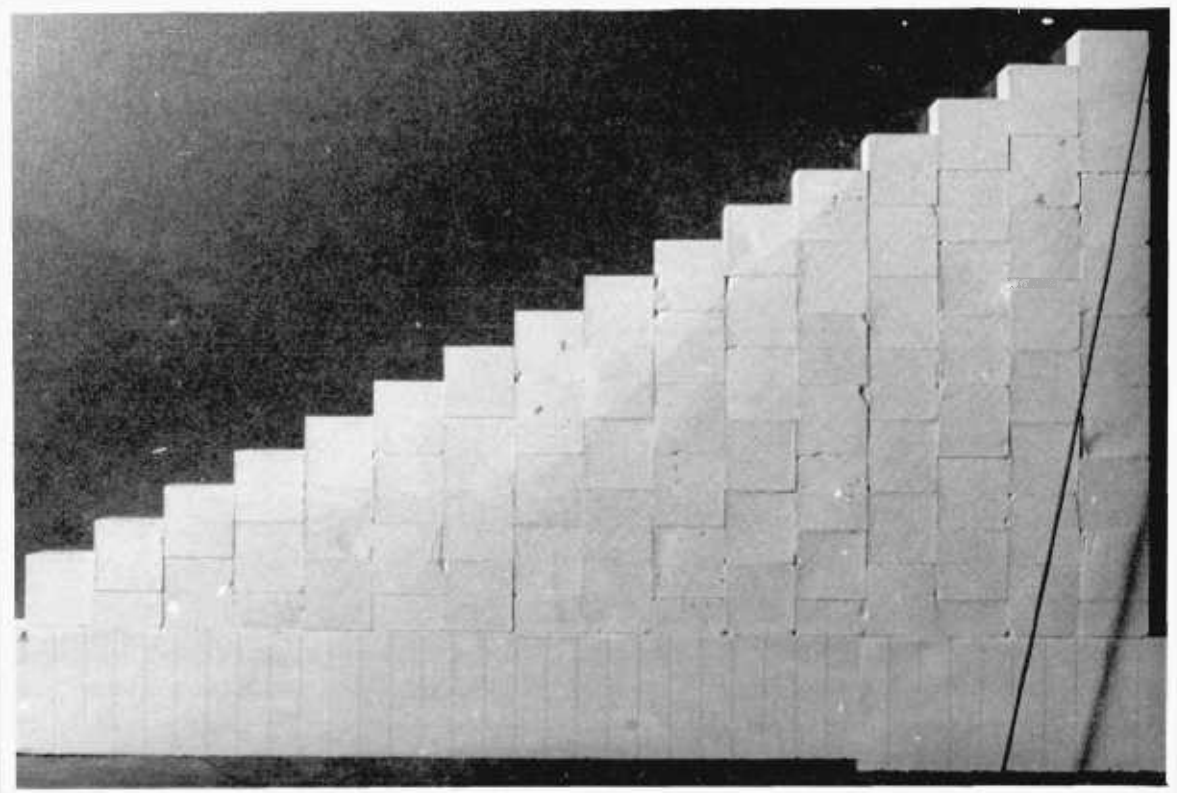
Displacements due to Excavation given at Upper Nodes

Model Parameters

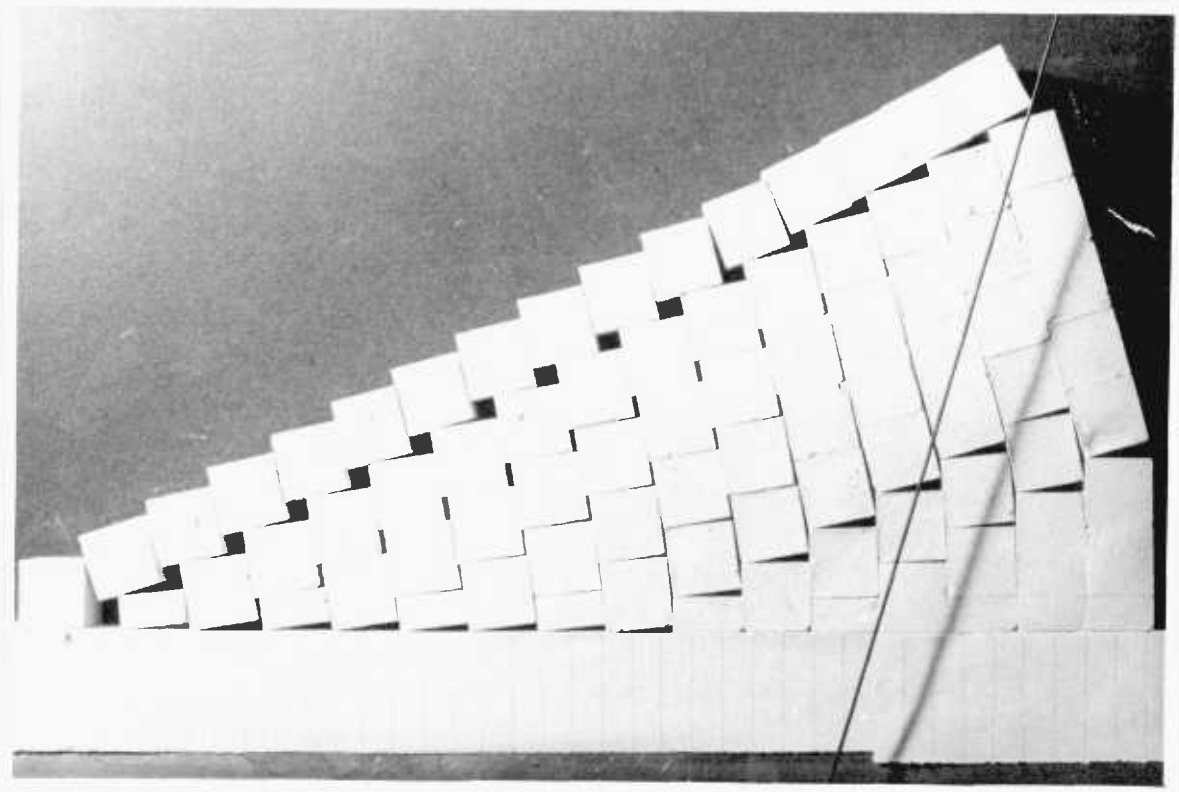
$E_r = 0{\cdot}1\times10^6$ $\quad \nu = 0{\cdot}2$

$K_n = 0{\cdot}1\times10^4$ $\quad K_s = 0{\cdot}1\times10^2$

FIGURE 4.23



Model before Failure



Model after Failure

FIGURE 4.24

A simple finite element idealization of a model of the type shown in Figure 4.24 was analysed. The results showed the typical block rotation that occurs, but not the toppling induced partings between blocks. The arching of rows of bricks was also apparent despite the small displacements.

4.5 EXTENSION TO MORE COMPLEX JOINT BEHAVIOUR

The computer simulation of jointed rock materials necessitates the assumption of particular behaviour for discontinuities. The simplest model is one of linear behaviour, up to a yield point, as proposed by Goodman et al (Ref. 1). As modified by Heuzé (Ref. 8) this model is satisfactory for joints exhibiting elastic-perfectly plastic behaviour in shear. It ignores the very important phenomenon of peak residual shear behaviour generally displayed by rock discontinuities. Furthermore it generates an arbitrary stiffness to limit joint closure under normal loading.

In order to simulate more general joint behaviour the author investigated the use of initial stress and initial strain techniques. These appear to have a considerable advantage, as regards computer time, over the variable stiffness method adopted by Heuzé (Ref. 8). A detailed comparison of these two techniques has recently been published by Goodman and Dubois (Ref. 21). The latter author is reported to be investigating a 'Constant Energy' method that is more efficient than either technique.

Before discussing the method of simulating complex joint behaviour it is pertinent to review the relevant properties of rock discontinuities in more detail than above (Section 4.4).

4.5.1 Further Properties of Discontinuities

Shear tests on both small and large samples of jointed rock have shown several important features of discontinuities under load.

(a) The shear strength is dependent upon the

normal stress and the previous shear displacement that has occurred.

(b) Discontinuities in shear usually exhibit marked peak residual behaviour. The degree too which this occurs depends upon the roughness of the discontinuity, the competence of the wall rock, the nature of any infilling, the normal stress and any previous shear displacement.

(c) A discontinuity may be strongly dilatant, or contractant, during shearing. The dilatancy will depend upon the normal loading and the shear displacement as well as the properties of the discontinuity itself.

(d) Discontinuities may exhibit very non-linear behaviour when subject to normal load. They are incapable of sustaining tension, unless they are healed. They have a maximum possible closure defined by the properties of any infilling and the initial void ratio of the fracture.

The behaviour of joints in shear has been reviewed by Goodman (Ref. 22) who provided some quantitative values for deformability and strength of rock joints. He particularly drew attention to the importance of joint infilling, as this may completely control the joint behaviour.

The models of joint behaviour presented by Patton (Ref. 23), Ladanyi and Archambault (Ref. 24) and other authors are interesting as they explore the mechanisms involved. The author has restricted his attention to the possibility of simulating observed joint properties.

4.5.2 Computer Simulation and Programming Assumptions

The behaviour of joints has been considered to comprise three

parts: shear force/displacement behaviour, normal force/displacement behaviour and dilatancy. Each of the properties can be specified numerically providing the necessary data can be determined from laboratory and field tests. Relevant values of each of these properties may then be calculated, at any point in the program, by linear interpolation between data points.

In this section each of the three components of joint behaviour will be treated independently so that the assumptions in the computer simulation are quite clear.

(a) Shear Force/Displacement Laws

A relationship between shear force per unit area and shear displacement may be described numerically as the shear strength at given displacement increments. Since it is impossible to have a separate relationship for every normal stress some method of normalizing the relationship is essential. Two methods of achieving this can be adopted. The first is based upon the assumption that the shear displacement to peak strength is independent of the normal stress. The second requires that the apparent shear stiffness to peak is independent of normal stress. The latter course is the more convenient of the two and appears to be in agreement with the published data of Krsmanovic et al (Ref. 25) and Barton (Ref. 26). The first approach was also investigated. It would, of course, be possible to specify any alternative relationship between shear displacement to peak strength and normal stress.

The non-dimensional shear force/shear displacement law is as follows: The shear stress is normalized by dividing by the residual shear strength. Assuming a purely frictional strength the normalized shear strength may be written:

$$\tau^* = \frac{\tau}{\sigma_n \, \mathrm{Tan}\phi_r} \qquad 4(10)$$

where σ_n is the normal stress and ϕ_r the residual friction

angle. So that the joint shear stiffness (k_s) describes the initial behaviour of the joint the shear displacement (δ_s) must be described in terms of an elastically related shear displacement (δ_{es}), where:

$$\delta_{es} = \frac{\sigma_n \, \text{Tan}\phi_r}{k_s} \qquad 4(11)$$

The non-dimensional shear displacement is therefore:

$$\delta^* = \frac{\delta_s}{\delta_{es}} \qquad 4(12)$$

The relationship can now be described numerically as in Figure 4.25. It is assumed that the joint will have reached residual conditions if the normalized shear displacement exceeds ten units.

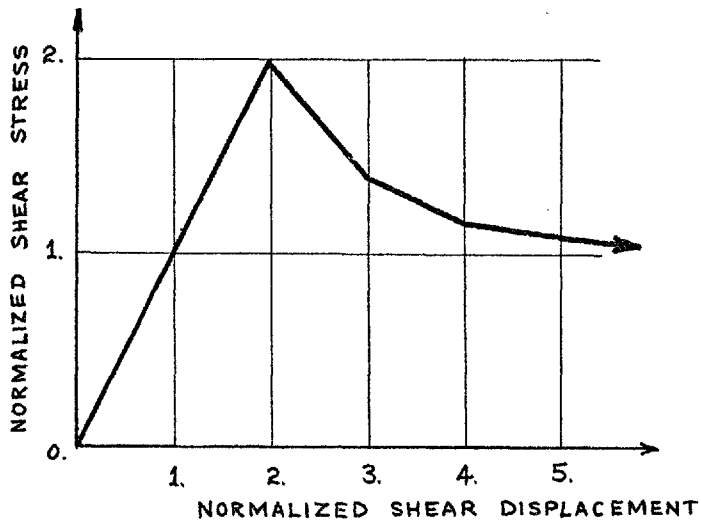


Figure 4.25

This behaviour is simulated by use of the initial stress method in much the same manner as for the ubiquitous joint slip case. Physically the process consists of shedding shear load in excess of that which should correspond to the existing shear displacement. Convergence may be slow due to a falling curve but methods of acceleration have not been explored.

In order to minimise the influence of history during the readjustment for any load increment it has been assumed that the relationship between shear displacement and stress is reversible. Alternative strategies could be adopted between increments but these only consist of more complex memories of past behaviour. The author knows of no records of the result of reversing the sense of shear displacement upon which to base such treatment.

Finally it should be noted that the computer program starts by calculating the shear displacements corresponding to the residual stress state prior to disturbance by excavation or loading. It is assumed that the shear stiffness describes the necessary relationship for this calculation (Figure 4.26).

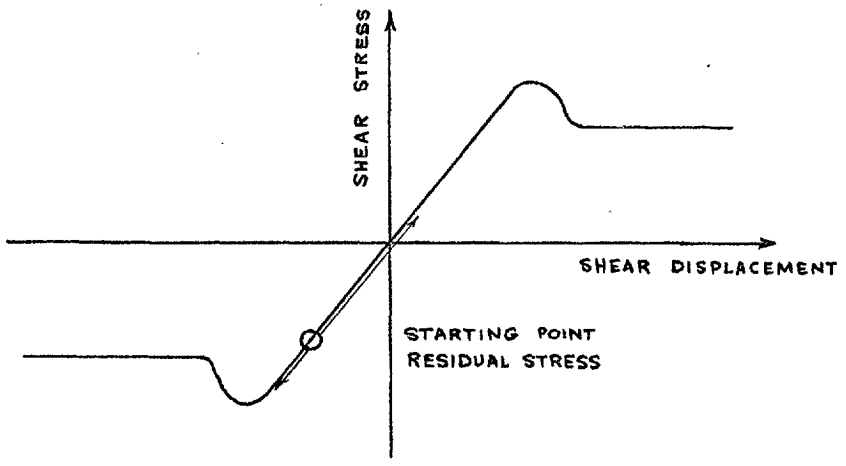


Figure 4.26

The analysis of non-linear problems in rock mechanics has already been discussed in this thesis. However, the methods have not been suitable for modelling work softening behaviour, such as displayed by rock joints. Indeed the method described in Section 4.4 may result in generation of negative joint stiffnesses if there is a significant fall in joint strength. The first publication of work considering the above type of behaviour was by Zienkiewicz et al (Ref. 27) who reported its use in conjunction with modified continuum elements. That of Goodman and Dubois (Ref. 21) is too recent to influence the work described in this thesis.

(b) Normal Stress/Displacement Law

Very little work appears to have been carried out to specifically determine the behaviour of a joint subject to normal load. Studies by Barton (Ref. 26) on a weak modelling material with tension induced discontinuities, revealed marked non-linear behaviour and considerable permanent deformation. This latter phenomenon was undoubtedly partially due to the presence of loose particles caused by the mode of preparation of the discontinuities, but probably it is observed also in nature. However, there is evidence from plate loading tests (Ref. 29) that joints may behave linearly over certain stress ranges.

A numerical relationship is used to define the proportion of the maximum permissible closure that may occur at a prescribed normal load. This is used to calculate the initial strain equivalent to the resistance to normal closure that is input for the next approximation. Obviously it is convenient if this relationship accords with the chosen joint normal stiffness (k_n) over the first normal load increment, i.e.

$$\delta_{n_1} = \frac{F_{n_1}}{k_n} \qquad 4(13)$$

where δ_{n_1} and F_{n_1} are the normal displacements and loads corresponding to the first load interval on the relationship given in Figure 4.27.

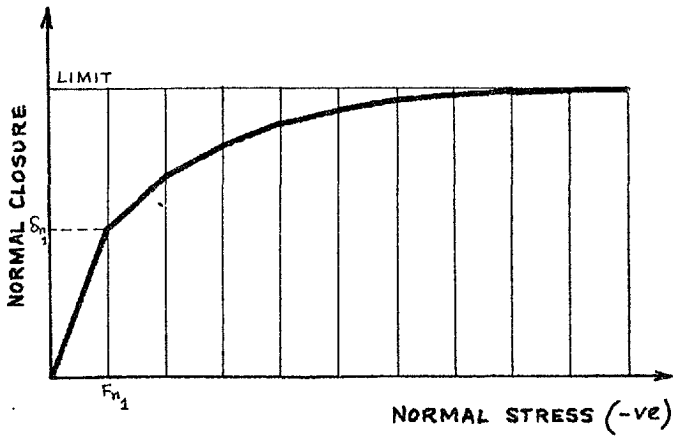


Figure 4.27

As stated above the resistance to closure is simulated using an initial strain method. This is illustrated by Figure 4.28. In this case convergence is generally rapid since the relationship takes the form of a rising curve.

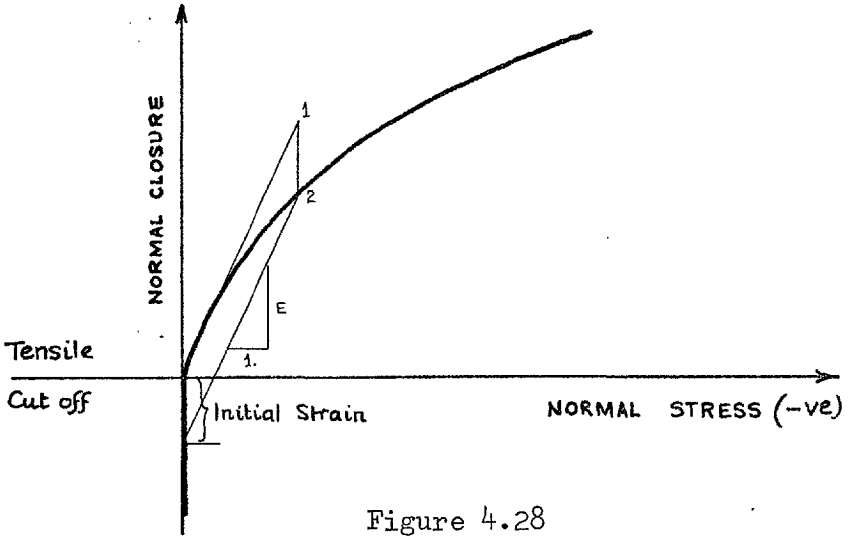


Figure 4.28

Finally it should be noted that the joint is assumed to have no tensile strength. The no-tension cut off is achieved using the initial stress method described earlier in this chapter. In the event of residual tensile or compressive stresses the corresponding displacement is calculated as for the shear stress case.

(c) Dilatancy during Shear

It is observed that a rough discontinuity exhibits dilatant behaviour during shear, due to a tendency to ride up roughnesses. Of course, if the sense of the shear displacement were reversed the joint may become contractant, although it would presumably achieve a minimum point after which it again became dilatant. Such a material may be termed bidilatant. A bicontractant material, as proposed by Goodman and Dubois (Ref. 21) is difficult to imagine. Barton (Ref. 26) did, in fact, note an initial contraction during shear, particularly at higher normal stresses. This is again probably due, in part, to the presence of small loose particles between the surfaces. Dilatancy is strongly dependent upon the

normal load and is reported to cease at stresses of the order of several thousand psi (Ref. 21).

Two interlinked aspects of dilatation must be represented. Firstly a normalized dilatation versus normalized shear displacement curve for zero normal load is defined. (The use of the normalized shear displacement of equation 4(12) ensures that peak strength and peak dilatation angle may coincide.) The first law is rescaled by means of a second numerical law defining the proportion of the normalized dilatation that occurs at the existing normal stress. These two relationships are given diagrammatically in Figure 4.29.

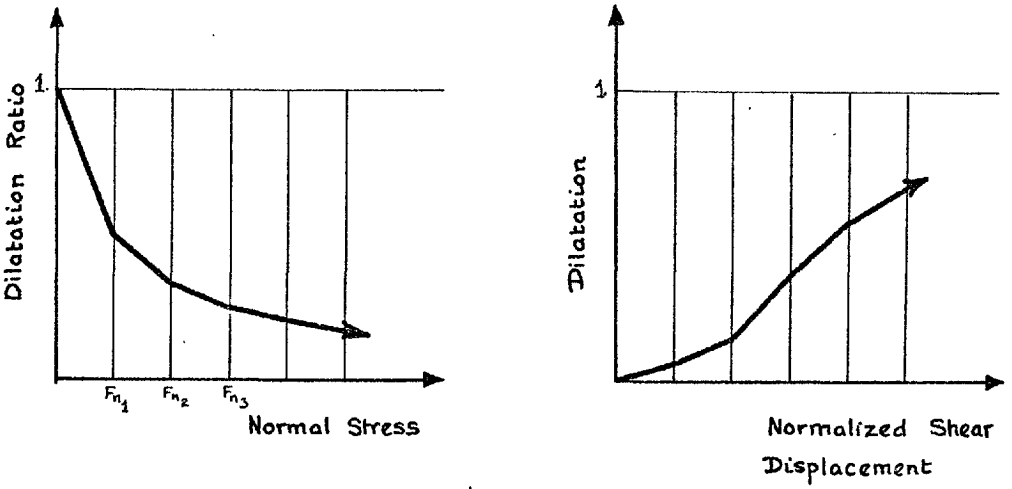


Figure 4.29

The dilatation is simulated using an initial strain as for limiting the normal closure. The total initial strain, for the next approximation, in any increment is thus a summation of that due to dilatation and resistance to normal closure.

The flow chart of the subroutine incorporating all these behaviours is given in Figure 4.30. The complete computer program, together with user instructions, is given in Appendix B.

4.5.3 Tests of the Computer Simulation

A number of small models have been studied in order to fully test all the options in the simulation program. As these model

SUBROUTINE JSTR

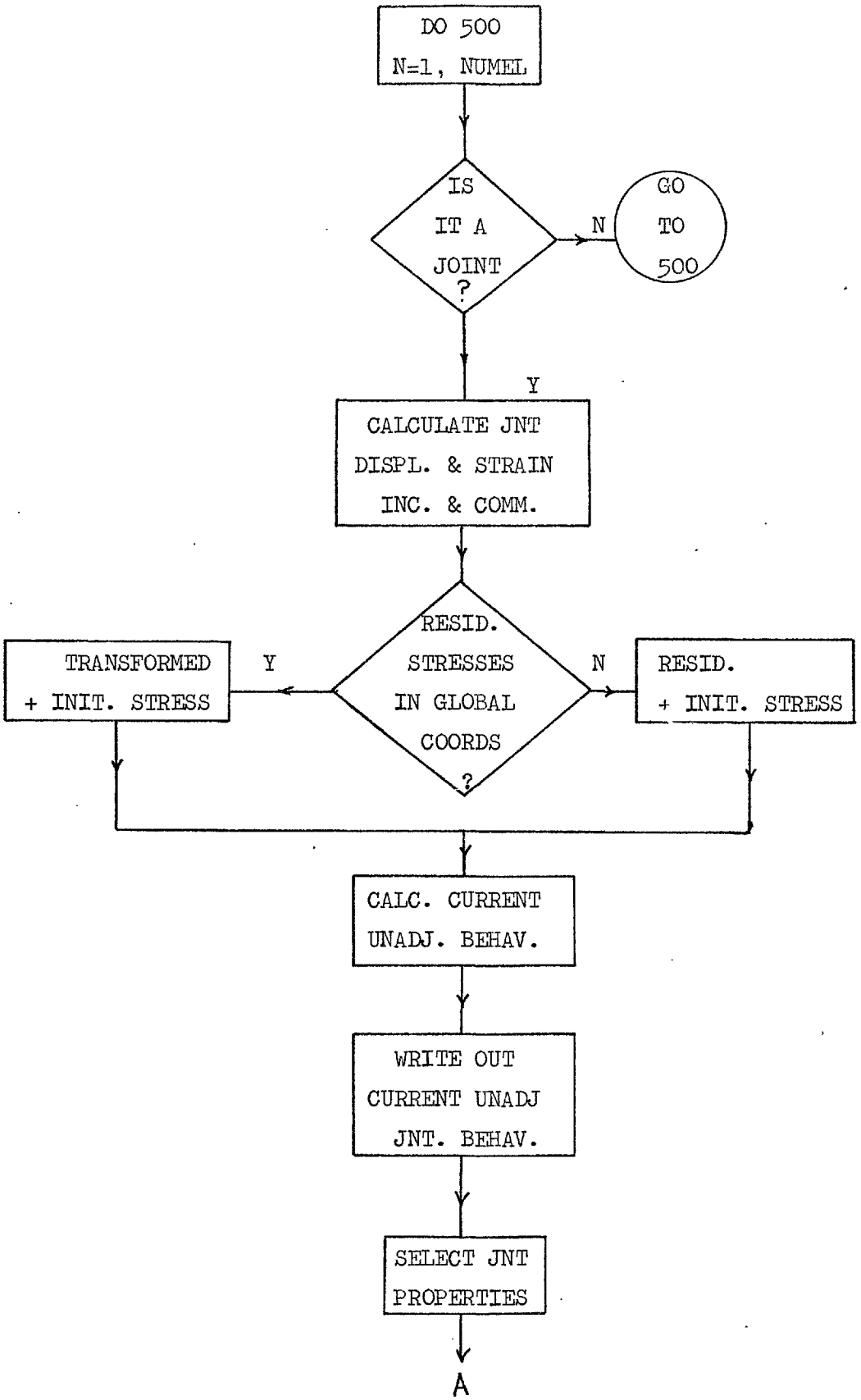


Figure 4.30

Continued .....

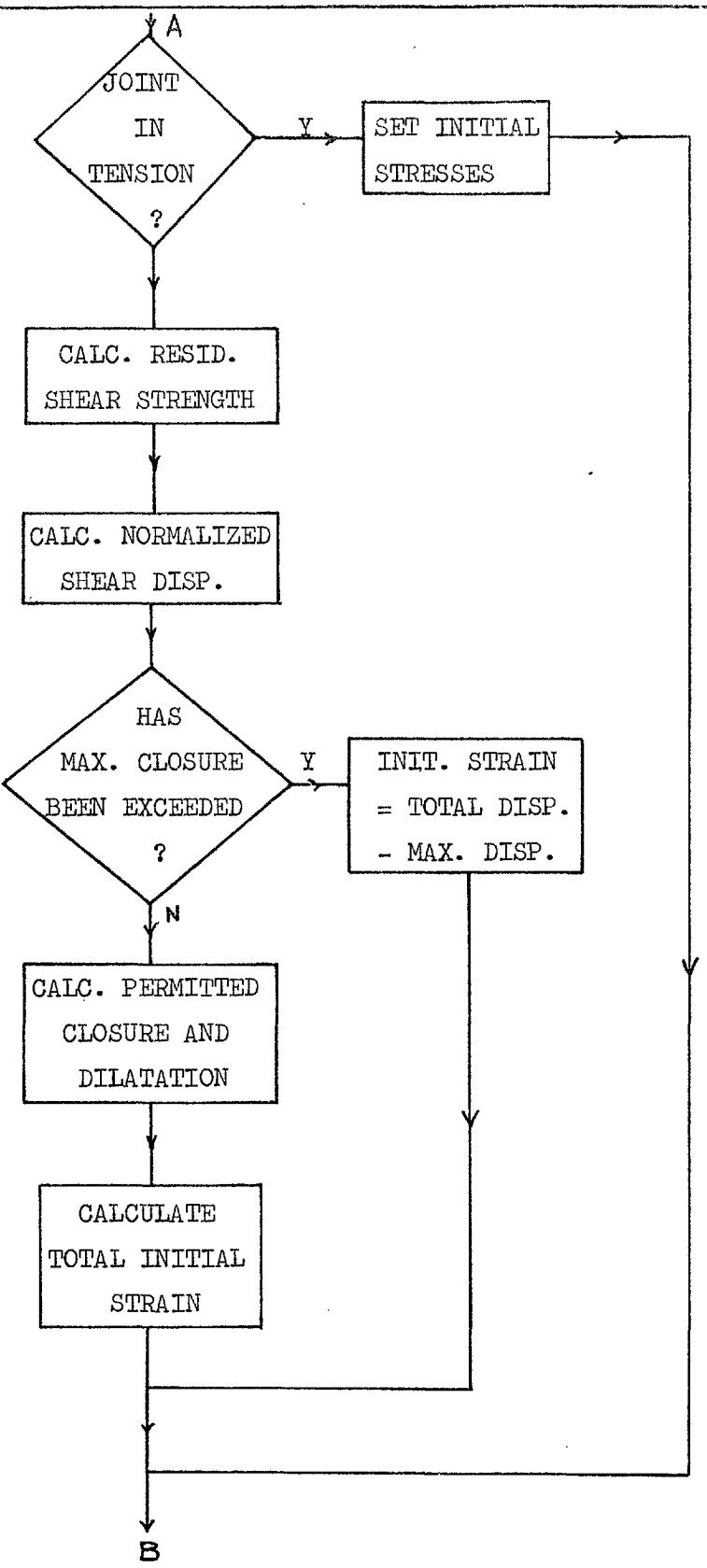


Figure 4.30

Continued .....

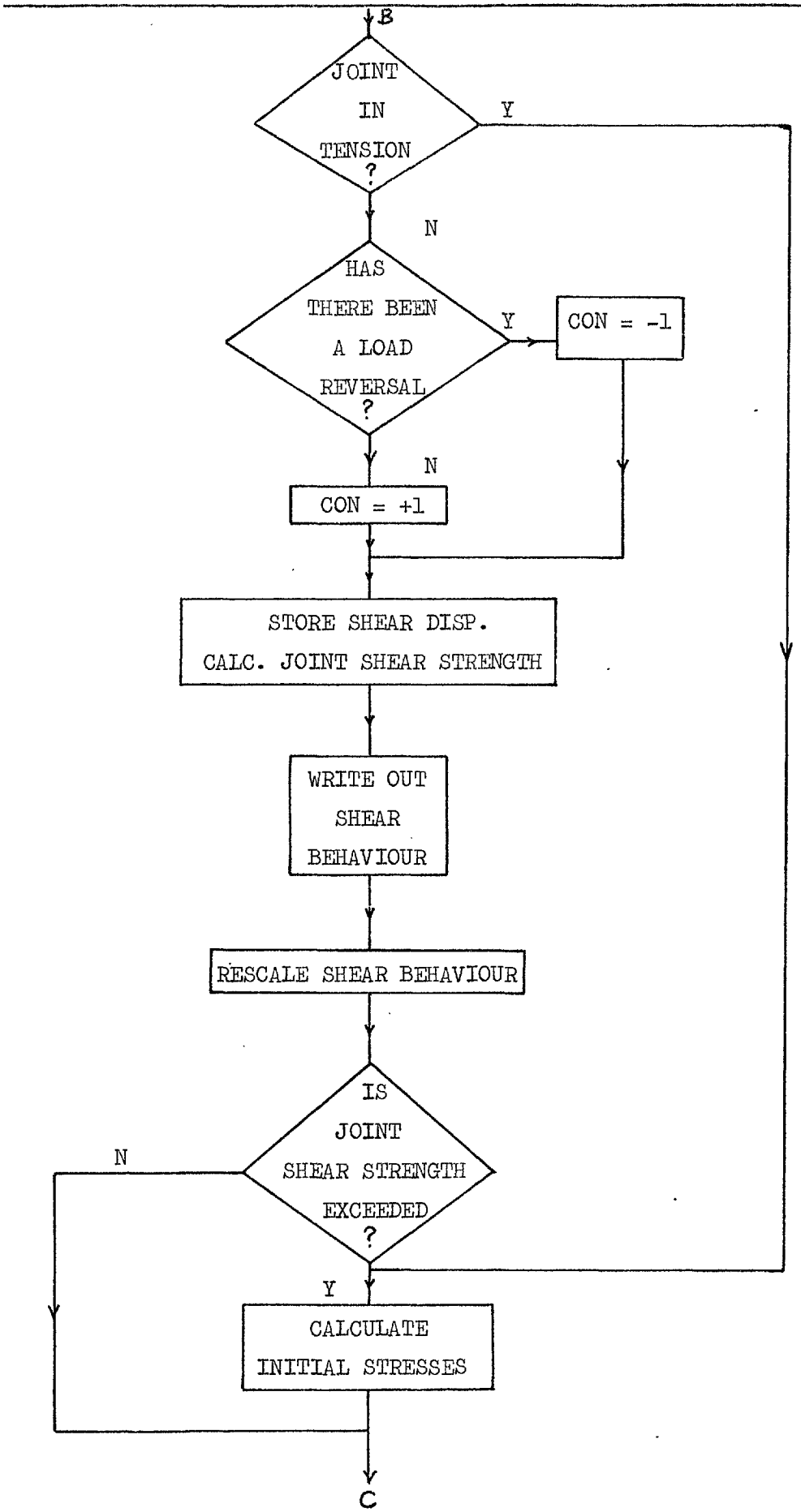


Figure 4.30

Continued .....

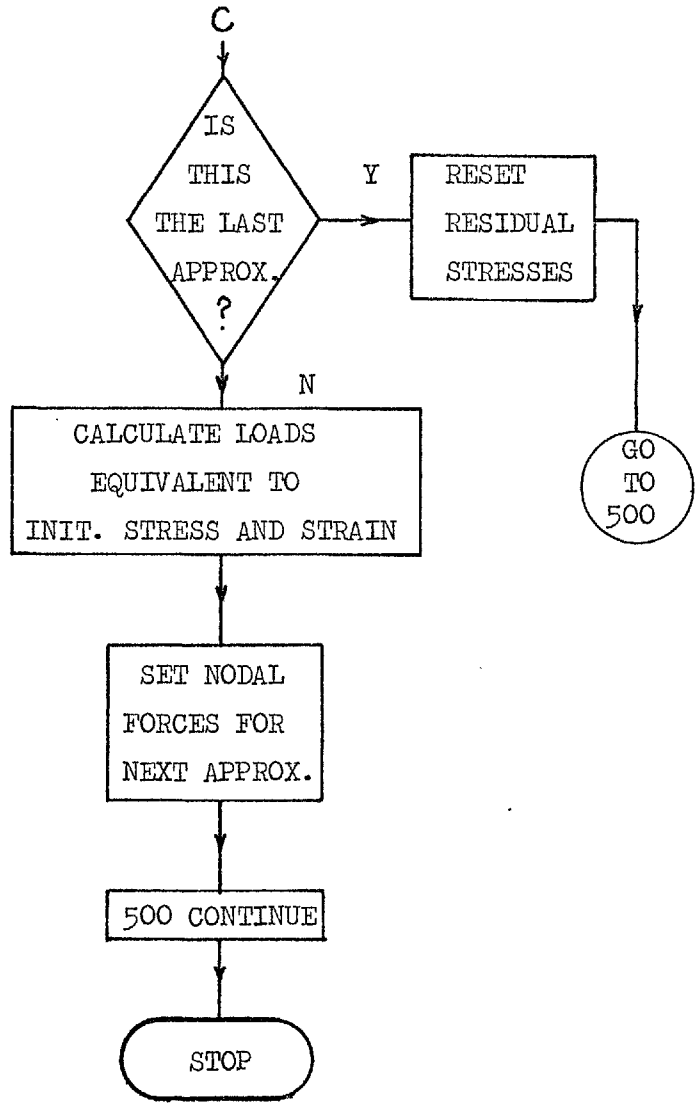

C
IS THIS THE LAST APPROX. ?
Y
RESET RESIDUAL STRESSES
GO TO 500
N
CALCULATE LOADS EQUIVALENT TO INIT. STRESS AND STRAIN
SET NODAL FORCES FOR NEXT APPROX.
500 CONTINUE
STOP

Figure 4.30

studies have no particular merit in themselves they are not reported in detail.

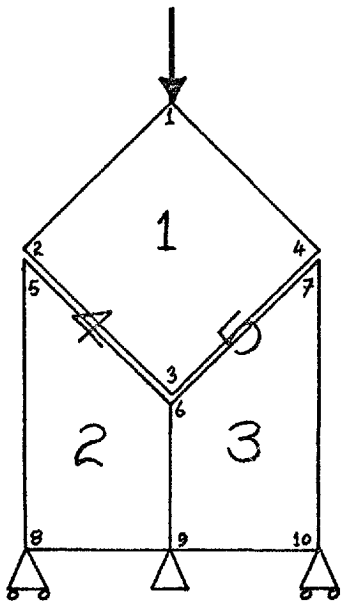


Figure 4.31

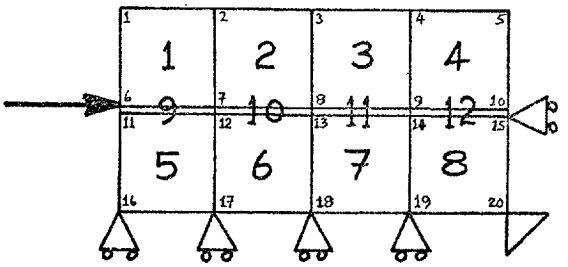
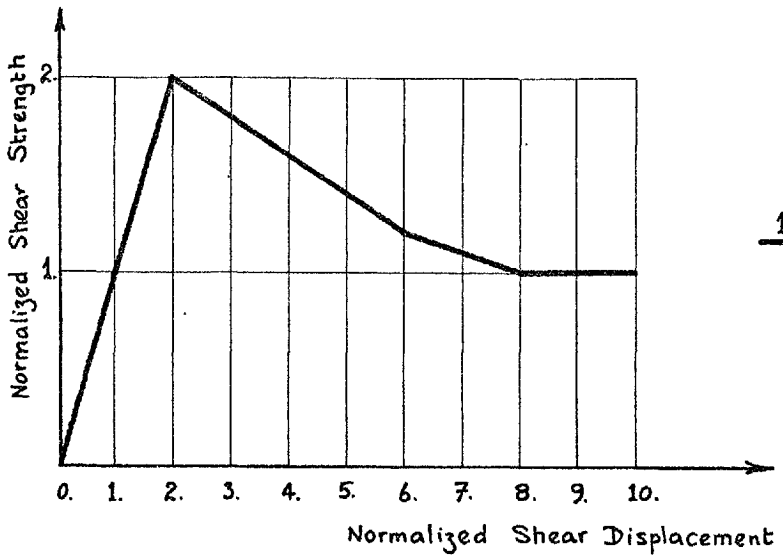
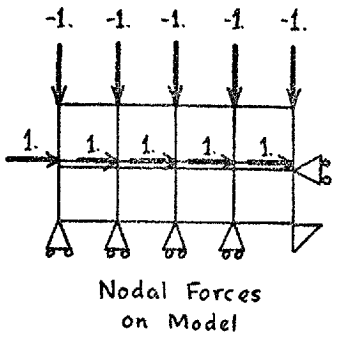


Figure 4.32

The symmetrical model of Figure 4.31 was analysed to test the necessary transformations. As anticipated, the results were symmetrical about the centre-line. The stiffness matrices of this model and that of Figure 4.32 were written onto cards so as to minimise computer cost during subsequent tests. Load conditions were then varied in an attempt to consider all possible cases.

Figure 4.33 shows the results of applying shear and normal loading to the simplified shear box model (Figure 4.32). The normalized shear force/displacement law assumed for the discontinuity is given, together with the results of the analysis. The latter shows that elements 9 and 10 are stressed beyond their peak strength, whilst 11 and 12 deform elastically. Yielding of the former two elements results in a progressive increase of load on the latter two, until a stable situation is reached. If the joint residual angle of friction is decreased the situation is no longer stable and slip will occur on all four elements. Exactly similar behaviour was observed for a prestressed model that was constrained normal to the direction of shear loading.





Residual Angle of Friction for Joint = 30°

Element	NORMALIZED Shear Strength	Shear F/A	Shear Displacement	Approx. No.
9	1·988	2·059	2·059	
10	1·994	2·031	2·031	
11	1·657	1·657	1·657	1
12	1·394	1·394	1·394	
9	1·982	2·019	2·090	
10	1·987	2·026	2·063	
11	1·679	1·679	1·679	2
12	1·407	1·407	1·407	
9	1·978	2·004	2·112	
10	1·983	2·010	2·085	
11	1·695	1·695	1·695	3
12	1·416	1·416	1·416	
9	1·968	1·970	2·160	
10	1·973	1·975	2·134	
11	1·728	1·728	1·728	10
12	1·436	1·436	1·436	

Figure 4.33

Further tests demonstrated parting in tension, dilatation during shear and resistance to normal load.

4.6 CONCLUSIONS

In the author's opinion the finite element method may be used to provide a satisfactory simulation of the behaviour of jointed rock slopes, providing small displacement theory is relevant to the case considered. Using the techniques outlined in this chapter, virtually any behaviour of rocky materials may be simulated providing it can be adequately defined. Each of the constitutive laws discussed in this chapter have been applied to simple models. In principle they may be applied to the real situation. However, the latter can only be adequately simulated if precise field data is available and these methods are extended to cover the general three dimensional case.

(1) Goodman, R.E., Taylor, R.L., & Brekke, T.L. A Model for the Mechanics of Jointed Rock. A.S.C.E. Vol. 94, S.M.3. May, 1968.

(2) Duncan, J.M. & Goodman, R.E. Finite Element Analyses of Slopes in Jointed Rock. Report to the U.S. Army Corps of Engineers, Vicksburg, Miss. Contract No. DACW39-67-C-0091 by Geotechnical Engineering, University of California, Berkeley.

(3) Tamuly Phukan, A.L., Lo, K.Y., & La Rochelle, P. Stresses and Deformations of Vertical Slopes in Elasto-Plastic Rocks. 11th Symp. Rock Mechanics 1969, Berkeley, California.

(4) Duncan, J.M. & Dunlop, P. Slopes in Stiff-Fissured Clays and Shales. A.S.C.E. Vol. 95, S.M.2. March, 1969.

(5) Perloff, W.H. Strain Distribution around Underground Openings. Tech. Report No. 1. Perdue University, Lafayette, Indiana. June, 1969.

(6) Judd, W.R. & Perloff, W.H. Strain Distribution around Underground Openings. Tech. Report No. 5. Perdue University, Lafayette, Indiana. March, 1971.

(7) Zienkiewicz, O.C., Valliapan, B.E. & King, I.P. Stress Analysis of Rock as a No Tension Material. Géotechnique 18.1.1968.

(8) Heuzé, F.E. The Design of Room and Pillar Structures in Competent Jointed Rock. Ph.D. Thesis 1970, University of California, Berkeley.

(9) Cundall, P.A. The Measurement and Analysis of Accelerations in Rock Slopes. Ph.D. Thesis, London University, 1971.

(10) Malina, H. The Numerical Determination of Stresses and Deformations in Rock taking into account Discontinuities. Rock Mechanics and Eng. Geol. Vol. 2/1, 1970.

(11) Hofmann, H. The Deformation Process of a Regularly Jointed Discontinuum during the Excavation of a Cut. 2nd International Cong. of I.S.R.M., Belgrade, 1970, Paper 7.1.

(12) Zienkiewicz, O.C., Valliapan, S., & King, I.P. Elasto-Plastic Solutions of Engineering Problems 'Initial Stress', Finite Element Approach. Int. Journal for Numerical Methods in Eng. Vol. 1. p. 75 - 100, 1969.

(13) Sharp, J. . Fluid Flow through Fissured Media. Ph.D. Thesis London University, 1970.

(14) Maini, Y.N. Measurement of In-situ Hydraulic Parameters. Ph.D. Thesis. London University, 1971.

(15) Goodman, R.E. Personal Communication. 1971.

(16) Trollope, D.H. The Mechanics of Discontinua or Clastic Mechanics. Rock Mechanics in Engineering Practice. Pub. J. Wiley & Sons, 1968.

(17) Trollope, D.H. & Burman, B.C. The Stability of Slopes in Hard Jointed Rock. 2nd International Cong. of I.S.R.M., Belgrade, 1970. Paper 7.11.

(18) Cundall, P.A. A Computer Model for Simulating Progressive Large-Scale Movements in Blocky Rock Systems. Symposium on Rock Fracture. Nancy, 1971. Paper II.8.

(19) Goodman, R.E. Personnal Communication. 1968.

(20) Ashby, J. Toppling Modes of Failure in Models and Rock Slopes. M.Sc. Dissertation. Imperial College, London University, 1971.

(21) Goodman, R.E. & Dubois, J. Duplication of Dilatant Behaviour in the Analysis of Jointed Rocks. For U.S. Army Corps of Engineers, Omaha District, Contract DACA-45-70-C0088 neg. September, 1971.

(22) Goodman, R.E. The Deformability of Joints. Determination of the In Situ Modulus of Deformation of Rock, A.S.T.M. S.T.P. 477.

(23) Patton, F.D. Multiple Modes of Shear Failure in Rock and Related Materials. Ph.D. Thesis, University of Illinois, 1966.

(24) Ladanyi, B. & Archambault, G. Simulation of Shear Behaviour of a Jointed Rock Mass. Proc. 11th Symposium on Rock Mechanics, 1969, Berkeley, California.

(25) Krsmanovic, D., Tufo, M. & Langof, Z. Shear Strength of Rock Masses and Possibilities of its Reproduction on Models. 1st Int. Congress I.S.R.M. 1966. Paper 3.52.

(26) Barton, N.R. A Model Study of the Behaviour of Steep Excavated Rock Slopes. Ph.D. Thesis, University of London, 1971.

(27) Zienkiewicz, O.C., Best, B., Dullage, C. & Stagg, K.G. Analysis of Non-Linear Problems in Rock Mechanics with particular reference to Jointed Rock Systems. 2nd International Congress I.S.R.M. 1970. Paper 8.14.

(28) Burland, J.B. & Lord, J.A. The Load-Deformation Behaviour of Middle Chalk at Mundford, Norfolk. Current paper 6/70 Building Research Station, Watford.

CHAPTER

5

THREE DIMENSIONAL ANALYSIS OF ROCK SLOPES

	Page
Chapter Index	159
Synopsis	160
5.1 Introduction	161
5.2 The Sliding of a Rigid Wedge	162
5.3 Stress Analysis of a Three Dimensional Excavation	167
5.4 Analysis of General Three Dimensional Structures in Jointed Rock	177
5.5 The Analysis of Wedge Type Structures by Finite Elements	179
5.6 An Extension to Vector Methods for Wedge Analysis	189
5.7 Conclusions	195
References	197

SYNOPSIS

The method of determining the stability, against sliding, of a wedge defined by two planes of weakness in a slope is presented briefly. Vector analysis is used, since this provides a basis for the presentation of an extension of this method that takes into account joint deformability.

The influence of slope plan is discussed with reference to analyses of axisymmetrical excavations. A fully three-dimensional Finite Element computer program capable of modelling jointed rock masses is presented. Results obtained for simple sliding wedge models, are discussed with particular reference to the importance of joint deformability. Reference is also made to the influence of initial stresses and computer simulation of progressive failure.

5.1 INTRODUCTION

The analysis of the previous chapters assumed that a rock slope can be considered to be of infinite lateral extent and that discontinuities always strike parallel to the slope face. These assumptions are now discarded and the fully three-dimensional problem examined, albeit in terms of very simple models.

Following the sequence of previous chapters, attention is given first to simple sliding wedge models, then to stress analysis assuming that rock behaves as a continuum, and finally to Finite Element simulation of jointed rock slopes.

5.2 THE SLIDING OF A RIGID WEDGE

The simple sliding wedge model of Section 1.3.1 may be extended to three dimensions by consideration of tetrahedral wedges defined by two planes of weakness passing through a rock slope. Such situations are amenable to analysis using graphical techniques based on stereographic projection (Refs. 1, 2), although only a vector-based method will be discussed below (Refs. 3, 4, 5).

5.2.1 Vector Definition of the Problem

In order to solve numerically for the forces on the planes of weakness defining a wedge in a slope, it is necessary to describe the geometry vectorially. The presentation here follows Wittke (Ref. 5) and is therefore brief, but hopefully sufficient for the purposes of development later in this chapter.

The orientation of the two planes of weakness OBD and OCD in Figure 5.1 are completely defined by the vectors $\vec{u}_1, \vec{v}_1$ and $\vec{u}_2, \vec{v}_2$ respectively. These represent the dip ($\vec{v}_{1,2}$) and strike direction ($\vec{u}_{1,2}$) of the planes according to the convention defined by Figure 5.1. Since these vectors lie on their respective planes, then the normal to each plane may be expressed as a vector product.

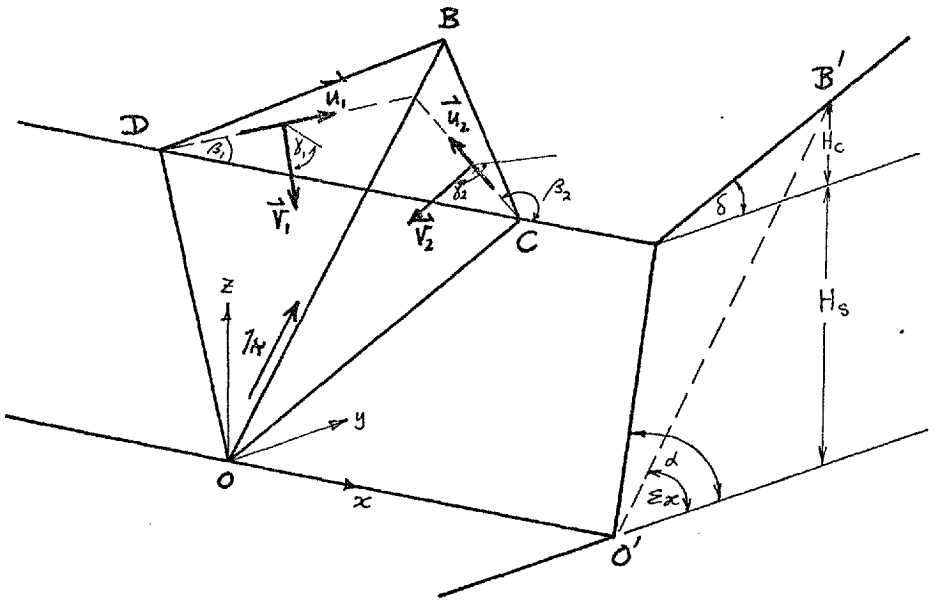


Figure 5.1

$$\vec{\omega}_{1,2} = \vec{u}_{1,2} \times \vec{v}_{1,2} \qquad 5(1)$$

In like manner the direction of the intersection of the two planes is obtained from the vector product of the normal to each.

$$\vec{x} = \vec{w}_1 \times \vec{w}_2 \qquad 5(2)$$

From the vector $\vec{x}$ which defines the intersection line OB the angle of the projection of OB on the YZ plane (ε_x) is given by:

$$\text{Tan}\,(\varepsilon_x) = \frac{x_z}{x_y} \qquad 5(3)$$

The total height of the wedge can be expressed in terms of the slope angle (α), the crest angle (δ) & the slope height (H_s)

$$H = H_S + H_C = H_S\left(1 + \frac{\tan\alpha - \tan\varepsilon_x}{\tan\varepsilon_x - \tan\delta} \cdot \frac{\tan\delta}{\tan\alpha}\right) \qquad 5(4)$$

where H_C is the height of the wedge apex above the crest of the slope.

The vectors defining OD, OC, OB, both in magnitude and direction, can now be determined from simple geometrical considerations, and from these the areas of the planes and the volume of the wedge can be expressed as:-

$$\text{Area OBD} = \frac{1}{2} \cdot \left| \vec{OD} \times \vec{OB} \right|$$

$$\text{Area OCB} = \frac{1}{2} \cdot \left| \vec{OC} \times \vec{OB} \right|$$

$$\text{Volume OBCD} = \frac{1}{6} \cdot h \cdot \left| \vec{OC} \times \vec{OD} \right|$$

where $h = \sin(\alpha - \varepsilon_x)\sqrt{(OB_y^2 + OB_z^2)}$

5.2.2 Stability Against Sliding

Ignoring rotational modes, sliding can occur in three possible ways:

(a) On face 1 only; parallel to the dip direction of plane 1.

(b) On face 2 only; parallel to the dip direction of plane 2.

(c) On both faces; parallel to the intersection.

The first two possibilities will occur if it is kinematically possible to slide parallel to the direction of dip of either of the two planes. (Should either plane 1 or plane 2 strike parallel to the face then (a) or (b) must occur, since a tetrahedral wedge is

not defined, and the problem reduces to the case of Section 1.3.1).

It is possible to determine whether sliding occurs on one or two planes by a simple vector comparison. Defining $\vec{y}_{1,2}$ as vectors of the normals to the planes by the following equation:

$$\vec{y}_{1,2} = \vec{v}_{1,2} \times \vec{x} \qquad 5(6)$$

It is then possible to compare the direction of $\vec{y}_{1,2}$ with the original normal vectors $\vec{w}_{1,2}$. They must be parallel but they may be in opposite directions. If either are in the opposite sense then sliding will occur on that plane alone. If both are in the same sense then sliding will occur along the intersection, i.e.

If either $\dfrac{\vec{y}_{1,2}}{|\vec{y}_{1,2}|} = -\vec{w}_{1,2}$ sliding $\parallel \vec{v}_{1,2}$

If both $\dfrac{\vec{y}_{1,2}}{|\vec{y}_{1,2}|} = \vec{w}_{1,2}$ sliding $\parallel \vec{x}$

The case of sliding on one plane only is trivial once the condition has been selected as being relevant, so attention will be restricted to consideration of sliding along the intersection.

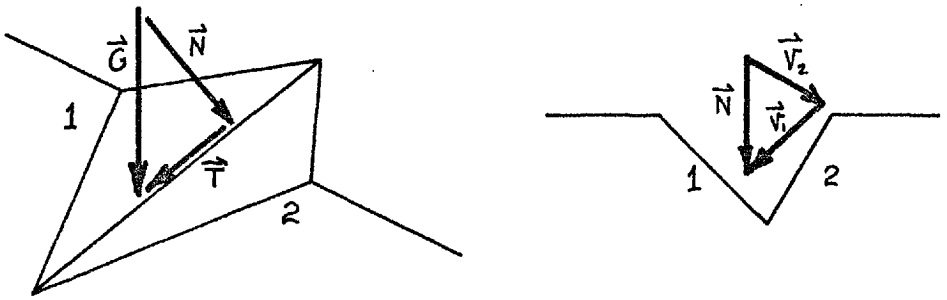


Figure 5.2

If the total weight of the wedge is expressed as the vector $\vec{G}$

then the force tending to cause sliding is:-

$$|\vec{T}| = \vec{G} \cdot \frac{\vec{x}}{|\vec{x}|} \qquad 5(8)$$

The vector $\vec{T}$ must have the same sense as $\vec{x}$ and have the magnitude defined by equation 5(8). Therefore:-

$$\vec{T} = \frac{1}{|\vec{x}|^2} \cdot |\vec{G} \cdot \vec{x}| \cdot \vec{x} \qquad 5(9)$$

And the component of weight normal to the intersection is:-

$$\vec{N} = \vec{G} - \vec{T} \qquad 5(10)$$

$\vec{N}$ clearly represents the resultant of the normal forces on the two planes. Since these forces must be parallel to the normals $\vec{\omega}_{1,2}$ then:-

$$\vec{N} = \vec{V}_1 + \vec{V}_2 = d_1 \cdot \vec{\omega}_1 + d_2 \cdot (-\vec{\omega}_2) \qquad 5(11)$$

where $\vec{V}_{1,2}$ are the vectors of the normal forces and have magnitudes $d_{1,2}$. The vector equation 5(11) can be written as three separate equations in terms of vector components and solved for the constants.

The total available shear force (T') resisting sliding, assuming a Coulomb strength law is:-

$$T' = c_1 \cdot A_1 + d_1 \tan\phi_1 + c_2 \cdot A_2 + d_2 \tan\phi_2 \qquad 5(12)$$

where $c_{1,2}$ and $\phi_{1,2}$ are, respectively, the cohesion and friction angles for the planes of weakness.

The factor of safety against sliding can therefore be written as:-

$$F.S. = \frac{T'}{|\vec{T}|} \qquad 5(13)$$

Alternatively, the angle of friction necessary to prevent sliding on either plane may be calculated if some assumption regarding cohesion is made. This approach has the advantage that it is immediately apparent which plane is the most critical. The method of analysis may then be treated as an aid to engineering judgement rather than a 'black-box' producing answers.

5.2.3 Implementation of Three-Dimensional Wedge Analysis

The vector analysis described briefly above is simple to program on a computer, particularly if a subroutine is used for all vector manipulations. Such a procedure is adopted in the program listed in Appendix C. This program is written so that only sliding is considered as a possible mode of failure and it is assumed that loading is due to an acceleration vector only. (This will normally be the acceleration due to gravity.) Additional forces and other shear strength criteria may, of course, be considered without complication.

The large number of possible variables in the sliding wedge situation preclude the deduction of general results. Hoek and Boyd (Ref. 6) considered the case of a gravity loaded wedge defined by two planes of weakness with equal angles of friction, and no cohesion, on each. For this model, they were able to draw up a series of charts relating the differences in dip and dip direction of the two planes with the necessary angle of friction to prevent sliding. The author considers that this paper is important because it demonstrates the fundamental simplicity of this type of analysis that is so often lost in a mass of vector equations and stereographic projections.

5.3 STRESS ANALYSIS OF A THREE-DIMENSIONAL EXCAVATION

Currently, it is not possible to analyse three dimensional excavations with arbitrary geometry in any great detail. Even an extension of the simple models of Chapter 3 is beyond the reasonable capabilities of present computers, except for the special case of axisymmetrical excavations. The methods of analysis described in Chapter 4 are, of course, available, and may readily be utilized on the arrival of larger and faster machines. Using the finite element programs listed in Appendices B and D in excess of 500 nodes may be used in any model if the full capacity of a CDC 6400 (45K Core Storage) computer is utilized. A single elastic analysis of such a model would require about 80 seconds computing time for the two-dimensional case and considerably more for the three-dimensional case. It is impossible to be more precise without reference to particular elements and the method of formulation of their properties. As far as the three-dimensional models are concerned the real limitation with the given program is the band width restriction. Any cross section is thus limited to representation with about twenty nodes. Alternative methods of solution of equation must be adopted if larger models are to be studied (Section 2.3).

5.3.1 Axisymmetric Analysis

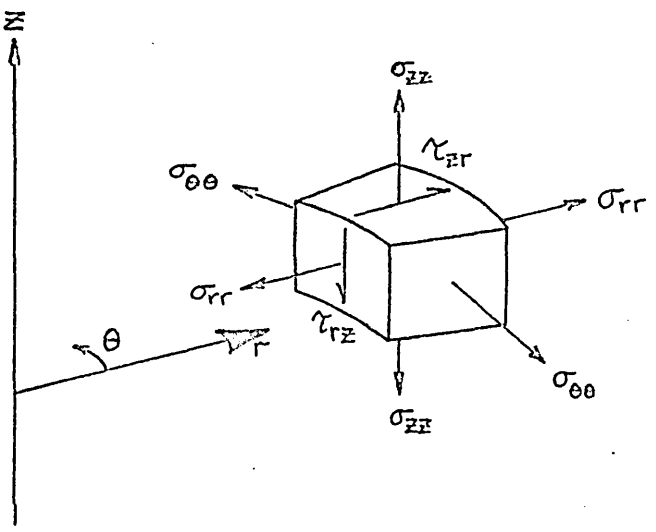


Figure 5.3

The analysis of axisymmetric situations can be achieved by modification of the finite element method as applied to the solution of two dimensional problems. By symmetry, the two in plane components of displacement (referred to r, z co-ordinates in Figure 5.3) completely define the state of strain and therefore the stress. The only modifications required to the two dimensional approach are therefore concerned with the consideration of ring rather than plate elements. The integration of the element properties must now be carried out over the volume of revolution.

Treatment of axisymmetric analysis is given in the text by Zienkiewicz and Cheung (Ref. 7). The program used by the author is a modified version of that given by Perloff (Ref. 8) for the analysis of elasto-plastic axisymmetric continua, and its basis is described by Wilson (Ref. 9).

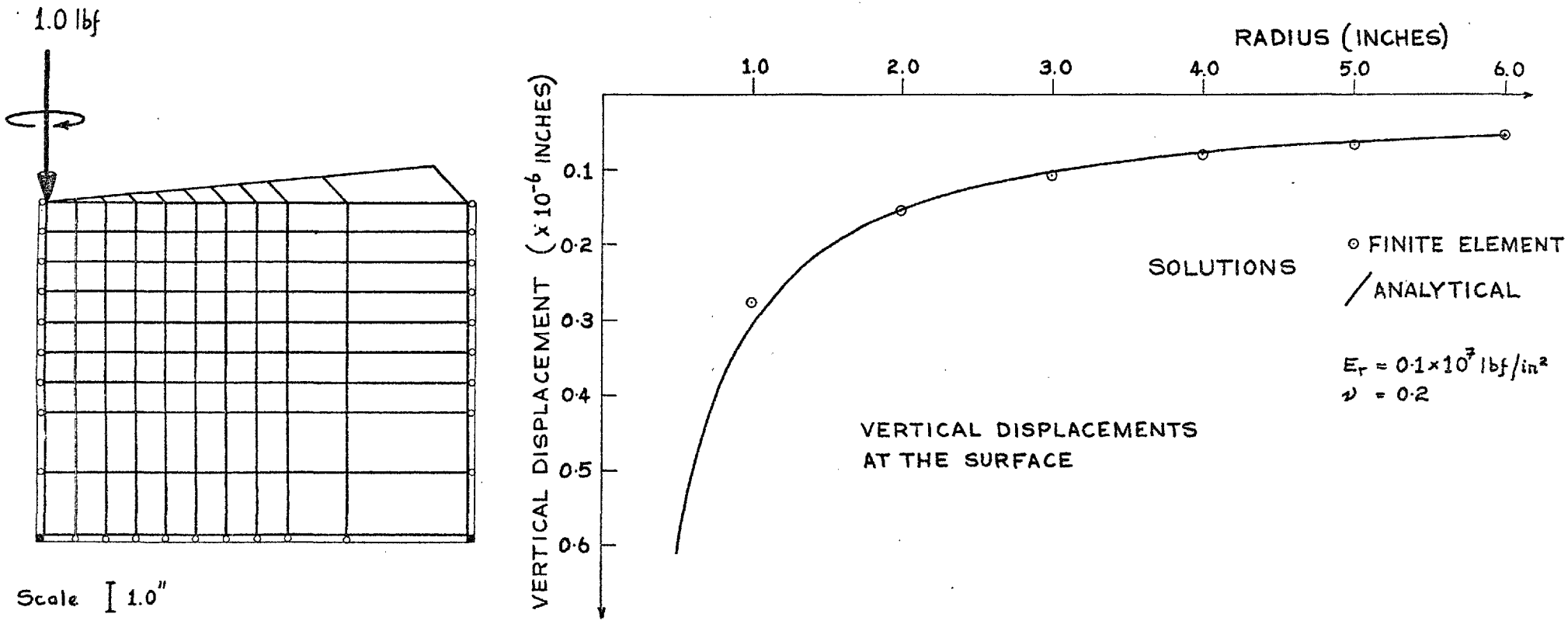
A comparison was made between analytical results for the point loading of an infinite elastic half space and a simple computer model of the same.

Even the small number of elements used provided a good approximation (Fig. 5.4). (The computer values in Figure 5.4 include a correction to take account of the limited vertical extent of the model.)

Since the agreement was excellent, further checks were restricted to the same model subject only to gravity loading. As anticipated, the circumferential and radial stresses were constant across any plane defined by constant z.

5.3.2 Axisymmetric Excavations

In open pit mines it has often been noted that the more stable portions of the excavation are those where the three dimensional shape of the pit is constricting. Conversely, promontories are observed to be less stable. This phenomenon is generally attributed to an increase in circumferential stresses in areas where the plan is concave. The discussion by Jenike and



AXISYMMETRIC MODEL OF POINT LOAD ON ELASTIC HALF SPACE

FIGURE 5.4

Yen (Ref. 10) concerning axisymmetric pits strictly refers only to the zone in plastic equilibrium around a circular shaft. The author therefore, considered it worthwhile to study the basis of the general assumption, given by Hoek (Ref. 11), concerning the importance of pit geometry (Fig. 5.5).

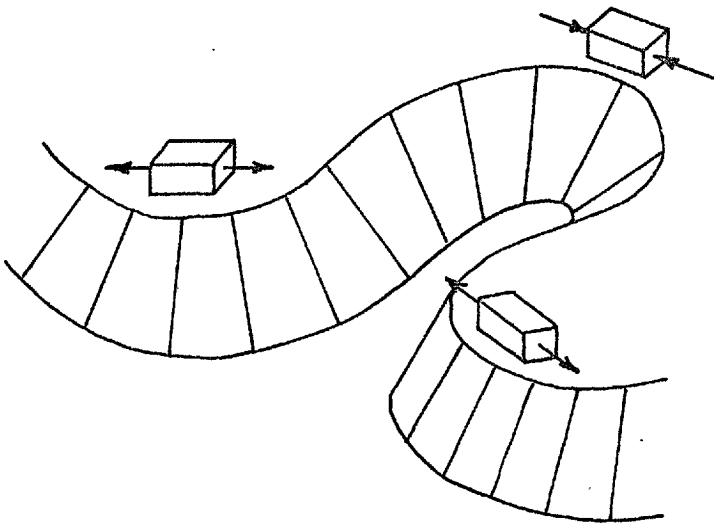


Figure 5.5

In order to study this problem a number of analyses of a 45^{o} slope were run for comparison. The several possibilities are:-

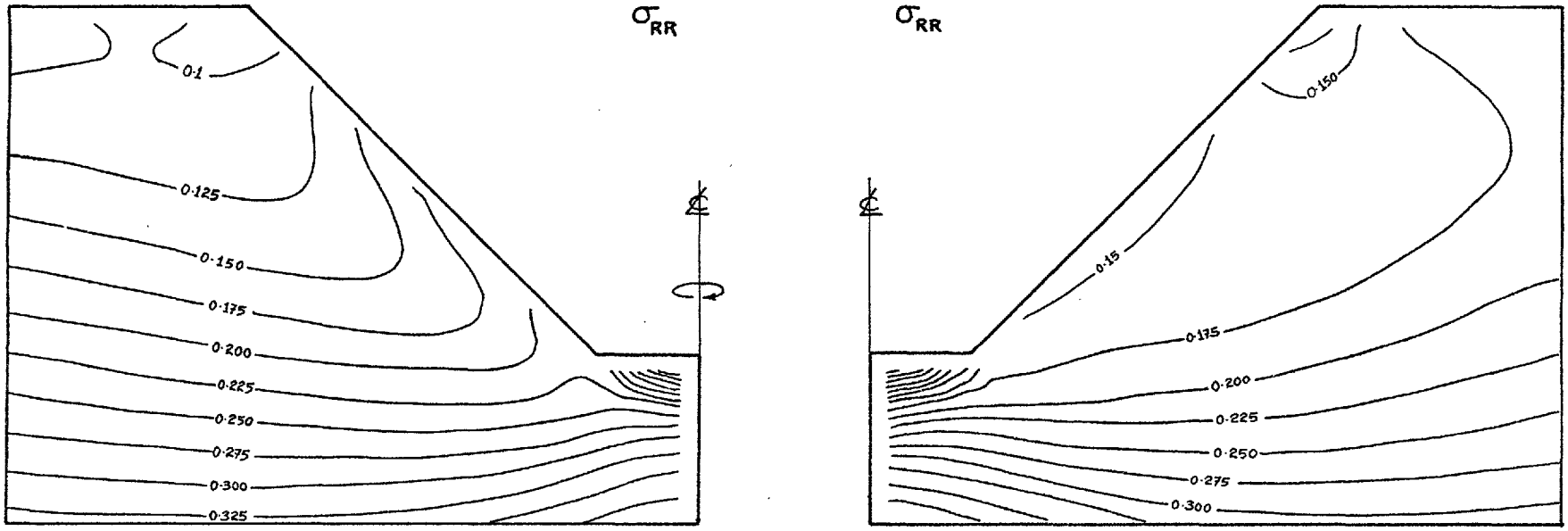
(a) Plane Stress - zero normal stresses by definition.

(b) Plane Strain - zero normal displacements by definition, so that the circumferential stress is given by:-

$$\sigma_{\theta\theta} = \nu . \left(\sigma_{rr} + \sigma_{zz} \right)$$

(c) The axisymmetric excavation, which for extreme cases is either a conical buttress or pit.

The results of analyses of the plain strain and axisymmetric pit, using the model type given in Section 3.6 are presented in Figures 5.6, 5.7 and 5.8. The two solutions are drawn opposite

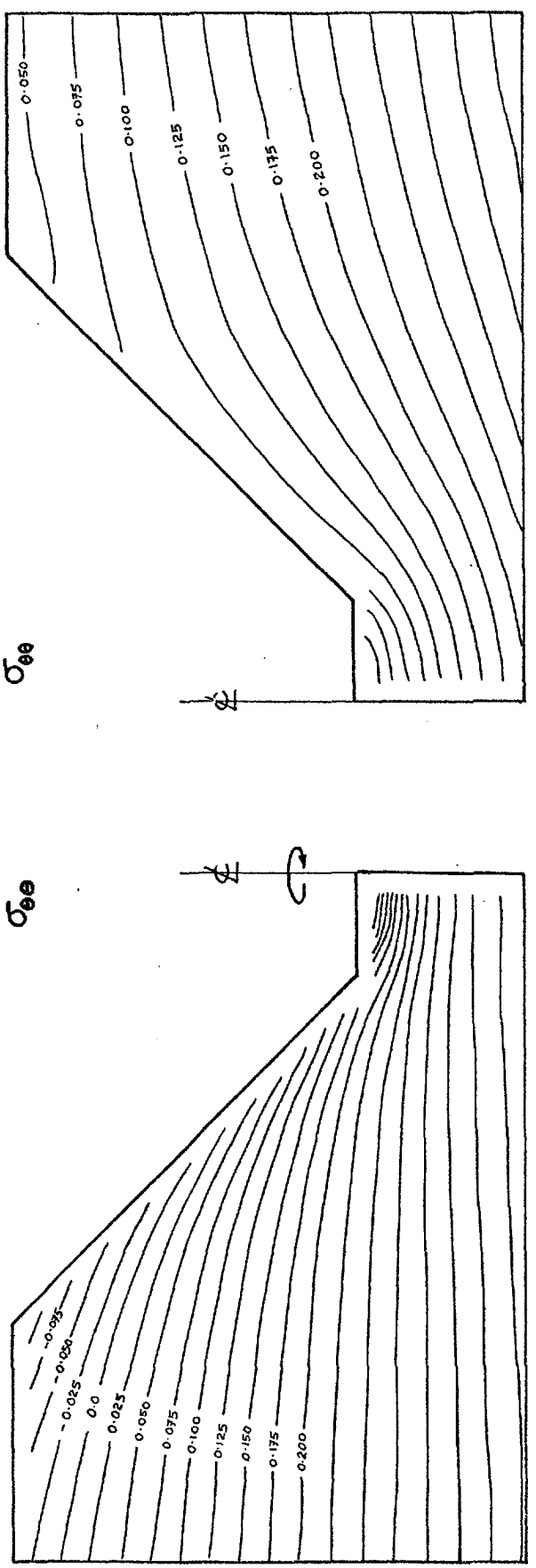


AXISYMMETRIC

PLANE STRAIN

NORMALIZED RADIAL STRESSES

FIGURE 5.6



NORMALIZED CIRCUMFERENTIAL STRESSES

FIGURE 5.7

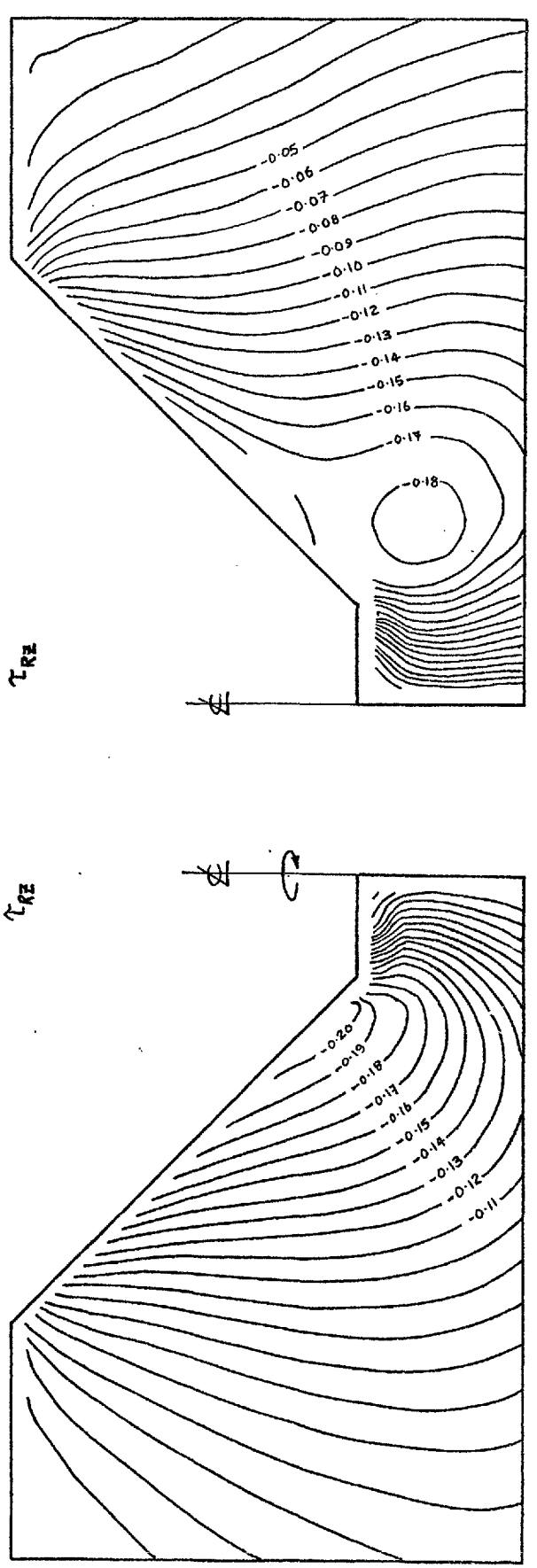

PLANE STRAIN
τ_{RZ}
-0·05
-0·06
-0·07
-0·08
-0·09
-0·10
-0·11
-0·12
-0·13
-0·14
-0·15
-0·16
-0·17
-0·18
NORMALIZED SHEAR STRESSES
AXSYMMETRIC
τ_{RZ}
-0·20
-0·19
-0·18
-0·17
-0·16
-0·15
-0·14
-0·13
-0·12
-0·11

FIGURE 5.8

each other for all except the vertical stresses, which were virtually identical. It is observed that there is a large reduction in radial stress behind the slope, comparing axisymmetric with plain strain solution. There is also a pronounced region of tensile hoop, or circumferential stress in the crest, which would result in radial cracking in a real situation. Although this is apparently in conflict with the expected presence of high compressive circumferential stresses, there is also a marked increase in confining stress in the lower portion of the slope. The latter is probably associated with the small radius of the toe. The effect will therefore become less marked as the radius increases, with the plain strain solution providing a limiting condition equivalent to an excavation of infinite diameter.

Cundall (Ref. 12) observed that the deformed state of the axisymmetric pit was equivalent to an outward rotation of the crest. This resulted in an increase in radius and therefore tensile circumferential stresses. The author's analysis of a 45° buttress (Fig. 5.9) revealed the same outward rotation of the crest, but in this case, a decrease in radius is occasioned. The circumferential stresses, therefore, tend to be higher in the crest region and lower in the main body of the slope.

Figure 5.9 reveals that although the circumferential stresses are low, they are not tensile as was expected. Comparison of the other stresses shows a general fall in radial stresses except on the slope face, and little change in vertical stresses. However, it should be noted that strict comparison is rather difficult since the models of conical 'pillar' and 'pit' are essentially dissimilar.

In order to evaluate the difference between the plain strain and conical pit analyses, a 'Ubiquitous Joint Analysis' was performed for each. The results given in Figure 5.10 for a 30° joint set are different, but consideration of the minimum Shearing Ratio (Section 3.11.3) for various joint orientations reveals little overall variation between the two cases. In any case, the necessary assumption of conical planes of weakness seems rather unrealistic, so the results are not reproduced in any detail.

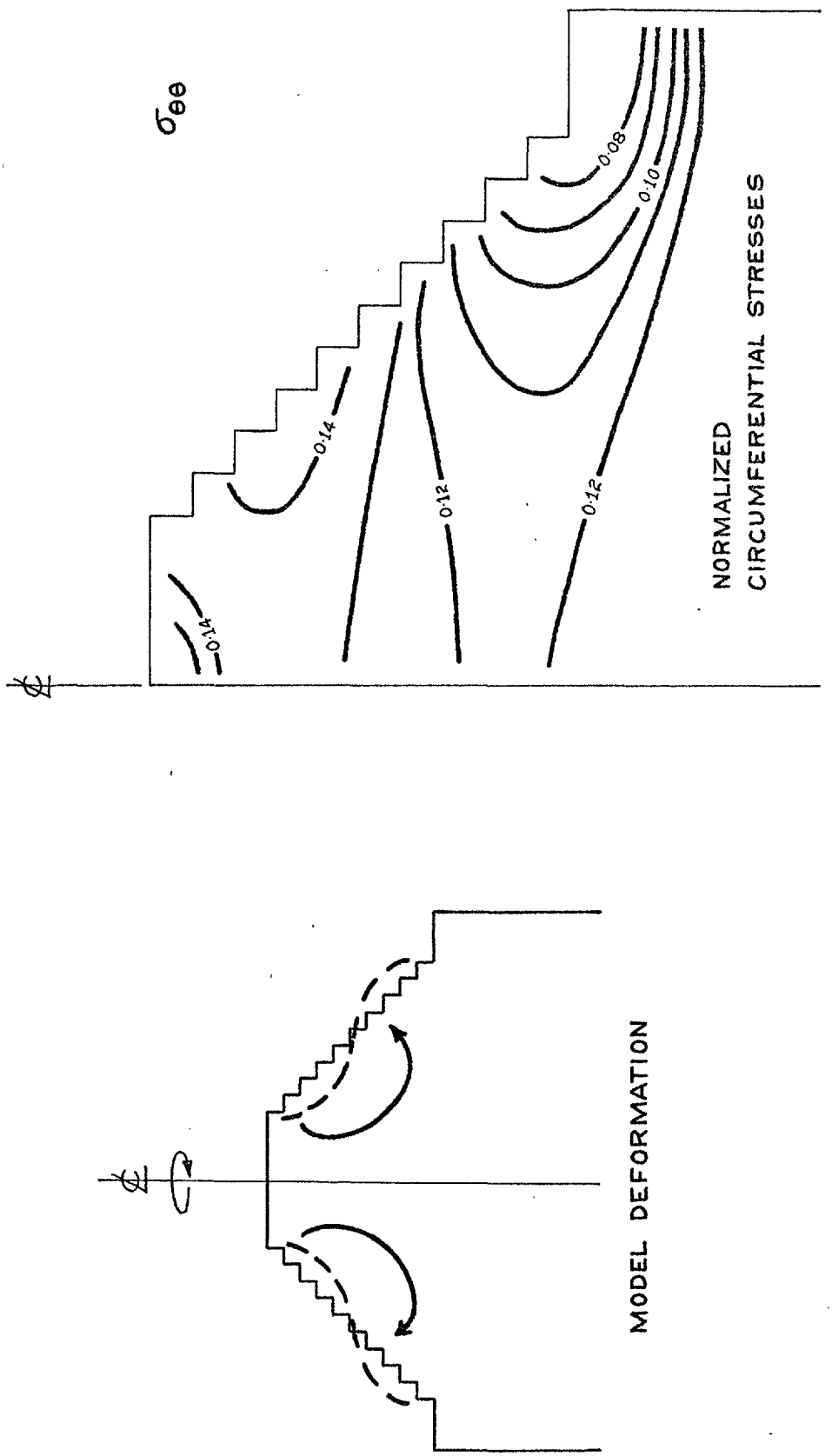
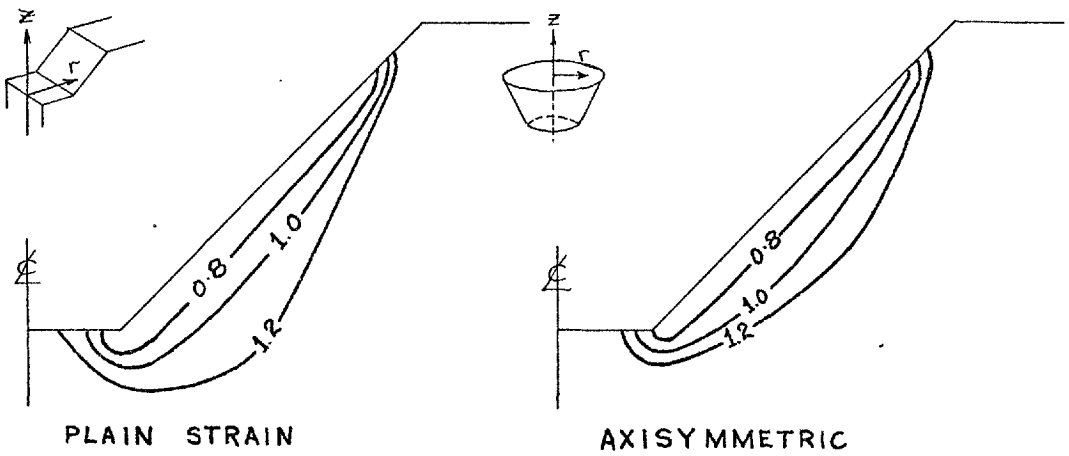

$\sigma_{\theta\theta}$
0·14
0·12
0·12
0·10
0·08
0·14
NORMALIZED
CIRCUMFERENTIAL STRESSES
AXSYMMETRIC BUTTESS ANALYSIS
MODEL DEFORMATION

FIGURE 5.9



Model as Figure 3.17
Figure 5.10

The general conclusion that may be drawn from all these analyses is that the stress distribution is unlikely to have a marked effect on stability. In a real situation the explanation of variation in stability is likely to be statistical (Fig. 5.11).

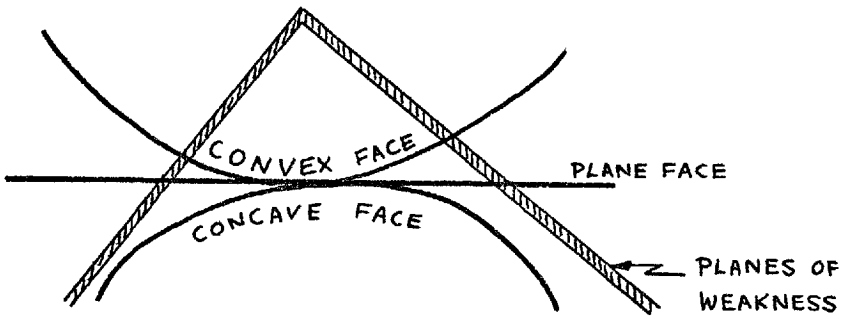


Figure 5.11

There is an increased likelihood that a 'kinematically feasible' block will be defined by planes of weakness if the slope is buttress shaped. In addition, this situation corresponds to the maximum possible volume of material involved in the potential slide, if all other things are equal.

5.3.3 Further Axisymmetric Models

The analyses discussed above consider only the case of rock behaving as a continuous, isotropic, homogeneous, linearly elastic solid. The only other cases that can be studied are conditions of transverse isotropy or horizontal jointing. All other cases involve physically unreasonable features in an axisymmetric situation, so treatment along the lines of Chapter 4 was not considered in this connection.

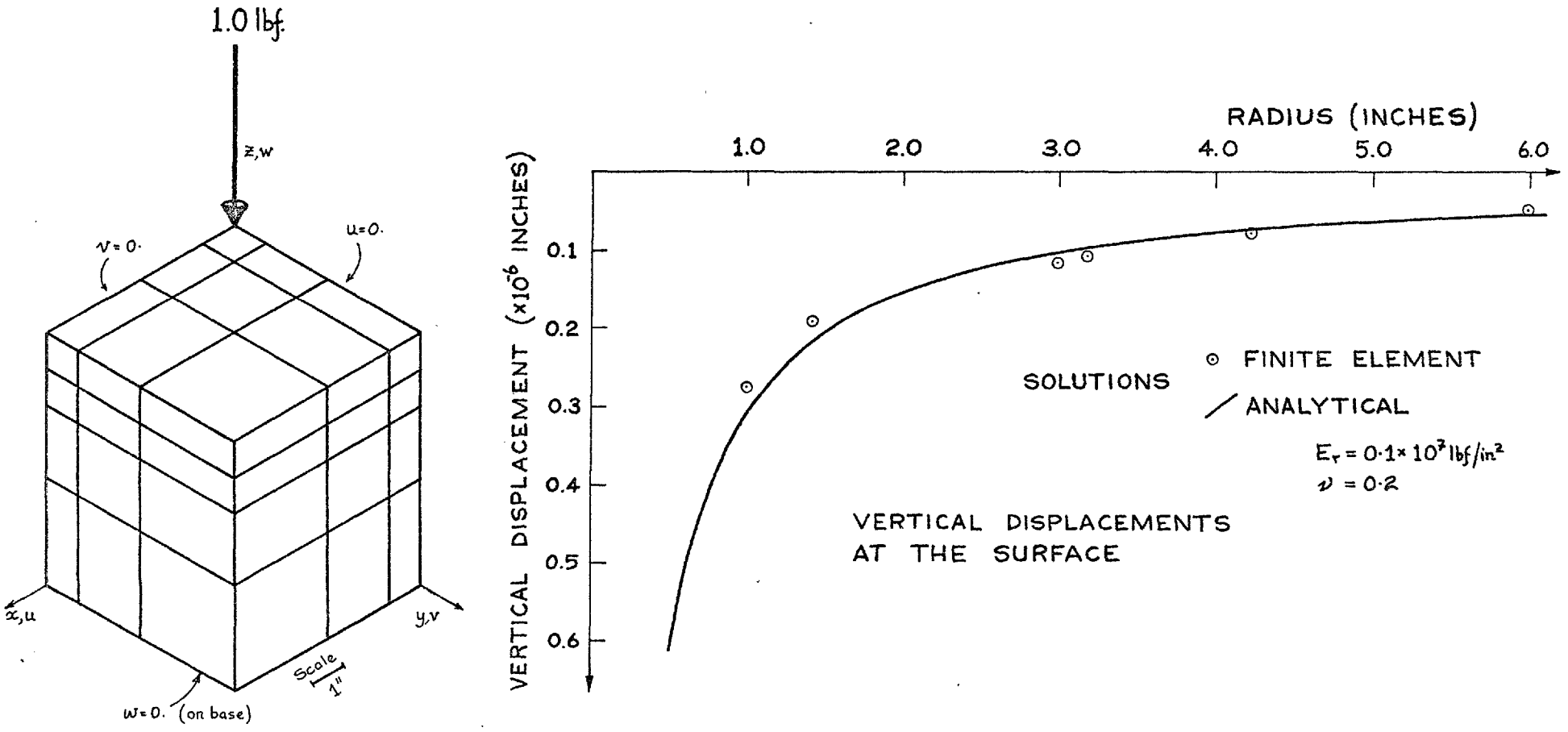
5.4 ANALYSIS OF GENERAL THREE DIMENSIONAL STRUCTURES IN JOINTED ROCK

Although it was stated above that it is not yet possible to analyse general structures in any detail, using the Finite Element method, simple models may be treated in order to assess the importance of assumptions inherent in current methods of analysis. The particular aim of the studies to be discussed below was to determine whether the sliding wedge models treated above ignore important physical parameters of the real situation.

5.4.1 Computer Programs and Verification

In the course of this study, two computer programs for the Finite Element Analysis of three dimensional structures in jointed rock were written. The purpose of this duplication was to provide a relatively independent check on the results obtained. The main difference between the two programs was that the first was built round tetrahedra based solid elements and triangular joint elements whilst the second was built on the natural co-ordinate elements described in more detail in Chapter 2. Since the earlier of these two programs has already been published by the author (Ref. 13) only the second is listed in Appendix C.

Verification of the programs is conveniently treated in two parts. The continuum elements may be tested against the Boussinesq solution used above (5.3.1). Again, making allowance for the limited vertical extent of the model, the results are reasonable despite the few elements used in the idealization (Fig. 5.12).



THREE DIMENSIONAL MODEL OF POINT LOAD ON ELASTIC HALF SPACE

FIGURE 5.12

The results using the earlier program are better than the later version, although for the various wedge models to be discussed below there was no appreciable difference.

Initial checks on the joint elements were carried out using elementary models, such as two rigid elements connected by a single joint. These provided a simple check on the transformation involved since the solutions were known from statics. A more rigorous check, using the model (Fig. 5.13) described by Goodman et al (Ref. 14), was made against the program for two dimensional structures. The model consisted of a single rough joint passing through a plate in plane strain and subject to shear loading. Agreement between the two solutions was excellent and the computer program was considered to be reasonably verified.

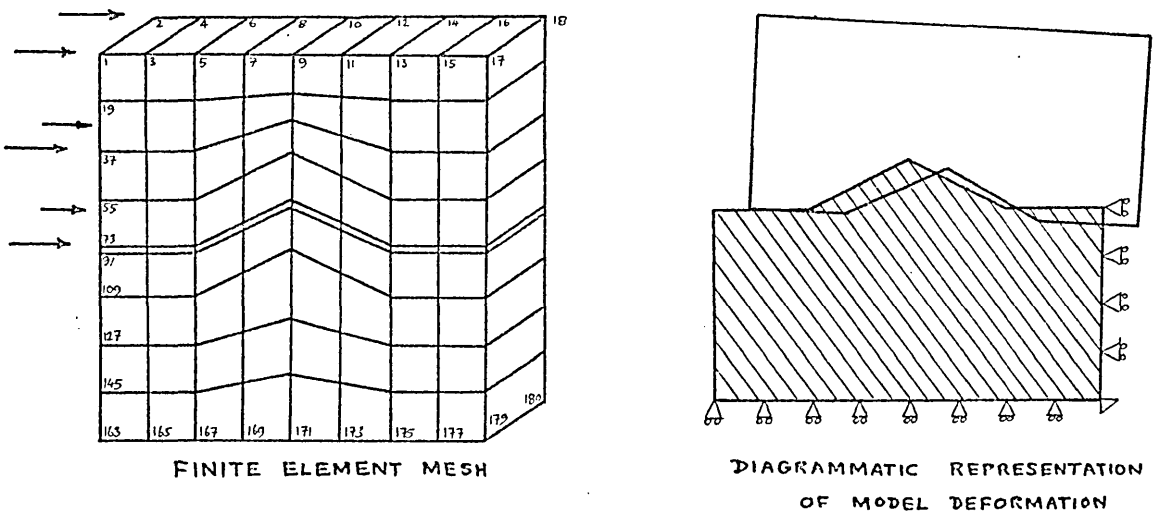


Figure 5.13

5.5 THE ANALYSIS OF WEDGE TYPE STRUCTURES BY FINITE ELEMENTS

The problem to be modelled is a vertical rock slope containing a symmetrical wedge defined by two planes of weakness (Fig. 5.14). For this case the geometrical variables are the wedge height, the aperture of the wedge and the dip of the intersection of the two planes of weakness.

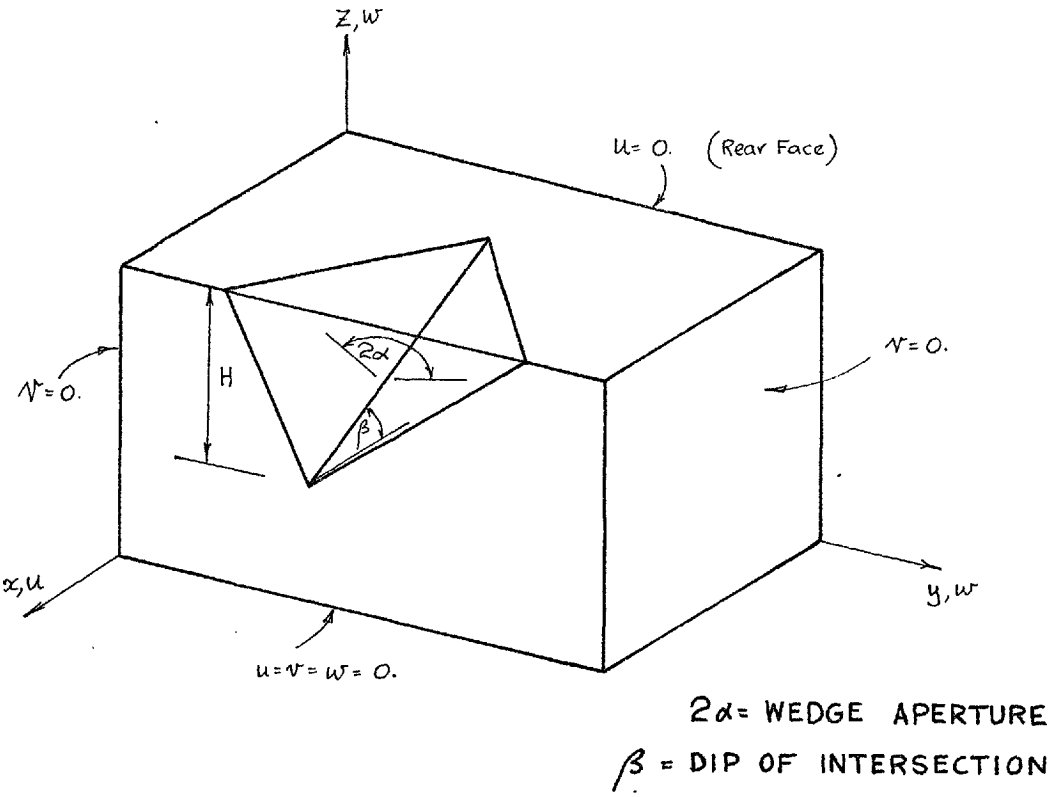


Figure 5.14

Of course the mechanical properties can be varied independently of the geometrical parameters defining the situation. In this case the solid rock is assumed to be isotropic, homogeneous, linearly elastic material so its behaviour is totally described by the Elastic Modulus and Poisson's Ratio. The joint is ascribed normal stiffness and shear stiffness. The latter is assumed to be independent of direction in the programs as they stand at present.

The mesh given in Figure 5.15 is typical of the Finite Element idealizations of this simple situation. The boundary conditions are chosen to suppress displacement on the base and permit only vertical displacement on the rear and sides of the model. In addition, the boundaries were placed sufficiently remote from the wedge to minimise any influence they might have on the result of analysis. (Mahtab & Goodman (Ref. 15) reported that the wedge should be at least its own width away from the boundaries.)

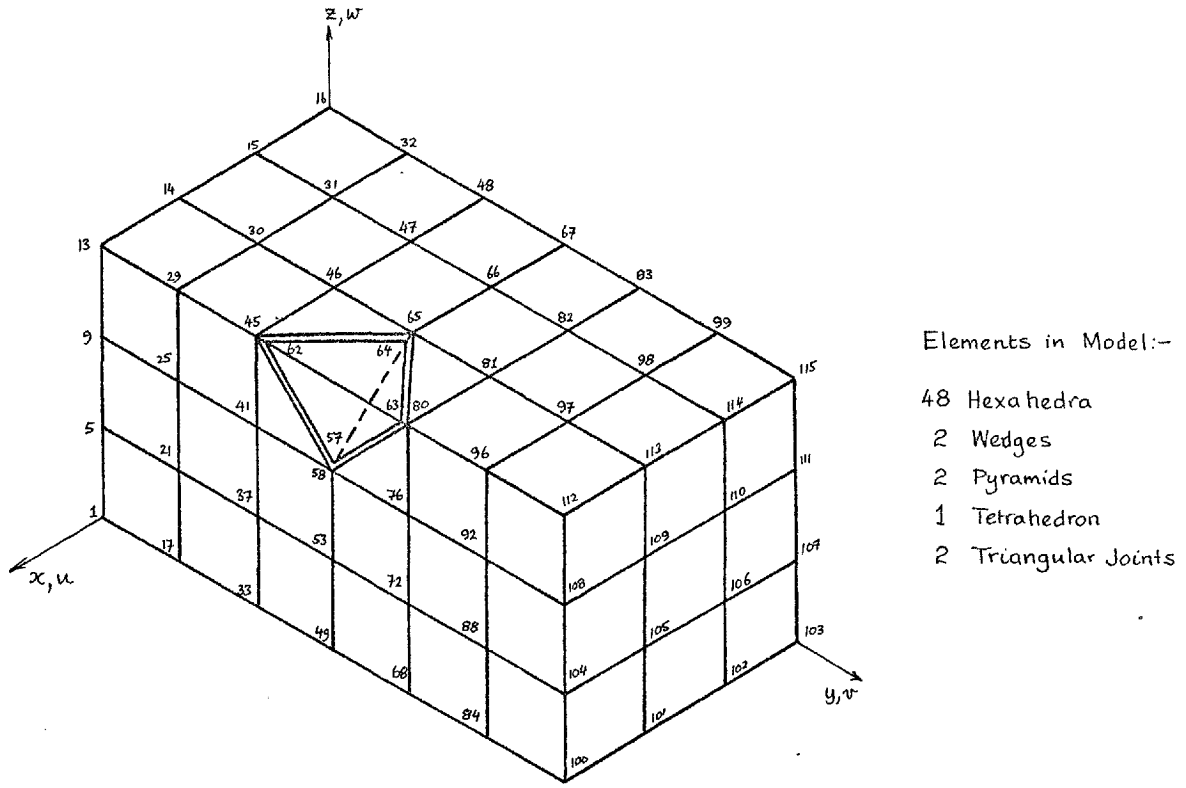


Figure 5.15

5.5.1 The Influence of Material Properties

Assuming a fixed geometry, analyses may be performed with various material properties. These reveal that the elastic modulus of the solid influences the displacements but not the stresses in the model. Additionally, it is noted that only the ratio of the joint stiffnesses influences the stresses on the joint, the magnitude again affecting only the displacements.

5.5.2 Influence of Joint Stiffness on Sliding Stability

Since the results of analysis were insensitive to the solid material properties, these and the wedge height were standardised at the values used by Mahtab & Goodman (Ref. 15) (Table 5.I). This was done partially with a view to obtaining a realistic comparison with their published results. The joint normal stiffness was likewise standardised and the shear stiffness varied to obtain different stiffness ratios. The results of analyses are shear

and normal forces per unit area on the joints. Assuming purely frictional behaviour, the limiting condition on each plane is:-

$$\phi_r \geq \mathrm{Tan}^{-1}\left(\frac{\tau}{\sigma_n}\right) \qquad 5(14)$$

where ϕ_r is the angle of friction required to prevent sliding.

σ_n is the normal force per unit area and τ the shear force per unit area. The output of the computer program is in fact the shear forces per unit area in the dip and strike directions, but the limiting condition is determined from the resultant of these two. Although this does not necessarily correspond with the possible direction of sliding of the wedge it is the correct limiting condition for the model to be valid.

The results of varying the joint stiffness ratio for the case of a wedge aperture of 30° and dip of intersection of 45° are plotted in Figure 5.16. From this figure it is apparent that as the stiffness ratio increases, the solution approximates more closely to that obtained from the rigid wedge analysis discussed above. For low stiffness ratios the results indicate that very high friction angles are required for limiting conditions in this particular case.

Model Parameters:

Included angle of wedge (2α) = 30°
Dip of joint intersection (β) = 45°
Wedge height (H) = 32·8 ft

Rock Properties:

E = 144. x 10^6 psf
ν = 0·25
γ = 149. pcf

Joint Properties:

k_n = 14·4 x 10^6 psf/ft
k_s = k_n / R
Cohesion = 0.

R	1.	10.	100.	RIGID
τ	-291·3	-245·8	-212·5	-211.
σ_n	- 64·5	-343·3	-714·6	-815.
ϕ_r	77·5	35·6	16·6	14.5

Table 5.I

Results of a Typical Series of Analyses

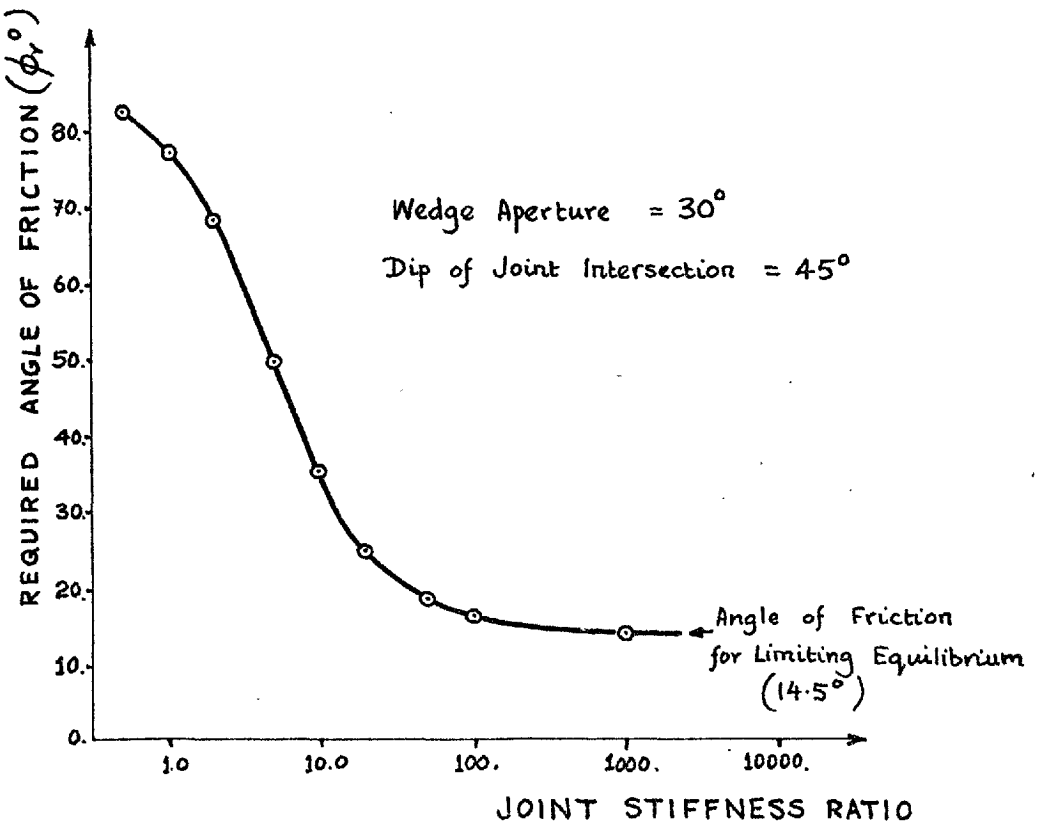
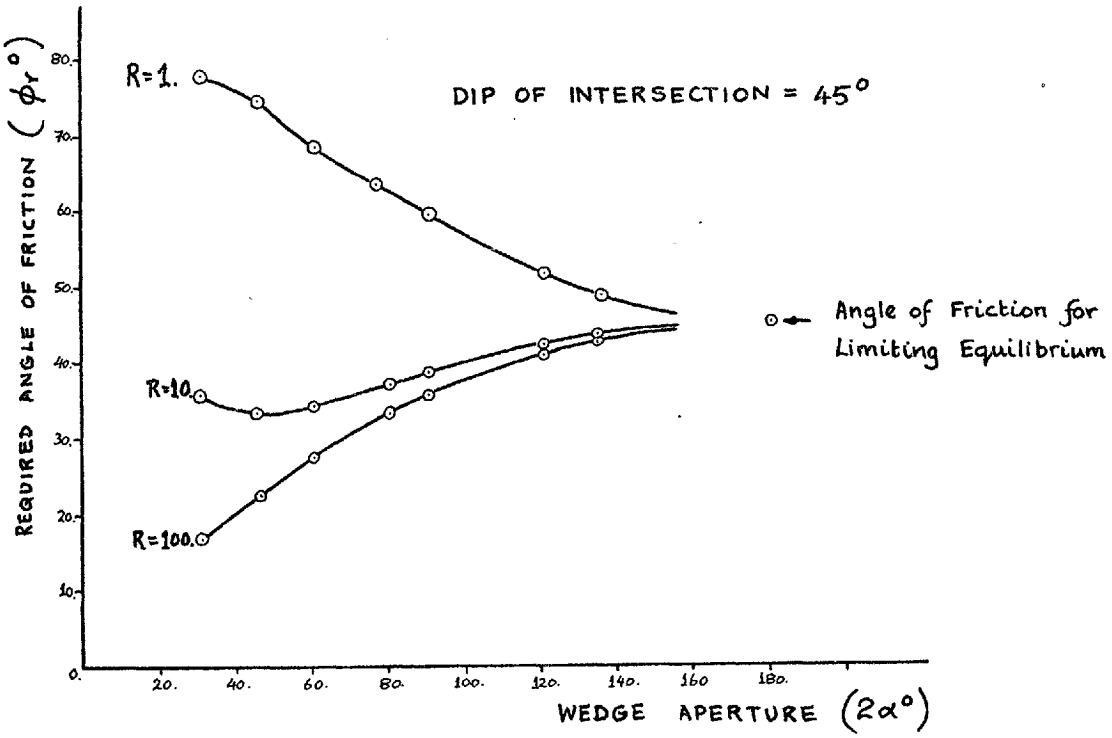


Figure 5.16

5.5.3 Influence of Wedge Aperture

If the analyses of 5.5.2 are run for various wedge apertures, the influence of the latter may be established. Figure 5.17 illustrates a decreasing influence of joint stiffness ratio as the wedge aperture increases. (It is also noticeable that the solutions converge on the rigid wedge analysis in every case, thereby providing additional justification for the computer program.)



VARIATION OF REQUIRED ANGLE OF FRICTION WITH WEDGE APERTURE AND JOINT STIFFNESS RATIO

Figure 5.17

Typical results from a 30° wedge aperture study are given in Table 5.I above. These differ markedly from those published by Mahtab & Goodman (Ref. 15). The reason for this disparity is not clear and it was this that prompted a writing of a second computer program. Not only are the actual results of analysis different, but also the method of assessing limiting conditions. Mahtab and Goodman (Ref. 15) chose to calculate the latter from the actual normal force per unit area and the component of weight of the

wedge tending to cause sliding in the direction of intersection. In the author's opinion, sliding will normally occur in another direction first, and therefore modify the whole situation. This will be discussed in greater detail in connection with progressive failure.

5.5.5 Progressive Failure of Wedge

If joint strength properties are assumed then a comparison of available shear strength and actual shear force per unit area may be made. If the latter exceeds the former then yielding, or slip, may be simulated by determining a new value for shear stiffness of the joint (Fig. 5.18).

$$K_s = \frac{\text{Available Shear Strength}}{\text{Maximum Shear Displacement}} \qquad 5(15)$$

If this procedure is adopted for the single element wedges discussed above then a progressive decrease in shear stiffness will occur until the available shear strength is equal to the actual shear force per unit area. If, however, the strength of the joint is such that rigid wedge calculations show that it would slide, then, except in the limiting case, the shear strength will always be less than the shear force per unit area, whatever the joint stiffness ratio.

The above statements amount to the conclusion that the standard rigid wedge analysis always provides the limiting conditions for stability. The parallel with the rigid wedge analysis is completed by the observation that as the stiffness ratio increases, the component of shear displacement normal to the direction of the joint intersection decreases. In the limit, as the stiffness ratio approaches infinity, then all shear displacement occurs in the expected direction since the kinematics of the situation preclude any other components.

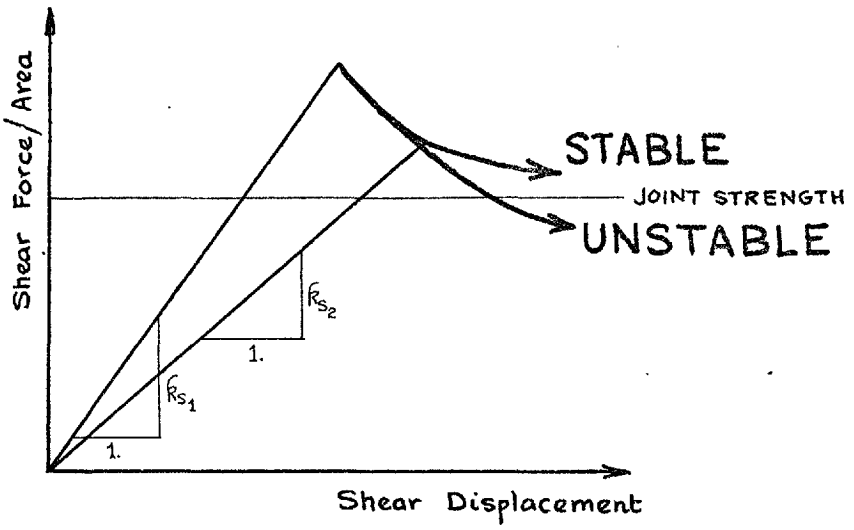


Figure 5.18

The very simple wedge models discussed above, give no indication of the stress distribution on each joint defining the wedge since the former are represented by a single constant stress element. Progressive failure can only be examined by use of a more complex model so alternative idealizations (Fig. 5.19) utilizing four plane triangular joint elements were studied. In this case the symmetry of the situation was used and only half the model analysed.

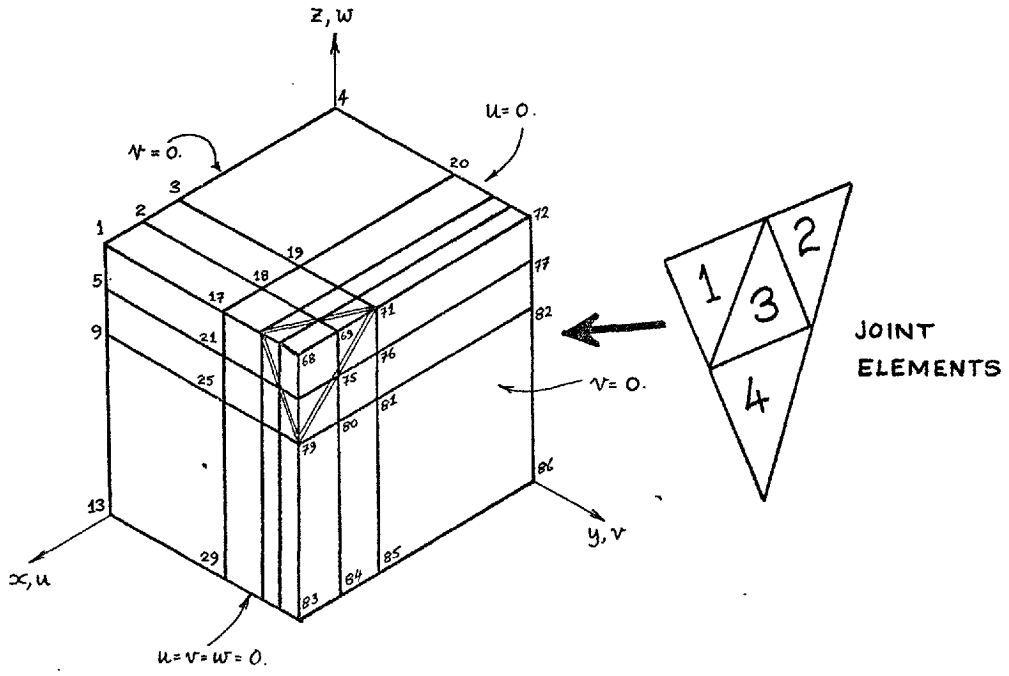


Figure 5.19

Assuming the same material constants and model dimensions as before, progressive analysis for the case of a 30° wedge aperture and 45° dip intersection was conducted. The joint friction angle was assumed to be 30°, since this was known to be stable from rigid wedge limiting equilibrium considerations. Table 5.II gives the joint stresses and required angles of friction determined from the analysis. Progressive readjustments for eight iterations resulted in a decrease in shear stiffness on all elements until a uniform friction angle of 30° was required to maintain the wedge in a state of limiting equilibrium.

Joint Element		Stresses & Angle of Friction Required to Prevent Slip		
		Iteration 1*	Iteration 4	Iteration 8
1	σ_n	- 50·7	-402·6	-389·7
	τ	300·2	239·6	225·7
	ϕ_r	80·4°	30·7°	30·1°
2	σ_n	- 53·7	-405·7	-408·1
	τ	284·4	241·5	236·4
	ϕ_r	79·3°	30·8°	30·1°
3	σ_n	- 32·1	-258·5	-261·9
	τ	185·1	156·3	152·0
	ϕ_r	80·4°	31·2°	30·0°
4	σ_n	- 81·8	-557·3	-585·6
	τ	405·8	328·7	338·9
	ϕ_r	78·6°	30·5°	30·0°

* Stiffness Ratio = 1·0

Table 5.II

5.5.6 Influence of Residual Stresses

The influence of initial stresses on the stability of wedges exposed during excavation can be studied with minor modifications to the computer programs. Results of such analysis reiterate the point that the measurement of initial stresses is of vital concern in slope stability.

The influence of initial horizontal stresses is illustrated by consideration of the possible cases of stresses either parallel or normal to the face created by the process of excavation. If the initial normal stresses are high and compressive then the joints tend to open when unloaded and there is a corresponding decrease in joint normal stress. Such a lessening of stress was noted in connection with two dimensional analysis. However, the same conditions of limiting equilibrium must still pertain despite the increase in angle of friction to prevent readjustment slip.

Figures 5.20 and 5.21 show some results of analyses conducted assuming high initial compressive stresses parallel to the free face. The stresses are considerably different, but the conditions for limiting equilibrium are unchanged. It is notable that the angle of friction required to prevent slip is reduced quite markedly for narrow aperture wedges. This effect decreases as the wedge aperture is increased. Although the joint displacements are dependent upon the residual stresses the deformation of the main body of the models is virtually unaltered.

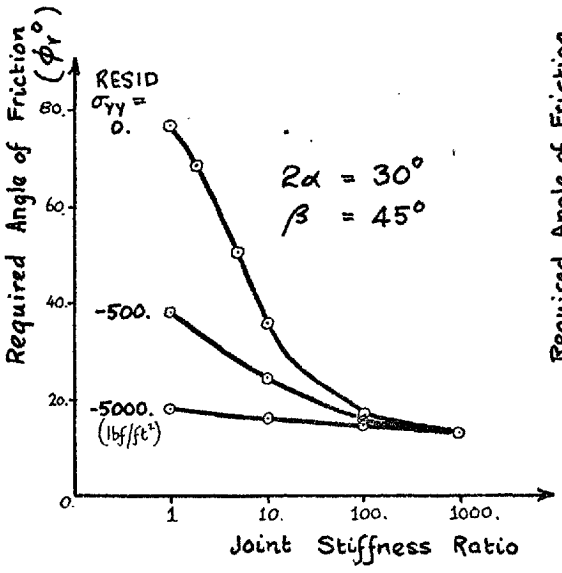


Figure 5.20

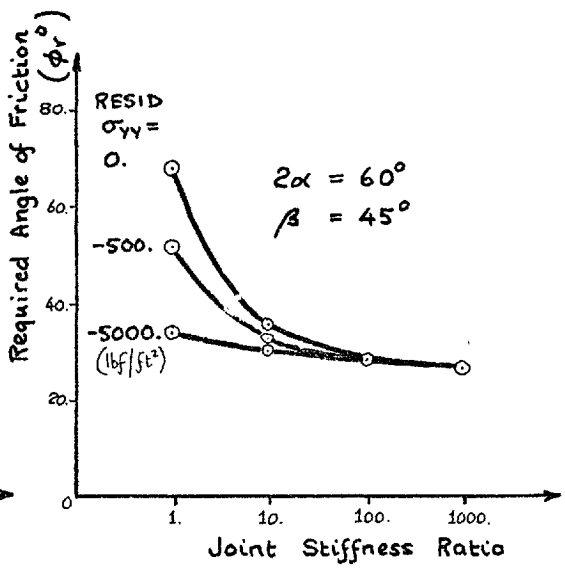


Figure 5.21

Influence of Residual Stresses on Required Angle of Friction

The discussion above has some bearing on the variation of stability with pit geometry. An examination of the stress distri-

bution for a particular case will indicate whether there is a net increase or decrease in the stresses parallel to the free face, and whether a corresponding variation in the angle of friction to prevent slip is likely to exist. Consideration of the stress distributions in Figure 5.8 suggests tight geometries are unlikely to result in less readjustment slip, particularly if the potential slide exits high up on the face or is quite superficial. (The validity of mental superposition of elastic stress distributions for axisymmetric cases and wedge analysis is dubious, but a qualitative assessment is all that is claimed.) Except when readjustment slip may result in modification of joint strength the stability of any wedge is unaffected by the stress conditions in the slope. The factor of safety can therefore be determined from limiting equilibrium calculations.

5.6 AN EXTENSION TO VECTOR METHODS FOR WEDGE ANALYSIS

One of the most interesting results of the Finite Element analysis of wedge type situations was the insensitivity of the solution to variations in the elastic modulus of the solid rock. This motivated the idea that it should be possible to modify the usual rigid wedge model to take account of joint deformability. If the elastic properties were really unimportant then good agreement should be obtained between the Finite Element and Modified Rigid Wedge analyses.

5.6.1 A Simplified Wedge Model with Deformable Joints

Consideration is given to the simplest possible model; a symmetrical tetrahedral wedge defined by two planes.

Using the notation given in Figure 5.22 the total weight of the wedge is:-

$$W = \frac{2}{3} . \gamma . A . H . \cos\beta . \sin\alpha \qquad 5(16)$$

where A is the area of each sliding face.

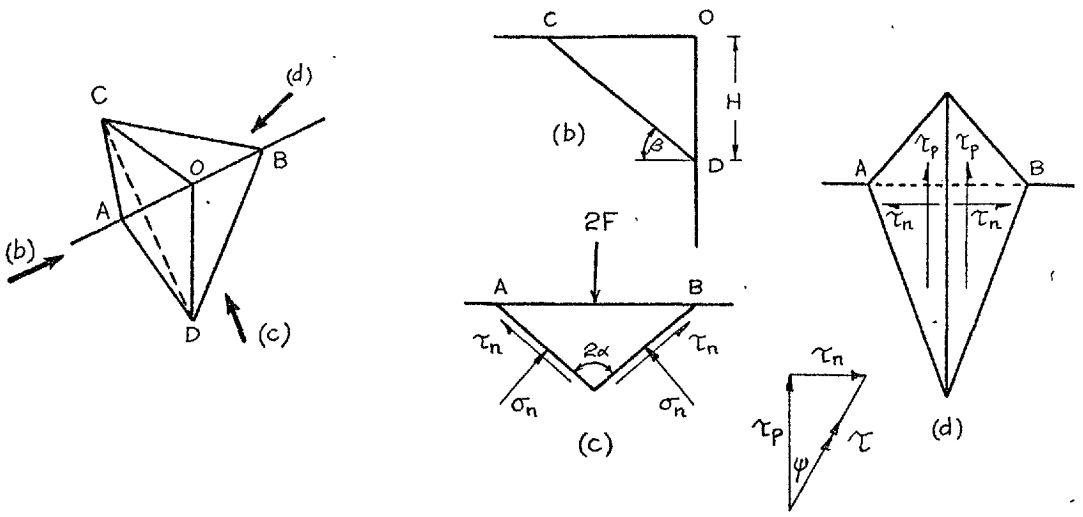


Figure 5.22

Resolving parallel to the intersection the average shear stress on the faces is:-

$$\tau_p = \frac{\gamma H}{3} . \, Sin\beta . \, Cos\beta . \, Sin\alpha \qquad 5(17)$$

The total force tending to drive the wedge into the joint intersection is:-

$$W Cos\beta = \frac{2}{3} . \, \gamma . H . A . Cos^2\beta . \, Sin\alpha \qquad 5(18)$$

If this results in a displacement δ normal to the joint intersection then, because the wedge and its seating are undeformable:-

$$\frac{\tau_n}{k_s . v . Cos\alpha} = \frac{\sigma_n}{k_n . v . Sin\alpha} \qquad 5(19)$$

τ_n and σ_n are the average stresses as defined in Figure

5.22 and v is the displacement of the wedge normal to the line of intersection and in the plane OCD.

Hence:

$$\tau_n = \frac{\sigma_n}{R} . \text{Cot}\,\alpha \qquad 5(20)$$

where

$$R = \frac{k_n}{k_s}$$

Resolving perpendicular to the intersection line:-

$$2A.(\sigma_n \text{Sin}\alpha + \tau_n \text{Cos}\,\alpha) = \frac{2}{3}\,\gamma A H \text{Cos}^2\beta \text{Sin}\alpha \qquad 5(21)$$

Substituting 5(20) in 5(21) and rewriting:-

$$\sigma_n = \frac{\gamma H R \text{Cos}^2\beta \text{Sin}^2\alpha}{3(R\text{Sin}^2\alpha + \text{Cos}^2\alpha)} \qquad 5(22)$$

$$\tau_n = \frac{\gamma H \text{Cos}^2\beta \text{Sin}\alpha \text{Cos}\alpha}{3(R\text{Sin}^2\alpha + \text{Cos}^2\alpha)} \qquad 5(23)$$

From these expressions it is apparent that, as for the Finite Element analysis, it is the ratio of the joint stiffnesses that is critical in determining the average stresses on the planes.

From equations 5(17) and 5(23) the maximum shear force per unit area is obtained by substitution in the expression:

$$\tau = \sqrt{(\tau_p^2 + \tau_n^2)} \qquad 5(24)$$

The angle of friction to prevent sliding is:-

$$\phi_r = \text{Tan}^{-1}\left(\frac{\tau}{\sigma_n}\right) = \text{Tan}^{-1}\left(\frac{\sqrt{(\tau_p^2 + \tau_n^2)}}{\sigma_n}\right) \qquad 5(25)$$

And the direction of shear with respect to the intersection line (Fig. 5.22) is:-

$$\psi = \text{Tan}^{-1}\left(\frac{\tau_n}{\tau_p}\right) \qquad 5(26)$$

In the limit, when the normal stiffness is very much larger than the shear stiffness then:-

$$k_n >> k_s \qquad R \longrightarrow \infty$$

$$\sigma_n \longrightarrow \frac{\gamma H}{3}.\text{Cos}^2\beta$$

$$\tau_n \longrightarrow 0.$$

And

$$\tau_p \longrightarrow \frac{\gamma H}{3}.\text{Sin}\beta\,\text{Cos}\beta\,\text{Sin}\alpha$$

$$\phi_r \longrightarrow \text{Tan}^{-1}(\text{Sin}\,\alpha\,\text{Tan}\beta)$$

$$\psi \longrightarrow 90^\circ$$

These conditions are exactly those resulting from the normal rigid wedge analysis in which joint deformability is ignored.

5.6.2 The Mechanism of Joint Stiffness Ratio Variation

Examination of the above expressions (5(17, 22, 23)) reveals the influence of joint stiffness ratio. As the joint shear stiffness decreases, with respect to the normal stiffness, then there is a corresponding decrease in the shear force normal to the intersection and an increase in the normal force per unit area on each face. For all situations, however, the shear force parallel to the intersection must be constant if equilibrium is to be satisfied. An increase in joint stiffness ratio will therefore

result in both an increase in normal force per unit area and a decrease in the maximum shear force per unit area on each of the sliding faces. As has already been stated, the direction of slip will correspond with the direction of maximum shear force per unit area. Although this is not a kinematically feasible possibility when total wedge failure by slip is concerned, it is a consequence of the assumed deformability of the planes of weakness. Only if the joint stiffness ratio is very high will this direction correspond with sliding parallel the intersection.

5.6.3 Generalisation of the Modified Rigid Wedge Analysis

The above modifications may be incorporated in the vector analysis described in Section 5.2. If the test of direction of sliding (5.2.2) reveals the composite condition to be the case, then equations 5(8) - 5(11) may be replaced by two vector equations that may be solved to determine the three components of stress on each plane of weakness.

Six vectors of average stress describe the state on the two planes:-

$$\vec{\sigma}_{n_{1,2}} \quad : \quad \vec{\tau}_{n_{1,2}} \quad : \quad \vec{\tau}_{P_{1,2}}$$

From equilibrium:

$$\vec{\sigma}_{n_1} + \vec{\sigma}_{n_2} + \vec{\tau}_{n_1} + \vec{\tau}_{n_2} + \vec{\tau}_{P_1} + \vec{\tau}_{P_2} = \vec{G} \qquad 5(27)$$

If the shear and normal stiffnesses of the discontinuities are $k_{s_{1,2}}$ and $k_{n_{1,2}}$ respectively, then:-

$$\vec{\delta}_{n_1} = \frac{\vec{\sigma}_{n_1}}{k_{n_1}} \quad \text{and} \quad \vec{\delta}_{n_2} = \frac{\vec{\sigma}_{n_2}}{k_{n_2}} \qquad 5(28)$$

With similar expressions describing the displacements due to the shear components of stress.

Since the wedge and its seating are rigid, then the displacements of the two faces must be related according to the following vector equation:-

$$\frac{\vec{\sigma}_{n_1}}{k_{n_1}} + \frac{\vec{\tau}_{p_1}}{k_{s_1}} + \frac{\vec{\tau}_{n_1}}{k_{s_1}} = \frac{\vec{\sigma}_{n_2}}{k_{n_2}} + \frac{\vec{\tau}_{p_2}}{k_{s_2}} + \frac{\vec{\tau}_{n_1}}{k_{s_2}} \qquad 5(29)$$

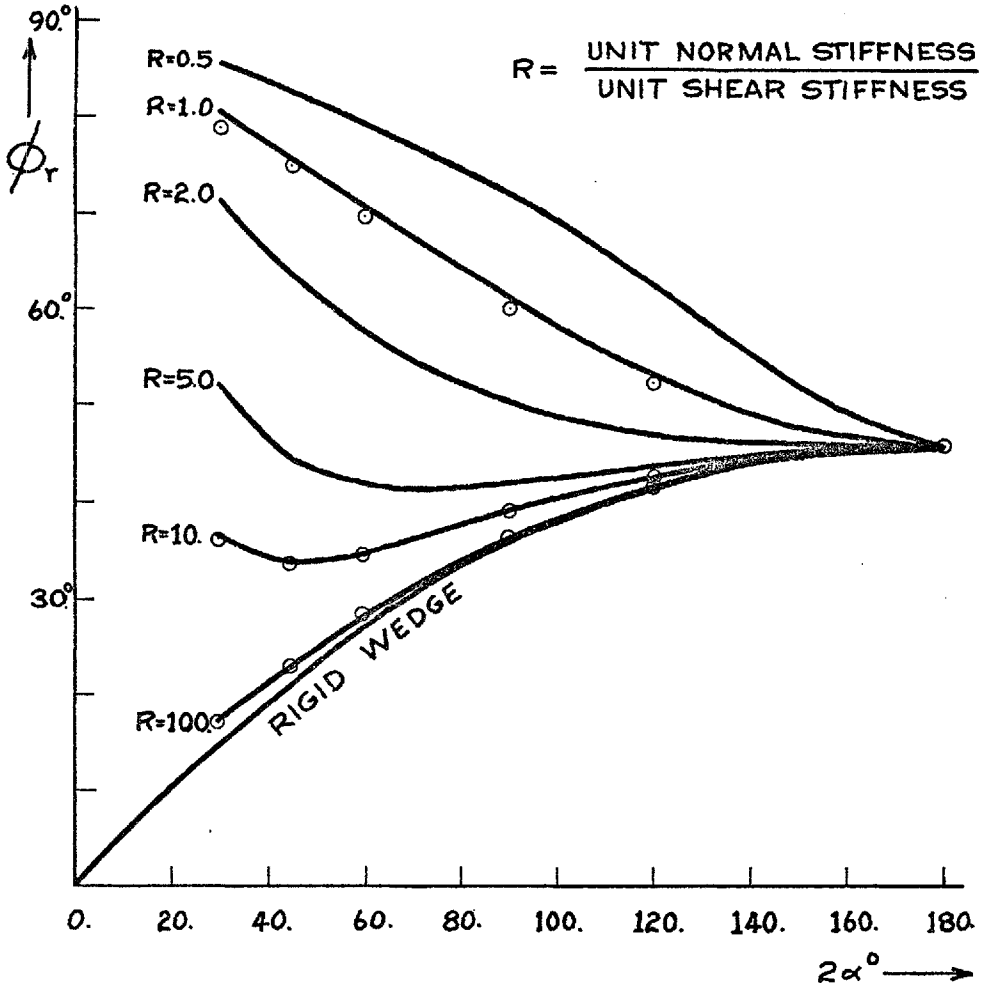
From the vector analysis in Section 5.2, the following relationships may be deduced.

$$\begin{aligned} \sigma_{n_1} &= C_1 \cdot \vec{\omega}_1 & \vec{\sigma}_{n_2} &= C_2 \cdot \vec{\omega}_2 \\ \vec{\tau}_{n_1} &= C_3 \cdot \left(\vec{\omega}_1 \times \frac{\vec{x}}{|\vec{x}|}\right) & \vec{\tau}_{n_2} &= C_4 \cdot \left(\vec{\omega}_2 \times \frac{\vec{x}}{|\vec{x}|}\right) \\ \tau_{p_1} &= C_5 \cdot \frac{\vec{x}}{|\vec{x}|} & \tau_{p_2} &= C_6 \cdot \frac{\vec{x}}{|\vec{x}|} \end{aligned} \qquad 5(30)$$

Substitution of equation 5(30) into equations 5(27) and 5(29) yields six simultaneous equations in the constants $C_1 - C_6$, which are the magnitudes of the stress vectors. Solution of these equations enables the conditions for limiting equilibrium of each plane of weakness to be determined.

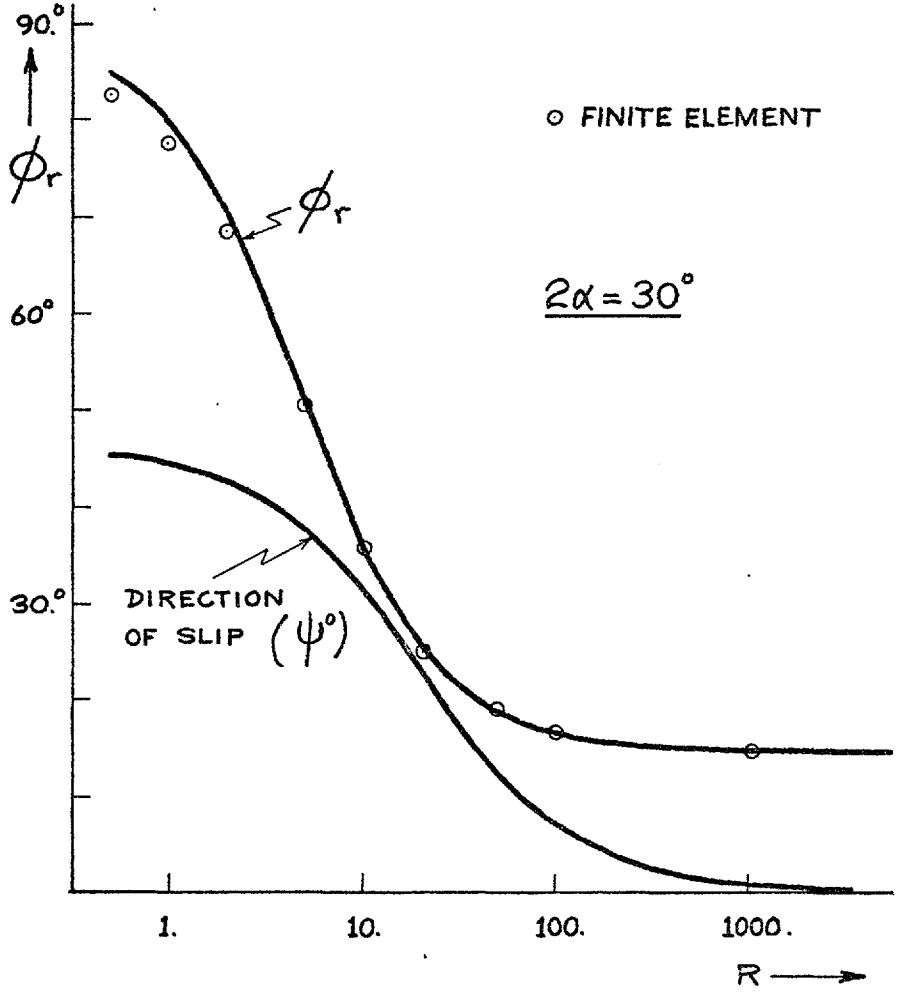
5.6.4 Results of Modified Rigid Wedge Analysis

The computer program for vector analysis for wedges given in the Appendix C contains a subroutine based on the method outlined in the above section. Using either the 'vector program' or by direct substitution in equations 5(17) to 5(26) results may be obtained for the situations discussed in Sections 5.5.2 and 5.5.3. Figures 5.23 and 5.24 show the very close agreement with the results of the Finite Element analysis.



WEDGE APERTURE (2α)
v REQUIRED FRICTION ANGLE (ϕ_r)

FIGURE 5.23



JOINT STIFFNESS RATIO (R)
v REQUIRED FRICTION ANGLE (ϕ_r)

45° DIP REAR INTERSECTION

FIGURE 5.24

The similarity of the results from the two methods of analysis supports the original observation concerning the relative unimportance of the properties of the solid rock. From this it may be concluded that this Modified Rigid Wedge analysis satisfactorily takes account of the influence of joint deformability on the stability of sliding wedges. It does, however, give no indication of the displacements of the rock mass and is simply a limiting equilibrium model.

The direction of slip (Fig. 5.24) shows clearly the importance of joint stiffness ratio. Criticisms based on the supposition that displacements can only occur parallel to the joint intersection are only valid if the normal stiffness is assumed to be very large with respect to the shear stiffness. This is obviously a special case of the general situation. The method is really applicable when soft joint infilling results in very deformable discontinuities.

5.7 CONCLUSIONS

The results of analyses of axisymmetrical excavations indicate that high circumferential stresses do not exist for conical pits. In fact, there is a considerably greater tensile zone at the slope crest than for a plane face. Based on these observations it is suggested that variations in stability with slope geometry are primarily due to the statistics of the planes of weakness that form possible failure units.

The analysis of simple wedge type slides showed that the limiting conditions, to prevent sliding, may be calculated using the standard Rigid Wedge methods. Finite Element and Modified Rigid Wedge analyses are in close agreement and there seems little advantage in using the former for stability calculations. In more complex situations, where initial stresses may be important and where the displacements due to excavation are of concern, then the Finite Element Method will provide a complete solution.

It is acknowledged that only small models may be studied using the computer programs developed. However, all the tools are

available, so, given larger and faster computers, the techniques discussed in connection with two dimensional analysis may be applied. Such a degree of sophistication is in advance of current methods of assessing the parameters defining the real situation. At present, therefore, time and money is probably more profitably spent improving the engineering assessment of the problem than on detailed numerical analysis.

(1) John, K.W. Graphical Stability Analysis of Slopes in Jointed Rock. J.Soil.Mech. & Foun. Div. A.S.C.E. Vol. 94, No. S.M.2. 1968.

(2) Londe, P., Vigier, G. & Vormeringer, R. Stability of Rock Slopes - Graphical Methods. J.Soil.Mech. & Foun. Div. A.S.C.E. Vol. 96, No. S.M.4. 1970.

(3) Goodman, R.E. & Taylor, R.L. Methods of Analysing Rock Slopes and Abutments, a Review of Recent Developments. Failure and Breakage of Rock. A.I.M.E. Chapter 12. 1967.

(4) Londe, P., Vigier, G & Vormeringer, R. Stability of Rock Slopes of a Three-Dimensional Study. J.Soil.Mech. & Found. Div. A.S.C.E. Vol. 95, No. S.M.1., 1969.

(5) Wittke, W.W. A Numerical Method of Calculating the Stability of Loaded and Unloaded Rock Slopes (in German) Felsmechanik and Ingenieurgeologie, Vol. 30 Suppl.II 1965 (English translation from Rock Mechanics Information Service, Imperial College, London.)

(6) Hoek, E. & Boyd, J.M. Stability of Slopes in Jointed Rock. Symposium on Rock Mechanics in Highway Construction, University of Newcastle, 1971.

(7) Zienkiewicz, O.C. & Cheung, Y.K. The Finite Element Method in Structural and Continuum Mechanics. McGraw-Hill, London, 1967.

(8) Perloff, W.H. Strain Distribution around Underground Openings - Tech. Report No. 1, Finite Element Analysis of Underground Openings. Purdue University. School of Civ. Eng., Lafayette, Indiana, June 1969.

(9) Wilson, E.L. Structural Analysis of Axisymmetric Solids. Journal of A.I.A.A. Vol. 3. No. 12, December, 1965.

(10) Jenike, A.W. & Yen, B.C. Slope Stability in Axial Symmetry in Rock Mechanics (Proc. 5th Symp. Rock. Mech. Univ. of Minnesota, 1962). Pergamon, 1963.

(11) Hoek, E. Estimating the Stability of Excavated Slopes in Opencast Mines. Trans. I.M.M. Vol. 79, October, 1970.

(12) Cundall, P. The Measurement and Analysis of Accelerations in Rock Slopes. Ph.D. Thesis, London University, 1971.

(13) St. John, C.M. Three Dimensional Analysis of Jointed Rock Slopes. Symp. on Rock Fracture. I.S.R.M. Nancy 1971.

(14) Goodman, R.E., Taylor, R.L. & Brekke, T.L. A Model for the Mechanics of Jointed Rock. Journal of Soil. Mech. & Found. Div. A.S.C.E. S.M.3., May 1968.

(15) Mahtab, M.A. & Goodman, R.E. Three Dimension Finite Element Analysis of Jointed Rock Slopes. 2nd International Cong. of I.S.R.M., Belgrade, 1970. Paper 7.12.

CHAPTER

6

OBSERVATIONAL METHODS

	Page
Chapter Index	198
Synopsis	199
6.1 Introduction	200
6.2 Slope Monitoring	200
6.3 Precise Survey Methods	204
6.4 Slope Monitoring at Gortdrum Mine, Ireland	216
6.5 Slope Movements at the Berkeley Pit	222
6.6 An Example of Comparison with Computer Prediction	223
6.7 An Example of Warning of Failure	227
6.8 Conclusions	
References	230

SYNOPSIS

A brief summary of methods of monitoring the behaviour of slopes precedes a more detailed discussion of a proposed system using precise surveying techniques. Some attention is given to the equipment considered essential for such measurements. Field trials consisting of repeated co-ordination of points in and around a small open pit are reported and conclusions are drawn regarding the practicality of such a monitoring scheme.

Finally, evidence of the uses of slope monitoring is found in current literature.

6.1 INTRODUCTION

"If we learn to pay more attention to the phenomenon itself and take this as teacher, we shall see more. Deformations are more precisely observed and more clearly assessed than the stresses calculated back from them."

Müller's (Ref. 1) comments above, have considerable relevance to one form of slope monitoring in open pit mines. Very precise determination of displacement will enable the full behaviour of rock slopes to be understood.

The methods discussed in this thesis, almost without exception, provide computed values for the displacements throughout an excavation, at any chosen moment in time. If these methods are valid, then comparison of real and predicted slope behaviour will provide a significant indication of stability. If, however, there is little agreement between theory and practice then the design methods and the assumed properties of rock masses must be reviewed.

Slope monitoring is also used in the prediction of the time of failure once a potential slide has been detected. The necessary measurements may then be less precise, since the movements prior to collapse are frequently large with respect to those anticipated in a 'no failure' situation.

6.2 SLOPE MONITORING

A wide variety of instrumentation has been used in connection with monitoring the behaviour of rock slopes. Basically they are either microseismic or displacement devices.

6.2.1 Microseismic Monitoring

Microseismic activity is associated with the break up of material and inter rock sliding and has therefore been used extensively to monitor the failure of laboratory specimens under load.

In the context of slope stability it is not possible to estimate the expected level of microseismic activity, although assessments might be made using the stress levels calculated from numerical analysis. Monitoring this phenomenon therefore constitutes a qualitative method, so it should be supplemented by displacement studies. The latter will quantify other data as well as provide evidence concerning the extent and mechanism of the failure.

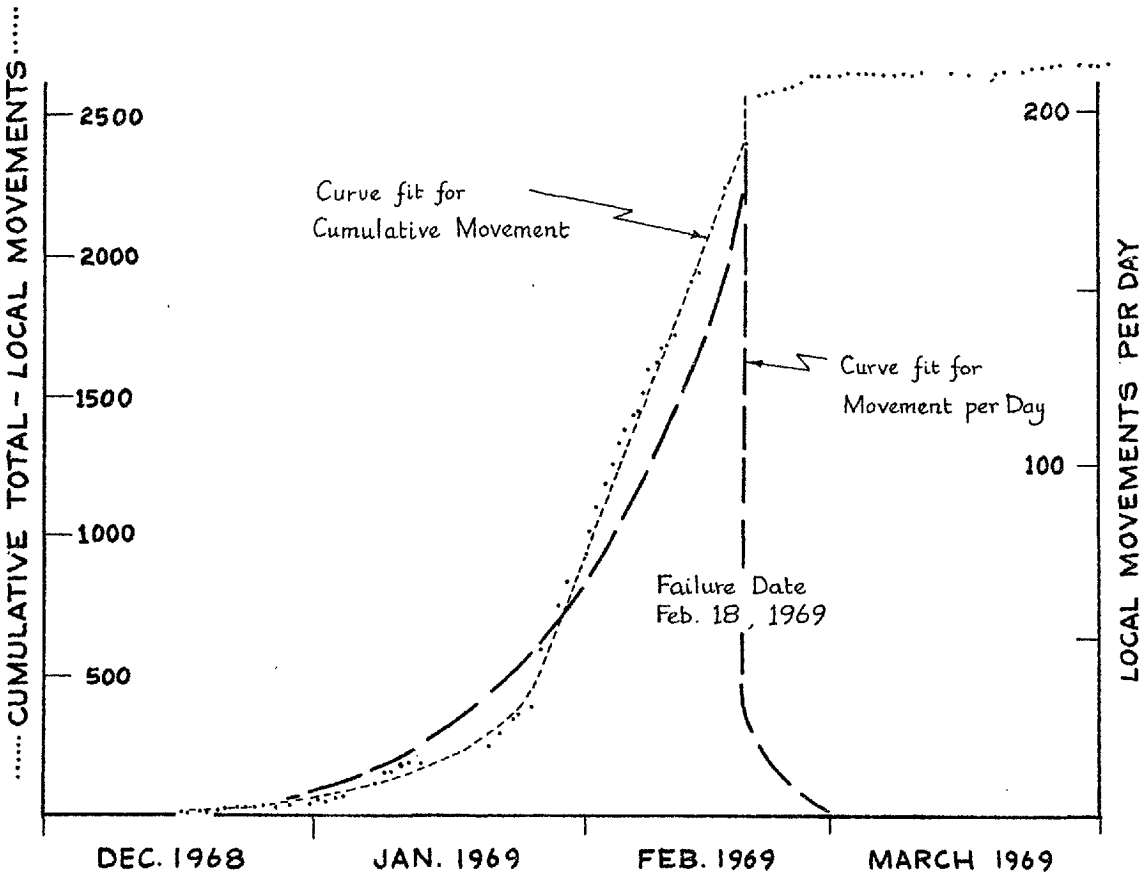
In deep underground mines where stresses are high and rock bursts are a problem, microseisms are monitored to detect potential danger areas (Ref. 2). In slopes the stresses are generally much lower and activity is associated with sliding and very local stress concentrations. Energy is radiated at around 1-10 Hz, which is fortunate since the higher frequencies found in deep level studies would be severely attentuated within the highly discontinuous rock mass.

During slope investigations at the Kimbley Pit (Ref. 3) three component seismographs were placed to detect radial, tangential and vertical motion with respect to the pit. Unfortunately, the reports on the work only state that activity was recorded during slope steepening, but ceased soon after excavation was complete.

Considerably more information is reported concerning slope failure at the Chuquicamata Mine in Chile (Ref. 4). Moving coil seismometers, recording events from 0·5 to 12·5 Hz were set for operation in the vertical plane and records kept of the number of events recorded per 24 hour period (Fig. 6.1). Fortunately it proved easy to differentiate between noise due to the excavation process, earthquakes and failure events. A very good correlation between the records of the last of these and displacement studies was achieved.

6.2.2 Displacement Monitoring

A catalogue of the various methods that have been used to measure displacements around slopes is beyond the scope of this thesis. They may, however, be broadly grouped into three types.



NUMBER OF SEISMIC EVENTS RECORDED (6. to 9. Hz)
v TIME (After Kennedy & Niermeyer 1970)

FIGURE 6.1

Down-the-hole Instrumentation

The many devices, such as borehole extensometers, the shear strip indicator and borehole tilt meters (Ref. 5), provide data on some component of displacement with respect to the borehole axis. Unless coupled with a collar survey only relative displacements may be determined, but the methods may serve to define the limits of a slide once the approximate location is known. Some of these devices are expensive, both to purchase and install, but they may be used for remote monitoring or automatic recording.

Crack Measuring Devices

Many methods of varying complexity have been used to measure the relative movement between two faces of a critical discontinuity. In essence the methods consist of measurements between two or more points either side of a crack. References 4 and 6 give typical examples.

These devices are usually used as failure warning instrumentation, since they can only be installed when critical discontinuities have been isolated. Even when used for this purpose, they are best employed in conjunction with survey techniques designed to detect gross movements.

Repeated Survey Techniques

Repeated Surveying of a number of points over a period of time (using any technique) will enable one or more components of displacement to be calculated. If failure is involved, then displacements can be large, and relatively crude methods may be adopted. For example; 'Tape and Transit' lines can be used where the topography and pit geometry are suitable. This involves measuring the departure of points from colinearity, using a theodolite, and taping of distances between the points. The latter technique is satisfactory over short ranges and where undisturbed taping lanes can be arranged.

Precise levelling is a rapid and accurate method of determining vertical displacements and, as such, has found wide usage both on its own and in conjunction with other techniques (Ref. 7). The alternative method of Trigonometrical Levelling is unsatisfactory except for relatively large movements and should therefore only be used when unavoidable.

In the author's opinion the most comprehensive and satisfactory method of determining the movement around an excavation is by repeated precise co-ordination of a number of reference points. In the past, this inevitably would have entailed repeated triangulation, but the advent of precise distance measuring equipment has provided preferable alternatives. Such methods will be discussed at greater length below.

6.3 PRECISE SURVEY METHODS

As has been stated above, the aim of precise survey measurements is either to detect the onset of failure or to determine the success of design procedures. If detailed computer analysis has been conducted to determine the displacements expected, departure from these will provide warning of potential slope failure. If no such analysis has been conducted, then estimations must be based on observed trends. This latter procedure has been proposed by Watt (Ref. 8), who assumed that a linear response was anticipated.

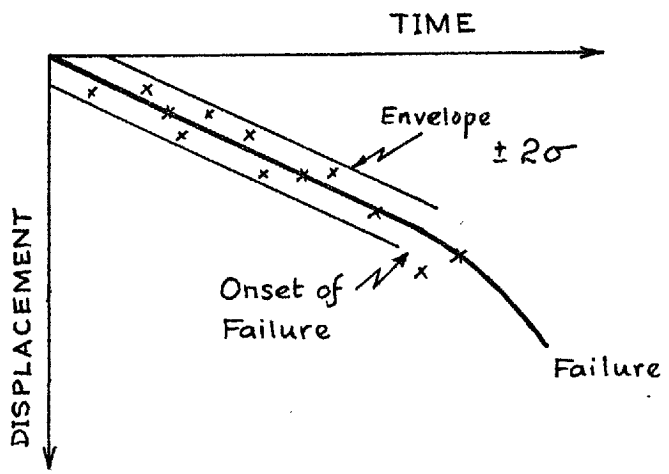


Figure 6.2

The precision required to successfully operate such a scheme will depend upon the expected displacements. The deformations given in Figure 6.3 refer to a 45^{o} slope for a pit 100 meters in depth and were obtained using an elastic analysis as discussed in Chapter 3. The author believes this to be a realistic estimate of the displacements that would occur due to excavation, since it seems improbable that discontinuities will contribute significantly to elastic recovery. (The discontinuities may, however, introduce an anisotropy that has a marked influence upon displacements into the excavation.)

Departures from the anticipated behaviour initially may be very small. Estimates of the standard deviation of the measurements are essential so that significant departures may be recognised. Clearly the smaller the standard deviation the sooner potential slope failure can be detected and remedial action taken.

6.3.1 A Proposed Method

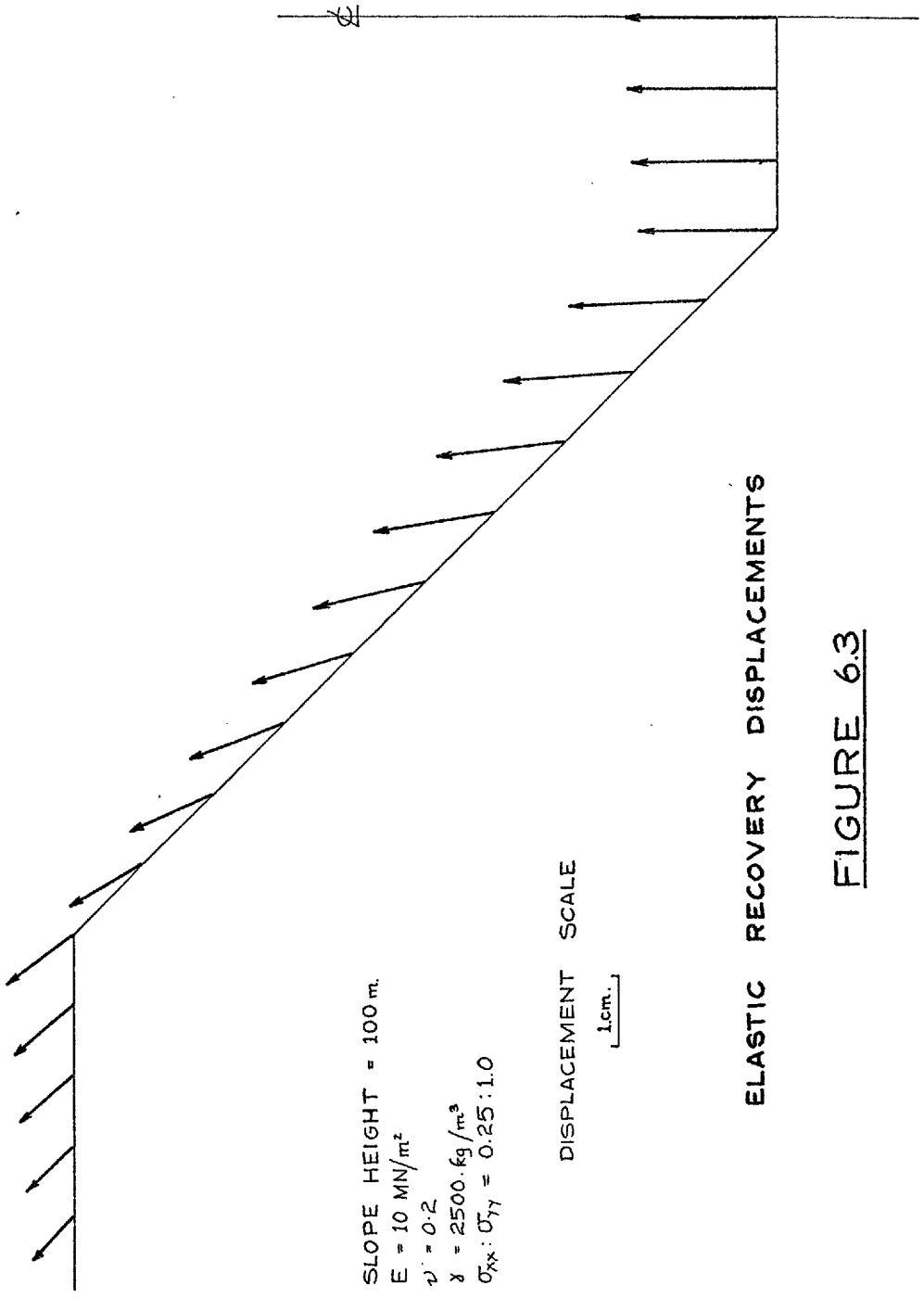
The aim of the method is to determine the three dimensional vector of movement of points in and around a slope during its excavation. In order to do this three types of monitoring stations are necessary.

Primary Stations

Elastic analyses of slopes indicate that Primary, or Reference, stations must be placed several diameters from the excavation. They should, of course, be sufficiently substantial and isolated to ensure that a continuous and reliable reference system is provided. Care should be taken to ensure that seasonal effects, such as shrinkage and swelling of soil with moisture variations, are overcome by suitable foundations on solid rock, where possible.

Secondary Stations

In many situations the most useful monitoring points are at



ELASTIC RECOVERY DISPLACEMENTS

FIGURE 6.3

the crest of the slope. Additionally, stations in this location provide vantage points from which the inside of the excavation may be observed. Such Secondary, or Crest, stations must again be substantial and should ideally take the form of pillars with special fittings facilitating rapid and accurate mounting of instrumentation. In general, surveying from Tripod setups should be avoided since differential movements causing rotation of the head are almost inevitable. In some situations, however, it may be impossible to construct pillars that will remain undamaged and buried monuments will be essential (Fig. 6.4).

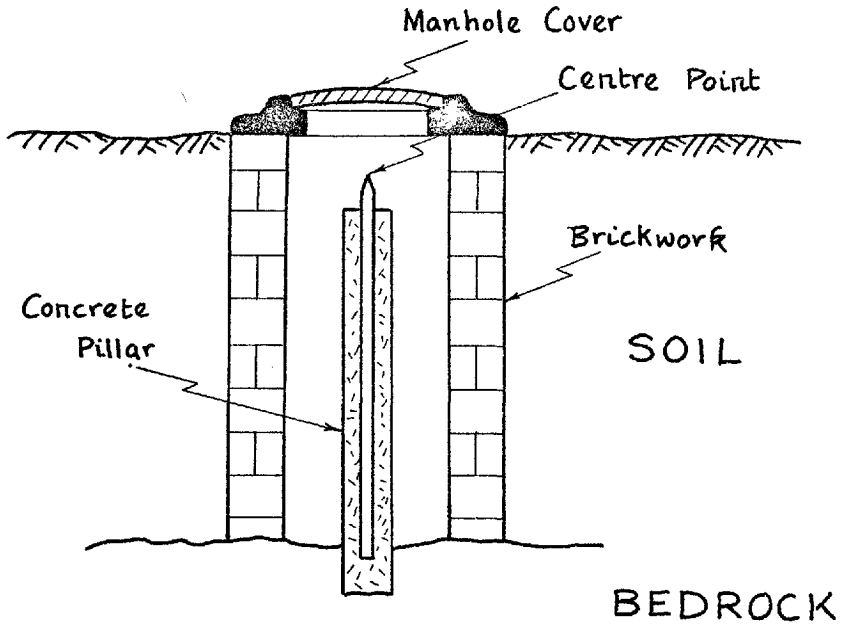
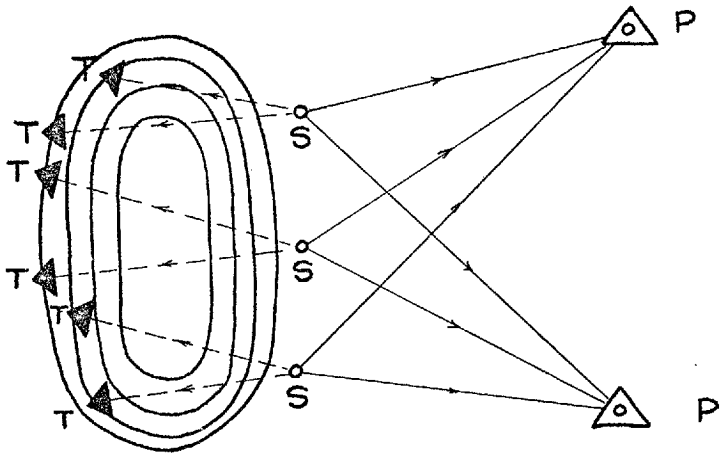


Figure 6.4

Pit Wall Targets

The nature of pit wall targets will depend upon the method of surveying adopted. One alternative is surveying by intersection. The station will then consist only of a simple optical target. For surveying by bearing and distance measurement a composite target including a reflector will be necessary. In the author's opinion stations within the pit should be permanent, and placed on the rock faces where they are remote from damage by rockfall or the process of excavation. In most cases therefore, a substantial rock bolt should provide anchorage. However, in

situations where surface spalling is serious some alternative strategy must be adopted, perhaps using buried monuments on benches.



P = Primary Station S = Secondary Station
T = Pit Wall Target

Figure 6.5

The survey splits itself into two parts which may or may not be done simultaneously. Firstly, the secondary stations must be co-ordinates with reference to the primary. Secondly, the movement of the pit wall targets can be detected by reference to the secondary stations. Figure 6.5 gives an idealised plan of this procedure for a small open pit. The method of surveying the secondary stations is either by triangulation (the measurement of angles) or trilateration (the measurement of distances). The advantages of the latter over the former have been discussed by St. John and Thomas (Ref. 9). Watt (Ref. 8) has given a diagrammatic comparison of the accuracy of distance and angle measuring instruments (Fig. 6.6). Here it is sufficient to state that angular measurement is not competitive on any criterion, over the ranges involved in pit monitoring. Whatever technique is used for surveying the secondary stations, it is essential that precise levelling be used to determine their elevations. Trigonometrical levelling is obviously unavoidable for the pit wall targets, but it is a poor alternative

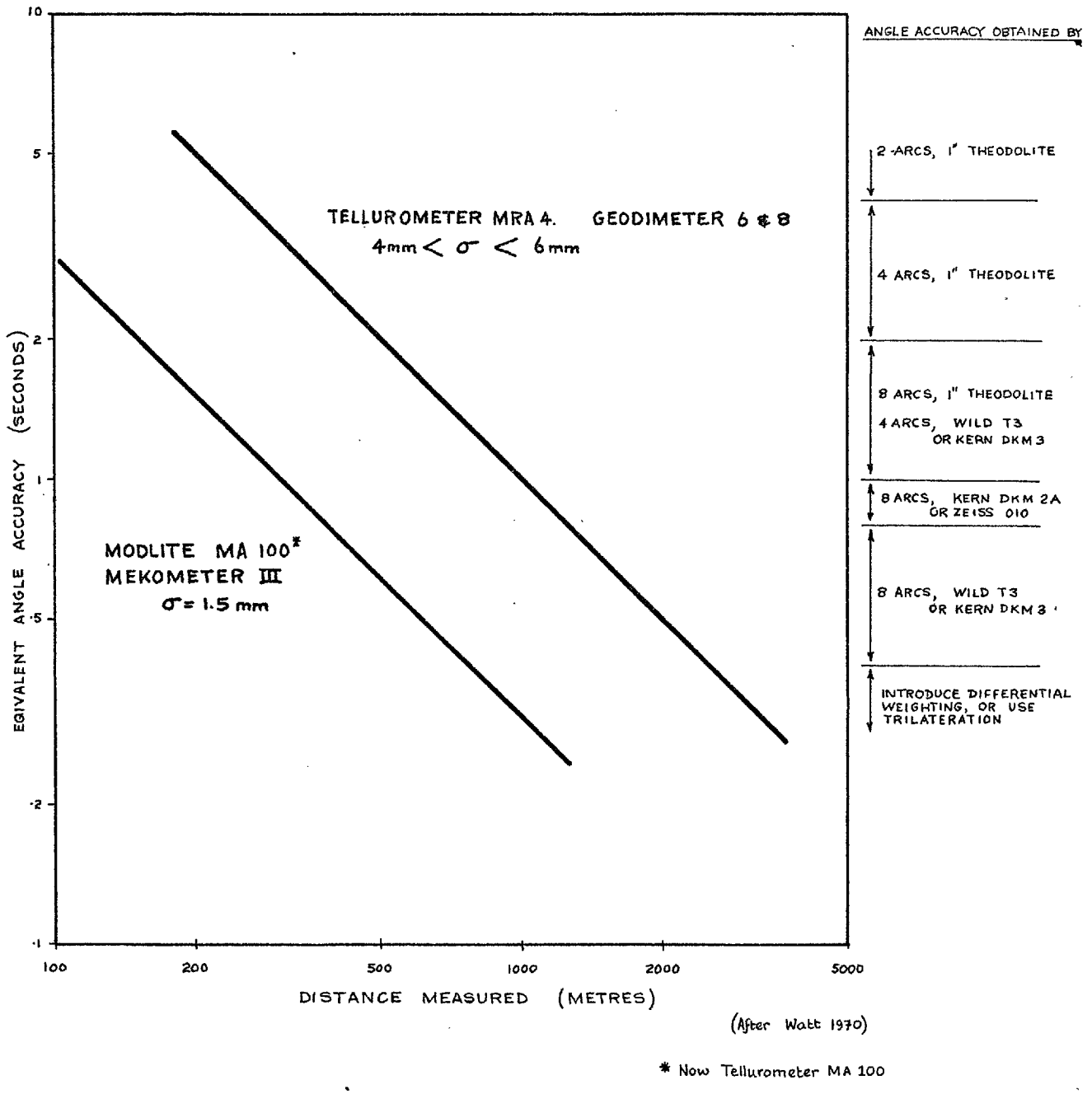

EQIVALENT ANGLE ACCURACY (SECONDS)
10
5
2
1
·5
·2
·1
100
200
500
1000
2000
5000
DISTANCE MEASURED (METRES)
TELLUROMETER MRA 4. GEODIMETER 6 & 8
4mm < σ < 6mm
MODLITE MA 100*
MEKOMETER III
σ = 1.5 mm
ANGLE ACCURACY OBTAINED BY
2 ARCS, 1" THEODOLITE
4 ARCS, 1" THEODOLITE
8 ARCS, 1" THEODOLITE
4 ARCS, WILD T3
OR KERN DKM 3
8 ARCS, KERN DKM 2A
OR ZEISS 010
8 ARCS, WILD T3
OR KERN DKM 3
INTRODUCE DIFFERENTIAL
WEIGHTING, OR USE
TRILATERATION
(After Watt 1970)
* Now Tellurometer MA 100

FIGURE 6.6

elsewhere. Surveying the pit wall targets may be achieved by intersection from two or more secondary stations or by bearing and distance from a single station. From the point of view of accuracy and speed, the author is in favour of the latter course, particularly if targets can be left in-situ. It also eliminates problems of intervisibility since there should be no difficulty where only one line of sight is necessary. Furthermore it is frequently difficult to achieve a well conditioned network if targets are fixed by intersection.

Complete determination by distance measurement from three or more points is theoretically feasible, but has practical disadvantages. Firstly, it necessitates either very complex targets or target adjustment between measurements. Secondly, it is frequently difficult to obtain a good spatial distribution of secondary stations from which observations can be made.

6.3.3 Instrumentation

It is relevant to make a few observations and recommendations concerning necessary instrumentation for the method proposed above.

Levels and Levelling

The precision automatic levels are likely to produce the best results in an open pit situation since they are less effected by the environment than the conventional tilting level. For precise work they should be fitted with parallel plate or pentaprism micrometers and used in conjunction with matched double graduated invar levelling staves. The Zeiss Koni 007 is a most satisfactory instrument since its totally sealed optics and micrometer are ideal in a dusty mine atmosphere.

Levelling should be done in closed traverses in order that errors may be detected. Watt (Ref. 8) suggests that no circuit closure error should exceed 3σ, where

$$\sigma = 0{\cdot}5\sqrt{(L/2)}\ \text{mm} \qquad 6(1)$$

and L is the perimeter in km.

Trigonometrical levelling does not require elaboration, although it is relevant to remark that computations are facilitated if observed vertical angles correspond with the slope of any distances measured.

Finally, any errors must be distributed and corrections made for refraction and curvature. The elevation of all stations is then determined and the data is required to reduce measured distances to horizontal. (To obtain elevations from Trigonometrical levelling the co-ordinates of the stations must be known. These may be taken from the previous survey.)

Theodolites and Angular Measurement

The choice of theodolite depends upon the required accuracy and, to some extent, the other equipment used in the scheme. Reference to Figure 6.6 provides a general guide to instruments and procedures required to achieve compatibility between angular and distance measurement. For repeated surveying it must be true that any instrument necessitating fewer observations is preferable.

For precise work it is vital that the theodolite mounting is rigid. Both from the point of view of stability and speed, pillars are desirable. These are particularly suitable if used in conjunction with a method for rapid and reproducable mounting of equipment. In this context the Kern system has proved to be excellent both on pillar and tripod setups.

Whatever instrument is used the surveyor must be fully aware of the misadjustments that may occur. In any case, compensated rounds of angles should always be observed and correction made for 'dislevelment' of the theodolite where steep sights are involved (Ref. 10).

Electromagnetic Distance Measuring Instruments

There are an increasing number of electromagnetic distance measuring instruments. Those with relatively short ranges, using modulated light waves and therefore employing passive reflectors, have application to displacement measurement if sufficiently accurate. Table 6.I gives a summary of the important properties of some of relevant instruments. Currently, the most accurate promises to be the Mekometer, which Kern intends to market as a geodetic instrument.

The choice of instruments is somewhat dictated by target considerations. All require retrodirective optical reflectors;6 cm. diameter corner cubes being in most common usage. The targets are relatively expensive and the large arrays necessary for some instruments are both costly and cumbersome.

Electromagnetic Distance Measurers

Instrument	Claimed Daylight Range	Claimed Accuracy	Targets for 1km Range*
Kern Mekometer ME 3000	3 Km	0.1mm $\pm$ 1ppm	1
Tellurometer MA 100	2 Km	1·5mm $\pm$ 1ppm	3
Hewlett Packard 3800A & 3800B	3 Km	3mm + 10ppm (-40°c to $+40^{\circ}$c)	1
Aga Geodimeter 6A	5 Km (Standard) Bulb	5mm + 1ppm	1
Wild DI 10 Distomat	1 Km	$\pm$ 1 cm	9
Zeiss SM-11 & Regelta 14	2 Km	$\pm$ 1 cm	7

* All use Retrodirective prisms

Table 6.I

Targets

For angular measurement precise traverse targets are necessary. If used in conjunction with distance measurement these should be completely interchangeable with the optical reflectors as well as the theodolite and distance measuring instrument. For pit wall targets, however, a composite arrangement including a reflector will be essential if these are to be left in situ.

The retrodirective reflectors possess the advantage of being non-critical as regards alignment with the line of sight. There is, however, a small error due to misalignment and this depends upon the method of mounting. The measurements by Cheney (Ref. 11) given in Figure 6.7 refer to a target with an axis of rotation about its rear apex.

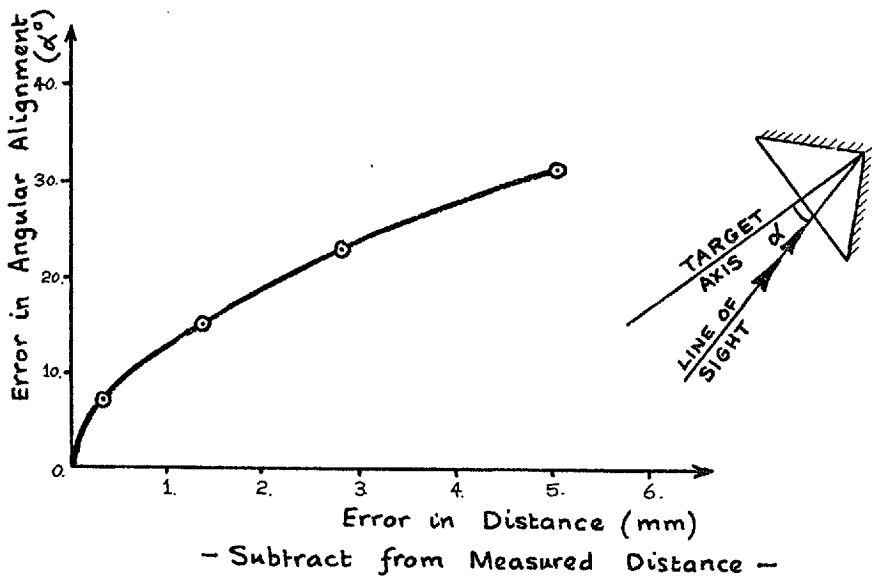
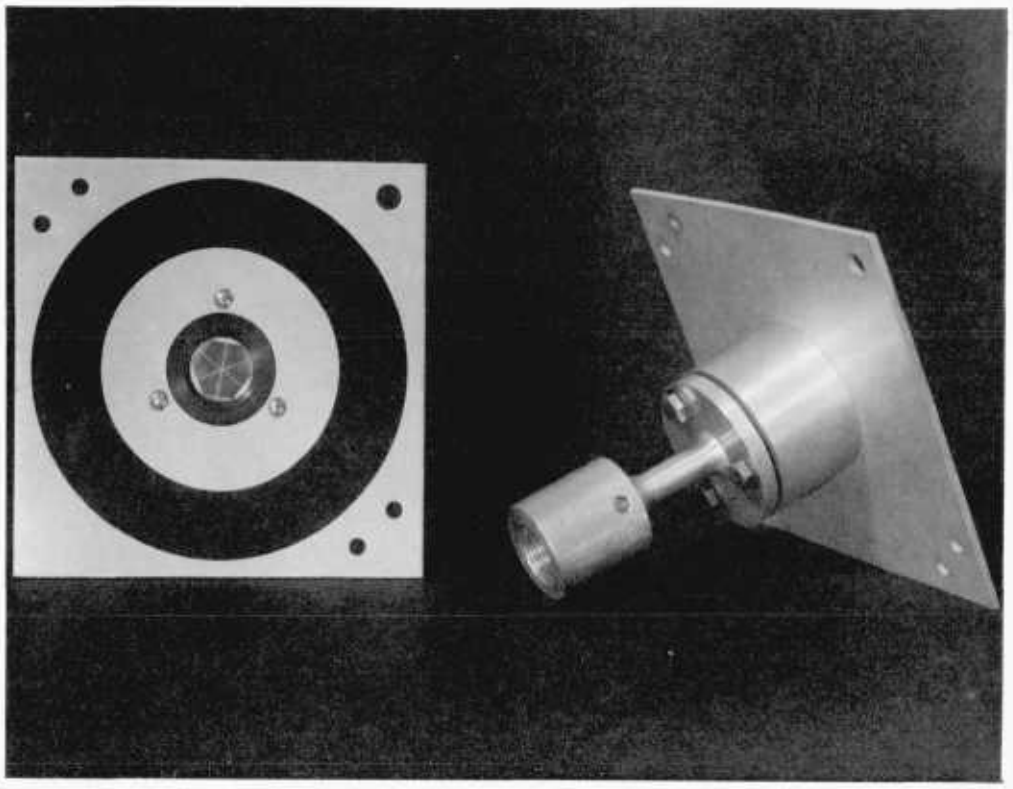


Figure 6.7

If the target is mounted correctly, with the axis somewhere within the reflector, then errors due to misalignment are cancelled by real changes in length. Based on the assumption that measurements are always made with reference to this axis, then alignment problems may be ignored when determining displacements of fixed targets by bearing and distance measurement from one station only.

Figure 6.8 shows a compound target constructed for use by the



ASSEMBLED TARGET



EXPLODED VIEW SHOWING CONSTRUCTION

FIGURE 6.8

author. This consists of a 6 inch square anodized metal target with the 'bulls eye' replaced by a 1 inch diameter corner cube. The housing for the corner cube is coupled, via a ball and socket fixture to 1 inch diameter studding which may be fixed as a resin bounded rock anchor. Using the Mekometer this target has a maximum useful range of about 1,000 ft.

It should be noted that the Mekometer requires reflectors to be stress free, since it utilizes elliptical polarisation modulation. The corner cubes, which are ground to a tolerance of better than 10 seconds, are therefore relatively expensive. Other instruments work on a different principle so there seems ample scope for investigating cheap reflectors which do not provide a financial deterrent to leaving them in situ.

6.3.4 Accuracy of Measurements

The accuracy of individual measurements has already been stated. It is, however, pertinent to remark that due attention must be given to the conditions in which the survey work is conducted. Open pits are very likely to give rise to anomalous air conditions so refraction and shimmer may be serious problems. Horizontal refraction over the pit is a particular problem which is not generally encountered elsewhere. It may have a significant influence on the accuracy of angular measurement but is unlikely to effect distance measurements. Proportional errors in electromagnetic distance measurement are 1 ppm for every $1^{o}C$ error in the temperature estimation. From all points of view, therefore, it would appear advisable to survey when the air conditions are most stable.

When all necessary corrections have been made and distances reduced to a common horizontal plane, the co-ordinates of all points may be calculated, if those of the reference scheme are known. Finally, displacements may be determined by comparison with previous results. (Of course, it is also possible to calculate displacements directly from differences in the reduced data.) In order to give meaning to these results it is necessary to have an

estimation of the likely error. Since estimates of the accuracy of individual observations can be made then it is possible to calculate the likely error in the co-ordinates determined for any station. This procedure has been discussed at length by Watt (Ref. 8) in connection with pre-analysis of a survey configuration to test whether it will yield the required accuracy. The method of calculating the so called 'error ellipses' (Fig. 6.9) will not be reproduced here.

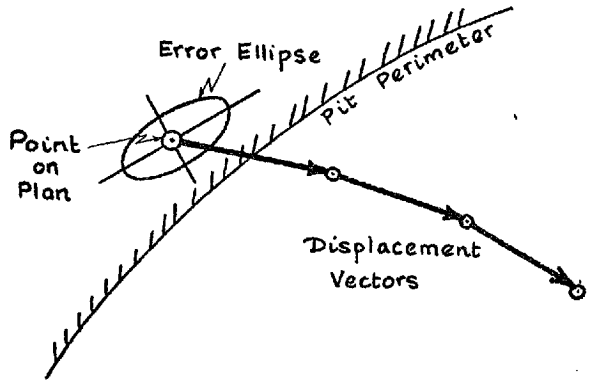


Figure 6.9

6.4 SLOPE MONITORING AT GORTDRUM MINE, IRELAND

Gortdrum is an open pit copper mine situated a few miles outside Tipperary, in the Republic of Ireland. The pit is small, measuring about 2,500 x 800 feet, but it is geologically complex. A large fault runs down the long axis of the pit and divides it into two halves with rather different characteristics.

Owing to the close proximity of the tailings dam to the pit and the economic necessity of mining at the maximum safe slope angle, some form of slope monitoring has been considered essential. The author was fortunate enough to try out ideas in this realistic situation. Also, since these measurements were not part of the scheme used by the mine, it was possible to place emphasis on assessing the practicality of the method rather than routinely producing results.

6.4.1 Operational Procedure

Since the monitoring project was to be relatively short-lived and the final geometry of the excavation was uncertain, the monuments were chosen to be simple and easy to construct. A station at the eastern end of the pit was assumed stable as it was relatively remote and development at that end limited. A station at the western end provided the far point of the main baseline running down the length of the pit. The orientation of this baseline could be checked by reference to a church spire with a conveniently ornate cross on the apex. Originally six other crest stations were positioned around the western end of the pit (Fig. 6.10), where the excavation was deepest. Some small failures had already occurred, on the southern side, in massively bedded sandstones and mudstones.

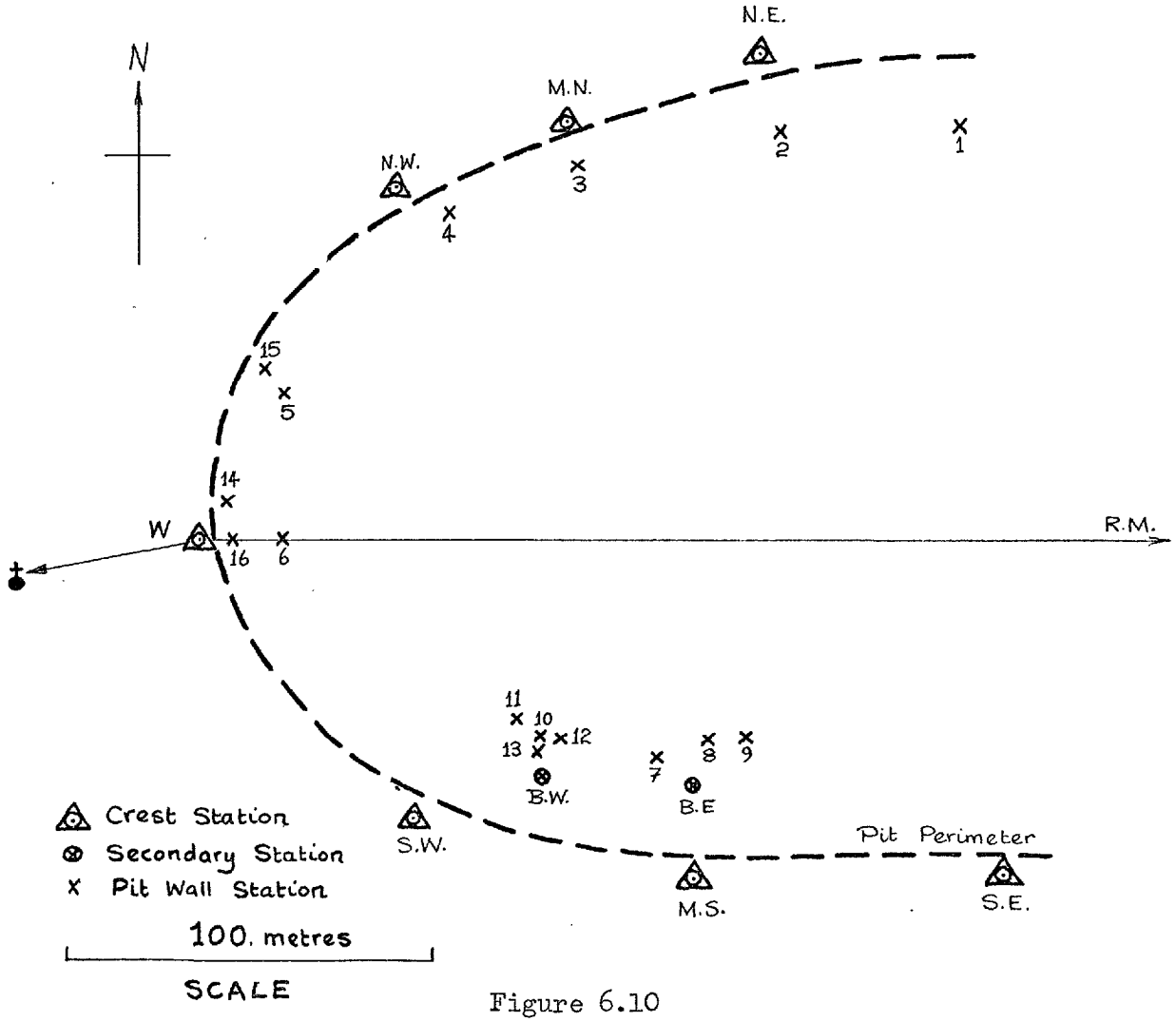


Figure 6.10

The crest stations consisted of metal tubes inset in concrete. For centering purposes a small plug could be inserted and for trigonometrical levelling an extension and crosspiece fixed as shown in Figure 6.11.

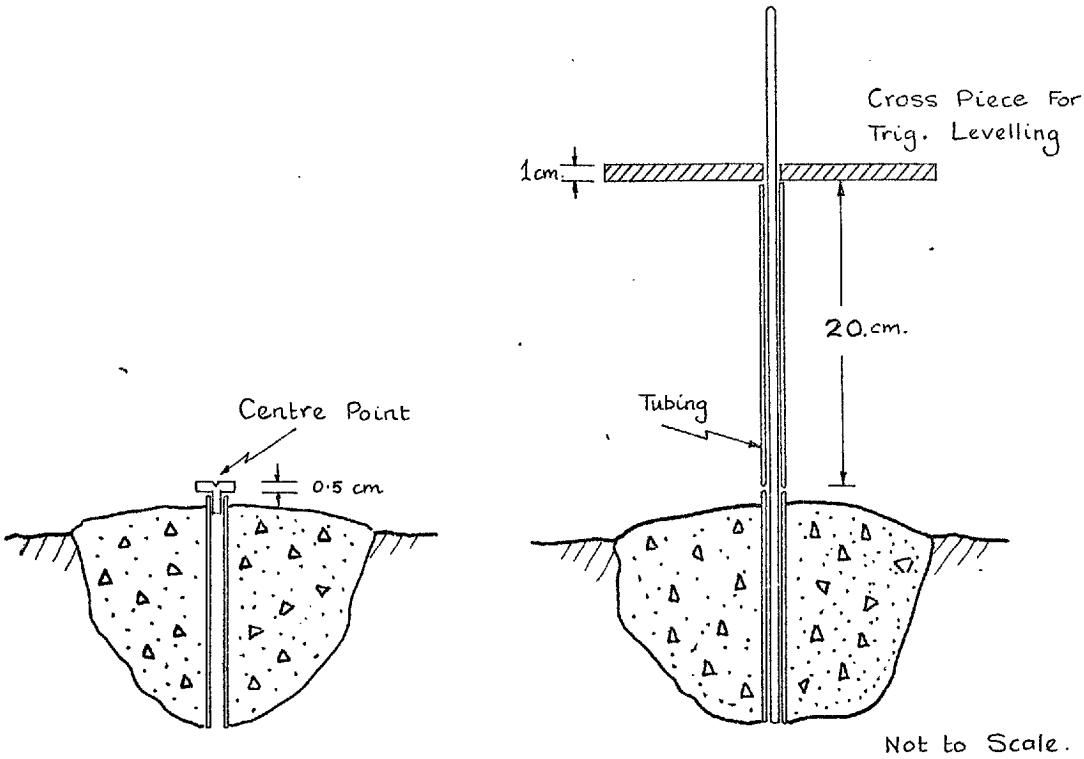


Figure 6.11

Despite the roughness of this scheme the results obtained using the Mekometer are fairly impressive. (The prototype of the instrument was kindly lent to the author by its originator Dr. K.D. Froome of the National Physical Laboratory, Teddington.) Table 6.II gives the results for repeated measurements of the main baseline throughout the period of the field trials. It should be noted that errors include those due to centering. For the latter purpose the self centering metal tripods manufactured by Kern were used. They proved very satisfactory providing a check was always made that the centering rod was not constrained by the centre mark.

Targets on the pit wall were surveyed by intersection so were simply $\frac{1}{4}$ inch screw heads or nuts. These proved very satisfactory for precise sighting but only the author could see them at the range involved! Clear identification was necessary and it was found useful to repaint both the sighting points and indicator

Measurements of Main Baseline Reduced to Horizontal

Date	Number of Observations	Horizontal Length cms
May 1970	2	75225·19
July 1970	1	75225·04
Oct. 1970	4	75225·20
Dec. 1970	2	75225·32
Feb. 1971	2	75225·36

Table 6.II

targets at the start of any series of measurements. The amount of swinging on the end of a rope and scrambling over broken material involved during the repainting, provided a practical demonstration of the convenience of targets that could be left undisturbed.

The surveying procedure consisted of trigonometrical levelling of the crest stations and then co-ordinating by trilateration, using the Mekometer. The pit wall targets were then intersected from two or more crest stations, two compensated rounds being taken at each with a Watts Microptic No. 2 theodolite. The scheme proved quite satisfactory and the author was able to complete all measurements, unaided, in about three days.

6.4.2 Surveying Calculations

Calculation of results was split up into five parts.

(1) Trigonometrical levelling for crest station elevations.

(2) Reduction of distances to horizontal.

(3) Trilateration calculations for co-ordinates of crest stations.

(4) Intersection of pit wall stations. A third ray was initially used as a check but was

dropped as the angle of intersection was very acute.

(5) Trigonometrical levelling for the pit wall target elevations.

Computations were performed with a Hewlett Packard 9100B, although use could have been made of larger computing facilities for such routine work. However, the author believes there is considerable advantage to be gained in breaking down the calculation into small steps as above and using one of the increasing number of programmable desk calculators. The advent of surveying equipment providing digital output onto punched paper tape may facilitate direct computer processing in the future.

6.4.3 Results of Measurements

Table 6.III gives records of movements of some stations throughout the period of measurement. Stations on the eastern side were lost, due to two small slides and the resulting clearing up operation, so they are not included.

The tight western end of the pit seemed most stable. This was anticipated since the structural features lie predominantly normal to western face. Two monolithic blocks on the southern side excited initial interest, but main mining operations transferred way from the area and the blocks appeared to stabilize. There was no evidence of massive movement on this southern side and therefore no immediate concern for the tailings dam.

6.4.4 Conclusions from Field Trials at Gortdrum

Although the measurements could be done quite rapidly, it was obvious that considerable time would be saved by the use of pillar instead of tripod set ups. These should have very substantial foundations and should be placed far enough back from the crest to minimise the risk of loss through a small bench failure.

	June 1970			July 1970			Oct. 1970			Dec. 1970			Feb. 1971		
Station	E	N	H	E	N	H	E	N	H	E	N	H	E	N	H
R.M.	0.	0.	0.	0.	0.	0.	0.	0.	0.	0.	0.	0.	0.	0.	0.
W.	0.	0.	0.	+0.2	0.	-0.2	+0.1	0.	-1.3	0.	0.	0.	-0.1	0.	0.
N.W.	+1.3	-1.5	-1.2	+1.7	+0.1	-0.2	+0.9	-0.6	-2.5	+1.1	-1.5	-1.2	+1.1	-1.7	-3.2
M.N.				+0.6	-0.3	-1.0	Original Station Lost								
N.E.	+1.2	+0.3	-1.	-0.4	-3.3	-1.5	Original Station Lost								
S.W.	Original Station Lost						+0.7	-0.4	-1.9	-0.7	-0.7	-1.5	-0.5	-0.1	-1.8
M.S.				+0.4	+0.1	+0.1	+2.0	+1.7	-0.4	+0.2	+0.6	-0.5	0.	+1.0	+0.6
S.E.	Original Station Lost						+2.0	+2.7	-0.4				-0.3	+0.3	-0.1
B.E.				+1.7	+1.5	+1.1	+2.5	+1.4	0.	+2.3	+0.9	+1.2	+1.7	+0.6	+0.2
9	0.0	+0.5	-1.	0.0	+2.0	-0.5	-1.0	+15.5	-5.5			Station	Lost		
8	+0.5	+0.5	0.	+1.0	+4.0	0.	+1.0	+4.0	-1.5	+1.3	+3.5	-0.7	+0.6	+4.0	-0.6
7	0.0	+1.0	0.	+1.0	+4.0	0.	+1.0	+3.0	-2.	+1.0	+4.0	-0.5	+0.2	+4.7	-1.9
B.W.	+2.1	-1.0	0.	+2.5	+3.0	-0.3	+5.5	+4.0	-3.	+3.7	+3.1	-0.3	+4.0	+4.1	-3.2
12	+1.0	+3.0	-1.	+2.5	+6.5	-1.	+2.5	+6.3	-3.	+3.0	+7.5	-2.5	+3.5	+8.8	-3.6
13	+1.0	+3.0	-0.5	+2.5	+3.5	-1.	+2.5	+6.0	-3.5	+2.9	+5.5	-3.	+3.6	+6.4	-4.5
10	+0.5	+3.0	-0.5	+2.5	+5.5	0.	+2.5	+6.5	-2.	+3.0	+5.0	-1.2	+2.9	+6.9	-2.0
11	0.0	+3.0	0.	+1.5	+5.0	0.	+1.0	+6.0	-2.				+1.5	+7.0	-1.1
16	+0.5	0.	0.	+0.5	0.	0.	0.	0.	-1.	+0.6	-1.0	-1.0	+0.5	-1.1	0.
14	0.	0.	0.	0.	0.	-0.5	+0.5	0.	-1.	+1.0	-1.5	-0.7	-0.9	-1.3	+0.3
6	+0.5	0.	0.	0.	0.	0.	0.	+1.0	-1.5	+0.7	-1.2	-0.8	+0.4	-0.9	+0.1
5	+0.5	0.	0.	0.	-0.5	+0.5	0.	0.	-1.	+0.3	-1.6	-0.5	+0.4	-1.7	+0.3
15	+0.5	0.	0.	0.	0.	+0.5	-0.5	+0.5	-1.	0.	-1.0	-0.5	-0.3	-1.0	+0.3
4	+2.5	-3.5	-2.0	+3.5	-2.5	-2.5	+3.0	-3.0	-3.5	+3.6	-4.5	-3.5	+3.3	-4.5	-2.7

Table 6.III
Displacements at Gortdrum - First Measurement May 1970

The weak point of the scheme was definitely the trigonometrical levelling of the crest stations. Not only was it comparatively inaccurate but it was inconvenient for calculation, as the vertical angles did not correspond with measured distance. The intersections at the pit wall targets were generally too acute (about 30^{o}). Unfortunately, the geometry of the excavation made it difficult to do otherwise without considerably increasing the length of the sights. Bearing and distance measurements would not be subject to this problem, and are therefore preferred by the author.

The quality of angular measurement was noticeably weather dependent. Vertical angles tended to be more consistent between rounds than horizontal angles. This was attributed to horizontal refraction, but could be due to differential expansion and subsidence of the tripod legs. In general, disagreements between consecutive rounds was of the order of one to two seconds for both horizontal and vertical angles.

There has been no attempt to draw any conclusions regarding slope stability at Gortdrum. The field measurements were not of sufficient duration to provide useful data and the geological and rock strength data is too limited to permit any meaningful numerical analysis.

6.5 SLOPE MOVEMENTS AT THE BERKELEY PIT

Anaconda's Berkeley Pit at Butte, Montana, has a history of small slope failures. The author visited this site for a few days and was provided with records of slope movements in an area where slope failure was anticipated. The information gathered is reported briefly as an example of typical field measurements.

Large movements were detected at the crest of the pit. In the particular location the slope was standing at about 50^{o} and the crest was some 330 feet above the next working level. The rock was predominantly weathered and unweathered granite, with about 130 feet of oxidized ore at the surface.

Cumulative movements of up to five feet were apparent, on a few major discontinuities, when the author visited the site. Measurements on a series of lines of posts had been made over the preceding four months. Typical results of taping between posts are given in Figure 6.12. Taking results from all lines, contours of displacement occurring over a particular time span may be plotted as in Figure 6.13. This provides a useful method of presenting data.

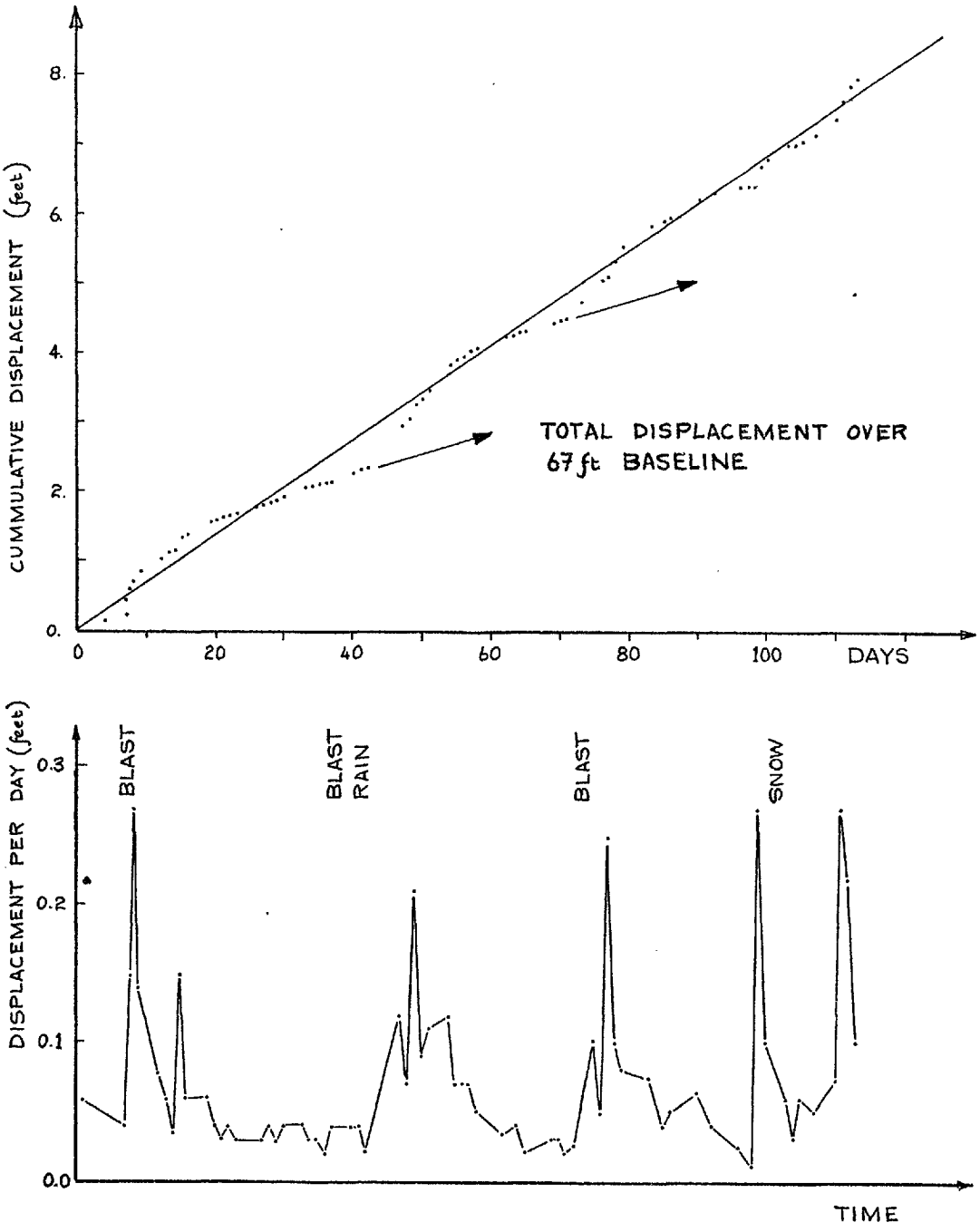
No mapping of surface cracking or geological structure had been carried out so the author spent some time collecting data summarized in Figure 6.14. Comparison between Figures 6.13 and 6.14 showsthe very strong structural control on the movements. On the basis of the geological measurements it appeared that the slide was either deep seated, or a local toppling failure. Cracking on lower benches, a large component of horizontal displacement and a total lack of evidence of movement in the toe region tended to support the latter as a possible explanation.

A later report revealed that the slope did not fail as anticipated, and it was eventually flattened to prevent further problems.

6.6 AN EXAMPLE OF COMPARISON WITH COMPUTER PREDICTION

The only example available in the literature appears to be that on work carried out at the Kimbley Pit by Kennecott Copper Corporation and the U.S.B.M. The original Finite Element analysis was conducted by Blake (Ref. 12) who considered the rock to be linearly elastic but took account of different rock types and residual stress states. He concluded that the stress state was low with respect to the rock strength and that it might reasonably be assumed that the rock would behave elastically.

A test during which the slope was steepened by excavation was carefully monitored in adits behind the slope face. This provided excellent data with which to compare further computer analysis since the total displacements resulting from the material removal



DISPLACEMENTS AT THE BERKELEY PIT

FIGURE 6.12

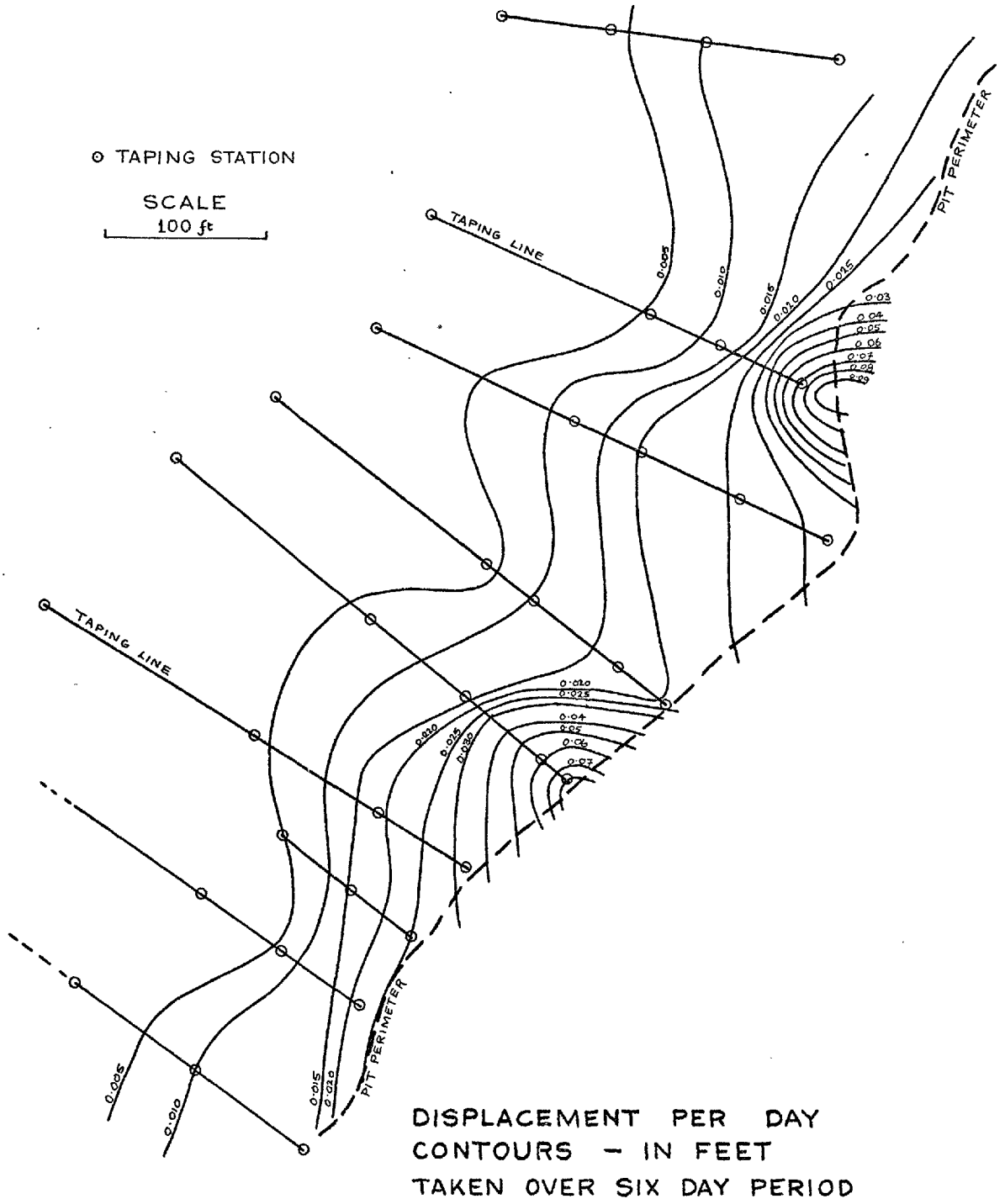

o TAPING STATION
SCALE
100 ft
TAPING LINE
TAPING LINE
PIT PERIMETER
PIT PERIMETER
0.005
0.010
0.015
0.020
0.025
0.030
0.035
0.040
0.045
0.050
0.055
0.060
0.065
0.070
0.075
0.080
0.085
0.090
0.095
DISPLACEMENT PER DAY
CONTOURS - IN FEET
TAKEN OVER SIX DAY PERIOD

FIGURE 6.13

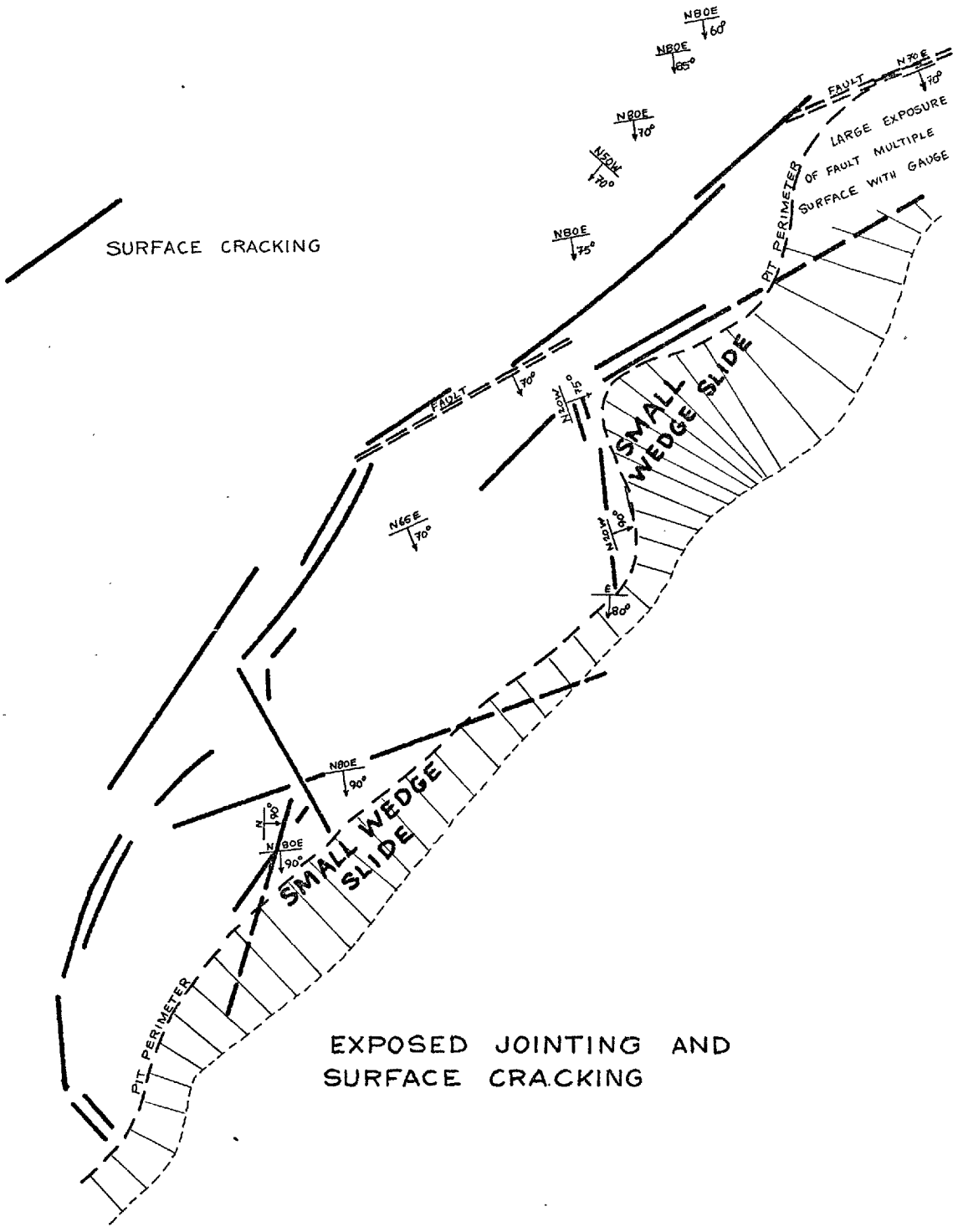

SURFACE CRACKING
FAULT
LARGE EXPOSURE OF FAULT MULTIPLE SURFACE WITH GAUGE
PIT PERIMETER
SMALL WEDGE SLIDE
SMALL WEDGE SLIDE
PIT PERIMETER
EXPOSED JOINTING AND SURFACE CRACKING

FIGURE 6.14

were measured. In the event, agreement between observed and computed behaviour was excellent (Ref. 13). The test has provided the only field data concerning the elastic recovery of a rock mass due to the excavation of a pit (Fig. 6.15).

It should be noted that correlation was achieved only because measurements commenced before the excavation started. In any displacement measurement system this is essential. All too often displacement studies start only after a slope has already deteriorated beyond recovery.

6.7 AN EXAMPLE OF WARNING OF FAILURE

The slide at the Chuquicamata pit in Chile provides an excellent and well documented example of displacement measurement used to predict slope failure (Ref. 4). In this case movements were large and relatively crude surveying methods proved to be satisfactory.

Measurements of displacements throughout the sliding area resulted in plots of cumulative displacement versus time for the fastest moving point (Fig. 6.16). This was used to predict the date of failure a month before it actually occurred. Although a considerable amount of guess work was involved in deciding exactly how much displacement could occur before total collapse, the estimate was correct to the day. Pit production was only slightly affected and there was no loss of life although 12 to 15 million tons of material were involved in the slide.

6.8 CONCLUSIONS

The prediction of time of collapse, or early warning, has been the main function of observational methods in connection with rock slopes in open pit mines. In this context, simple displacement measurements and records of microseismic activity are proven techniques. Undoubtedly, others will be used in the future. Already Terrestrial and Air Photogrammetry (Ref. 14) are attracting attention as methods of monitoring displacements.

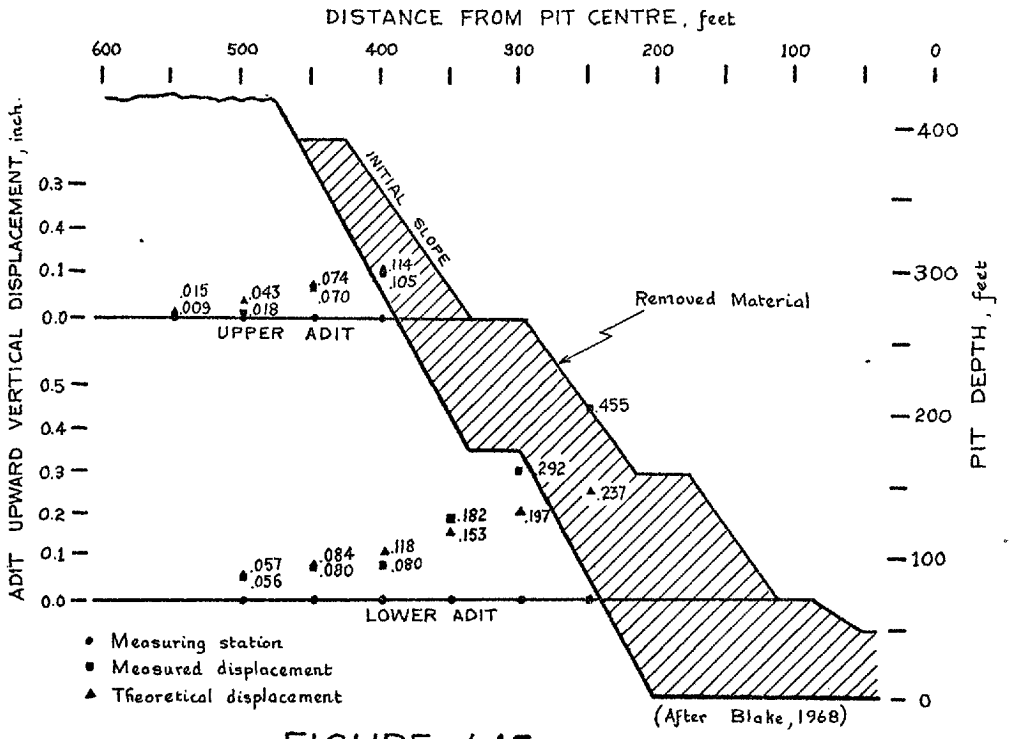
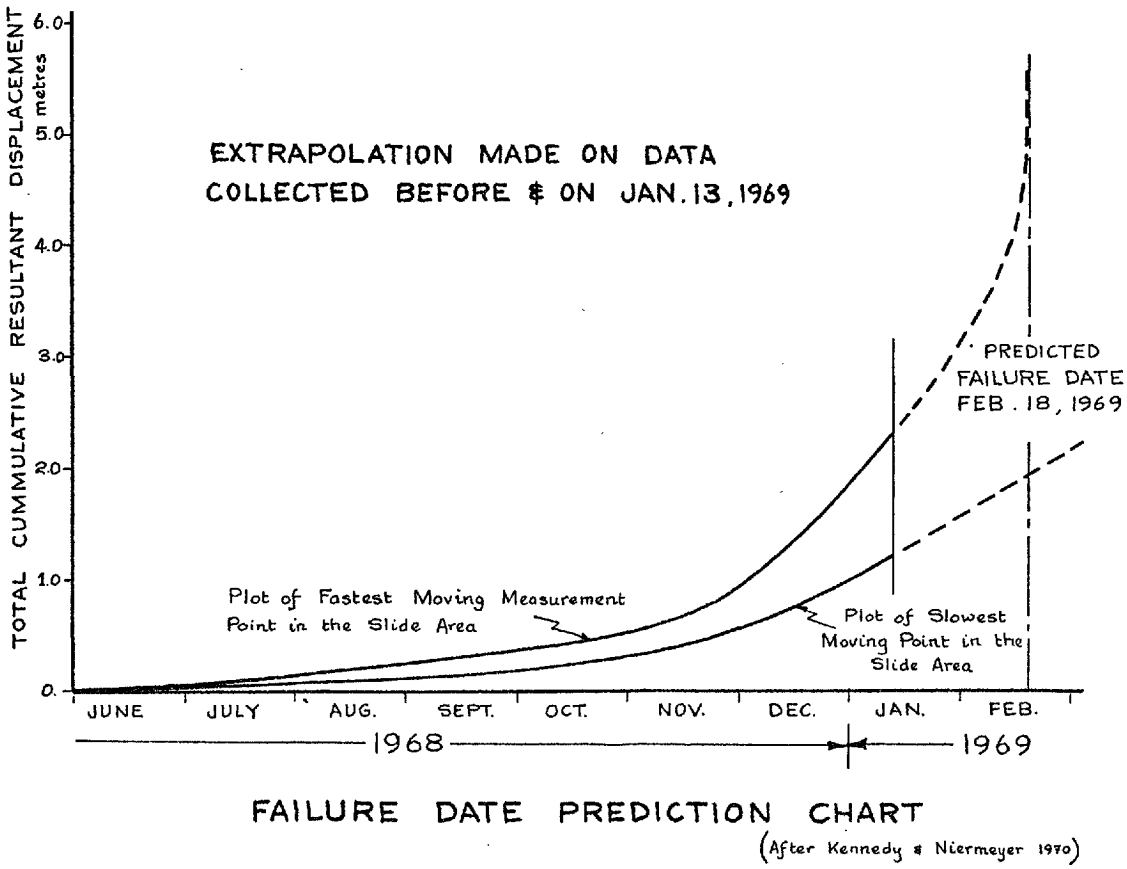


FIGURE 6.15



FAILURE DATE PREDICTION CHART
(After Kennedy & Niermeyer 1970)

FIGURE 6.16

The precise determination of surface displacements by surveying techniques has been discussed in detail. The advent of accurate distance measuring equipment is certain to have a profound impact in this field as displacements may now be monitored with great precision and relatively little effort. If such information can be gathered from the start of an operation early warning of potential slope failure will be possible. Field studies of this type are vital to the advance of the subject of slope stability since only then can the modern numerical techniques be evaluated.

(1) Müller, L. The Stability of Rock Bank Slopes and the Effect of Rock Water on the Same. Int. J. Rock Mech. Mining Sci. Vol. 1 pp 475-504, 1964.

(2) Blake, W. & Leighton, F. Recent Developments and Application of the Microseismic Method in Deep Mines. Rock Mechanics - Theory & Practice. (Proc. 11th Symp. Rock Mech. University of California) Pub. A.I.M.M. & P.E. 1970.

(3) Merrill, R.H. Bureau Contribution to Slope Angle Research at the Kimbley Pit, Ely, Nevada. Trans. Soc. Mining Engineers A.I.M.E. Vol. 241, December, 1968.

(4) Kennedy, B.A. & Niermeyer, K.E. Slope Monitoring Systems used in the Prediction of Major Slope Failure at the Chuquicamata Mine, Chile. Planning Open Pit Mines (Proc. Symp. on the Theoretical Background to the Planning of Open Pit Mines with special reference to Slope Stability) Pub. S.A.I.M.M. 1971.

(5) Hartman, B. Slope Stability Instrumentation. Status of Practical Rock Mechanics (Proc. 9th Symp. Rock Mech. Colorado) Pub. A.I.M.E. 1968.

(6) Dodds, R.K. Rock Movement along Fractures during Failure. Proc. 1st Cong. I.S.R.M. Lisbon 1966. Paper 6.1.

(7) Mathews, K.E. & Edwards, D.B. Rock Mechanics Practice at Mount Isa Mines Limited, Australia. Proc. 9th Commonwealth Mining & Metallurgical Congress, 1969. Paper 32.

(8) Watt, I.B. Control for Early Warning of Potential Danger in Open Pits. Planning Open Pit Mines (Proc. Symp. on the Theoretical Background to the Planning of Open Pit Mines with special reference to Slope Stability) Pub. S.A.I.M.M. 1971.

(9) St. John, C.M. & Thomas, T.L. The N.P.L. Mekometer and its Application in Mine Surveying and Rock Mechanics. Trans. I.M.M. Vol. 79 p A31-A36.

(10) Sheppard, J.S. Theodolite Errors and Adjustments. Pub. Stanley London, 1965.

(11) Cheney, J. Personal Communication 1970. Building Research Station, Watford.

(12) Blake, W. Stresses and Displacements Surrounding an Open Pit in a Gravity-Loaded Rock. U.S.B.M. Rept. of Inv. 7002.

(13) Blake, W. Finite Element Model Study of Slope Modification at the Kimbley Pit. Trans. Soc. of Mining Engs. A.I.M.E. Vol. 241, December, 1968.

(14) Curran, J. Case History of Use of Analytical Aerial Photogrammetry in Slope Failure Analysis for Mine Planning. Presented at the Fall Meeting, Society of Mining Engineers, A.I.M.E. 1971.

CHAPTER

7

A STUDY OF A PHYSICAL MODEL AND THE MODELLING MATERIAL

	Page
Chapter Index	231
Synopsis	232
7.1 Introduction	233
7.2 The Model	233
7.3 The Material and the Properties of Discontinuities	235
7.4 Idealized Behaviour for Computer Simulation	236
7.5 Computer Studies	242
7.6 Conclusions	258
References	260

Synopsis

The properties of a modelling material, and discontinuities introduced into it, are discussed with reference to the material behaviour proposed in Chapter 4. The idealized relationships necessary for computer analysis are obtained from reported laboratory test data.

A physical model of a multijointed rock slope is analysed using some of the two dimensional finite element techniques discussed in this thesis. A comparison is made between the displacements of the physical model and the various computer simulations.

7.1 INTRODUCTION

A number of computer techniques for modelling rock slopes have been discussed in this thesis. No justification by comparison with real situations has been possible. Any examples have been idealized models studied for the purposes of illustration. Unfortunately the author does not have access to a sufficiently well documented study of slope behaviour on which to conduct an exhaustive computer analysis. Indeed, it is probable that no such case exists as the procedures of precise slope monitoring and jointed rock testing are relatively new and unpractised.

The most comprehensive computer simulations discussed in this thesis are two dimensional and are immediately an approximation to the real situation. Of course these techniques are readily extended to the full three dimensional case. Doubtless this will be done in the future. For the present, however, the ideal check is against a well documented, two dimensional model of a jointed rock slope. Obviously it is important that the physical characteristics of the model should be representative of the real situation.

Barton (Ref. 1) has described a number of studies of jointed rock slopes. These are well documented with details of boundary conditions, excavation procedure and displacements prior to failure. He also gives extensive information concerning the characteristics of both the solid material and the discontinuities introduced by tensile fracturing. Tests on the latter provided evidence on which to base the idealized behaviours discussed in Chapter 4. Altogether, Barton's study provides an excellent opportunity to demonstrate the use of the numerical methods, discussed in this thesis, to study a practical problem. It is also possible to compare observed and computed behaviour.

7.2 THE MODEL

The model was constructed from 16" square slabs, 1" in thickness, of a material comprising read lead sand/ballotini and plaster of paris (Ref. 2). Regular sets of parallel joints were produced in these slabs by propagating a tensile fracture through them by

means of a specially designed guillotine. The strength of these discontinuities was carefully matched with the material density to give geometric and stress scaling factors of 500 : 1 and 666 : 1 respectively. (For the purposes of computer analysis the real model properties will be used throughout.)

The completed model, measuring 8' long and 4' high, was assembled from 18 slabs with the loading rig in the horizontal position. It was then rotated slowly to the vertical while the horizontal loading was increased to retain a constant ratio with the vertical loading due to gravity. In its final position, under plane stress conditions, a pit was excavated in the centre of the model by means of a spatula and a vacuum cleaner.

The model to be discussed was designated number L.M.3 by Barton (Ref. 1). It contained three joint sets at half inch spacing and was symmetrical about the centre line (Figure 7.1). The boundary conditions were carefully controlled so that the initial horizontal stresses were one half of the self weight vertical stresses. The lower boundary was fixed but the side boundaries provided a partially following load.

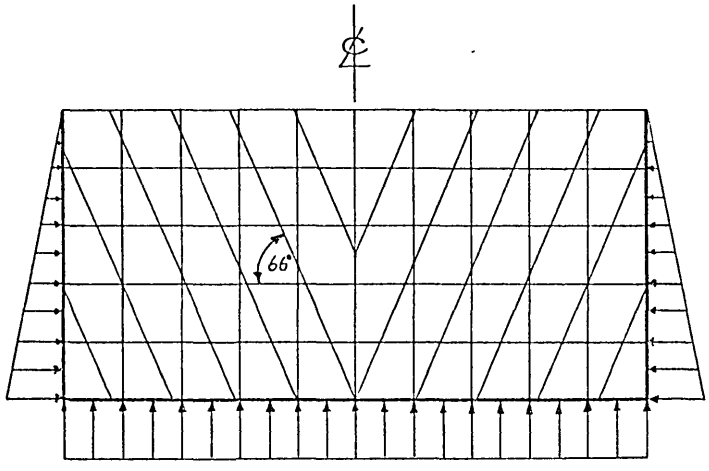


Figure 7.1

Excavation was performed in a series of steps. At the end of each the new displaced condition was recorded photographically. Displacements of a number of sample points were thereby known to

an accuracy of about 0.006 inch. Those recorded at the crest of the slope were larger than elsewhere and are given in Table 7.I. In general the displacements decreased towards the toe, where they were predominantly horizontal. Final collapse occurred with a symmetrical excavation 31·2" in depth, about 6" across the base and a slope angle of around 82°.

Depth (Inches)	Displacement (Inches)	Inclination to Horizontal Dipping into the Excavation (Degrees)
0·	0·	0·
8·	0·034	21·
16·	0·031	15·
25·	0·049	14·
30·	0·086	16·
31·2	F A I L U R E	

Table 7.I

7.3 THE MATERIAL AND THE PROPERTIES OF DISCONTINUITIES

The elastic properties of the solid material were determined from uniaxial compression tests on specially prepared specimens. The following apply to the material from which the model was constructed.

Density	=	0.07 lbf/in^3
Youngs Modulus (50% U.C.S.)	=	1.07×10^4 lbf/in^2
Poisson's Ratio (Estimated)	=	0.15
Uniaxial Compressive Strength	=	20.14 lbf/in^2

The joints produced in the slabs by the guillotine were rough but continuous unless stopped by pre-existing discontinuities. Three different types of joints were distinguished according to their order of occurrence (Figure 7.2). The differences between their properties are seen clearly in Figures 7.3 - 7.6.



Primary Joint — Continuous



Primary Crossed Joint — Continuous, but influenced by secondary jointing



Secondary Joint — Discontinuous

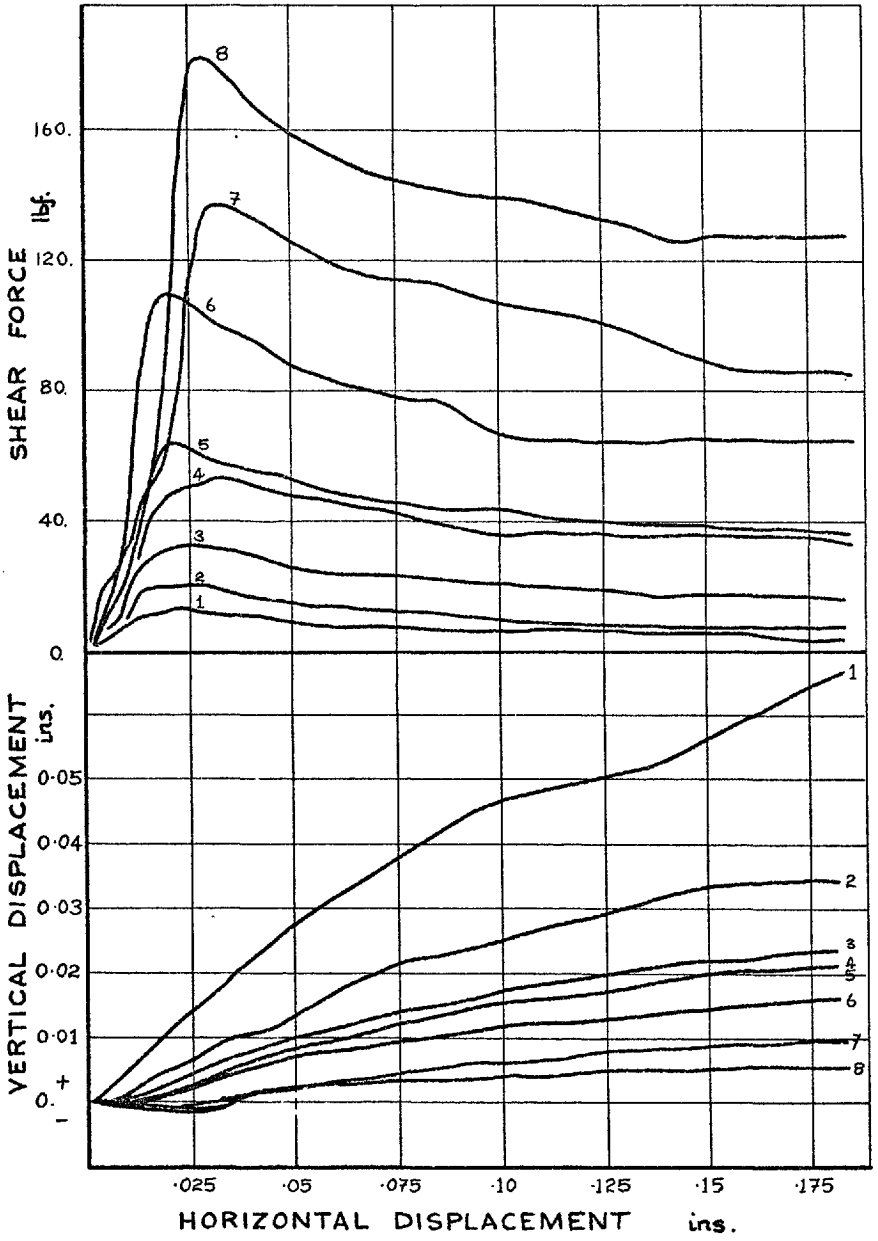
Figure 7.2

7.4 Idealized Behaviour for Computer Simulation

The upper portion of Figure 7.3 shows the relationship between shear force and shear displacement resulting from direct shear tests on 2·32" x 1·0" samples containing a single primary discontinuity. Barton (Ref. 3) suggests that these provide evidence that the displacement to peak is independent of normal stress. In view of the scatter of results the author feels justified in retaining the constant shear stiffness approach discussed in section 4.5.2.

Figure 7.4 indicates that the residual angle of friction for the primary jointing is close to 45°. Figure 7.5 shows that over the normal stress range relevant to the model study the ratio of peak to residual shear strength is about 2. The residual shear strength per unit area is 1·0 lbf/in^2. If the displacement to peak strength is taken as 0.02" then the required shear stiffness to match the initial shear behaviour is 100 lbf/in^2/in. The approximation of the joint shear behaviour, based on the above information, may now be drawn as in Figure 7.7.

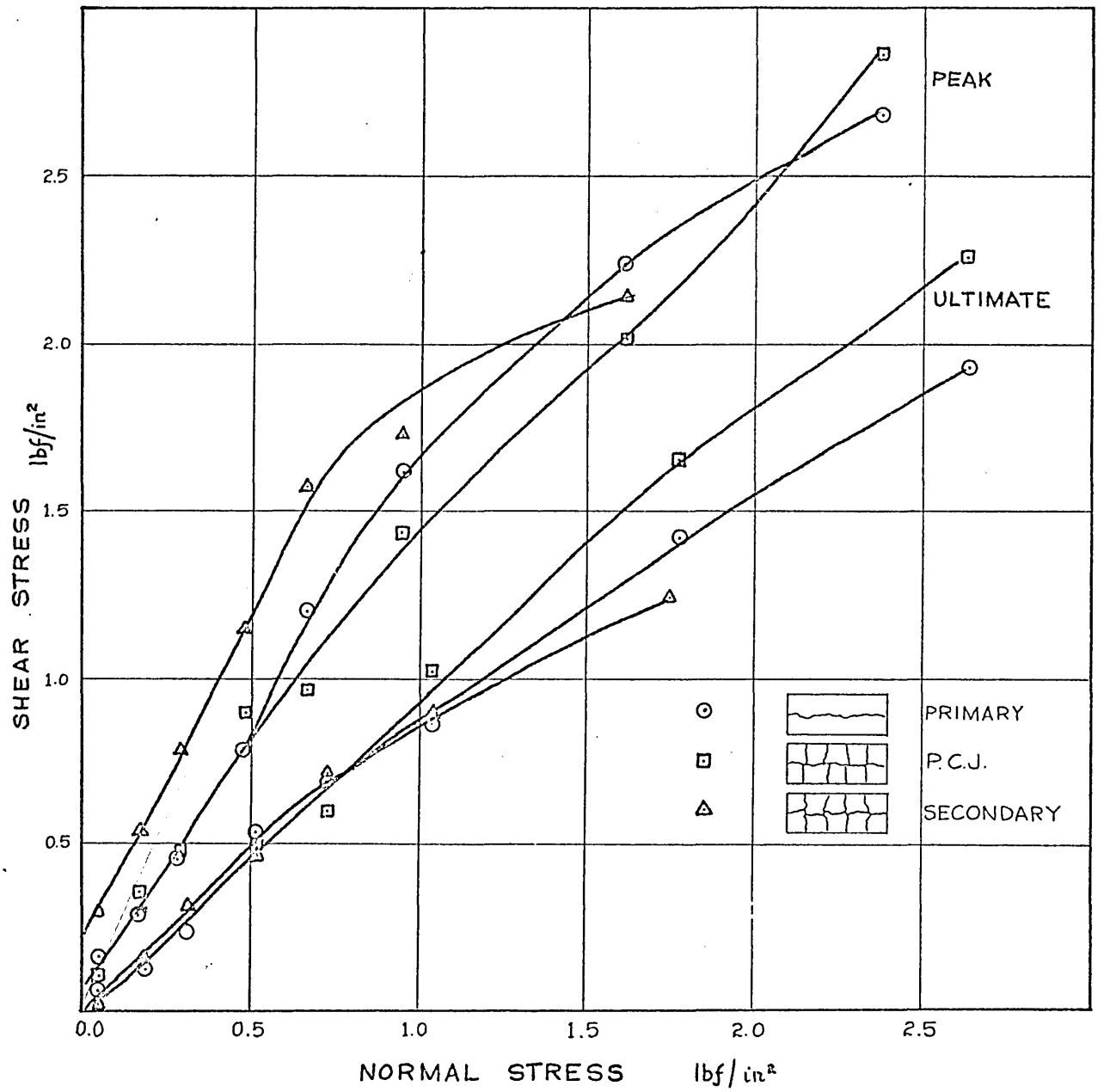
The lower portion of Figure 7.3 shows the dilatation of the joint during shear whilst subject to a variety of normal stresses. For the purposes of simulation this behaviour is split into two



SHEAR FORCE - DISPLACEMENT AND DILATATION
PRIMARY TENSION JOINT (After N. Barton)

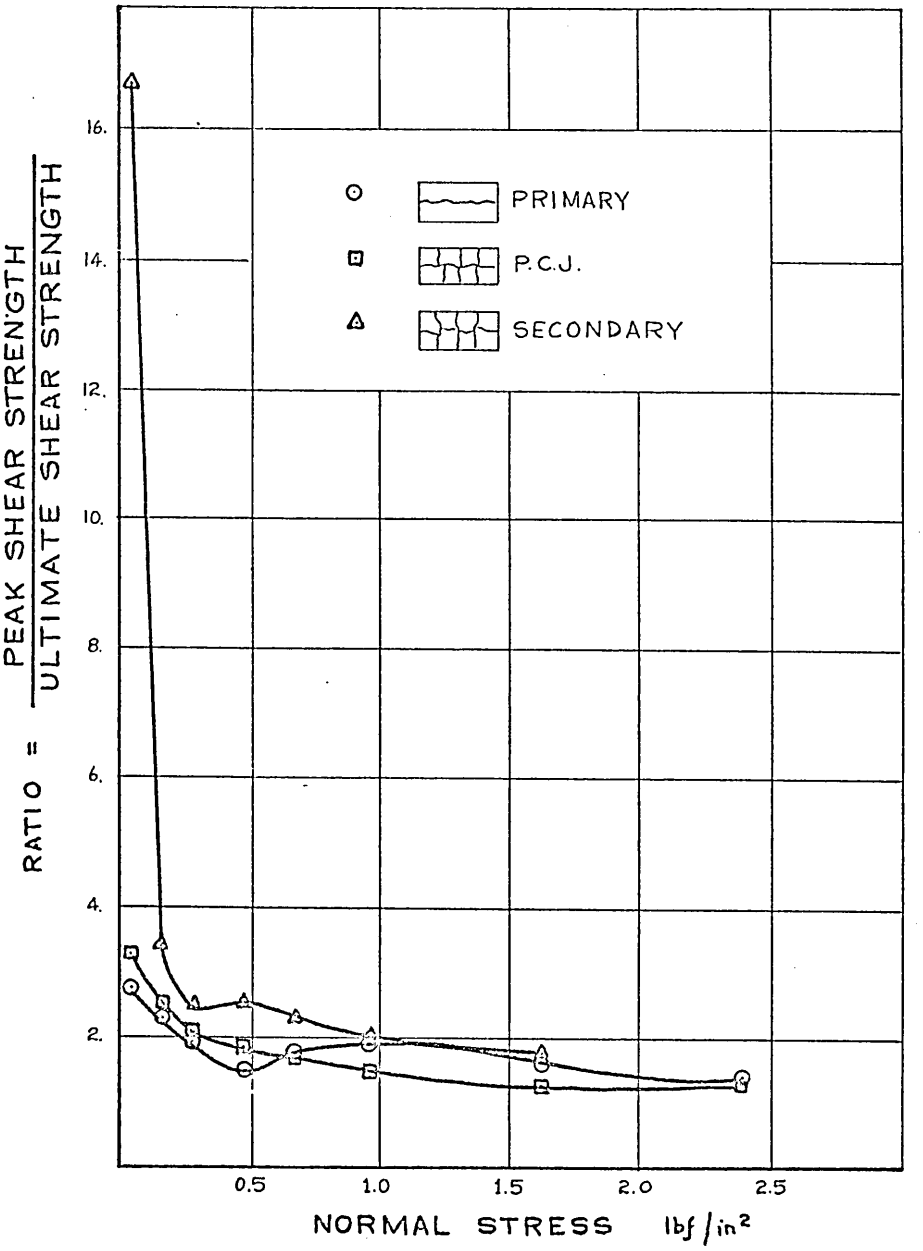
KEY	NORMAL STRESS
1	0·044
2	0·168
3	0·286
4	0·477
5	0·668
6	0·954
7	1·620
8	2·383

FIGURE 7.3



SHEAR STRENGTH ENVELOPES FOR THE THREE JOINT TYPES (After N. Barton)

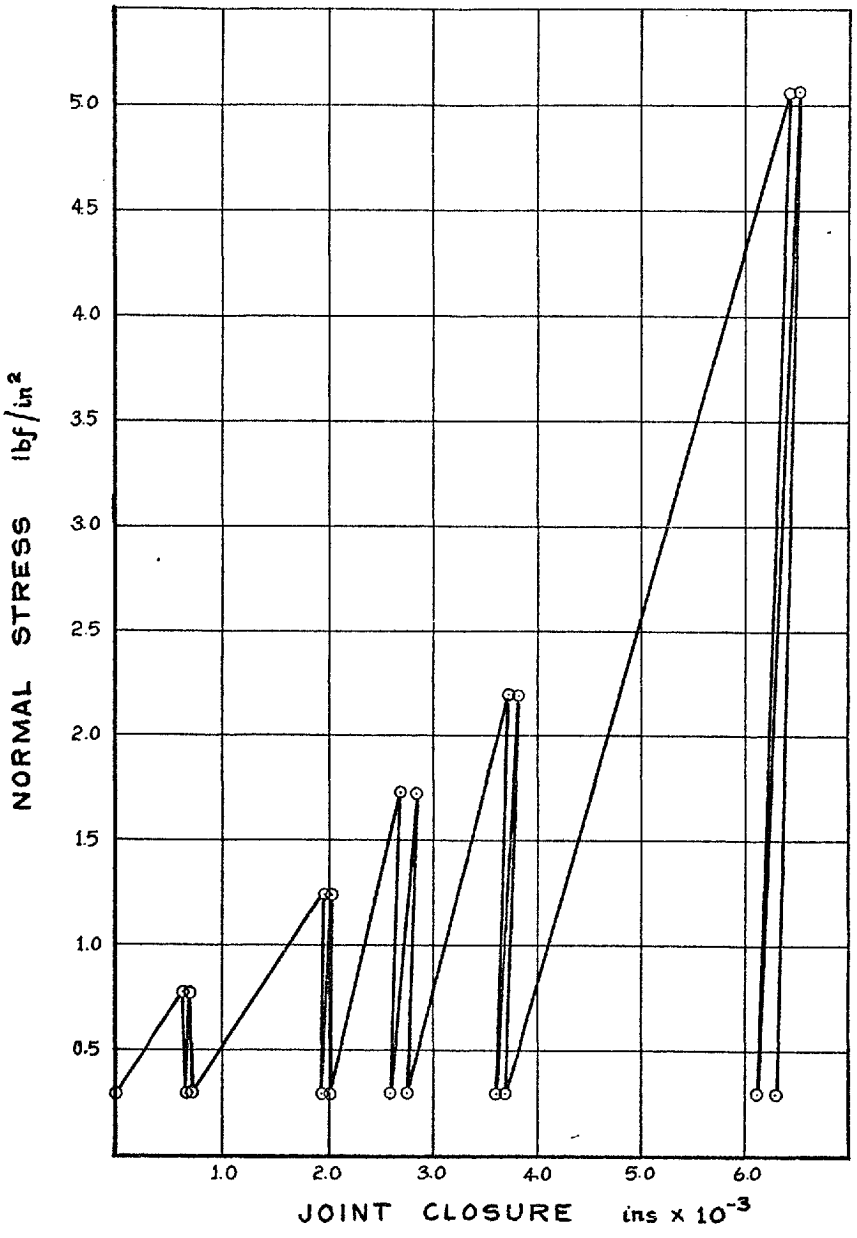
FIGURE 7.4



RATIO OF PEAK TO ULTIMATE SHEAR STRENGTH AS A FUNCTION OF NORMAL STRESS

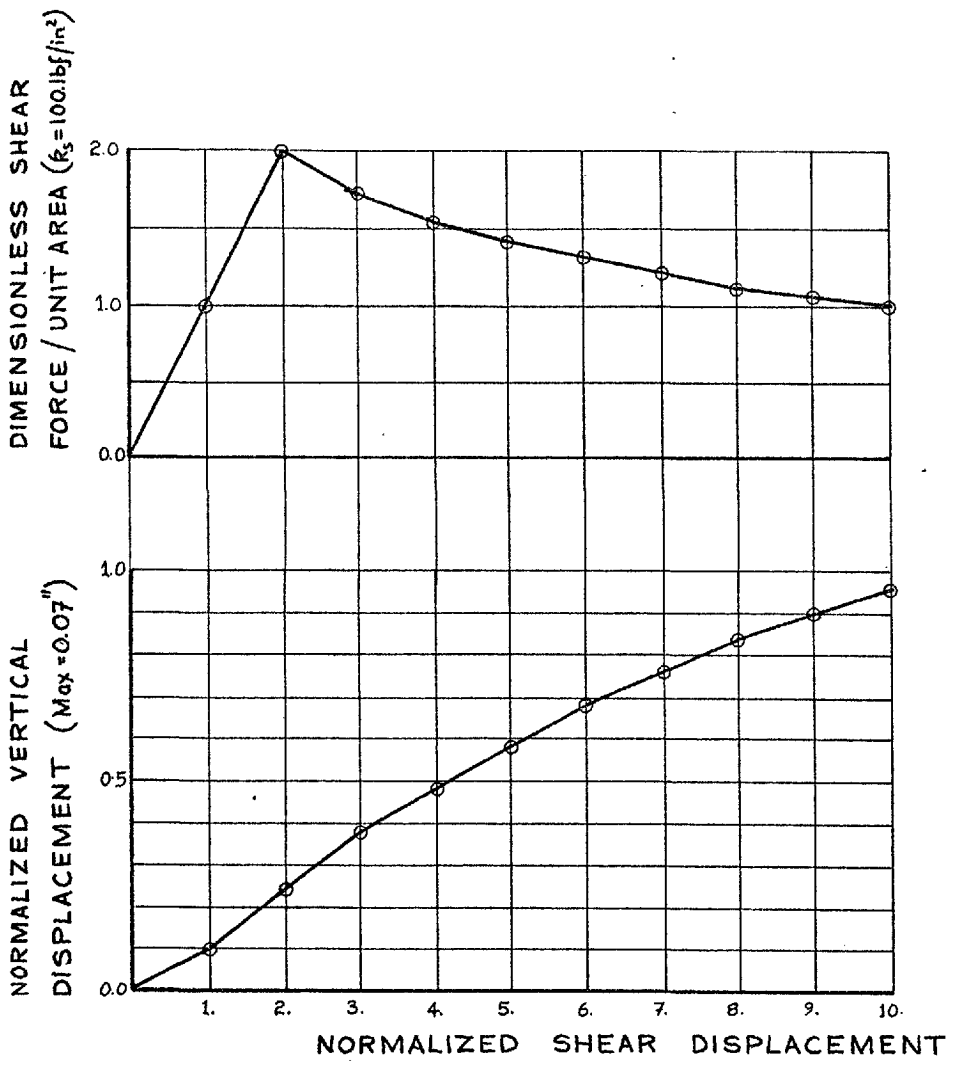
(After N. Barton)

FIGURE 7.5



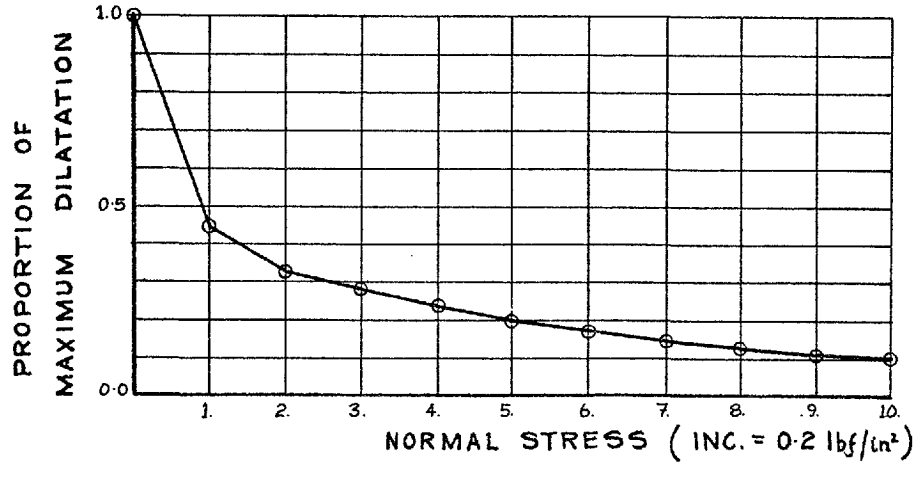
CLOSURE OF PRIMARY JOINT UNDER CYCLIC NORMAL LOAD (After N. Barton)

FIGURE 7.6



NORMALIZED SHEAR AND DILATATION FOR PRIMARY JOINTS

FIGURE 7.7



DILATATION v NORMAL STRESS

FIGURE 7.8

parts which are recoupled in the analysis. Figure 7.7 shows the dependence of dilatation on the normal stress and Figure 7.8 the dilatation that occurs at 'zero' normal loading.

Finally a normal stress displacement relationship is necessary. Figure 7.6 shows that the overall normal behaviour is strongly non-linear although the joint deforms fairly linearly once any consolidation stress is reached. The joint normal stiffness was chosen as $2. \times 10^5$ lbf/in^2/in to match the behaviour at the relevant stress state. The process of excavation is primarily one of unloading and the normal stiffness is selected accordingly.

The method of analysis discussed in section 4.4 did not take account of the complex behaviour laws described above. In order to apply the method to this model, properties representative of pre-peak response of the three joint sets were therefore selected. These are given in Table 7.II and can mainly be deduced from Figures 7.3 - 7.6.

Joint Set	Normal Stiffness lbf/in^2/in	Shear Stiffness lbf/in^2/in	Cohesion lbf/in^2	Angle of Friction
66° (Primary)	$2. \times 10^5$	23.	0.1	58°
Vertical (P.C.J.)	$2. \times 10^5$	30.	0.1	58°
Horizontal (S)	$1. \times 10^5$	80.	0.2	60°

Table 7.II

7.5 COMPUTER STUDIES

In order to attempt to test the range of computer programs, two finite element models were used. The first of these was for continuum analysis. Both isotropic and joint controlled anisotropic behaviour were considered. The second model attempted to simulate the discontinuum by the inclusion of joint elements. Unfortunately the real model comprised some forty thousand discrete units so the finite element approximation was necessarily poor (Figure 7.10).

7.5.1 Continuum Analysis

A relatively coarse mesh of 270 elements and 304 nodal points was used as only the order of magnitude and the direction of displacements were of real interest. Only half the model was studied and the mesh was constrained to excavate to an 82° slope at the full depth of 32".

The results of the elastic, isotropic analysis, using actual modelling material properties, draws attention to the very small contribution of elastic behaviour to the total deformation. The displacements shown in the upper portion of Figure 7.9 are those due to excavation to full depth. They are too small to have been recorded during the model study as the displacement measuring accuracy was about 0·006". It would, however, be wrong to conclude that the elastic recovery of a slope on unloading is always insignificant (Ref. 4).

The method of superimposing deformabilities to calculate joint controlled anisotropic material constants was then used. The bulk properties of the jointed model material were deduced from the intact elastic properties and the stiffness given in Table 7.II. The resulting displacements from an analysis assuming this behaviour are given in the lower part of Figure 7.9. Again these do not correspond with those measured in practice. Although the displacements are of the right order of magnitude they occur in the wrong place and in the wrong directions. Elastic recovery of both the solid and the jointing clearly plays an important role despite the marked influence of the steeply dipping joint set. In reality the behaviour of discontinuities is not reversible.

For the sake of completeness the stress distributions were plotted for the above studies. These revealed that the horizontal stresses in the region of slope were lower for the anisotropic case. In fact a zone of tension parallel to the slope face persisted over much of its height. A ubiquitous joint analysis for the 66° joint set, using the properties listed in Table 7.II, showed a much larger slip zone for the anisotropic case.

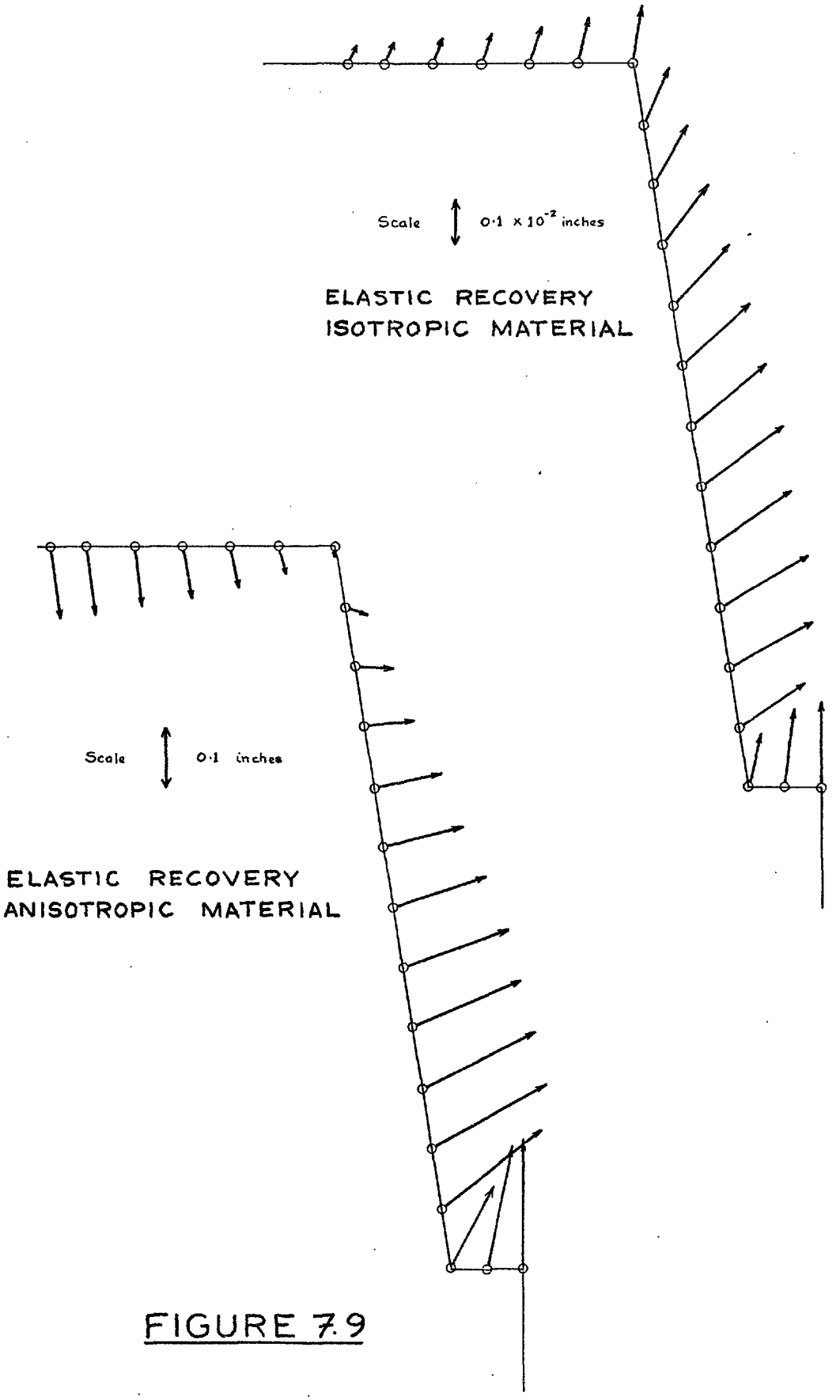

Scale 0·1 x 10⁻² inches
ELASTIC RECOVERY
ISOTROPIC MATERIAL
Scale 0·1 inches
ELASTIC RECOVERY
ANISOTROPIC MATERIAL

FIGURE 7.9

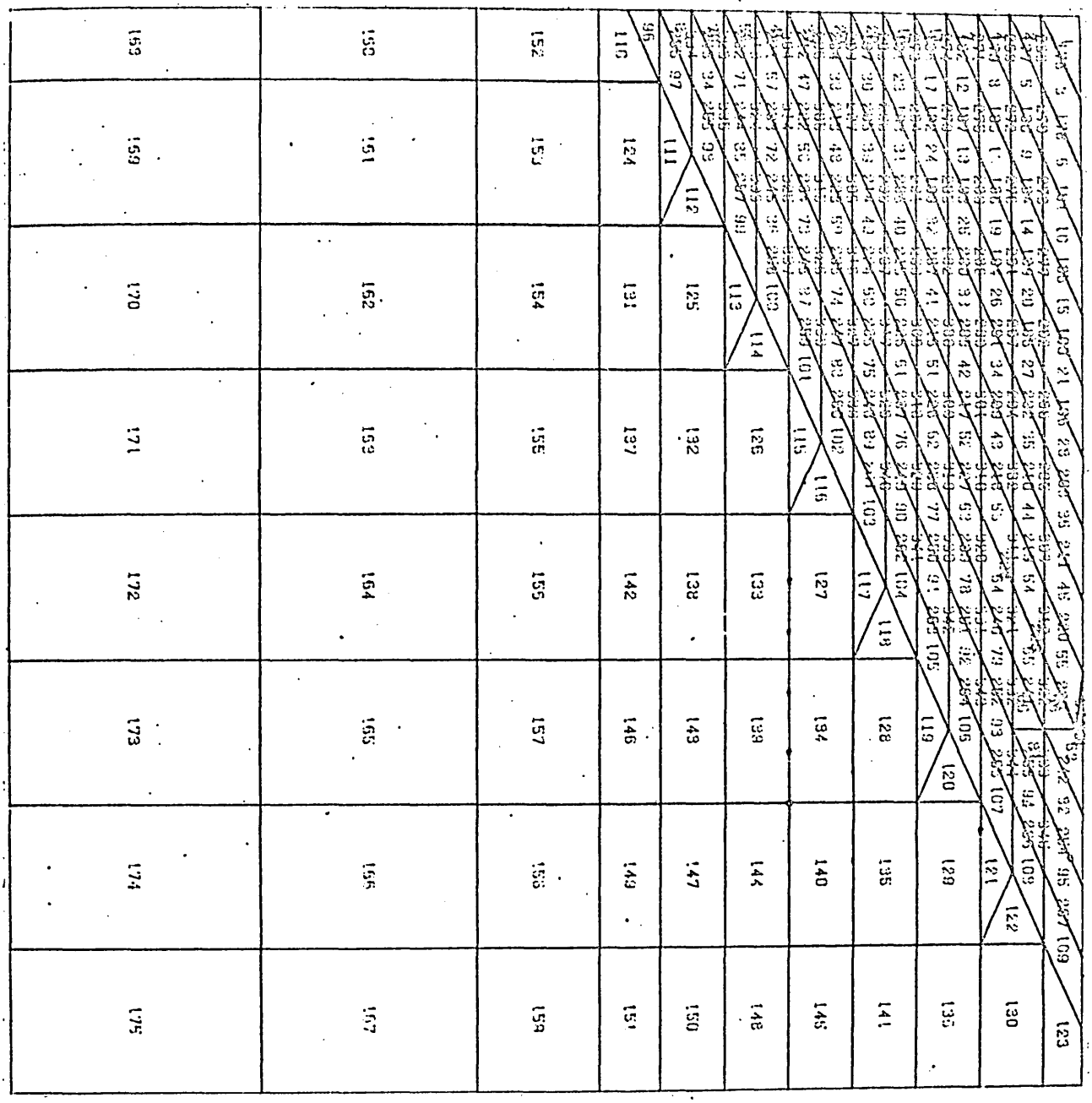
7.5.2 Elastic Analysis of the Jointed Model

The finite element model given in Figure 7.10 is almost the largest that can be treated using the program listed in Appendix B. It does not take account of the horizontal set, but includes as many as possible of the vertical and steeply dipping joints near the final slope profile.

A single step excavation to full depth resulted in the displacements shown in Figure 7.11. These displacements contain no component due to slip as they are the elastic response of the model to unloading. The chief difference between these values and those recorded during the model study is the much larger horizontal displacements recorded in the latter case. Progressive reduction of shear stiffness on over stressed discontinuities would result in displacements parallel to the steeply dipping joint set. Only toppling or dilatant behaviour for the joints could result in large horizontal components of displacement.

The most interesting feature of this analysis was the presence of tensile stresses on the steeply dipping joints at the slope face. This is not a physically reasonable phenomenon and is probably due to the relatively coarse mesh used. The erroneous result arises because of the assumption of constant stress elements when calculating the excavation loads equivalent to the residual stress state.

Attempts to model progressive slip on overstressed joints failed owing to the generation of negative shear stiffnesses. Examination of Figure 4.11 shows that this occurs if the residual shear stress is greater than the current shear strength. The latter condition requires some arbitrary resetting of shear stiffness that was not included in the existing program. It is possible that the problem might not occur if a multistage excavation were performed. However, this approach was not pursued. The above discussion provides a good example of the difficulty of modelling a work softening material using a direct iterative approach.



FINITE ELEMENT MESH

FIGURE 7.10

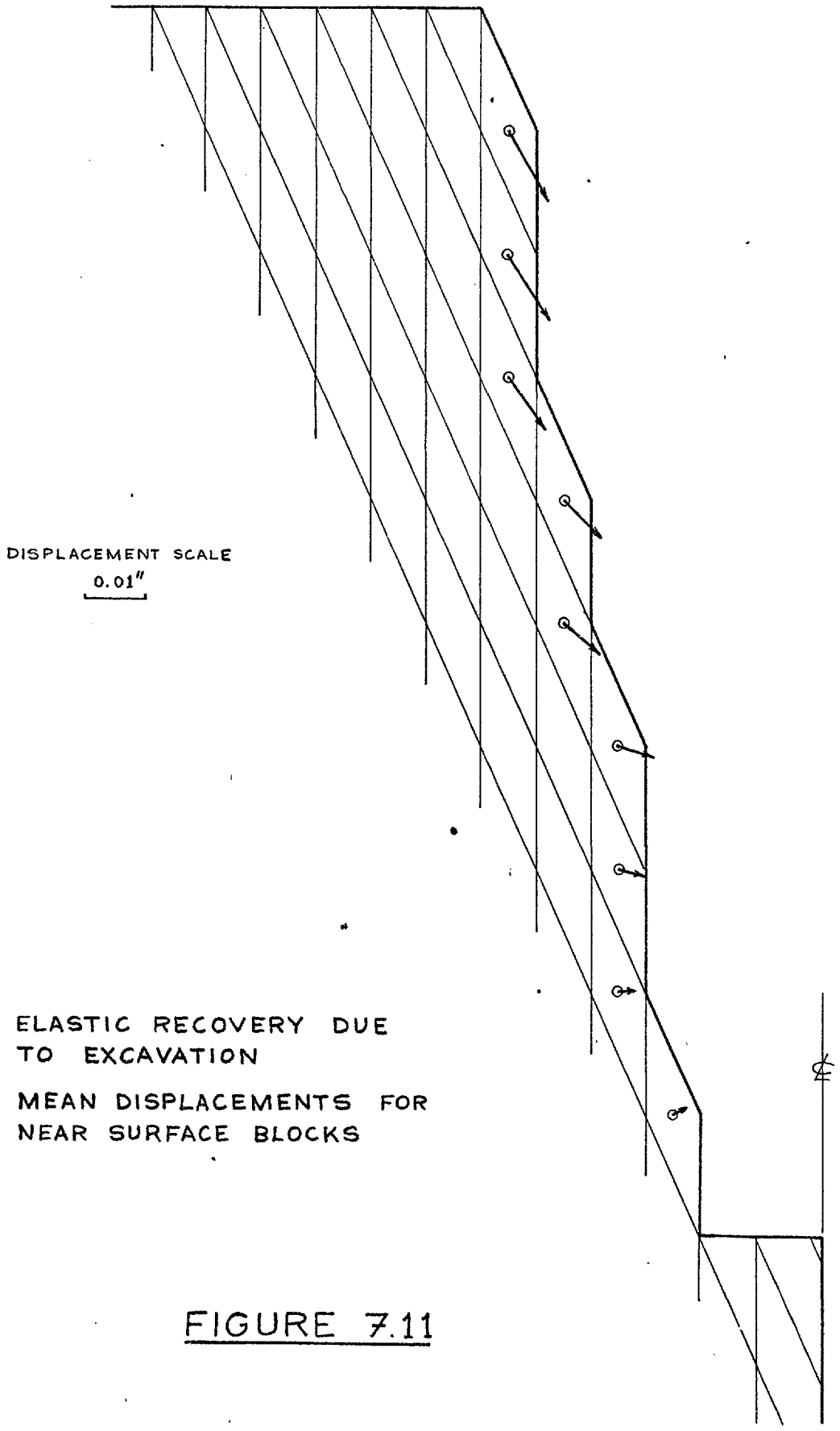

DISPLACEMENT SCALE
0.01"
ELASTIC RECOVERY DUE TO EXCAVATION
MEAN DISPLACEMENTS FOR NEAR SURFACE BLOCKS

FIGURE 7.11

For interest, it is perhaps worthwhile to record the computer requirements for the above analysis. Using a variable stiffness version of the computer program given in Appendix B the storage requirement was 37,000 words of central memory. For every iteration, by formation and inversion of the stiffness matrix, about 62 seconds of central processor time were used on the C.D.C. 6400 at Imperial College.

7.5.3 Analysis Using Comprehensive Material Laws

The first study was carried out assuming the excavation to be made to full depth in a single step. The comprehensive material properties given in Figure 7.8 were used. The initial cycle of the calculation gave results differing from the elastic analysis described above (Fig. 7.11) by virtue of the different initial stiffnesses of the joints. There was, of course, the same tendency that was observed previously for very low, to tensile, stresses on the steeply dipping joints near the surface.

Examination of the existing and permitted joint stresses and displacements revealed several interesting facts. Firstly, there was an area of tension on the joints along the crest. Secondly, it was noted that most joints not in tension were within their shear strength and should therefore behave elastically in shear. The line of joints one above that passing through the toe was most critical, with slip predicted on the lowest two elements (Fig. 7.12). Thirdly, it was observed that the dilatation corresponding to the existing shear displacement was generally several orders of magnitude greater than the permitted normal closure.

Resubmission of the model for the next iteration gave rather unexpected results. The displacements appeared reasonable but the joint normal stresses had increased throughout the model by orders of magnitude. The dilatation was therefore automatically reduced to zero for succeeding iterations. This erroneous result was seen to be caused by very high dilatations and dilatational forces input from the previous iteration. In fact the errors in the calculation of the dilatation component of behaviour were much greater than the

```
  232  -15.44    -1.60    .3110E-01    .8142E-01    .4826E-06    .1555E-06    .6046E-03    .8142E-03
 JOINT IN TENSION
 NC SHEAR STRENGTH
  233  -14.00    -4.80   -.6587E-01    .1286E+00    .6521E-06   -.3294E-06    .6578E-03    .1286E-02
 DILATATION=     .1445E-01 PERMITTED NORMAL CLOSURE=    .3294E-06
NORMALIZED SHEAR BEHAVIOUR   SHEAR STRENGTH=   1.953 SHEAR F/A=    1.953 DISP.=   1.953
  234  -12.56    -8.00   -.1202E+00    .1758E+00    .1035E-05   -.6012E-06    .7105E-03    .1758E-02
 DILATATION=     .7903E-02 PERMITTED NORMAL CLOSURE=    .6012E-06
NORMALIZED SHEAR BEHAVIOUR   SHEAR STRENGTH=   1.463 SHEAR F/A=    1.463 DISP.=   1.463
  235  -11.12   -11.20   -.1469E+00    .2217E+00    .1555E-05   -.7346E-06    .7498E-03    .2217E-02
 DILATATION=     .7366E-02 PERMITTED NORMAL CLOSURE=    .7346E-06
NORMALIZED SHEAR BEHAVIOUR   SHEAR STRENGTH=   1.509 SHEAR F/A=    1.509 DISP.=   1.509
  236   -9.68   -14.40   -.1468E+00    .2648E+00    .2210E-05   -.7340E-06    .7615E-03    .2648E-02
 DILATATION=     .9463E-02 PERMITTED NORMAL CLOSURE=    .7340E-06
NORMALIZED SHEAR BEHAVIOUR   SHEAR STRENGTH=   1.804 SHEAR F/A=    1.804 DISP.=   1.804
  237   -8.24   -17.60   -.1761E+00    .3029E+00    .2718E-05   -.8806E-06    .7234E-03    .3029E-02
 DILATATION=     .7667E-02 PERMITTED NORMAL CLOSURE=    .8806E-06
NORMALIZED SHEAR BEHAVIOUR   SHEAR STRENGTH=   1.720 SHEAR F/A=    1.720 DISP.=   1.720
  238   -6.80   -20.80   -.7375E-01    .3359E+00    .3884E-05   -.3688E-06    .6351E-03    .3359E-02
 DILATATION=     .2989E-01 PERMITTED NORMAL CLOSURE=    .3688E-06
NORMALIZED SHEAR BEHAVIOUR   SHEAR STRENGTH=   1.467 SHEAR F/A=    4.556 DISP.=   4.556
  239   -5.36   -24.00   -.1501E+00    .3749E+00    .4157E-05   -.7506E-06    .6059E-03    .3749E-02
 DILATATION=     .1314E-01 PERMITTED NORMAL CLOSURE=    .7506E-06
NORMALIZED SHEAR BEHAVIOUR   SHEAR STRENGTH=   1.875 SHEAR F/A=    2.498 DISP.=   2.498
```

COMPUTER OUTPUT FOR JOINT ELEMENTS 232-239

FIGURE 7.12

original normal stresses.

By way of experiment the above procedure was repeated without horizontal residual stresses. Exactly the same problem of very high normal stresses due to dilatation was met. It was therefore decided to alter the joint properties in such a way as to limit the dilatation. This was achieved by reducing the joint normal stiffness, increasing the permitted maximum closure and decreasing the maximum dilatation. The revised joint properties were:-

Normal Stiffness	$0{\cdot}2 \times 10^{4}$ lbf/in^2/in
Maximum Closure	$-\ 0{\cdot}1 \times 10^{-2}$ in
Maximum Dilatation	$0{\cdot}7 \times 10^{-3}$ in
Normal Stress Increment	$0{\cdot}2 \times 10^{1}$ lbf/in^2

The first test using the altered joint parameters was carried out with a model excavated to half the full depth. The results were considerably more satisfactory as the dilatation and permitted normal closure were more comparable. It was, however, observed, from the iterations that were performed, that the no-tension condition was resulting in a divergent rather than a convergent solution. The author therefore decided to cut the tension elimination calculation out of the program for further analysis. (It is retained in the program listed in Appendix B as it functioned satisfactorily during test runs.)

The final analysis of the model simulated a cut to full depth in a single step. The initial elastic displacements for this model, as obtained from the first iteration, are shown in Figure 7.13. For simplicity only the displacement of the centroids of the blocks at the surface are plotted. Slip and dilatation were then permitted according to the prescribed laws. After four iterations a distinct structure bounded by tension and slip developed. This is shown in Figure 7.14, together with the existing displacements. Further iterations resulted in increased displacements into the excavation (Fig. 7.15). However, stresses were generally too erratic for any conclusions regarding the stability of the slope to be drawn.

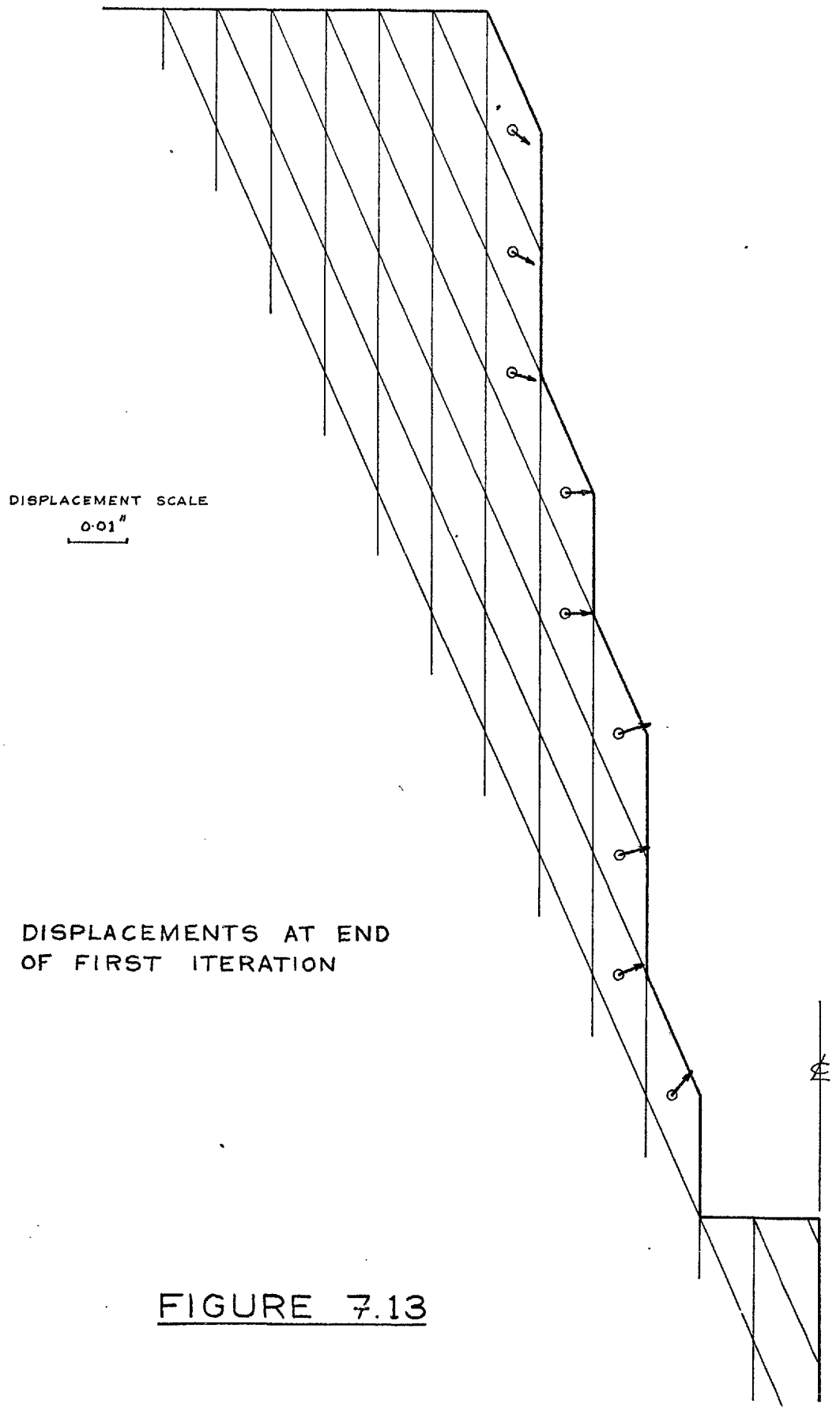

DISPLACEMENT SCALE
0·01"
DISPLACEMENTS AT END
OF FIRST ITERATION

FIGURE 7.13

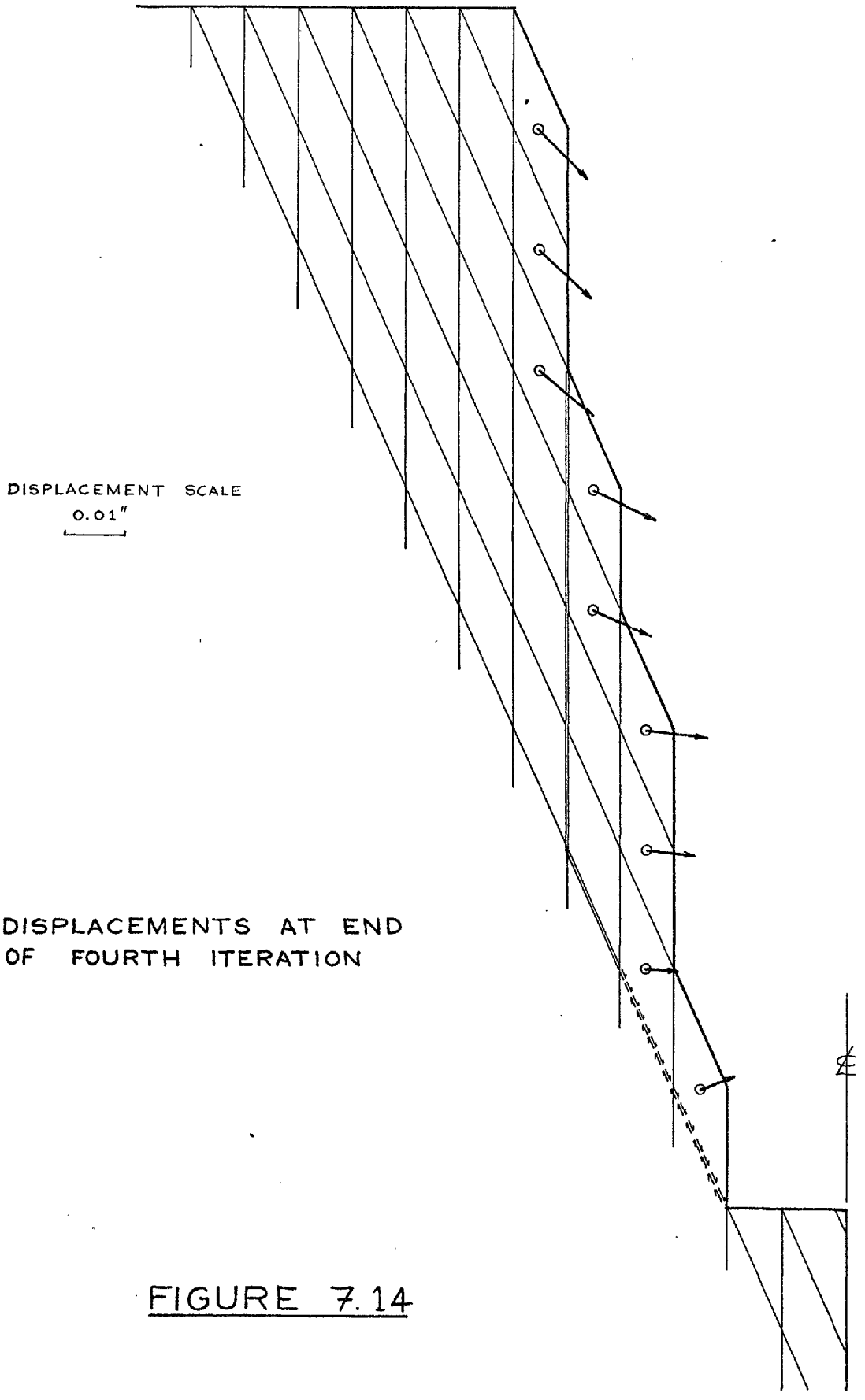

DISPLACEMENT SCALE
0.01"
DISPLACEMENTS AT END
OF FOURTH ITERATION

FIGURE 7.14

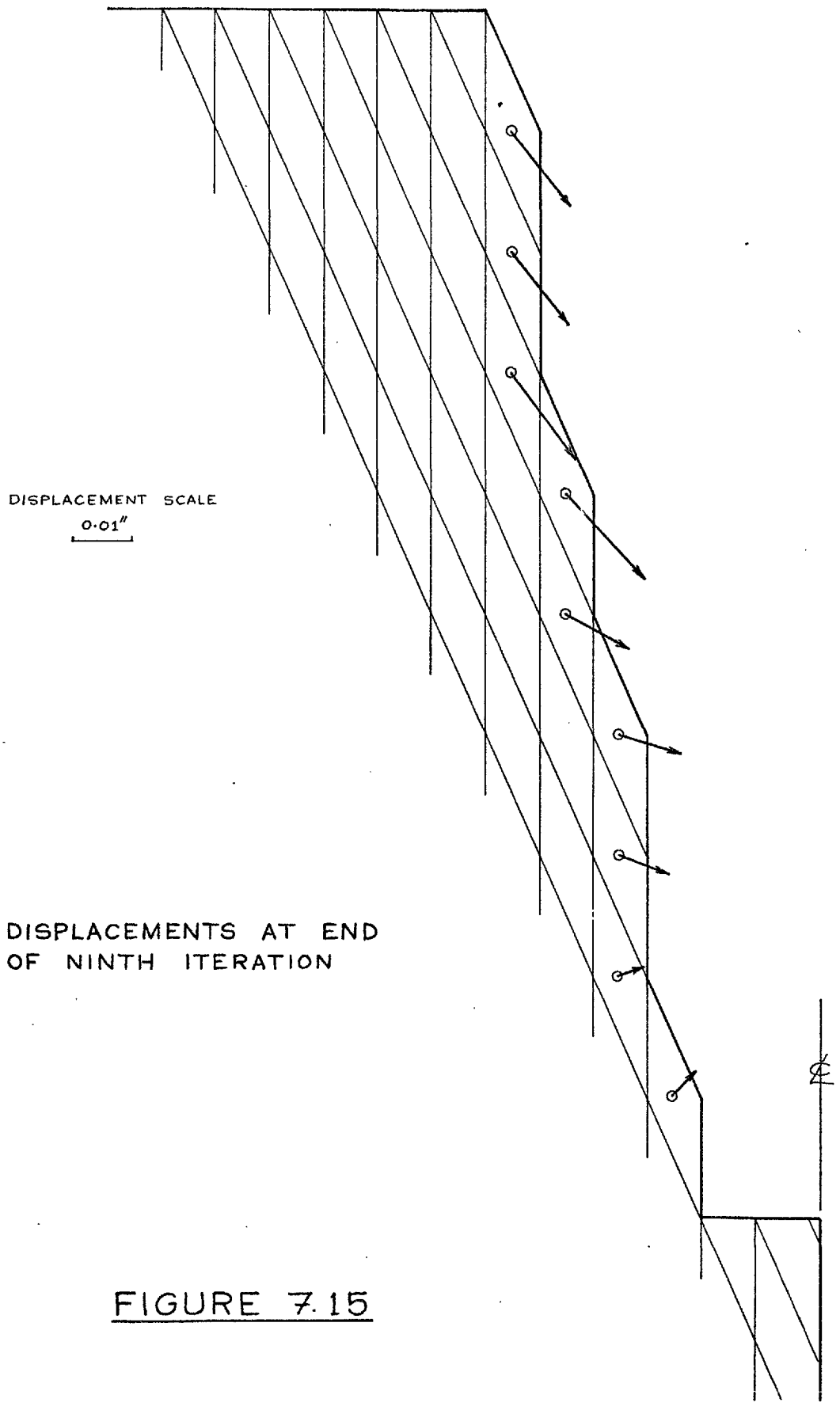

DISPLACEMENT SCALE
0·01"
DISPLACEMENTS AT END
OF NINTH ITERATION
℄

FIGURE 7.15

7.5.4 Practical Considerations

It is probably of some interest to state the procedure and computer requirements for the above analysis. With this end in view the flow chart given in Figure 7.16 has been constructed. (Further details are given in Appendix B.)

Clearly it is impractical to run a lengthy analysis in one pass. Not only is it impossible to state beforehand how many iterations are necessary for any increment, but it is improbable that it is convenient from a computing standpoint. Figure 7.16 shows how the analysis may be performed as a multipass exercise. The logic of the flow chart is internal to the computer program and the path followed is determined by the data cards submitted on any run. All that is required externally is to ensure that the correct files are ready, and contain the anticipated information. Three basic conditions exist:-

(1) First run with the model:-
All data read from cards.

(2) Not the first run. The last increment was complete:-
Read data from tape.

(3) Not the first run. The last increment is to be continued:-
Read data from tape.
Recover element properties tape.
Recover reduced stiffness matrix tape.

Of course, at the end of any of these runs the necessary tapes for restarting the calculate must be saved, either physically or by storing their contents on another file.

Running the program listed in Appendix B required 42,000 words of central memory on the CDC 6400 at Imperial College. The computer time for the model discussed above was about 68 seconds for an iteration involving a recalculation of the model stiffness matrix and 23 seconds for iterations involving only load perturbations.

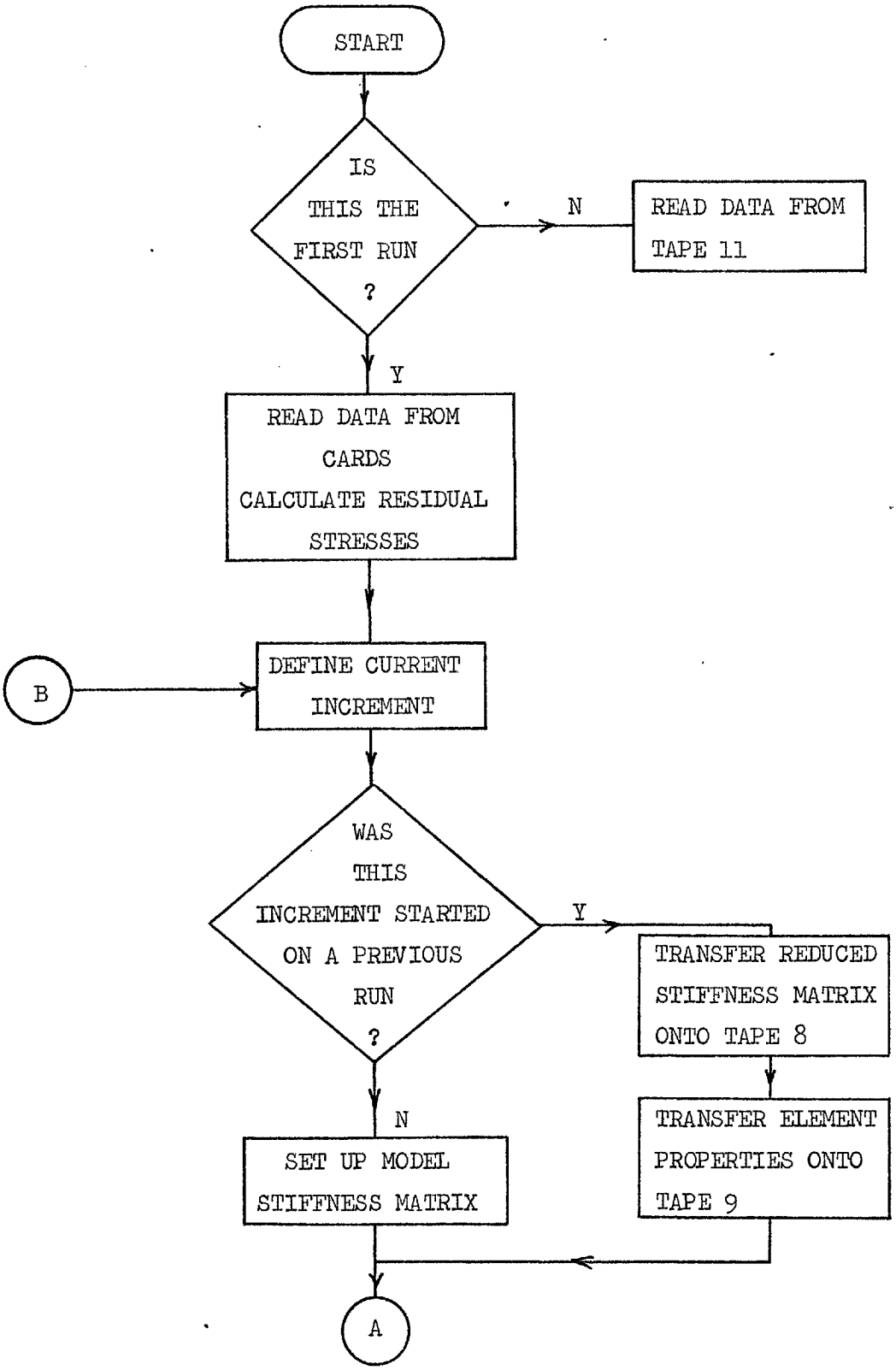
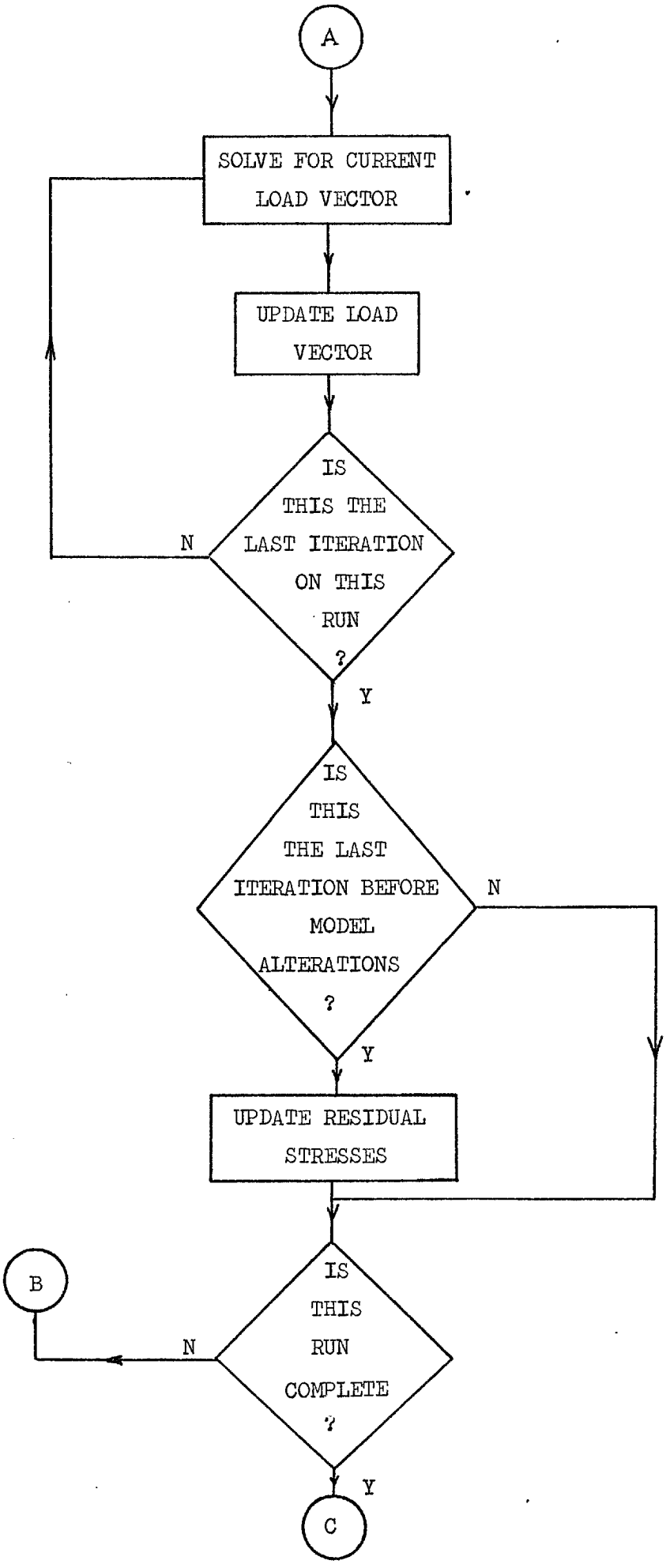


Figure 7.16

Continued


A
SOLVE FOR CURRENT LOAD VECTOR
UPDATE LOAD VECTOR
IS THIS THE LAST ITERATION ON THIS RUN ?
N
Y
IS THIS THE LAST ITERATION BEFORE MODEL ALTERATIONS ?
N
Y
UPDATE RESIDUAL STRESSES
B
IS THIS RUN COMPLETE ?
N
Y
C

Continued

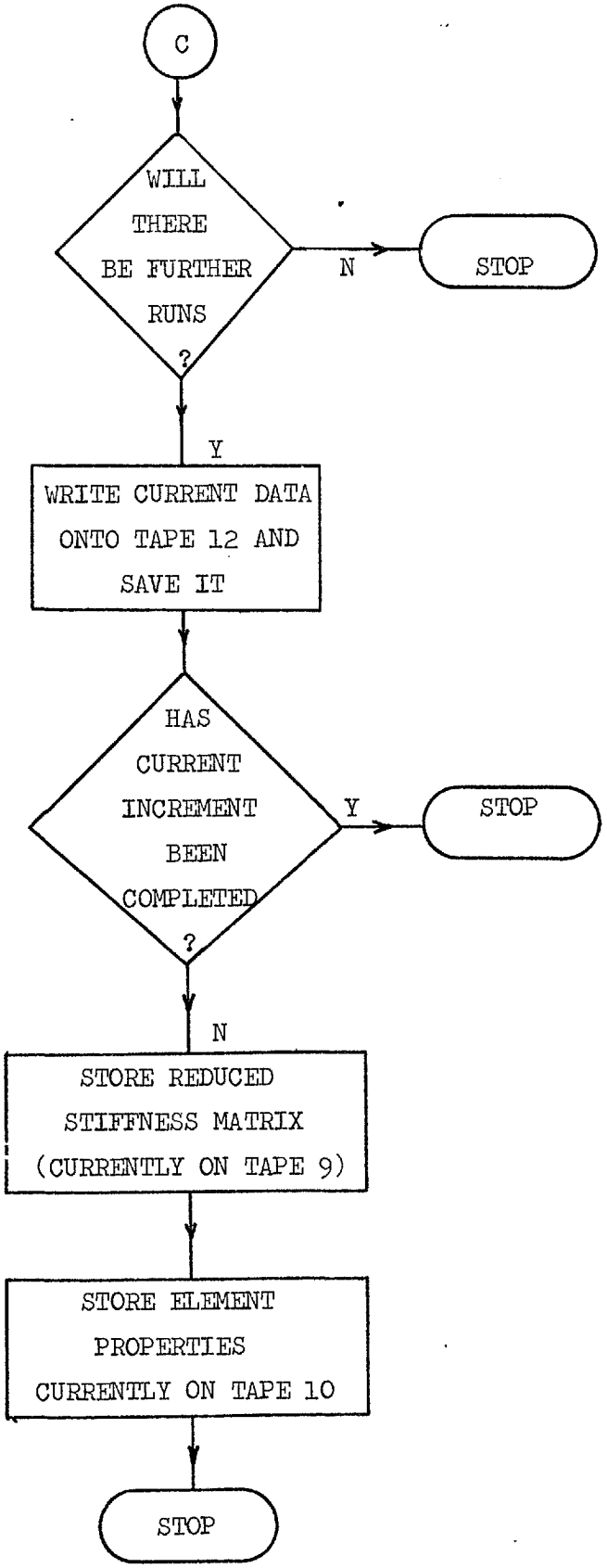

C
WILL THERE BE FURTHER RUNS ?
N
STOP
Y
WRITE CURRENT DATA ONTO TAPE 12 AND SAVE IT
HAS CURRENT INCREMENT BEEN COMPLETED ?
Y
STOP
N
STORE REDUCED STIFFNESS MATRIX (CURRENTLY ON TAPE 9)
STORE ELEMENT PROPERTIES CURRENTLY ON TAPE 10
STOP

Figure 7.16

This should be compared with 62 seconds for each iteration using the variable stiffness method.

7.6 CONCLUSIONS

It has been demonstrated how input parameters for numerical analysis may be determined from laboratory testing of a jointed material. Those obtained were utilized in a number of simulations of a physical model.

The computed displacements of the elastic continuum model were very different from those reported for the prototype. The elastic recovery of the joints made a significant contribution in the case of the anisotropic model. Such behaviour was not observed in the prototype and is unlikely to be observed in nature. To overcome this problem the calculation could be done iteratively, with elements ascribed properties according to whether they were loaded or unloaded over the current increment.

The discontinuum model was first studied using the variable stiffness method described in Chapter 4. This was found to fail owing to the presence of negative joint stiffnesses generated during unloading by excavation. In the context of slope stability this problem is likely to occur if this method of analysis is adopted.

The discontinuum model was then studied using the comprehensive computer program listed in Appendix B and described in Chapter 4. This approach broke down owing to very low joint normal stresses occurring with very large dilatations. This problem is perhaps common to slope situations, but also reflects the very rough discontinuities present in the prototype.

By adopting adjusted joint properties the model was successfully simulated. However, the results were rather erratic. This was probably due to two reasons. Firstly, there may be a problem connected with the calculation of dilatation from the total stress state rather than stress disturbances. Secondly, it is essential

that such a complex model be simulated in very small increments of change so that a realistic history is followed. Such a procedure is lengthy and expensive and was not attempted within this study.

Although the results of the model simulation are not conclusive the author believes the exercise to be a useful illustration of the methods discussed in this thesis. The short comings are discussed briefly above and point the way to further work in this field.

The comprehensive simulation that has been developed is potentially a useful tool in rock mechanics. The way appears to be open to model virtually any prescribed behaviour. The computer program listed in Appendix B may serve as a basis for further investigation. Such a study could usefully examine the importance of considering finite, rather than infinitesimal, strain. At all times further development should be made in parallel with physical models simple enough to permit a reasonable representation to be achieved using the numerical models. In retrospect the model discussed in this chapter was too large and too complex to provide a useful test case at the current stage of development.

References

(1) Barton, N.R. A Model Study of the Behaviour of Steep Excavated Rock Slopes. Ph.D. Thesis, University of London, 1971.

(2) Barton, N.R. A Low Strength Model Material for Simulations of the Mechanical Properties of Intact Rock in Rock Mechanics. 2nd Congress Int. Soc. Rock Mechanics, Belgrade, 1970. Paper 3.15.

(3) Barton, N.R. A Model Study of Rock Deformation. To be published.

(4) Blake, W. Finite Element Model Study Modification at the Kimbley Pit. Trans. Soc. of Minings Engs. A.I.M.E. Vol. 241, December, 1968.

APPENDIX

A

PLOTTING INPUT AND OUTPUT OF TWO DIMENSIONAL FINITE ELEMENT STUDIES

1) Data Checking and Mesh Plotting
2) Contour Plotting Program (a)
3) Contour Plotting Program (b)

DATA CHECKING AND MESH PLOTTING

PURPOSE:- To check the nodal point and element data for the 2-D programs. There is the option to plot the mesh.

INPUT:- Deck of nodal point and element data as used for the finite element program. Plotting data if required.

OUTPUT:- Complete listing of data and model bandwidth. Plot of finite element mesh with the element number at each centroid.

INPUT INSTRUCTIONS AND PROGRAM NOTATION			FORMAT
CARD 1	NUMEL	Number of Elements	3I5
	NUMNP	Number of Nodes	
	NPLOT	= 0 if plot not required	
CARDS 2	N	Nodal point number	I5,F5.0,2F10.0
	CODE(N)	Displacement code	
	R(N)	X ordinate	
	Z(N)	Y ordinate	
CARDS 3	M	Element number	6I5
	IX(M,1)	List of nodes defining element	
	IX(M,2)		
	IX(M,3)		
	IX(M,4)		
	IX(M,5)	Material identification	
CARD 4	ANG	Orientation of element number (+ve anticlockwise from horizontal)	
	FACT	Scale factor.Plots twice size if equal to 2.	3F5.0
	SIZE	Size of number	
	ENDPLOT	Enplot value for Calcomp Plotter	
CARD 5	XSHIFT	Shift origin of model for plotting in	2F5.0
	YSHIFT	X and Y directions respectively	

```
                PROGRAM STJO(INPUT,OUTPUT,TAPE5=INPUT,TAPE6=OUTPUT,TAPE62)
000002          DIMENSION IX(700,5),R(700),Z(700),CODE(700)
000002          READ(5,1002) NUMEL,NUMNP,NPLOT
000014          LBAD=0
                C     READ AND PRINT OF NODAL POINT DATA
                C****           *       *       *       *
000015          L=0
000016          WRITE(6,2000)
000021           2000 FORMAT(12HNODAL DATA )
                C*****
000021             60 READ(5,1002) N,CODE(N),R(N),Z(N)
000035              NL=L+1
000037              IF(L.EQ.0) GO TO 90
000042              ZX=N-L
000043              DR=(R(N)-R(L))/ZX
000045              DZ=(Z(N)-Z(L))/ZX
000050             70 L=L+1
000052              IF(N-L) 100,90,80
000055             80 CODE(L)=0.0
000056              R(L)=R(L-1)+DR
000060              Z(L)=Z(L-1)+DZ
000062              GO TO 70
000063             90 WRITE(6,1004) (K,CODE(K),R(K),Z(K),K=NL,N)
000103              IF(L.EQ.0) L=1
000105              IF(NUMNP-N) 100,110,60
000110            100 WRITE (6,2009) N
000116            110 CONTINUE
000116           1002 FORMAT(I5,F5.0,2F10.0)
000116           1004 FORMAT(I5,F5.0,2F10.2)
000116           2009 FORMAT(4HBAD=,I10)
000116              WRITE(6,3000)
000122           3000 FORMAT(12HELEMENT DATA  )
                C****           *       *       *
                C       READ AND PRINT OF ELEMENT PROPERTIES
                C****           *       *       *
000122              N=0
000123            130 READ(5,1003) M,(IX(M,I),I=1,5)
000141            140 N=N+1
000143              IF (M-N) 170,170,150
000151            150 IX(N,1)=IX(N-1,1)+1
000152              IX(N,2)=IX(N-1,2)+1
000153              IX(N,3)=IX(N-1,3)+1
000154              IX(N,4)=IX(N-1,4)+1
000155              IX(N,5)=IX(N-1,5)
000156            170 WRITE(6,1003) N,(IX(N,I),I=1,5)
000174              IF (M-N) 180,180,140
000177            180 IF (NUMEL-N) 190,190,130
000202            190 CONTINUE
000202           1003 FORMAT(6I5)
                C     DETERMINE BAND WIDTH
                C*****
000202            314 J=0
000203              DO 340 N=1,NUMEL
000205              DO 340 I=1,4
000206              DO 325 L=1,4
000207              KK=IABS(IX(N,I)-IX(N,L))
000215              IF(KK.LE.39) GO TO 315
000217              WRITE (6,2018) N
000225                 LBAD=LBAD+1
000227            315 IF(KK-J) 325,325,320
000232            320 J=KK
000234            325 CONTINUE
000236            340 CONTINUE
000243              MBAND=2*J+2
000245              WRITE (6,2012) MBAND
000252              WRITE (6,2019) LBAD
000260              IF (LBAD.NE.0) STOP
000263              IF(NPLOT.GT.0) CALL EYORE(NUMNP,NUMEL,IX,R,Z)
000270           2012 FORMAT (/6HMBAND= I5 /)
000270           2018 FORMAT (24H ELEMENT CARD ERROR  N=  I4)
000270           2019 FORMAT (* LBAD =* I5)
000270              STOP
000272              END

UNUSED COMPILER SPACE
017100
```

```
                SUBROUTINE EYORE(NUMNP,NUMEL,IX,R,Z)
000007          DIMENSION IX(700,5),R(700),Z(700)
000007          REAL LEN
000007          READ(5,1001) ANG,FACT,SIZE,ENDPLT
000022          WRITE(6,2000) ANG,SIZE,FACT,ENDPLT
000041     2000 FORMAT(*   ELEMENT PLOTTING  */*   ORIENTATION OF NUMBER= * ,
                1 F10.4, * SIZE OF NUMBER = *,F10.4,* SCALING FACTOR =*,F10.5,
                2 *  END PLOT AT * F10.2, *INCHES*)
000044          A=ANG*0.01745
000046     1001 FORMAT(4F5.0)
000046          READ(5,1001) XSHIFT,YSHIFT
000056          DO 50 N=1,NUMNP
000070          R(N)=(R(N)-XSHIFT)*FACT
000072          Z(N)=(Z(N)-YSHIFT)*FACT
000073       50 CONTINUE
000074          CALL 'START(2)
000076          CALL PLOT(1.0,1.0,-3)
000101          DO 10 N=1,NUMEL
000107          XCEN=0.0
000107          YCEN=0.0
000110          M=IX(N,1)
000111          XCEN=XCEN+R(M)/4.0
000114          YCEN=YCEN+Z(M)/4.0
000116          CALL PLOT(R(M),Z(M),+3)
000126          M=IX(N,2)
000130          XCEN=XCEN+R(M)/4.0
000133          YCEN=YCEN+Z(M)/4.0
000136          CALL PLOT(R(M),Z(M),+2)
000146          M=IX(N,3)
000150          XCEN=XCEN+R(M)/4.0
000153          YCEN=YCEN+Z(M)/4.0
000156          CALL PLOT (R(M),Z(M),+2)
000166          IF(M.EQ.IX(N,4)) GO TO 15
000171          M=IX(N,4)
000172          XCEN=XCEN+R(M)/4.0
000175          YCEN=YCEN+Z(M)/4.0
000200          CALL PLOT(R(M),Z(M),+2)
000210          GO TO 16
000211       15 XCEN=XCEN/1.75
000217          YCEN=YCEN/0.75
000214       16 EL=N
000215          M=IX(N,1)
000217          CALL PLOT(R(M),Z(M),+2)
                C*
                C****ANGLE DEFINES ORIENTATION OF NUMBERING***
                C***FACT=SCALING FACTOR---SIZE=HT. OF NUMBER---CHOOSE MULT. OF 0.035
                C**FIND NUMBER OF DIGITS
000227          D=2.0
000230          IF(N.GT.99) D=3.0
000235          IF(N.LT.10) D=1.0
000241          LEN=D*SIZE/2.0
000243          YC=YCEN-LEN*SIN(A)-SIZE*COS(A)/2.0
000254          XC=XCEN-LEN*COS(A)+SIZE*SIN(A)/2.0
                C**PLOT ELEMENT NUMBER WITH CENTER AT CENTROID OF ELEMENT
000266          CALL NUMBER(XC,YC,SIZE,EL,ANG,-1)
000275       10 CONTINUE
000300          CALL ENPLOT(ENDPLT)
000301          RETURN
000302          END

UNUSED COMPILER SPACE
017200
```

CONTOUR PLOTTING PROGRAM (a)

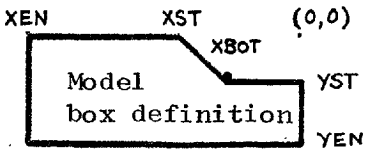
PURPOSE:- To plot stresses for models for which the elements are laid out to be topologically equivalent to a regular mesh

INPUT:- Direct stresses at the centroids of the elements and plotting instructions.

OUTPUT:- The output is one or more of the following options:

(1) The direct stresses XX, YY, XY
(2) The major and minor principal stresses and directions.
(3) Maximum shear stress, mean normal stress and maximum shear stress directions.

Each of these groups is plotted three across the page (30 inches on a Calcomp Plotter). Contours are drawn at specified intervals and the direction vectors are of uniform magnitude.

INPUT INSTRUCTIONS AND PROGRAM NOTATION			FORMAT
CARD 1	IROW	Number of rows in mesh	4I5,3F10.0
	ICOL	Number of columns in mesh	
	NPLOT	Number of plots	
	NUMEL	Total number of elements	
	UZMAX	Any value above this will not be plotted	
	SCALE	Geometric scaling factor	
	TSCL	Stress scaling factor	
CARD 2	CINT(N)	List of values to give contour interval or vector magnitude of each plot	9F5.0
CARD 3	XXPL	≠0. if XX, YY, XY required	3F5.0
	SIGPL	≠0. if principal stresses required	
	SUMPL	≠0. if maximum shear stress etc. required.	
CARD 4	XST		6F10.0
	XEN		
	YST		
	YEN		
	XBOT		
CARDS 5	N	Element Number	I5,2F10.2,3E12.4
	RR(N)	X-ord	
	ZZ(N)	Y-ord	
	SIG1(N)	XX-stress	
	SIG2(N)	YY-stress	
	SIG3(N)	XY-stress	

```
      PROGRAM CONTUR(INPUT,OUTPUT,      TAPE5=INPUT,TAPE6=OUTPUT,TAPE25,
     1 TAPE27)
      DIMENSION  RR(800),ZZ(800),SIG1(800),SIG2(800),SIG3(800),SIG4(800)
     1,SIG5(800),SIG6(800)
      COMMON/TPL/XST,XEN,YST,YEN,XBOT,XP(30,30),YP(30,30),CINT(10),NUMPL
      COMMON/TRA/ SIG(6),THETA
      COMMON/ARR/SMAX,DIRS,TSCL,R,Z
      COMMON/STR/ F(800),IROW,ICOL,UZMAX
      DIMENSION HED(3)
      INTEGER PAPER
      READ(5,9000) PAPER,HED
 9000 FORMAT(I5,3A10)
      NUMPL=0
      READ(5,1) IROW,ICOL,NPLOT,NUMEL,UZMAX,SCALE,TSCL
    1 FORMAT(4I5,3F10.0)
      READ (5,2) (CINT(N),N=1,NPLOT)
    2 FORMAT (10F5.0)
      WRITE(6,1010)(CINT(N),N=1,NPLOT)
 1010 FORMAT(1H1,*   CONTOUR INTERVALS  * / 10E12.4)
      READ(5,3) XXPL,SIGPL,SUMPL
    3 FORMAT (3F5.0)
      READ(5,6) XST,XEN,YST,YEN,XBOT
    6 FORMAT(6F10.0)
      WRITE(6,15)
   15 FORMAT (1H1,3X,4HELEM,3X,5HX-ORD,4X,5HY-ORD,5X,9HXX-STRESS,2X,9HYY
     1-STRESS,3X,9HXY-STRESS)
      DO 1007 N=1,NUMEL
      READ(5,4) N,RR(N),ZZ(N),SIG1(N),SIG2(N),SIG3(N)
      SUM=SIG1(N)+SIG2(N)+SIG3(N)
      IF(SUM) 1007,1008,1007
 1008 CONTINUE
      SIG1(N)=UZMAX+1.0
      SIG2(N)=UZMAX+1.0
      SIG3(N)=UZMAX+1.0
 1007 CONTINUE
      DO 1009 N=1,NUMEL
      IF(ABS(SIG1(N)).GT.UZMAX) GO TO 1019
      SIG1(N)=SIG1(N)/TSCL
      SIG2(N)=SIG2(N)/TSCL
      SIG3(N)=SIG3(N)/TSCL
      GO TO 1009
 1019 SIG1(N)=ABS(SIG1(N))
      SIG2(N)=ABS(SIG2(N))
      SIG3(N)=ABS(SIG3(N))
 1009 CONTINUE
    4 FORMAT(I5,2F10.2,3E12.4)
    5 FORMAT(1H ,I5,2F10.2,3E12.4)
      CALL START
C****DEFINE LIMITS FOR PLOTTING
      XST=XST/SCALE
      XEN=XEN/SCALE
      YST=YST/SCALE
      YEN=YEN/SCALE
      XBOT=XBOT/SCALE
      XT=XBOT
      YT=-0.25
      XN=XEN
      YN=YEN+0.5
      SHIFT=XEN+1.0
      YSHIFT=YEN+1.0
      SHIFTY=-2.0*YSHIFT-1.0
C***  TRANSFORM FROMLINEAR ARRAY TO MATRIX
      DO 10 I=1,ICOL
      DO 10 J=1,IROW
      K=(I-1)*IROW+J
      XP(J,I)=RR(K)/SCALE
      YP(J,I)=ZZ(K)/SCALE
   10 CONTINUE
C***   XX,YY,XY-STRESS PLOT OPTION
      IF(XXPL.EQ.0.) GO TO 1000
      DO 101 N=1,NUMEL
  101 F(N)=SIG1(N)
      CALL PLOT (0.0,1.0,-3)
      CALL TPLOT
      CALL SYMBOL (XT,YT,0.15,9HXX-STRESS,180.0,9)
      DO 102 N=1,NUMEL
  102 F(N)=SIG2(N)
      CALL PLOT(0.0,YSHIFT,-3)
      CALL TPLOT
      CALL SYMBOL (XT,YT,0.15,9HYY-STRESS,180.0,9)
      DO 103 N=1,NUMEL
  103 F(N)=SIG3(N)
      CALL PLOT(0.0,YSHIFT,-3)
      CALL TPLOT
      CALL SYMBOL (XT,YT,0.15,9HXY-STRESS,180.0,9)
      CALL SYMBOL(XN,YN,0.14,HED,180.0,30)
C****SHIFT PLOTTING ORIGIN
C
      IF(SIGPL.EQ.0.) GO TO 3000
      CALL PLOT(SHIFT,SHIFTY,-3)
 1000 CONTINUE
C****COMPUTE PRINCIPAL STRESSES AND THEIR DIRECTIONS
C
      DO 50 N=1,NUMEL
      IF(SIG1(N).GT.UZMAX) GO TO 50
      SIG(1)=SIG1(N)
      SIG(2)=SIG2(N)
      SIG(3)=SIG3(N)
      CALL PRINC
      SIG1(N)=SIG(4)
      SIG2(N)=SIG(5)
      SIG3(N)=SIG(6)
   50 CONTINUE
C***   COMPUTATION OF MAXIMUM SHEAR STRESS AND DIRECTION
      DO 100 N=1,NUMEL
      SIG4(N)=(SIG1(N)+SIG2(N))/2.0
      SIG5(N)=(SIG1(N)-SIG2(N))/2.0
      SIG6(N)=SIG3(N)+45.0
      IF(SIG1(N).GT.UZMAX) SIG5(N)=SIG1(N)
      IF(SIG6(N).GT.90.) SIG6(N)=SIG6(N)-90.
  100 CONTINUE
      WRITE(6,17)
      WRITE(6,7) (N,SIG1(N),SIG2(N),SIG3(N),SIG4(N),SIG5(N),SIG6(N),
     1N=1,NUMEL  )
C***   PRINCIPAL STRESS PLOT OPTION
C****PLOT MAJOR PRINCIPAL STRESSES
```

```
000436          DO 104 N=1,NUMEL
000444      104 F(N)=SIG1(N)
000446          CALL PLOT(0.0,1.0,-3)
000450          CALL TPLOT
000451          CALL SYMBOL(XT,YT,0.15,10HMAX-STRESS,180.,10)
        C****PLOT MINOR PRINCIPAL STRESSES
000455          DO 105 N=1,NUMEL
000463      105 F(N)=SIG2(N)
000465          CALL PLOT(0.0,YSHIFT,-3)
000467          CALL TPLOT
000470          CALL SYMBOL(XT,YT,0.15,10HMIN-STRESS,180.,10)
        C****PLOT PRINCIPAL STRESS DIRECTIONS
000474          NUMPL=NUMPL+1
000476          SMAX=CINT(NUMPL)
000500          CALL PLOT(0.0,YSHIFT,-3)
000503          CALL BOX(XST,XEN,YST,YEN,XBOT)
000507          DO 80 N=1,NUMEL
000511          IF (SIG1(N).GT.UZMAX) GO TO 80
000517          DIRS=SIG3(N)
000520          R=RR(N)/SCALE
000522          Z=ZZ(N)/SCALE
000524          CALL ARROW
000525       80 CONTINUE
000530          CALL SYMBOL(XT,YT,0.15,9HDIRECTION,180.0,9)
        C****SHIFT ORIGIN
000534       2000 CONTINUE
        C***    OPTION TO PLOT SHEAR STRESS AND DIRECTIONS
000534          IF (SUMPL.EQ.0.) GO TO 3000
000535          CALL PLOT(SHIFT,SHIFTY,-3)
000540          DO 106 N=1,NUMEL
000546      106 F(N)=SIG4(N)
000550          CALL PLOT(0.0,1.0,-3)
000552          CALL TPLOT
000553          CALL SYMBOL(XT,YT,0.15,14HMEAN NORM.STR.,180.,14)
000567          DO 107 N=1,NUMEL
000565      107 F(N)=SIG5(N)
000567          CALL PLOT(0.0,YSHIFT,-3)
000571          CALL TPLOT
000572          CALL SYMBOL(XT,YT,0.15,14HMAX.SHEAR STR.,180.,14)
000576          NUMPL=NUMPL+1
000600          SMAX=CINT(NUMPL)
000602          CALL PLOT(0.0,YSHIFT,-3)
000605          CALL BOX(XST,XEN,YST,YEN,XBOT)
000611          DO 90 N=1,NUMEL
000617          IF (SIG1(N).GT.UZMAX) GO TO 90
000621          R=RR(N)/SCALE
000622          Z=ZZ(N)/SCALE
000624          DIRS=SIG6(N)
000626          CALL ARROW
000627       90 CONTINUE
000632          CALL SYMBOL(XT,YT,0.15,9HDIRECTION,180.0,9)
000636       3000 CONTINUE
000636          CALL ENPLOT(SHIFT)
000640        7 FORMAT(1H ,I5,5E12.4,F10.2)
000640       17 FORMAT (1H1,1X,4HELEM,2X,10HMAX-STRESS,2X,10HMIN-STRESS,
                11X,11HPRIN-DIRECT,3X,8HPPIN-SUM,3X,9HMAX-SHEAR,2X,12HDIRECT-SHEAR)
000640          STOP
000642          END
```

```
        $IBFTC *FRN*
              SUBROUTINE PRINC
000001        COMMON /TRA/ SIG(6),THETA
        C***  CALCULATE PRINCIPAL STRESS
000001        CC=(SIG(1)+SIG(2))/2.0
000004        BB=(SIG(1)-SIG(2))/2.0
000006        CR=SQRT(BB**2+SIG(3)**2)
000013        SIG(4)=CC+CR
000014        SIG(5)=CC-CR
000016        EPS=ATAN2(SIG(3),BB)/2.0
000021        SIG(6)=57.296*EPS
000023        RETURN
000024        END
              SUBROUTINE ARROW
000001        COMMON /ARR/T,D,TSCL,R,Z
000001        AL=T/2.0
000003        A=D/57.296
000005        A1=AL*COS(A)
000010        A2=AL*SIN(A)
000014        X1=A1+R
000015        Y1=A2+Z
000017        X2=-A1+R
000020        Y2=-A2+Z
000021        X3=A2+R
000022        Y3=-A1+Z
000023        X4=-A2+R
000024        Y4=A1+Z
000026        CALL PLOT (X1,Y1,3)
000030        CALL PLOT (X2,Y2,2)
000033        CALL PLOT (X3,Y3,3)
000036        CALL PLOT (X4,Y4,2)
000041        RETURN
000042        END
              SUBROUTINE TPLOT
000001        COMMON/TPL/XST,XEN,YST,YEN,XBOT,XP(30,30),YP(30,30),CINT(10),NUMPL
000001        COMMON/STR/ F(800),IROW,ICOL,UZMAX
000001        DIMENSION C(30,30)
000001        NUMPL=NUMPL+1
000003        DC=CINT(NUMPL)
000005        DO 5 I=1,ICOL
000006        DO 5 J=1,IROW
000021        K=(I-1)*IROW+J
000022      5 C(J,I)=F(K)
000030     10 CALL BOX(XST,XEN,YST,YEN,XBOT)
000034        CALL CONTOR(IROW,ICOL,C,XP,YP,DC,DS,UZMAX)
000044        RETURN
000045        END
              SUBROUTINE BOX(XST,XEN,YST,YEN,XBOT)
000007        CALL PLOT   (0.0,YEN,3)
000011        CALL PLOT   (0.0,YST,2)
000017        CALL PLOT(XBOT,YST,2)
000024        CALL PLOT   (XST,0.0,2)
000031        CALL PLOT   (XEN,0.0,2)
000037        CALL PLOT   (XEN,YEN,2)
000044        CALL PLOT   (0.0,YEN,2)
000052        RETURN
000053        END
```

```
      CIRFIC *INI*
            SUBROUTINE INIT(IET,IS,JS,I,J,K,XP,YP,Z)
000013      DIMENSION XP(30,30),YP(30,30),Z(30,30)
000013      DIMENSION LTR(4,2),LFLAG(8)
000017      COMMON/OWN/IFLAG(30,30,2),IE,ISO,JSO,N,IROW,ICOL
           /     ,DS,C,X(200),Y(200),E1,E2,UZMAX,XM,YM,ZM
C           HAVE ENTERED ON LOCAL SIDE IE OF LOCAL SQUARE ISO,JSO.
000013      DATA LTR(1,1),LTR(1,2),LTR(2,1),LTR(2,2),LTR(3,1),
           1 LTR(3,2),LTR(4,1),LTR(4,2)/8,5,5,6,6,7,7,9/
000013      IF(IS.LT.1.OR.IS.GE.IROW) RETURN
000022      IF(JS.LT.1.OR.JS.GE.ICOL) RETURN
000037      ISO=IS
000037      JSO=JS
000040      IE=IET
000041      N=1
000042      IFLAG(I,J,K)=2
000043      IEDGE=IE
000046      CALL INTER(IEDGE,X(1),Y(1),XP,YP,Z)
000056      MFLAG=0
000057      IP = ISO + 1
000061      JP = JSO + 1
000062      IF(Z(ISO,JSO).GT.UZMAX.OR.Z(IP,JSO).GT.UZMAX
           / .OR.Z(IP,JP).GT.UZMAX.OR.Z(ISO,JP).GT.UZMAX) RETURN
000133    20 XM = (XP(ISO,JSO)+XP(ISO,JP)+XP(IP,JSO)+XP(IP,JP))/4.0
000137      YM = (YP(ISO,JSO)+YP(ISO,JP)+YP(IP,JSO)+YP(IP,JP))/4.0
000144      ZM = ( Z(ISO,JSO)+ Z(ISO,JP)+ Z(IP,JSO)+ Z(IP,JP))/4.0
000150      IF(ABS(ZM-C) .LT. E1) ZM = C + E1
C           SET LOCAL FLAGS
000161      LFLAG(1)=IFLAG(ISO,JSO,1)
000165      LFLAG(2)=IFLAG(ISO,JP,2)
000170      LFLAG(3)=IFLAG(IP,JSO,1)
000174      LFLAG(4)=IFLAG(ISO,JSO,2)
000177      DO 1 IT=5,8
000204      IEDGE = IT
000204      LFLAG(IEDGE)=1
000207      CALL INTER(IEDGE,XX,YY,XP,YP,Z)
000214      IF(IEDGE .LT. 0) LFLAG(IT) = 0
000223    1 CONTINUE
C           THREAD THROUGH SQUARE
000225      IE=IE
000226    9 ITEMP = LTR(IE,2)
000230      IF(LFLAG(ITEMP)) 3,3,5
000233    3 ITEMP = LTR(IE,1)
000235      IF(LFLAG(ITEMP)) 4,4,6
000240    4 JJ = 0
000241      ISIDE = IE
000243      GO TO 7
000245    5 JJ = 2
000244      ISIDE = ITEMP
000246      GO TO 7
000246    6 JJ=1
000247      ISIDE=ITEMP
000251    7 IF(N .LT. 200) GO TO 70
000254      WRITE(6,99)
000257   99 FORMAT(32H MORE THAN 200 POINTS ON CONTOUR)
000263      GO TO 78
000263   70 N = N + 1
000265      CALL INTER(ISIDE,X(N),Y(N),XP,YP,Z)
000276      LFLAG(ISIDE)=LFLAG(ISIDE)-1
000301      IF(JJ) 10,10,8
000307    8 IE=MOD(IE+2*JJ,4)+1
000315      GO TO 9
C           RESET GLOBAL FLAGS
000315   10 IF(LFLAG(ISIDE)) 40,40,41
000320   41 MFLAG=1
000321      LFLAG(ISIDE)=0
000331   40 IFLAG(ISO,JSO,1)=LFLAG(1)
000334      IFLAG(ISO,JP,2)=LFLAG(2)
000335      IFLAG(IP,JSO,1)=LFLAG(3)
000337      IFLAG(ISO,JSO,2)=LFLAG(4)
000343      IE=MOD(ISIDE+1,4) + 1
000350      ISO=ISO+MOD(IE,2)*(2-IE)
000355      JSO=JSO+MOD(IE-1,2)*(IE-3)
000367      IF(ISO.LT.1.OR.ISO.GE.IROW) GO TO 30
000402      IF(JSO.LT.1.OR.JSO.GE.ICOL) GO TO 30
000411      IP=ISO+1
000412      JP=JSO+1
000414      IF(Z(ISO,JSO).GT.UZMAX.OR.Z(IP,JSO).GT.UZMAX
           1 .OR.Z(IP,JP).GT.UZMAX.OR.Z(ISO,JP).GT.UZMAX) GO TO 30
000450      IF(MFLAG) 20,20,30
000451   30 CALL SMOOTH(X,Y,DS,N)
000454      RETURN
000455      END
            SUBROUTINE INTER(IEDGE,XX,YY,XP,YP,Z)
000010      DIMENSION Z(30,30),XP(30,30),YP(30,30)
000010      COMMON /OWN/ IFLAG(30,30,2),IE,ISO,JSO,N,IROW,ICOL
           /     ,DS,C,X(200),Y(200),E1,E2,UZMAX,XM,YM,ZM
000010      IF(IEDGE .GT. 4) GO TO 10
000017      I1 = ISO + IEDGE/3
000022      J1 = JSO + MOD(IEDGE/2,2)
000024      I2 = ISO + MOD(IEDGE/2,2)
000025      J2 = JSO + 1 - IEDGE/3
000030      X1 = XP(I1,J1)
000034      Y1 = YP(I1,J1)
000036      Z1 =  Z(I1,J1)
000040      X2 = XP(I2,J2)
000044      Y2 = YP(I2,J2)
000046      Z2 =  Z(I2,J2)
000051      GO TO 20
000053   10 X1 = XM
000054      Y1 = YM
000055      Z1 = ZM
000057      I2 = ISO + MOD((IEDGE-4)/2,2)
000065      J2 = JSO + 1 - (IEDGE-4)/3
000071      X2 = XP(I2,J2)
000075      Y2 = YP(I2,J2)
000077      Z2 =  Z(I2,J2)
000101      IF(ABS(Z2-C) .LT. E1) Z2 = C + E1
000107      IF(ABS(Z1-C) + ABS(C-Z2) .LE. ABS(Z1-Z2)+E2) GO TO 20
000121      IEDGE = - IEDGE
000122      RETURN
000123   20 F = (C - Z1)/(Z2 - Z1)
000126      XX = X1 + F*(X2-X1)
000131      YY = Y1 + F*(Y2-Y1)
000135      RETURN
000135      END
```

```
      *IDFTC *FOR*
            SUBROUTINE CONTOR(IP,IC,Z,XP,YP,     DCC,DST,UZMAXT)
000017      DIMENSION Z(30,30),XP(30,30),YP(30,30)
000017      COMMON/OWN/IFLAG(30,30,2),IE,ISQ,JSQ,N,IROW,ICOL
           /   ,DS,C,X(200),Y(200),E1,E2,UZMAX,XM,YM,ZM
000012      IF(IROW .LE. 30 .AND. ICOL .LE. 30) GO TO 100
000022      WRITE(6,99)
000025   99 FORMAT(33H GRID OUTSIDE 30*30 LIMIT ALLOWED  )
000031      STOP
000033  100 DC = ABS(DCC)
000034      IF(DC.GT.0.0) GO TO 101
000037      WRITE(6,98)
000042   98 FORMAT(///40H ZERO CONTOUR INTERVAL NOT PERMITTED      )
000046      STOP
000050  101 UZMAX = UZMAXT
000051      IROW = IP
000052      ICOL = IC
000053      DS = DST
000055      E1 = .0001*DC
000057      E2 = .00001*DC
000060      IRM = IROW - 1
000062      ICM = ICOL - 1
            C     FIND THE MINIMUM AND MAXIMUM VALUES OF Z
000064      ZMIN = Z(1,1)
000065      DO 5 I = 1,IROW
000067      DO 6 J = 1,ICOL
000070      IF(Z(I,J) .LT. ZMIN) ZMIN = Z(I,J)
000075    6 CONTINUE
000105    5 CONTINUE
000107      ZMAX = ZMIN
000111      DO 35 I=1,IROW
000112      DO 35 J=1,ICOL
000113      IF(Z(I,J).LT.UZMAX.AND.Z(I,J).GT.ZMAX) ZMAX = Z(I,J)
000121   35 CONTINUE
            C     FIND LOWEST CONTOUR
000137      K = ZMIN/DC + 0.5
000142      C = FLOAT(K-1)*DC
            C
000145      DO 50 IJK= 1,1000
000146      C = C + DC
000147      IF(C .GE. ZMAX) RETURN
            C     SET FLAGS ON ALL EDGES FOR CONTOUR C
000153      DO 10 I = 1,IROW
000155      DO 15 J = 1,ICOL
000156      ZZ = Z(I,J)
000161      IF(ABS(ZZ-C) .LT. E1) ZZ = C + E1
000167      IF(J .EQ. ICOL) GO TO 16
000171      ZJ = Z(I,J+1)
000174      IF(ABS(ZJ-C) .LT. E1) ZJ = C + E1
000202      IFLAG(I,J,1) = 0
000206      IF(ZZ .GE. UZMAX .OR. ZJ .GE. UZMAX) GO TO 16
000216      IF(ABS(ZZ-C) + ABS(C-ZJ) .LE. ABS(ZZ-ZJ) + E2) IFLAG(I,J,1)=1
000227   16 IF(I .EQ. IROW) GO TO 15
000235      ZI = Z(I+1,J)
000240      IF(ABS(ZI-C) .LT. E1) ZI = C + E1
000246      IFLAG(I,J,2) = 0
000252      IF(ZZ .GE. UZMAX .OR. ZI .GE. UZMAX) GO TO 15
000262      IF(ABS(ZZ-C) + ABS(C-ZI) .LE. ABS(ZZ-ZI) + E2) IFLAG(I,J,2)=1
000277   15 CONTINUE
000302   10 CONTINUE
            C     SEARCH AROUND BOUNDARIES FOR EDGES STARTING THERE
000304      DO 20 J = 1, ICM
000306      IF(IFLAG(1,J,1) .EQ. 1) CALL INIT(1,1,J,1,J,1,XP,YP,7)
000323      IF(IFLAG(IROW,J,1) .EQ. 1) CALL INIT(3,IRM,J,IROW,J,1,XP,YP,7)
000351   20 CONTINUE
000354      DO 21 I = 1, IRM
000355      IF(IFLAG(I,1,2) .EQ. 1) CALL INIT(4,I,1,I,1,2,XP,YP,7)
000371      IF(IFLAG(I,ICOL,2) .EQ. 1) CALL INIT(2,I,ICM,I,ICOL,2,XP,YP,7)
000417   21 CONTINUE
            C     SEARCH THROUGH USER BOUNDARY SQUARES
000422      DO 70 I = 1,IRM
000423      DO 75 J = 1,ICM
            C     IS IT A BOUNDARY SQUARE
000424      IF(Z(I,J) .GT. UZMAX) GO TO 71
000432      IF(Z(I+1,J) .GT. UZMAX) GO TO 71
000435      IF(Z(I,J+1) .GT. UZMAX) GO TO 71
000440      IF(Z(I+1,J+1) .GT. UZMAX) GO TO 71
000443      GO TO 75
            C
            C     FIND AN EDGE IN SQUARE WITH IFLAG = 1
000443   71 IF(IFLAG(I,J,1) .EQ. 1) GO TO 81
000450      IF(IFLAG(I,J+1,2) .EQ. 1) GO TO 82
000452      IF(IFLAG(I+1,J,1) .EQ. 1) GO TO 83
000454      IF(IFLAG(I,J,2) .EQ. 1) GO TO 84
000456      GO TO 75
            C
000456   81 CALL INIT(3,I-1,J,I,J,1,XP,YP,7)
000472      GO TO 75
000476   82 CALL INIT(4,I,J+1,I,J+1,2,XP,YP,7)
000512      GO TO 75
000516   83 CALL INIT(1,I+1,J,I+1,J,1,XP,YP,7)
000532      GO TO 75
000536   84 CALL INIT(2,I,J-1,I,J,2,XP,YP,7)
            C
000556   75 CONTINUE
000561   70 CONTINUE
            C     SEARCH THROUGH INTERNAL EDGES
000563      DO 25 I = 1,IRM
000565      DO 25 J = 1,ICM
000566      IF(IFLAG(I,J,1) .EQ. 1) CALL INIT(1,I,J,I,J,1,XP,YP,7)
000603      IF(IFLAG(I,J,2) .EQ. 1) CALL INIT(4,I,J,I,J,2,XP,YP,7)
000631   25 CONTINUE
000636   50 CONTINUE
000640      RETURN
000641      END

UNUSED COMPILER SPACE
015600


            SUBROUTINE SMOOTH(X,Y,DS,N)
000006      DIMENSION X(200),Y(200)
000006      IF(N .LT. 2) RETURN
000010      II = 3
000011      DO 5 I = 1,N
000013      CALL PLOT(X(I),Y(I),II)
000022      II = 2
000023    5 CONTINUE
000025      RETURN
000025      END
```

CONTOUR PLOTTING PROGRAM (b)

PURPOSE:- To plot stresses for plane strain and axisymmetrical models where the mesh is not regular. Elements may be triangular or quadrilateral.

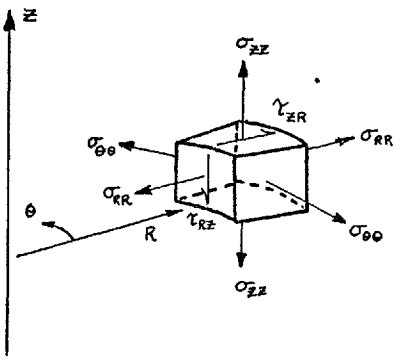
INPUT:- Stresses at element centroids, a list of nodes defining each element and plotting instructions.

OUTPUT:- A list of input data and contoured plots of direct stresses (RR, ZZ, TT, RZ)

INPUT INSTRUCTIONS AND PROGRAM NOTATION			FORMAT
CARD 1	NUMEL	Number of elements	2I5,F10.0
	NUMNP	Number of nodes	
	UZMAX	Maximum value to be plotted	
CARD 2	NPLOT	Number of plots	
	NC	Number of contour values to each plot	4I5,3F10.0
	NO	Number of coordinates to describe structure	
	NA	Number of steps between contour labels	
	SCA	Geometric scale factor	
	XM	Distance between plots in the X direction	
	YM	Distance between plots in the Y direction	

Note that the program was written for plotting on Kingmatic paper size 1 and it spaces the plots two across the page. If the geometric scaling factor is 2. then the model is plotted half size.

CARD 3	BASE(I)	Minimum contour value for each plot (NPLOT of them)	6F10.0
CARD 4	CINT(I)	Contour interval (NPLOT of them)	6F10.0
CARD 5	Z(I),W(I)	Coordinates defining the structure (NO pairs)	6F10.0
CARDS 6	((IX(N,I),I=1,4),N=1,NUMEL)	List of nodes defining each element. If the third and fourth nodes are the same then the element is triangular	24I3
CARDS 7	N	Element Number	
	X(N) Y(N)	Coordinates of centroid	I5,2F8.2,3E12.4
	RR(N) ZZ(N) TT(N) RZ(N)	Stresses from analysis	



```
000002            PROGRAM AXI(INPUT,OUTPUT,TAPE5=INPUT,TAPE6=OUTPUT,TAPE25,TAPE27)
                  C       UMCP005----ST.JOHN    **ROCK MECHANICS**
000002            DIMENSION XS(600),YS(600),TS(600),SS(600)
000002            COMMON NUMEL,NUMNP,UZMAX,NPLOT,NO,SCA,XM,YM,IX(600,4),
                 1 X(600),Y(600),XX(600),YY(600),XY(600),BASE(10),CINT(10),
                 2Z(40),W(40),NOD(10),TT(600)
000002            COMMON/TRIF/ S(600,4),XN(600),YN(600),CT(40),JA(40),NC,NA
000002            EQUIVALENCE (S(1,1),XS),(S(1,2),YS),(S(1,3),TS),(S(1,4),SS)
000002            READ(5,1000) NUMEL,NUMNP,UZMAX
000014     1000   FORMAT(2I5,F10.0)
000014            WRITE(6,2000) NUMEL,NUMNP,UZMAX
000026     2000   FORMAT(1H1,20HNUMBER OF ELEMENTS=  , I5 , /
                 1        20HNUMBER OF NODES    = , I5 ,/
                 2    24HMAXIMUM VALUE PLOTTED =  ,F10.2 )
                C***READ PLOTTING INSTRUCTIONS***
000026            READ(5,1002) NPLOT,NC,NO,NA,SCA,XM,YM
000050            WRITE(6,2007) NPLOT,NC,NO,NA,SCA,XM,YM
000072     2003   FORMAT(1H0,17HNUMBER OF PLOTS = ,I5,  /
                 1  I5,9HCONTOURS,I5,20HCOORDS FOR STRUCTURE,
                 2  I5,20HSTEPS BETWEEN LABELS,4X,17HSCALE FACTOR= ,F10.2,  /
                 3 2HDISTANCE BETWEEN PLOTS- X= ,F10.2,2HY= , F10.2 )
000072            READ(5,1003) (BASE(I),I=1,NPLOT)
000101            WRITE(6,2004) (BASE(I),I=1,NPLOT)
000110     2004   FORMAT(1H ,19HCONTOUR BASE VALUES  , / 6F10.2 )
000110            READ(5,1003) (CINT(I),I=1,NPLOT)
000117            WRITE(6,2005) (CINT(I),I=1,NPLOT)
000126     2005   FORMAT(1H ,17HCONTOUR INTERVALS  ,/ 6F10.2)
000126            READ(5,1003) (Z(I),W(I),I=1,NO)
000143            WRITE(6,2006) (Z(I),W(I),I=1,NO)
000160     2006   FORMAT(1H ,34HCOORDINATES DEFINING THE STRUCTURE / 6F10.2)
000160     1002   FORMAT(4I5,3F10.0)
000160     1003   FORMAT(6F10.0)
                C****ELEMENT DATA******
000160            READ(5,1005) ((IX(N,I),I=1,4),N=1,NUMEL)
000200     1005   FORMAT(24I3)
000200            READ(5,1001) (N,X(N),Y(N),XX(N),YY(N),TT(N),XY(N),N=1,NUMEL)
000226     1001   FORMAT(I5,2F8.2,4E12.4)
000226            WRITE(6,2001)
000232     2001   FORMAT(1H0,1X,7HELEMENT,2X,10HNODAL LIST,4X,4HXORD,4X,4HYORD,4X,
                 1 9HXX-STRESS,5X,9HYY-STRESS,5X,9HTTSTRESS,5X,9HXY-STRESS )
000232            WRITE(6,2002)(N,IX(N,1),IX(N,2),IX(N,3),IX(N,4),X(N),Y(N),
                 1 XX(N),YY(N),TT(N),XY(N),N=1,NUMEL)
000270     2002   FORMAT(1H ,1X,5I4,2F8.2,4E12.4)
000270            DO 10 N=1,NO
000300            Z(N)=Z(N)/SCA
000301            W(N)=W(N)/SCA
000302       10   CONTINUE
                C****CREATE NODES AND STRESSES FROM ELEMENT DATA***
000303            DO 100 N=1,NUMNP
000304            K=0
000305            DO 200 M=1,NUMEL
000306            DO 300 I=1,4
000316            IF(IX(M,I).EQ.N) GO TO 150
000317       300  CONTINUE
000321            GO TO 200
000321       150  IF(XX(M).GE.UZMAX) GO TO 200
000324            K=K+1
000326            NOD(K)=M
000330       200  CONTINUE
                C***FIND CENTROID ELEMENT LIST
000333            IF(K.GT.1) GO TO 99
000337            M=NOD(1)
000340            XN(N)=X(M)/SCA
000342            YN(N)=Y(M)/SCA
000343            XS(N)=XX(M)
000345            YS(N)=YY(M)
000347            SS(N)=XY(M)
000350            TS(N)=TT(M)
000352            GO TO 100
000352        99  XN(N)=YN(N)=XS(N)=YS(N)=TS(N)=SS(N)=0.0
000362            DO 400 J=1,K
000372            SK=K
000373            SCAK=SCA*SK
000374            JK=NOD(J)
000376            XN(N)=XN(N)+X(JK)/SCAK
000400            YN(N)=YN(N)+Y(JK)/SCAK
000402            XS(N)=XS(N)+XX(JK)/SK
000405            YS(N)=YS(N)+YY(JK)/SK
000407            TS(N)=TS(N)+TT(JK)/SK
000411            SS(N)=SS(N)+XY(JK)/SK
000412       400  CONTINUE
000414       100  CONTINUE
                C****PLOT UNITS ONE AT A TIME----3 ACROSS PAGE----
000417            CALL START
000420            CALL PLOT(1.3,1.0,-3)
000423            DO 500N=1,NPLOT
000425            CALL PRETRI(N)
000426            IF(N-2) 502,501,502
000430       501  CALL PLOT(XM,-YM,-3)
000434            GO TO 500
000435       502  CALL PLOT(0.0,YM,-3)
000440       500  CONTINUE
000443            CALL ENPLOT(30.)
000444            STOP
000446            END

UNUSED COMPILER SPACE
016100
```

```
                SUBROUTINE PRET*I(NP)
000002          COMMON NUMEL,NUMNP,UZMAX,NPLOT,NO,SCA,XM,YM,IX(600,4),
               1 X(600),Y(600),XX(600),YY(600),XY(600),BASE(10),CINT(10),
               2Z(40),N(40),NOD(10),TT(600)
000002          COMMON/TRIP/ S(600,4),XN(600),YN(600),CT(40),JA(40),NC,NA
          C****PLOT SHAPE OF STRUCTURE****
000002          CALL PLOT(Z(1),N(1),3)
000005          DO 50 N=2,NO
000010          CALL PLOT(Z(N),N(N),2)
000014       50 CONTINUE
          C****ESTABLISH CONTOUR INFORMATION****
000017          F=0.0
000020          DO 10 N=1,NC
000032          CT(N)=BASE(NP)+CINT(NP)*F
000033          F=F+1.0
000034       10 CONTINUE
000035          DO 20 JI=1,NC
000042          JA(JI)=0
000043       20 CONTINUE
          C***PLOT ELEMENTS ONE AT ATIME
000044          DO 100 M=1,NUMEL
000045          I=IX(M,1)
000050          J=IX(M,2)
000051          K=IX(M,3)
000053          L=IX(M,4)
000054          IF(K.EQ.L) GO TO 490
000062          L1 = ((XN(I)-XN(K))**2+(YN(I)-YN(K))**2)
000066          L2=((XN(J)-XN(L))**2+(YN(J)-YN(L))**2)
000072          IF(L1.LE.L2) GO TO 480
000075          CALL TRIPLT(K,L,J,NP)
000100          CALL TRIPLT(K,L,I,NP)
000105          GO TO 100
000107       480 CALL TRIPLT(K,L,I,NP)
000114       490 CALL TRIPLT(I,J,K,NP)
000121       100 CONTINUE
000124          RETURN
000124          END

UNUSED COMPILER SPACE
017600
```

```
                SUBROUTINE TRIPLT(II,JJ,KK,KT)
000006          DIMENSION A(40),B(40),C(40),D(40),JC(40)
000006          COMMON/TRIP/ S(600,4),XN(600),YN(600),CT(40),JA(40),NC,NA
000006          DO 82 JI=1,NC
000014          A(JI)=0.
000015          B(JI)=0.
000015          C(JI)=0.
000015          D(JI)=0.
000016          JC(JI)=0
000016       82 CONTINUE
000017          IF(S(II,KT).GT.S(JJ,KT))GO TO 11
000036          SS1=S(II,KT)
000037          SS2=S(JJ,KT)
000040          XX1=XN(II)
000042          XX2=XN(JJ)
000043          ZZ1=YN(II)
000045          ZZ2=YN(JJ)
000047          GO TO 12
000056       11 SS1=S(JJ,KT)
000057          SS2=S(II,KT)
000060          XX1=XN(JJ)
000062          XX2=XN(II)
000063          ZZ1=YN(JJ)
000065          ZZ2=YN(II)
000067       12 NN=1
000070          GO TO 30
000071       13 NN=2
000072          IF(S(JJ,KT).GT.S(KK,KT)) GO TO 14
000107          SS1=S(JJ,KT)
000110          SS2=S(KK,KT)
000111          XX1=XN(JJ)
000113          XX2=XN(KK)
000114          ZZ1=YN(JJ)
000116          ZZ2=YN(KK)
000120          GO TO 15
000127       14 SS1=S(KK,KT)
000130          SS2=S(JJ,KT)
000131          XX1=XN(KK)
000133          XX2=XN(JJ)
000134          ZZ1=YN(KK)
000136          ZZ2=YN(JJ)
000140       15 CONTINUE
000140          GO TO 30
000141       16 NN=3
000142          IF(S(II,KT).GT.S(KK,KT)) GO TO 17
000157          SS1=S(II,KT)
000160          SS2=S(KK,KT)
000161          XX1=XN(II)
000163          XX2=XN(KK)
000164          ZZ1=YN(II)
000166          ZZ2=YN(KK)
000170          GO TO 18
000177       17 SS1=S(KK,KT)
000200          SS2=S(II,KT)
000201          XX1=XN(KK)
000203          XX2=XN(II)
000204          ZZ1=YN(KK)
000206          ZZ2=YN(II)
```

```
000210     18    CONTINUE
000210     30    CONTINUE
000210           DIFF=ABS(SS2-SS1)
000213           IF(DIFF.LT.0.0001) GO TO 60
000215           DO 21 N=1,NC
000217           IF(CT(N).LT.SS1.OR.CT(N).GT.SS2) GO TO 21
000232           XX=(CT(N)-SS1)*(XX2-XX1)/(SS2-SS1)+XX1
000237           YY=ZZ1+(CT(N)-SS1)*(ZZ2-ZZ1)/(SS2-SS1)
000245           JC(N)=JC(N)+1
000247           JS=JC(N)
000250           GO TO (70,71,72),JS
000257     70    A(N)=XX
000260           B(N)=YY
000262           GO TO 21
000264     71    C(N)=XX
000265           D(N)=YY
000267           GO TO 21
000270       72  DXC=(A(N)-C(N))**2+(B(N)-D(N))**2
000275           IF(DXC.GT.0.0001) GO TO 21
000301           C(N)=XX
000302           D(N)=YY
000304     21    CONTINUE
000307     60    CONTINUE
000307           GO TO (13,16,24) NN
000316     24    DO 25 JI=1,NC
000320           IF(JC(JI).EQ.0) GO TO 25
000321           CALL PLOT (A(JI),B(JI),+3)
000324           CALL PLOT(C(JI),D(JI),+2)
000330           IF(JA(JI).EQ.0) GO TO 26
000334           JA(JI)=JA(JI)-1
000336           GO TO 25
000337       26  CALL NUMBER(A(JI),B(JI),0.07,CT(JI),0.0,3)
000346           JA(JI)=NA
000353     25    CONTINUE
000356           RETURN
000356           END

UNUSED COMPILER SPACE
016700
```

APPENDIX

B

TWO DIMENSIONAL SIMULATION OF JOINTED ROCK STRUCTURES BY FINITE ELEMENTS

COMPUTER PROGRAM FOR JOINTED ROCK MASSES

TWO DIMENSIONAL ANALYSIS

PLANE STRESS AND PLANE STRAIN

Purpose

The program is designed to simulate complex behaviour of jointed rock systems. The following material behaviours are treated using initial stress and strain methods.

(1) Limited or zero tensile strength for solid materials

(2) Shear on a ubiquitous joint set in solid materials

(3) Non linear shear force displacement law for joints; including peak residual behaviour.

(4) Dilatancy during shear

(5) Zero tensile strength for joints

(6) Non-linear closure under normal load; according to a prescribed law.

Comment

The program was written for the CDC 6400/6600 installation at London University. It is based on earlier two dimensional finite element programs developed at the University of California, Berkeley (1965-1969).

Input Data

(1) Title of Problem (12A6)

Columns 1-72 on the first data card of the set contains a title that will be printed at the head of output.

(2) Control Information (4I5, 2F10.2, 5I5)

Columns		Program Notation
1 - 5	Number of Nodal Points	NUMNP
6 - 10	Number of Elements	NUMEL
11 - 15	Number of Material Types	NUMMAT
16 - 20	Number of Boundary Pressure Cards	NUMPC
21 - 30	Acceleration in X direction	ACELX
31 - 40	Acceleration in Y direction	ACELY
41 - 45	Number of Steps on this run	NSTEP
46 - 50	0 if a second data set follows	NEND
51 - 55	Residual Stress Code*	NRES
56 - 60	Joint Cut-off Number. Materials with a higher number are all joints	NSHELL
61 - 65	Material type with Non Existant Properties	NONEX

* NRES = 0 No Residual Stresses
NRES = 1 Residual Stresses. In Local Coords for Joints
NRES = 2 Residual Stresses. In Global Coords for Joints.

(3) Tape Storage Card (2I5)

1 - 5	Reads Data and Previous Output from TAPE 11	NREAD
6 - 10	Write Data and Current Output onto TAPE 12 if not zero	NWRITE

(See Note (D))

(4) Model Control Card (5F10.0)

1 - 10	Scale Factor for nodal point co-ordinates used for changing scale, units, etc.	SCALE
11 - 20	Set greater than zero if Residual Stresses are to be calculated (NRES will have been zero if so)	RCALC
21 - 30	Datum for Residual Stress Calculations May be necessary to shift co-ordinate origin for residual stress calculations	DATUM
31 - 40	Ratio of Horizontal to Vertical Residual Stresses	RATIO
41 - 50	Code for Plane Stress (=1) or Plane Strain (=0)	PLANE

(5) Material Property Cards Set for each material type.

Solid Materials:

First Card:(I5, F10.0)

1 - 5	Material Identification	MTYPE
6 - 15	Material Density	RO

Second Card (7F10.0)

1 - 10	Tensile Strength of Material	E(1,MTYPE)
11 - 20	E - Compression	E(2,MYTPE)
21 - 30	ν	E(3,MYTPE)
31 - 40	E - Tension	E(4,MTYPE)
41 - 50	Direction of Ubiquitous Joint set. (Measure Anticlockwise from X axis) OR Area for Bar Elements.	E(5,MTYPE)
51 - 60	Cohesion for Joints OR Initial Stress for Bar Elements	E(6,MTYPE)
61 - 70	Friction Angle for Joints	E(7,MTYPE)

Joint Materials:

First Card: (I5)

1 - 5	Material Identification	MTYPE

Second Card: (5F10.0)

1 - 10	Normal Stiffness	E(1,MTYPE)
11 - 20	Shear Stiffness	E(2,MTYPE)
21 - 30	Joint Cohesion (usually zero)	E(3,MTYPE)
31 - 40	Joint Friction Angle	E(4,MTYPE)
41 - 50	Maximum Normal Closure (Must be negative)	E(5,MTYPE)

Third Card: (I5)

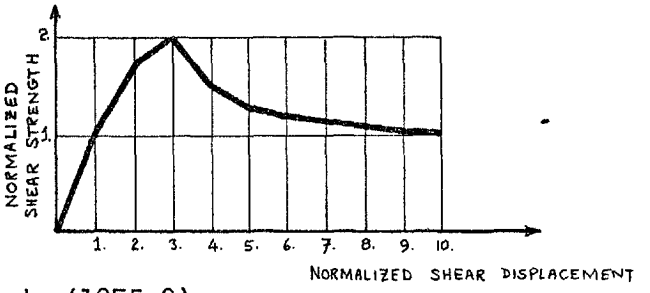
1 - 5	Joint Number	JTYPE

Fourth Card: (2F10.0)

1 - 10	Maximum Possible Dilatation at zero normal load	DINC
11 - 20	Normal Load Increment for Dilation law	FINC

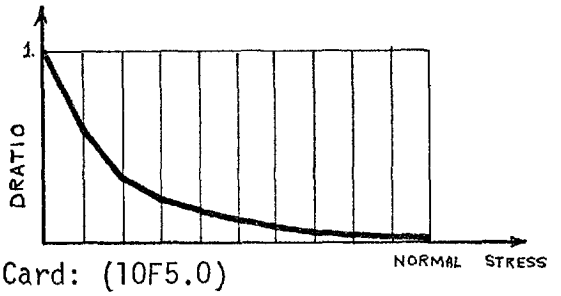
Fifth Card: (10F5.0) SHEAR

List of Normalized Shear Stresses at unit increments of Normalized Shear Displacement. The shear stress at unit displacement should be 1.0 for the joint shear stiffness to describe its behaviour



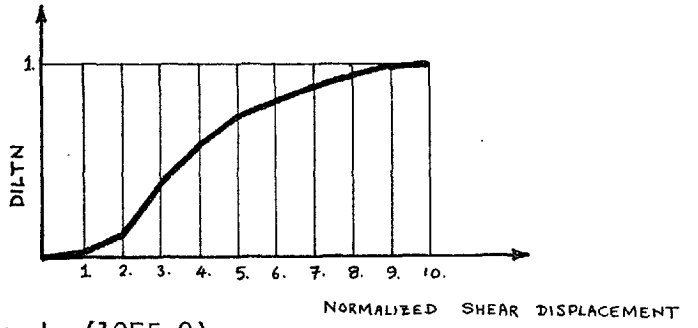
Sixth Card: (10F5.0) DRATIO

List of the Proportion of Maximum Dilatation that may occur. Given at specifield increments of normal stress (FINC).



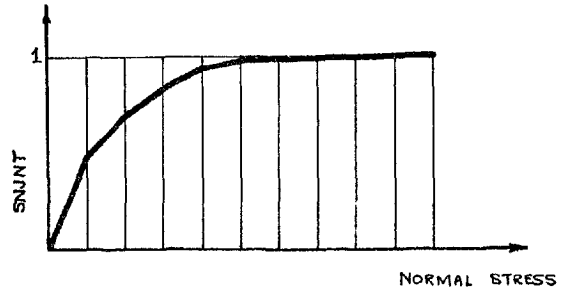
Seventh Card: (10F5.0) DILTN

List of Normalized Dilatation (Dilatation/DINC) that occurs at zero normal stress. Given at unit intervals of Normalised Shear Displacement.



Eighth Card: (10F5.0) SNJNT

List of the Proportion of Maximum Closure that may occur. Given at specified normal stress increments (FINC). Note that it is convenient if the normal stiffness corresponds to this relationship over the first increment.



(6) Nodal Point Cards (2I5, 4F10.0)

1 - 5	Nodal Point Number	N
6 - 10	Nodal Point Load or Displacement Identifier*	CODE
11 - 20	X - ordinate	R
21 - 30	Y - ordinate	Z
31 - 40	X - Load or X - Displacement	UR
41 - 50	Y - Load or Y - Displacement	UZ

*Nodal Coding

Loads or displacements are indicated, depending on the nodal code

Code	0	1	2	3	
X-direction	L	D	L	D	D = Displacement
Y-direction	L	L	D	D	L = Load

Missing nodal points in the data presented are generated automatically by linear interpolation. In the event of interpolation the nodal code and the loads are set to zero. If CODE is negative then it refers to the angle measured anti-clockwise from the global axes to local axes in which a load/displacement is specified.

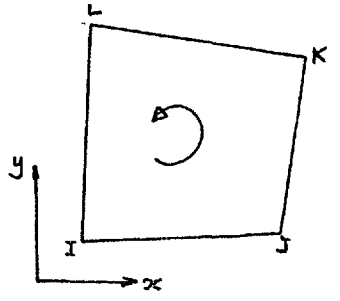
This is used for skew boundaries (See Note A following).

(7) Element Cards (6I5)

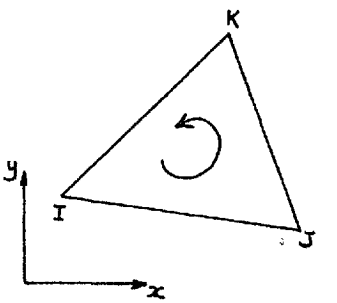
1 - 5	Element Number	M
6 - 10	I	IX (1)
11 - 15	J	IX (2)
16 - 20	K	IX (3)
21 - 25	L	IX (4)
26 - 30	Material Type	IX (5)

Missing elements are supplied by adding one to each nodal point number of the last specified element. This element also defines the material type. The last element must appear on the last data card of this series.

Solid Element



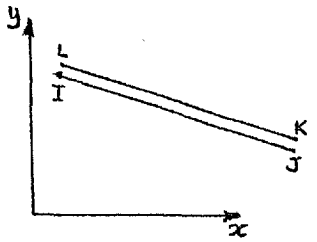
Labelled I, J, K, L



Labelled I, J, K, K

Maximum difference between nodal point numbers of an element is 39.

Joint Element



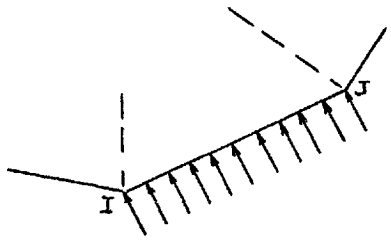
Labelled I, J, K, L - Nodes I and L have the same co-ordinates so do J and K.

A one dimensional Bar Element is identified as I, J, J, I.

(8) Pressure Cards (2I5, 1F10.0)

One card for each boundary element subject to normal pressure.

1 - 5	Nodal Point I	IBC
6 - 10	Nodal Point J	JBC
11 - 20	Normal Pressure	PR



As shown above, the boundary element must be on the left with reference to the direction I to J. Surface tensile force is input as a negative pressure. Joints cannot be placed on the boundaries.

(9) Residual Stress Cards (I5, 2X, 3E15.4)

1 - 5	Element	N
6 - 7	Blank	
8 - 22	X - stress	RESID(N,1)
23 - 37	Y - stress	RESID(N,2)
38 - 52	XY - stress	RESID(N,3)

If the residual stress refers to joint elements then if the former are in the joint local co-ordinate system:

X - stress = Normal Stress

Y - stress = 0.0

XY - stress = Shear Stress

If cards in this set are omitted, then the stresses are assumed equal to those on the last card. If all the elements have the same stresses, then only the first and last element stresses need by supplied.

(10) Construction, Excavation or Loading Control Card (6I5)

One card of this type is required to head each set of increment instructions. There are NSTEP increments.

1 - 5	Number of Elements which are to have their material code altered.	NELCUT
6 - 10	New Material Code for altered elements	MCUT
11 - 15	Number of Nodal points to be altered	NBOUN
16 - 20	Number of first approximation in this computer run	NFIRST
21 - 25	Number of last approximation in this computer run	NLAST
26 - 30	Total Number of approximations for this load increment	NP

Note: If NP is greater than NLAST then further approximations on a later computer run are anticipated. The residual stress state and the displacements are then not updated before the results of the run are written onto tape.

(11) Altered Node Cards(I5, F5.0, 2F10.0)

There will be NBOUN of these for each load step.

1 - 5	Node Number	N
6 - 10	Displacement or Load Code	CODE
11 - 20	X-Load or Displacement	UR
21 - 30	Y-Load or Displacement	UZ

Note: These are total loads or displacements, not additional to those pre-existing.

(12) Altered Element Cards (6I5)

List of Elements to be given material type MCUT. Six Element Numbers per card. NCUT

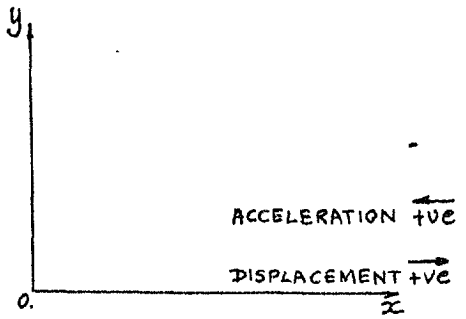
COMPUTER OUTPUT

The following output is obtained:

1) Printout of entire data, if this has been read from cards
2) Residual Stress state at beginning of each increment
3) Incremental and total displacements up to the start of the current increment. Given for each approximation.
4) Stresses at the centroid of each solid element. Given for each approximation.
5) Stresses and relative displacements of each joint element. Given for each approximation.

ADDITIONAL REMARKS ON DATA AND COMPUTER OUTPUT

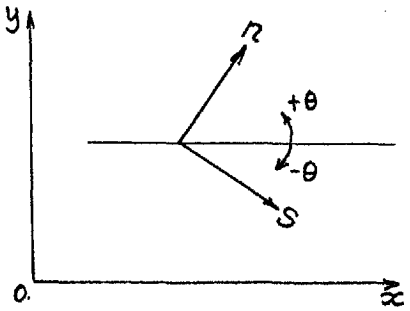
(a) Co-ordinate Systems



The right-handed xy co-ordinate system is as shown above.

Displacements have the same sign.

Accelerations have the opposite sign.



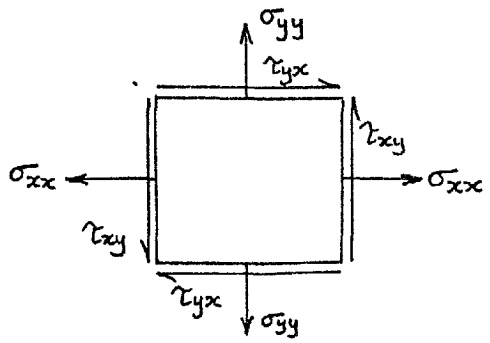
The ns co-ordinate system for skew boundaries is defined by the angle +ve clockwise from the x-axis to the s-axis. It must always be negative in the range -0.001 to -180.0 degrees. (Note +1.0 ≡ - 179.0).

The terms in columns 31-50 of the nodal point card are now interpreted as:

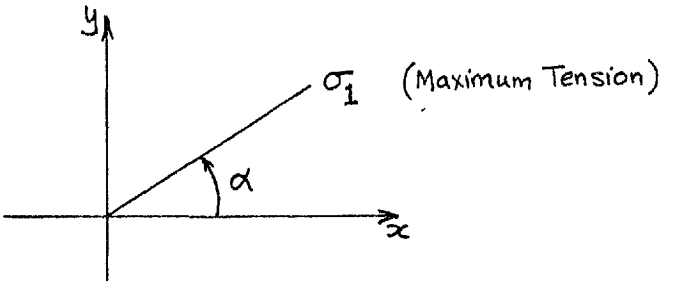
UR is the specified load in the s-direction
UZ is the specified displacement in the n- direction

The displacement printed in the output are given in this local co-ordinate system for these nodes.

(b) Continuum Element Stresses

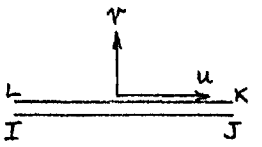


Direct Stresses Sign Convention (Tension +ve)

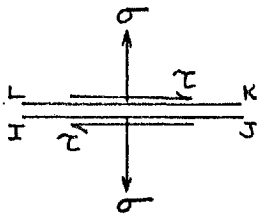


Principal Stress Direction Sign Convention α is measured anti-clockwise from the x-axis.

(c) Joint Element Stresses and Displacements



Positive displacements of top face relative to bottom face



Positive Stresses

The stresses and displacements for the joint are the mean values and are given at the mid point. Residual stresses have the same sign convention unless they are given in global co-ordinates (NRES = 2)

(d) Tape Handling of Data and Output

The following procedure has been adopted for storing data and output on tape units 11 and 12. It is designed for permanent file usage. The essence of the procedure is that the permanent file cycle is written as TAPE 12 and read as TAPE 11.

	NREAD	NWRITE
RUN (1)	0	1

Read Data from Cards
Write output and Data on TAPE 12
Catalog TAPE 12
as Permanent File (P.F.) Named; (e.g.) (EXCAV, CY=1)
(where CY is the cycle number)

RUN (2)	1	1

Attach TAPE 11 - P.F. (EXCAV, CY=1)
Read Data and Previous Output from TAPE 11
Write Output and Data on TAPE 12
Catalog TAPE 12 - P.F. (EXCAV,CY=2)

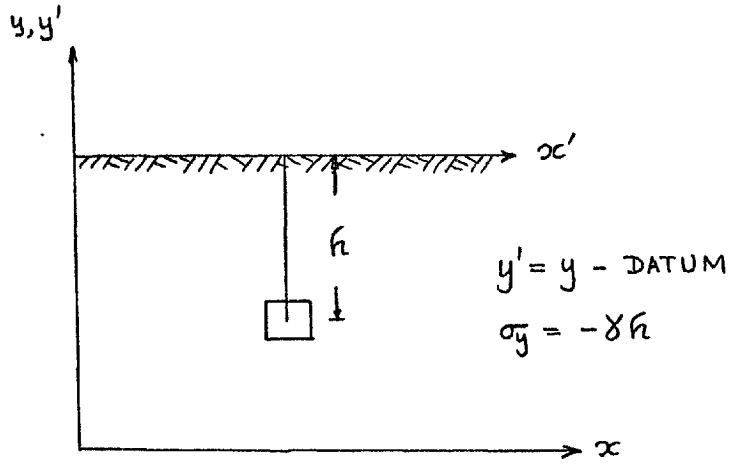
RUN (N) 1 1

Attach TAPE 11 - P.F. (EXCAV, CY=N-1)
Read Data and Output from RUN (N-1)
Write Final Output and Data on TAPE 12
Catalog TAPE 12 - P.F.(EXCAV, CY = N)

Clearly the cycle numbers need not be successive and only the output of the current and preceding runs need be on file at the same time. If a real tape is used then the output of the current run may overwrite the preceding run by using only tape 11 or tape 12 for both reading and writing. However, it is probably good practice to retain the preceding output until the current run has been checked.

(e) Model Control Card

If RCALC is greater than zero then the residual stress slate in the model will be calculated from the given co-ordinates. In most cases, the depth of overburden will control the vertical stress. It is then essential that the origin of the co-ordinate system for the model is constrained to lie on the upper free surface. This is done using DATUM as shown below.



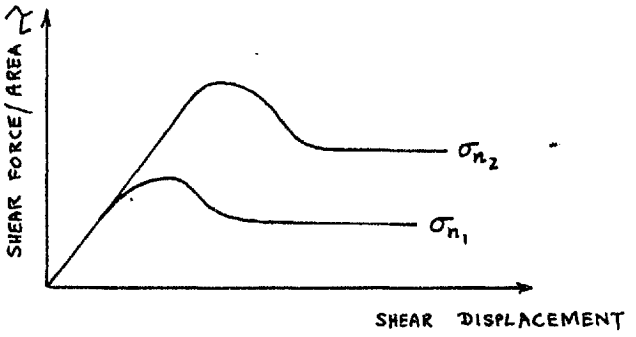
RATIO defines the ratio of the residual horizontal stress to the vertical,

$$\text{i.e.} \quad \sigma_x = \text{RATIO} \times \sigma_y$$

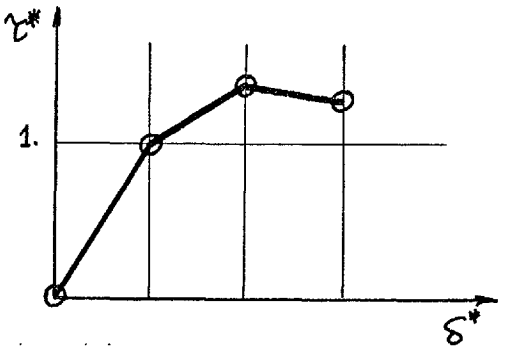
Note that SCALE alters the data in store whilst DATUM does not.

(f) Shear Force/Displacement Law

The law is defined so that the initial shear stiffness (k_s) is independent of the normal stress.



The normalised relationship between shear force per unit area and shear displacement is arrived at via the joint shear stiffness and the residual angle of friction (ϕ_r). It is convenient if the shear stiffness defines the behaviour at least over the first increment of normalised shear displacement. (If residual stresses exist at the start of the calculation the corresponding displacements are calculated from the shear stiffness).

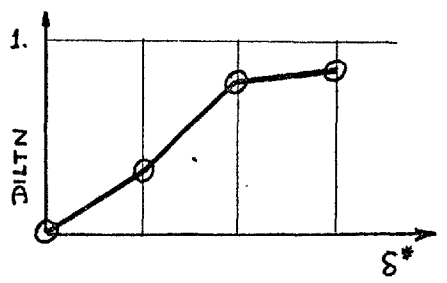


$$\tau^* = \frac{\tau}{\sigma_n \tan \phi_r}$$

$$\delta^* = \frac{\delta_s \cdot ks}{\sigma_n \tan \phi_r}$$

(g) Dilation Laws

Shear tests on joints may be used to determine the joint dilatancy. This has been divided into two parts. Firstly the dilatation during shear at zero, or very low, normal stress is defined. The maximum dilatation recorded is DINC. This is used to define a normalised dilatation at zero normal load. It is specified numerically at intervals of the normalised shear displacement defined in note (f).



Dilatation at zero normal load
= (DILTN) X (DINC)

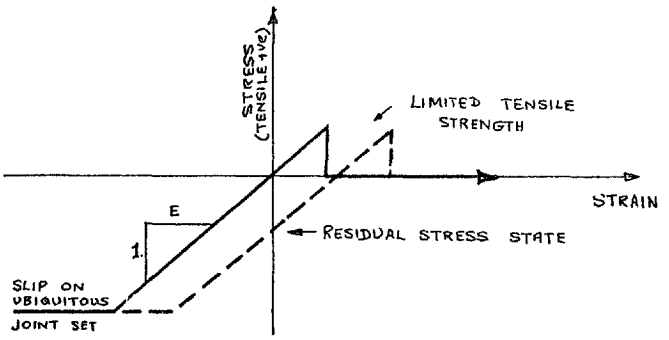
In order to take account of the influence of normal stress on dilatancy a second law is defined. This specifies the proportion of the maximum dilatation that occurs and is given at the increments of normal stress as defined by FINC.

Note: Because the dilatation law is defined in terms of the normalised shear displacement, it is possible to ensure that the peak dilatation angle coincides with peak shear strength.

(h) Normal Closure Law

The maximum permissible normal closure is given by E(5,MTYPE) on the second joint property card of each set. Up to the maximum value any relationship between normal force per unit area and normal displacement may be specified. SNJNT defines the proportion of the maximum that is permitted at the given increments of normal stress (FINC).

(i) Solid Element Properties



Slip will occur on the 'jointing' in the solid elements if the shear stress exceeds the shear strength at the existing normal stress.

$$\tau \text{ available} = c + \sigma_n \text{ Tan } \phi$$

where ϕ is the angle of friction
and c is the joint cohesion

```
      PROGRAM GEN(INPUT,OUTPUT,TAPE5=INPUT,TAPE6=OUTPUT,TAPE7
     1 ,TAPE8,TAPE9,TAPE10,TAPE11,TAPE12)
C     ST.JOHN   UMCR005
C     PLANE STRAIN WITH JOINTS, CUMULATIVE LOADING, NON LINEAR ALONG TANGENT
000002      COMMON NUMNP,NUMEL,NUMMAT,NUMPC,ACELX,ACELY,N,VOL,NRES,MTYPE,
     1 HED(12),E(8,12),RO(12),XXNN(12),R(500),Z(500),UR(500),UZ(500),
     2 CODE(500),IBC(200),JBC(200),PR(200),ANGLE(4),LBAD,NNN,NP,
     3 EPS(400),NSHELL,RSTRST(400,3),KN(400),KS(400)
000002      COMMON /ARG/ RRR(5),ZZZ(5),S(10,10),P(10),TT(4),LM(4),DD(3,3),
     1 HH(6,10),RR(4),ZZ(4),C(4,4),H(6,10),B(6,6),F(6,10),TP(6),XI(10)
     2,EE(7),IX(400,5),MTAG(400),RSTRS(4),RESID(400,3)
000002      COMMON /BANARG/ MBAND,NUMBLK,B(160),A(160,80),ND
000002      COMMON /EXC/ NCUT(100),NONEX
000002      COMMON /CUM/ BST(1000),STRN(400,4),NS
000002      COMMON /PLN/ PLANE
000002      REAL KN,KS
C*****
C     READ AND PRINT OF CONTROL INFORMAT AND MATERIAL PROPERTIES
C*****
C*****
000002      LBAD=0
000003   50 READ(5,1000)  HED,NUMNP,NUMEL,NUMMAT,NUMPC,ACELX,ACELY,
     1 NSTEP,NEND,NRES,NSHELL,NONEX
000037      WRITE(6,2000) HED,NUMNP,NUMEL,NUMMAT,NUMPC,ACELX,ACELY,NSTEP,
     1 NSHELL
000065      READ(5,1003) NREAD,NWRITE
000075      READ(5,1005) SCALE,RCALC,DATUM,RATIO,PLANE
000113      WRITE(6,3005) SCALE,RCALC,DATUM,RATIO
000127      IF(PLANE.EQ.0.) WRITE(6,2030)
000134      IF(PLANE.EQ.1.) WRITE(6,2031)
C
000142      IF (NSHELL .EQ. 0)  NSHELL= 13
000144   56 DO 59 M=1,NUMMAT
000146      READ (5,1001) MTYPE,RO(MTYPE)
000155      IF (MTYPE .GT.NSHELL) GO TO 560
000161      WRITE(6,2011) MTYPE,RO(MTYPE)
000170      READ  (5,1005) (E(J,MTYPE),J=1,7)
000177      WRITE (6,2010) (E(J,MTYPE),J=1,7)
000206      GO TO 59
000207  560 READ(5,1005) (E(J,MTYPE),J=1,5)
000216      WRITE (6,2017)  MTYPE
000224      WRITE(6,2016) (E(J,MTYPE),J=1,5)
000233      CALL PROPS
000234   59 CONTINUE
000237      IF(NREAD.EQ.0.) GO TO 7000
000240      READ(11) R,Z,UR,UZ,CODE,IX,IBC,LBC,PR,NRES,RESID,
     1 RSTRST,STRN,BST,EPS,MTAG,NUMBLK,ND,KN,KS
000313      GO TO 7001
000314 7000 CONTINUE
C
C*****
C     READ AND PRINT OF NODAL POINT DATA
C*****
C
000314      WRITE (6,2004)
000320      L=0
000321   60 READ  (5,1002) N,CODE(N),R(N),Z(N),UR(N),UZ(N)
000344      R(N)=R(N)*SCALE
000345      Z(N)=Z(N)*SCALE
000346      NL=L+1
000347      ZX=N-L
000351      DR=(R(N)-R(L))/ZX
000353      DZ=(Z(N)-Z(L))/ZX
000355   70 L=L+1
000357      IF(N-L) 100,90,80
000362   80 CODE(L)=0.0
000363      R(L)=R(L-1)+DR
000365      Z(L)=Z(L-1)+DZ
000367      UR(L)=0.0
000370      UZ(L)=0.0
000371      GO TO 70
000371   90 WRITE(6,2002) (K,CODE(K),R(K),Z(K),UR(K),UZ(K),K=NL,N)
000415      IF(NUMNP-N) 100,110,60
000420  100 WRITE (6,2009) N
000426      LBAD=1
000427      GO TO 60
000430  110 CONTINUE
000430      NI=NUMNP+1
C*****  TO BE VARIED WITH DIMENSION STATEMENT
000432      DO 111 N=NI,500
000436      UR(N)=0.0
000437  111 UZ(N)=0.0
C*****
C     READ AND PRINT OF ELEMENT PROPERTIES
C*****
000440      WRITE (6,2001)
000444      N=0
000445  130 READ  (5,1003) M,(IX(M,I),I=1,5)
000463  140 N=N+1
000465      IF(M-N) 170,170,150
000473  150 IX(N,1)=IX(N-1,1)+1
000474      IX(N,2)=IX(N-1,2)+1
000475      IX(N,3)=IX(N-1,3)+1
000476      IX(N,4)=IX(N-1,4)+1
000477      IX(N,5)=IX(N-1,5)
000500  170 WRITE(6,2003) N,(IX(N,I),I=1,5)
000516      IF (M-N) 180,180,140
000521  180 IF (NUMEL-N) 190,190,130
000524  190 CONTINUE
C*****
C     READ AND PRINT OF PRESSURE BOUNDARY CONDITION
C*****
000524      IF (NUMPC.EQ. 0) GO TO 310
000525  290 WRITE (6,2005)
000531      DO 300 L=1,NUMPC
000533      READ  (5,1004) IBC(L),JBC(L),PR(L)
000544  300 WRITE(6,2007) IBC(L),JBC(L),PR(L)
000561  310 CONTINUE
C*****
C     READ AND PRINT OF INITIAL DATA FOR THE PROBLEM
C*****
000561      DO 32 N=1,NUMEL
000563      DO 31 I=1,3
000572      RESID(N,I)=0.0
000573   31 CONTINUE
000574   32 CONTINUE
```

```
000576          IF(NRES.EQ.0) GO TO 45
000577          L=0
000600       47 READ  (5,1007) N,(RESID(N,I),I=1,3)
000616          NL=L+1
000620       43 L=L+1
000622          IF(N-L)40,41,42
000624       42 DO 46 I=1,3
000634       46 RESID(L,I)=RESID(L-1,I)
000636          GO TO 43
000637       41 CONTINUE
000637          IF(NUMEL-N) 40,45,47
000642       40 WRITE (6,1008) N
000650          LBAD=1
000651       45 CONTINUE
000651          IF(RCALC.EQ.0.0) GO TO 145
000652          OVB=RO(1)*ACELY
000654          DO 141 N=1,NUMEL
000657          YCEN=0.0
000660          NNOD=4
000661          IF(IX(N,3).EQ.IX(N,4)) NNOD=3
000664          DO 142 I=1,NNOD
000675          J=IX(N,I)
000676      142 YCEN=YCEN+Z(J)
000703          DIV=FLOAT(NNOD)
000704          RESID(N,2)=OVB*(YCEN/DIV-DATUM)
000710          RESID(N,1)=RESID(N,2)*RATIO
000712      141 RESID(N,3)=0.0
000716          NRES=2
000717      145 CONTINUE
            C*****
            C    SOLVE NON-LINEAR STRUCTURE BY SUCCESSIVE APPOXIMATIONS
            C*****
000717          DO 350 N=1,NUMEL
000726          MTAG(N)=1
000727          EPS(N)=0.0
000727          STRN(N,1)=0.0
000730          STRN(N,2)=0.0
000730          STRN(N,3)=0.0
000731          STRN(N,4)=0.0
000731      350 CONTINUE
000733          DO 605 NL=1,NUMEL
000734          DO 605 IJ=1,3
000743          RSTRST(NL,IJ)=0.0
000744      605 CONTINUE
000747          NF=2*NUMNP
000751          DO 505 N=1,NF
000755      505 DST(N)=0.0
000757     7001 CONTINUE
            C*****
            C    DETERMINE BAND WIDTH
            C*****
000757      314 J=0
000760          DO 340 N=1,NUMEL
000762          DO 340 I=1,4
000763          DO 325 L=1,4
000764          KK=IABS(IX(N,I)-IX(N,L))
000772          IF(KK.LE.39) GO TO 315
000774          WRITE (6,2018) N
```

```
001002          LBAD=LBAD+1
001004      315 IF(KK-J) 325,325,320
001007      320 J=KK
001011      325 CONTINUE
001013      340 CONTINUE
001020          MBAND=2*J+2
001022          WRITE (6,2012) MBAND
001027          WRITE (6,2019) LBAD
001035          IF (LBAD.NE.0) STOP
            C*****
            C**** PROVISION FOR EXCAVATION
001040          DO 1500 NS=1,NSTEP
001042          READ(5,1003) NELCUT,MCUT,NBOUN,NFIRST,NLAST,NP
001061          IF(NBOUN.EQ.0) GO TO 901
001062          WRITE(6,3001)
001066          DO 900 NB=1,NBOUN
001070          READ(5,1002)  K,CODE(K),UR(K),UZ(K)
001103          WRITE(6,1002) K,CODE(K),UR(K),UZ(K)
001117      900 CONTINUE
001122      901 IF(NELCUT.EQ.0) GO TO 903
001123          WRITE(6,3002)
001127          READ(5,1003) (NCUT(I),I=1,NELCUT)
001136          WRITE(6,1003)(NCUT(I),I=1,NELCUT)
001145          DO 902 NC=1,NELCUT
001155          M=NCUT(NC)
001156          IX(M,5)=MCUT
001156      902 CONTINUE
001160      903 CONTINUE
            C***** PRINT RESIDUAL STRESSES AT START OF INCREMENT  (NOT FIRST INC.)
001160          IF(NFIRST.GT.1) GO TO 351
001164          WRITE(6,1006)
001167          WRITE(6,1007) (K,(RESID(K,I),I=1,3),K=1,NUMEL)
            C
            C     FORM STIFFNESS MATRIX
            C
001211          CALL STIFF
001212      351 CONTINUE
001212          NN=ND/2
001214          DO 500 NNN=NFIRST,NLAST
001216          IF(NNN.EQ.1) GO TO 352
001220          NB=0
001221      353 NB=NB+1
001223          DO 354 NR=1,NN
001236          K=NN*(NB-1)+NR
001237          KK=2*(NR-1)
001240          B(KK+1)=UR(K)
001241      354 B(KK+2)=UZ(K)
001246          WRITE(8) (B(N),N=1,ND)
001254          IF(NUMBLK-NB)352,352,353
001257      352 CONTINUE
            C
            C     SOLVE FOR DISPLACEMENTS
            C
001257          CALL BANSOL(NNN)
            C
001261          WRITE(6,2006)(N,B(2*N-1),B(2*N),BST(2*N-1),BST(2*N),N=1,NUMNP)
            C     COMPUTE STRESSES
            C
```

```
001307          CALL STRESS
001310          CALL JSTR
001311      500 CONTINUE
001314          IF(NLAST.LT.NP) GO TO 1500
                C**** CUMULATIVE DISPLACEMENTS UPDATED AT END OF INCREMENT
001316          DO 1510 N=1,NF
001323          BST(N)=BST(N)+B(N)
001324      1510 CONTINUE
                C**** SET NODAL LOADS BACK TO ZERO FOR NEXT INCREMENT
001325          DO 1511 N=1,NUMNP
001333          UR(N)=0.0
001334      1511 UZ(N)=0.0
                C****NRES=2 IF RESIDUAL STRESS FOR JOINT IN GLOBAL COORDINATES
001335          NRES=1
001336      1500 CONTINUE
001341          IF(NWRITE.EQ.0) GO TO 5000
001342          WRITE(12)R,Z,UR,UZ,CODE,IX,IBC,LBC,PR,NRES,RESID,
                1 RSTRST,STRN,BST,EPS,MTAG,NUMBLK,ND,KN,KS
001415          WRITE(6,3006)
001421      5000 CONTINUE
001421          IF(NEND.EQ.0) GO TO 50
                C
                C
001422      1000 FORMAT(12A6/4I5,2F10.2,6I5)
001422      1001 FORMAT(I5,F10.0)
001422      1002 FORMAT(I5,F5.0,5F10.0)
001422      1003 FORMAT(6I5)
001422      1004 FORMAT(2I5,F10.0)
001422      1005 FORMAT(7F10.0)
001422      1006 FORMAT (25H1INITIAL STRESSES IN ROCK//8H ELEMENT 4X 9H X-STRESS 6X
                1 9H Y-STRESS 6X 10H XY-STRESS//)
001422      1007 FORMAT (I5,2X,3E15.4)
001422      1008 FORMAT (31H RESIDUAL STRESS INPUT ERROR N= I5)
001422      2000 FORMAT (1H1 12A6/
                    130H0 NUMBER OF NODAL POINTS------ I3 /
                    230H0 NUMBER OF ELEMENTS---------- I3 /
                    330H0 NUMBER OF DIFF  MATERIALS--- I3 /
                    430H0 NUMBER OF PRESSURE CARDS---- I3 /
                    530H0 X-ACCELERATION------------- E12.4/
                    630H0 Y-ACCELERATION------------- E12.4/
                    7 30H0 NUMBER OF APPROXIMATIONS----    I3/
                    8 30H0 JOINT CUT OFF NUMBER--------   I3 )
001422      2001 FORMAT (49H1ELEMENT NO.     I     J     K     L    MATERIAL    )
001422      2002 FORMAT (I12, F12.2, 2F12.3, 2E24.7)
001422      2003 FORMAT (1I13,4I6,1I12)
001422      2004 FORMAT (1H8H1NODAL POINT        TYPE   X-ORDINATE  Y-ORDINATE X LO
                1AD OR DISPLACEMENT  Y LOAD OR DISPLACEMENT                )
001422      2005 FORMAT (29H0PRESSURE BOUNDARY CONDITIONS/ 24H      I     J   PRESS
                1URE )
001422      2006 FORMAT(1H1,11HN.P. NUMBER,18X,2HUX,18X,2HUY,17X,4HCUMX,17X,
                1 4HCUMY, /(1I12,4E20.7))
001422      2007 FORMAT (2I6,F12.3)
001422      2008 FORMAT(*0NODAL POINT  X DISPLACEMENT       Y DISPLACEMENT      CUM
                1 X DISPLACEMENT  CUM Y DISPLACEMENT*)
001422      2009 FORMAT (25H0NODAL POINT CARD ERROR N= I5)
001422      2010 FORMAT(20X,12HCOMP MODULUS,3X,14HPOISSONS RATIO,3X,
                1  12HTENS MODULUS  ,/(F15.5,6E15.5))
001422      2011 FORMAT (17H0MATERIAL NUMBER= I3, 15H, MASS DENSITY= E12.4)
001422      2012 FORMAT (/6HMBAND= I5 /)
001422      2016 FORMAT (*0       KN              KT              C            PHI
                1       MAX.CLOSURE   */ 5E15.4 )
001422      2017 FORMAT (1H010X,16H MATERIAL NUMBERI5)
001422      2018 FORMAT (24H ELEMENT CARD ERROR  N=  I4)
001422      2019 FORMAT (* LOAD =* I5)
001422      2030 FORMAT(*  PLANE STRAIN ANALYSIS OF JOINTED STRUCTURES *)
001422      2031 FORMAT(*  PLANE STRESS ANALYSIS OF JOINTED STRUCTURES *)
001422      3001 FORMAT(1H0,13HNODES ALTERED )
001422      3002 FORMAT(1H0,18HELEMENTS EXCAVATED  )
001422      3005 FORMAT(1H0,*  SCALE FACTOR = *,E12.4,//
                1 *  RESIDUAL STRESS CALCULATION. RCALC= *,F5.0,*  DATUM= *,E12.4
                2 ,*RATIO= *,E12.4,//)
001422      3006 FORMAT(1H0,30H RESULTS WRITTEN ONTO TAPE       )
001422          STOP
001424          END

UNUSED COMPILER SPACE
012300
```

```
                SUBROUTINE PROPS
000001          COMMON /MAT/ SHEAR(4,10),ORATIO(4,10),DILTN(4,10),DINC(4),FINC(4)
               1 ,SNJNT(4,10)
000001          READ(5,1000) J
000007          READ(5,1001) DINC(J),FINC(J)
000017          WRITE(6,2001) J,DINC(J),FINC(J)
000031          READ(5,1002)  (SHEAR(J,I),I=1,10)
000044          WRITE(6,2002) (SHEAR(J,I),I=1,10)
000057          READ(5,1002)  (ORATIO(J,I),I=1,10)
000072          WRITE(6,2003) (ORATIO(J,I),I=1,10)
000105          READ(5,1002)  (DILTN(J,I),I=1,10)
000120          WRITE(6,2004) (DILTN(J,I),I=1,10)
000133          READ(5,1002) (SNJNT(J,I),I=1,10)
000146          WRITE(6,2005) (SNJNT(J,I),I=1,10)
000161        1 CONTINUE
000161     1000 FORMAT(I5)
000161     1001 FORMAT(2F10.0)
000161     1002 FORMAT(10F5.0)
000161     2001 FORMAT( 10X,* JOINT TYPE *,I5,*  DILATATION CONSTANT * ,E12.4,
               1 *  NORMAL STRESS INCREMENT * ,E12.4 )
000161     2002 FORMAT( *  SHEAR STRENGTH AT UNIT INTERVALS OF DISPLACEMENT * /
               1 10F10.3)
000161     2003 FORMAT( * DILATATION AND NORMAL DISPLACEMENT RATIO  */,10F10.3)
000161     2004 FORMAT(*  DILATATION AT UNIT INTERVALS OF SHEAR DISPLACEMENT *
               1 / 10F10.3)
000161     2005 FORMAT(*  NORMAL DISPLACEMENT AT NORMAL STRESS INCREMENTS *,
               1  /,10E10.3)
000161          RETURN
000162          END

UNUSED COMPILER SPACE
017500
```

```
                SUBROUTINE STIFF
000001          COMMON NUMNP,NUMEL,NUMMAT,NUMPC,ACELX,ACELY,N,VOL,NRES,MTYPE,
               1 HED(12),E(8,12),RO(12),XXNN(12),R(500),Z(500),UR(500),UZ(500),
               2 CODE(500),IBC(200),JBC(200),PR(200),ANGLE(4),LBAD,NNN,NP,
               3 EPS(400),NSHELL,RSTRST(400,3),KN(400),KS(400)
000001          COMMON /ARG/ RRR(5),ZZZ(5),S(10,10),P(10),IT(4),LM(4),JD(6,3),
               1 HH(6,10),RR(4),ZZ(4),C(4,4),H(6,10),D(6,6),F(6,10),TP(6),XI(10)
               2,EE(7),IX(400,5),MTAG(400),RSTRS(4),RESID(400,3)
000001          COMMON /BANARG/ MBAND,NUMBLK,B(160),A(160,80),ND
000001          COMMON /EXC/ NCUT(100),NONEX
      C*****
      C     INITIALIZATION
      C*****
000001          REWIND 8
000003          REWIND 10
000005          NB =  40
      C****NB IS CONTROLLED BY COMPUTER BANDWIDTH
      C****   DIMENSIONS OF A AND B MUST CORRESPOND
000006          ND=2*NB
000010          ND2=2*ND
000011          LBAD=0
000012          NUMBLK=0
000013          DO 50 N=1,ND2
000015          B(N)=0.0
000016          DO 50 M=1,ND
000026       50 A(N,M)=0.0
      C*****
      C     FORM STIFFNESS MATRIX IN BLOCKS
      C*****
000033       60 NUMBLK=NUMBLK+1
000034          NH=NB*(NUMBLK+1)
000036          NM=NH-NB
000037          NL=NM-NB+1
000040          KSHIFT=2*NL-2
000043          DO 210 N=1,NUMEL
      C***BYEPASS STATEMENTS FOR NON-EXISTANT ELEMENTS
000044          IF(IX(N,5).EQ.NONEX) GO TO 210
000046          IF (IX(N,5)) 210,210,65
000050       65 DO 80 I=1,4
000052          IF (IX(N,I)-NL) 80,70,70
000056       70 IF (IX(N,I)-NH) 90,90,80
000063       80 CONTINUE
000065          GO TO 210
000066       90 IF (IX(N,5) .LE. NSHELL) GO TO 92
000071          CALL JTSTIF
000072          GO TO 165
000073       92 CALL QUAD
000074          IX(N,5)=-IX(N,5)
000076          IF (VOL.LE.0.) LBAD=1
000101          IF (VOL.GT. 0.) GO TO 144
000104          WRITE (5,2003) N
000111      144 IF (IX(N,3).EQ.IX(N,4)) GO TO 165
000114      145 DO 150 II=1,9
000117          CC=S(II,10)/S(10,10)
000121          P(II)=P(II)-CC*P(10)
000123          DO 150 JJ=1,9
000134      150 S(II,JJ)=S(II,JJ)-CC*S(10,JJ)
000141          DO 160 II=1,8
```

```
000144          CC=S(II,9)/S(9,9)
000146          P(II)=P(II)-CC*P(9)
000150          DO 160 JJ=1,8
000161      160 S(II,JJ)=S(II,JJ)-CC*S(9,JJ)
            C******ADD ELEMENT STIFFNESS TO TOTAL STIFFNES****
000166      165 DO 166 I=1,4
000177      166 LM(I)=2*IX(N,I)-2
000201          DO 200 I=1,4
000203          DO 200 K=1,2
000204          II=LM(I)+K-KSHIFT
000206          KK=2*I-2+K
000210          B(II)=B(II)+P(KK)
000214          DO 200 J=1,4
000215          DO 200 L=1,2
000216          JJ=LM(J)+L-II+1-KSHIFT
000222          LL=2*J-2+L
000224          IF(JJ) 200,200,175
000226      175 IF(ND-JJ) 180,195,195
000231      180 WRITE (6,2004)  N
000237          LBAD = 1
000240          GO TO 210
000241      195 A(II,JJ)=A(II,JJ)+S(KK,LL)
000250      200 CONTINUE
000260      210 CONTINUE
000263          IF(LBAD.NE.0) GO TO 475
            C*****ADD CONCENTRATED FORCES WITHIN BLOCK *****
000264          DO 250 N=NL,NM
000275          K=2*N-KSHIFT
000277          B(K)=B(K)+UZ(N)
000301      250 B(K-1)=B(K-1)+UR(N)
            C***** BOUNDARY CONDITIONS *****
            C***        1.PRESSURE B.C.    ***
000304          IF (NUMPC) 260,310,260
000305      260 DO 300 L=1,NUMPC
000307          I=IBC(L)
000312          J=JBC(L)
000313          PP=PR(L)/2.0
000315          DZ=(Z(I)-Z(J))*PP
000320          DR=(R(J)-R(I))*PP
000323      264 II=2*I-KSHIFT
000325          JJ=2*J-KSHIFT
000326          IF (II) 280,280,265
000330      265 IF (II-ND) 270,270,280
000333      270 SINA=0.0
000334          COSA=1.0
000335          IF (CODE(I)) 271,272,272
000340      271 SINA=SIN(CODE(I))
000342          COSA=COS(CODE(I))
000347      272 B(II-1)=B(II-1)+(COSA*DZ+SINA*DR)
000354          B(II)=B(II)-(SINA*DZ-COSA*DR)
000356      280 IF(JJ) 300,300,285
000360      285 IF(JJ-ND) 290,290,300
000363      290 SINA=0.0
000364          COSA=1.0
000365          IF (CODE(J))291,292,292
000370      291 SINA=SIN(CODE(J))
000372          COSA=COS(CODE(J))
000377      292 B(JJ-1)=B(JJ-1)+(COSA*DZ+SINA*DR)
000404          B(JJ)=B(JJ)-(SINA*DZ-COSA*DR)
000406      300 CONTINUE
            C***        2. DISPLACEMENT B.C.
000411      310 DO 400 M=NL,NH
000413          IF (M-NUMNP) 315,315,400
000415      315 U=UR(M)
000417          N=2*M-1-KSHIFT
000421          IF (CODE(M)) 390,400,316
000423      316 IF (CODE(M)-1.) 317,370,317
000426      317 IF (CODE(M)-2.) 318,390,318
000431      318 IF (CODE(M)-3.) 390,380,390
000434      370 CALL MODIFY(A,B,ND2,MBAND,N,U)
000440          GO TO 400
000441      380 CALL MODIFY(A,B,ND2,MBAND,N,U)
000445      390 U=UZ(M)
000447          N=N+1
000451          CALL MODIFY(A,B,ND2,MBAND,N,U)
000455      400 CONTINUE
            C***** WRITE BLOCK OF EQUATIONS ON TAPE AND SHIFT UP LOWER BLOCK *****
000460          WRITE(8) ((A(N,M),M=1,MBAND),N=1,ND)
000477          WRITE(8) (B(N),N=1,ND)
            C**** TRANSFER B VECTOR INTO UR,UZ ONE BLOCK AT THE TIME
000505          DO 419 N=NL,NM
000515          K=2*N-KSHIFT
000517          UZ(N)=B(K)
000520      419 UR(N)=B(K-1)
000523          DO 420 N=1,ND
000525          K=N+ND
000526          B(N)=B(K)
000527          B(K)=0.0
000531          DO 420 M=1,ND
000543          A(N,M)=A(K,M)
000544      420 A(K,M)=0.0
            C***** CHECK FOR LAST BLOCK   *****
000550      475 IF(NM-NUMNP) 60,480,480
000553      480 CONTINUE
000553          IF (LBAD .EQ. 0) GO TO 500
000554          WRITE (6,2005) LBAD
000562          STOP
000564      500 RETURN
000565     2003 FORMAT (26HONEGATIVE AREA ELEMENT NO. I4)
000565     2004 FORMAT (29HOBAND WIDTH EXCEEDS ALLOWABLE I4)
000565     2005 FORMAT ( * LABO= *I5)
000565          END

UNUSED COMPILER SPACE
015300
```

```
            SUBROUTINE QUAD
000001      COMMON NUMNP,NUMEL,NUMMAT,NUMPC,ACELX,ACELY,N,VOL,NRES,MTYPE,
           1 HED(12),E(8,12),RD(12),XXNN(12),R(500),Z(500),UR(500),UZ(500),
           2 CODE(500),IBC(200),JBC(200),PR(200),ANGLE(4),LBAD,NNN,NP,
           3 EPS(400),NSHELL,RSTRST(400,3),KN(400),KS(400)
000001      COMMON /ARG/ RRR(5),ZZZ(5),S(10,10),P(10),TT(4),LM(4),DD(3,3),
           1 HH(6,10),RR(4),ZZ(4),C(4,4),H(6,10),D(6,6),F(6,10),TP(6),XI(10)
           2,EE(7),IX(400,5),MTAG(400),RSTRS(4),RESID(400,3)
000001      COMMON /BANARG/ MBAND,NUMBLK,B(160),A(160,80),ND
000001      COMMON /TEN/ HRES(3,10)
000001      COMMON /PLN/ PLANE
000001      I=IX(N,1)
000003      J=IX(N,2)
000004      K=IX(N,3)
000006      L=IX(N,4)
000007      MTYPE=IX(N,5)
      C*****  FORM STRESS STRAIN RELATIONSHIP FOR PLAIN STRAIN *****
000011      DO 105 KK=1,7
000020    105 EE(KK)=E(KK+1,MTYPE)
000022      IF (MTAG(N)-2) 82,84,83
000025     82 EE(3)=EE(1)
000027      GO TO 84
000027     83 EE(1)=EE(3)
000033     84 EE(1)=EE(1)/(1.-EE(2)**2)
000035      EE(3)=EE(3)/(1.-EE(2)**2)
000037      EE(2)=EE(2)/(1.-EE(2))
000041      XX=EE(1)/EE(3)
000042      COMM=EE(1)/(XX-EE(2)**2)
000045      C(1,1)=COMM*XX
000045      C(1,2)=COMM*EE(2)
000046      C(1,3)=0.0
000050      C(2,1)=C(1,2)
000050      C(2,2)=COMM
000051      C(2,3)=0.0
000052      C(3,1)=0.0
000053      C(3,2)=0.0
000053      C(3,3)=.5*EE(1)/(XX+EE(2))
000057      SS=SIN(EPS(N))
000061      CC=COS(EPS(N))
000067      S2=SS*SS
000070      C2=CC*CC
000071      SC=SS*CC
000071      D(1,1)=S2
000072      D(1,2)=C2
000073      D(1,3)=0.0
000074      D(1,4)=-SC
000075      D(2,1)=C2
000076      D(2,2)=S2
000076      D(2,3)=0.0
000077      D(2,4)=SC
000100      D(3,1)=2.*SC
000102      D(3,2)=-D(3,1)
000103      D(3,3)=0.0
000103      D(3,4)=-C2+S2
000105      DO 88 II=1,3
000106      DO 88 JJ=1,4
000107      H(II,JJ)=0.0
000112      DO 88 KK=1,3
000124        H(II,JJ)=H(II,JJ)+C(II,KK)*D(KK,JJ)
000126     88 CONTINUE
000133        DO 89 II=1,4
000135        DO 89 JJ=1,4
000136        C(II,JJ)=0.0
000140        DO 89 KK=1,3
000154        C(II,JJ)=C(II,JJ)+D(KK,II)*H(KK,JJ)
000156     89 CONTINUE
      C*****
      C    REPLACE RESIDUAL STRESS FOR NTH ELEMENT BY RSTRS(IJ)
      C*****
000163        IF(NRES.EQ.0) GO TO 112
000164        DO 111 IJ=1,3
000175    111 RSTRS(IJ)=RESID(N,IJ)+RSTRST(N,IJ)
000200        GO TO 114
000200    112 DO 113 IJ=1,3
000205    113 RSTRS(IJ)=0.0
000214    114 RSTRS(4)=RSTRS(3)
      C***** FORM QUADRILATERAL STIFFNESS MATRIX *****
000215        RRR(5)=(R(I)+R(J)+R(K)+R(L))/4.0
000221        ZZZ(5)=(Z(I)+Z(J)+Z(K)+Z(L))/4.0
000225        DO 94 M=1,4
000226        MM=IX(N,M)
000232     93 RRR(M)=R(MM)
000235     94 ZZZ(M)=Z(MM)
000240        DO 100 II=1,10
000241        P(II)=0.0
000242        DO 95 JJ=1,6
000251     95 HH(JJ,II)=0.0
000253        DO 96 JJ=1,3
000260     96 HRES(JJ,II)=0.0
000262        DO 100 JJ=1,10
000270    100 S(II,JJ)=0.0
000274        DO 119 II=1,4
000304        JJ=IX(N,II)
000305    119 ANGLE(II)=CODE(JJ)/57.3
      C*****  FORM BAR STIFFNESS *****
000311        IF (IX(N,2)-IX(N,3)) 250,240,250
000315    240 TT(1)=-EE(6)
000316        TT(2)=-EE(6)
000317        DR=R(J)-R(I)
000321        DZ=Z(J)-Z(I)
000324        XL=SQRT(DR**2+DZ**2)
000337        RRR(5)=(R(I)-R(J))/2.-2.*EE(4)*DZ/XL
000343        ZZZ(5)=(Z(I)+Z(J))/2.+2.*EE(4)*DR/XL
000351        CALL TRISTF(1,2,5)
000353        GO TO 130
000354    250 CONTINUE
000354        IF (K.NE. L) GO TO 125
000356    120 CALL TRISTF(1,2,3)
000361        RRR(5)=(RRR(1)+RRR(2)+RRR(3))/3.0
000365        ZZZ(5)=(ZZZ(1)+ZZZ(2)+ZZZ(3))/3.0
000370        VOL=XI(1)
000372        IF(VOL.GT.0.) GO TO 130
000374        WRITE (6,1000) N
000401        RETURN
000402    125 VOL=0.0
000403        CALL TRISTF(4,1,5)
```

```
000406          CALL TPISTF(1,2,5)
000411          CALL TRISTF(2,3,5)
000414          CALL TRISTF(3,4,5)
000417          IF(VOL.GT. 0.) GO TO 126
000422          WRITE (6,1000) N
000427      126 DO 140 II=1,6
000431          DO 140 JJ=1,10
000440          HH(II,JJ)=HH(II,JJ)/4.0
000441      140 CONTINUE
000444      130 CONTINUE
000444          WRITE(10) RRR,ZZZ,C,HH,S,P,VOL,HPES
000467          RETURN
000470     1000 FORMAT (* NEGATIVE AREA ,ELEMENT NO.* I5)
000470     2001 FORMAT (1H ,4E12.4)
000470          END

UNUSED COMPILER SPACE
015500
```

```
                SUBROUTINE TRISTF(II,JJ,KK)
000005          COMMON NUMNP,NUMEL,NUMMAT,NUMPC,ACELX,ACELY,N,VOL,NRES,MTYPE,
                1 HED(12),E(8,12),RO(12),XXNN(12),P(500),Z(500),UR(500),UZ(500),
                2 CODE(500),IBC(200),JBC(200),PR(200),ANGLE(4),LBAD,NNN,NP,
                3 EPS(400),NSHELL,RSTRST(400,3),KN(400),KS(400)
000005          COMMON /ARG/ RRR(5),ZZZ(5),S(10,10),P(10),TT(4),LM(4),DD(3,3),
                1 HH(6,10),RR(4),ZZ(4),C(4,4),H(6,10),D(6,6),F(6,10),TP(6),XI(10)
                2,EE(7),IX(400,5),MTAG(400),RSTRS(4),RESID(400,3)
000005          COMMON /BANARG/ MBAND,NUMBLK,B(160),A(160,80),ND
000005          COMMON /TEN/ HRES(3,10)
                C       1. INITIALIZATION
                C
000010          LM(1)=II
000010          LM(2)=JJ
000011          LM(3)=KK
                C
000012          RR(1)=RRR(II)
000014          RR(2)=RRR(JJ)
000015          RR(3)=RRR(KK)
000017          RR(4)=RRR(II)
000017          ZZ(1)=ZZZ(II)
000021          ZZ(2)=ZZZ(JJ)
000022          ZZ(3)=ZZZ(KK)
000024          ZZ(4)=ZZZ(II)
                C
000025       85 DO 100 I=1,6
000027          DO 90 J=1,10
000036          F(I,J)=0.0
000037       90 H(I,J)=0.0
000040          DO 100 J=1,6
000050      100 D(I,J)=0.0
                C
                C       3. FORM INTEGRAL(G)T*(C)*(G)
                C
000056          COMM=RR(2)*(ZZ(3)-ZZ(1))+RR(1)*(ZZ(2)-ZZ(3))+RR(3)*(ZZ(1)-ZZ(2))
000066          XI(1)=COMM/2.0
000067          IF(XI(1).GT.0.0) GO TO 102
000072          WRITE(6,1000) II,JJ,KK,N
000105          LBAD=1
000106          RETURN
000107      102 CONTINUE
000107          VOL=VOL+XI(1)
                C
000111      107 D(2,2)=XI(1)*C(1,1)
000113          D(2,6)=XI(1)*C(1,2)
000114          D(3,3)=XI(1)*C(4,4)
000116          D(3,5)=XI(1)*C(4,4)
000120          D(5,5)=XI(1)*C(4,4)
000121          D(6,6)=XI(1)*C(2,2)
                C
000123      108 DO 110 I=1,6
000125          DO 110 J=I,6
000135      110 D(J,I)=D(I,J)
                C
                C       4. FORM COEFFICIENT-DISPLACEMENT TRANSFORMATION MATRIX
                C
000144          DD(1,1)=(RR(2)*ZZ(3)-RR(3)*ZZ(2))/COMM
000147          DD(1,2)=(RR(3)*ZZ(1)-RR(1)*ZZ(3))/COMM
```

```
000154          DD(1,3)=(RR(1)*ZZ(2)-RR(2)*ZZ(1))/COMM
000160          DD(2,1)=(ZZ(2)-ZZ(3))/COMM
000162          DD(2,2)=(ZZ(3)-ZZ(1))/COMM
000164          DD(2,3)=(ZZ(1)-ZZ(2))/COMM
000165          DD(3,1)=(RR(3)-RR(2))/COMM
000170          DD(3,2)=(RR(1)-RR(3))/COMM
000172          DD(3,3)=(RR(2)-RR(1))/COMM
        C
000175          DO 120 I=1,3
000215          J=2*LM(I)-1
000217          H(1,J)=DD(1,I)
000220          H(2,J)=DD(2,I)
000224          H(3,J)=DD(3,I)
000230          H(4,J+1)=DD(1,I)
000234          H(5,J+1)=DD(2,I)
000237      120 H(6,J+1)=DD(3,I)
        C
        C       ROTATE UNKNOWNS IF REQUIRED
        C
000251          DO 125 J=1,2
000254          I=LM(J)
000255          IF (ANGLE(I)) 122,125,125
000260      122 SINA=SIN(ANGLE(I))
000263          COSA=COS(ANGLE(I))
000266          IJ=2*I
000270          DO 124 K=1,6
000303          TEM=H(K,IJ-1)
000304          H(K,IJ-1)=TEM*COSA+H(K,IJ)*SINA
000306      124 H(K,IJ)= -TEM*SINA+H(K,IJ)*COSA
000313      125 CONTINUE
        C
        C         5. FORM ELEMENT STIFFNESS MATRIX (H)T*(D)*(H)
        C
000315          DO 130 J=1,10
000317          DO 130 K=1,6
000320          IF (H(K,J)) 128,130,128
000323      128 DO 129 I=1,6
        C
000341      129 F(I,J)=F(I,J)+D(I,K)*H(K,J)
000346      130 CONTINUE
000352          DO 140 K=1,6
000354          DO 140 I=1,10
000355          IF (H(K,I)) 138,140,138
000360      138 DO 139 J=1,10
000375      139 S(I,J)=S(I,J)+H(K,I)*F(K,J)
000402      140 CONTINUE
        C
        C
        C     FORM RESIDUAL LOAD MATRIX
        C
000406      150 DO 160 I=1,10
000426      160 P(I)=P(I)+XI(1)*H(2,I)*(     -RSTRS(1))
                1          +XI(1)*H(6,I)*(     -RSTRS(2))
                2          +XI(1)*H(3,I)*(     -RSTRS(3))
                3          +XI(1)*H(5,I)*(     -RSTRS(3))
000442           DO 165 I=1,10
000464           HRES(1,I)=HRES(1,I)+H(2,I)*XI(1)
000470           HRES(2,I)=HRES(2,I)+H(6,I)*XI(1)
000472      165 HRES(3,I)=HRES(3,I)+(H(3,I)+H(5,I))*XI(1)
        C
        C       ACCELERATION LOADS
        C
000505          COMM=RO(MTYPE)*XI(1)/3.0
000510          DO 170 I=1,3
000524          J=2*LM(I)-1
000526          P(J)=P(J)-ACELX*COMM
000530      170 P(J+1)=P(J+1)-ACELY*COMM
        C
        C       FORM STRAIN TRANSFORMATION MATRIX
        C
000535      400 DO 410 I=1,6
000537          DO 410 J=1,10
000546      410 HH(I,J)=HH(I,J)+H(I,J)
        C
000555      415 RETURN
000556     1000 FORMAT(28HZERO OR NEGATIVE AREA, TRI.    3I4,11HELEMENT NO. I5)
        C
000556          END

UNUSED COMPILER SPACE
015500
```

```
                SUBROUTINE JTSTIF
000001          COMMON NUMNP,NUMEL,NUMMAT,NUMPC,ACELX,ACELY,N,VOL,NRES,MTYPE,
               1 ME0(12),E(6,12),RO(12),XXNN(12),R(500),Z(500),UR(500),UZ(500),
               2 CODE(500),IBC(200),JBC(200),PR(200),ANGLE(4),LBAD,NNN,NP,
               3 EPS(400),NSHELL,RSTRST(400,3),KN(400),KS(400)
000001          COMMON /ARG/ RRR(5),ZZZ(5),S(10,10),P(10),TT(4),LM(4),DD(3,3),
               1 HH(6,10),RR(4),ZZ(4),C(4,4),H(6,10),D(6,6),F(6,10),TP(6),XI(10)
               2,EE(7),IX(400,5),MTAG(400),RSTRS(4),RESID(400,3)
000001          COMMON /CUM/ BST(1000),STRN(400,4),NS
000001          DIMENSION A(4,4),TR(2,2),ESTIF(10,10),PPP(8)
000001          EQUIVALENCE(S(10,10),ESTIF(10,10))
000001          DATA A/2.,1.,-1.,-2.,1.,2.,-2.,-1.,-1.,-2.,2.,1.,-2.,-1.,1.,2./
000001          REAL KS,KN,L
000001          II=IX(N,1)
000003          JJ=IX(N,2)
000004          DR=R(JJ)-R(II)
000007          DZ=Z(JJ)-Z(II)
000012          L=SQRT(DR*DR+DZ*DZ)
000015          IF(L.EQ.0.) GO TO 201
000020          MAT=IX(N,5)
000021          IX(N,5)=-IX(N,5)
          C***  MATERIAL PROPERTIES ****
000022          IF(NNN.GT.1) GO TO 50
000031          KN(N)=E(1,MAT)
000031          KS(N)=E(2,MAT)
000036       50 COMS=KS(N)*L/6.
000037          COMN=KN(N)*L/6.
          C***  INITIALIZE ****
000041          DO 100 II=1,8
000043          P(II)=0.0
000044          DO 100 JJ=1,8
000053      100 ESTIF(II,JJ)=0.0
          C***  DEVELOP RESIDUAL STRESS CONTRIBUTIONS TO THE LOAD VECTOR
          C******
          C THE FOLLOWING SIGN CONVENTION IS ADOPTED.THE NORMAL STRESS IS POSITIVE
          C WHEN DIRECTED OUTWARDS THE ELEMENT ON THE FACE(II,JJ).THE SHEAR STRESS
          C IS POSITIVE WHEN DIRECTED FROM IT TO JJ AND KK TO LL INSIDE THE ELEMT.
          C BESIDES,AND FOR EXAMPLE,S2 IS THE SQUARE OF THE COSINE OF THE ANGLE
          C BETWEEN THE GLOBAL X DIRECTION AND THE LOCAL NORMAL STRESS DIRECTION.
000061          SC=(DR*DZ)/(L**2)
000063          S2=(DZ/L)**2
000064          C2=(DR/L)**2
000065          IF(NPES.EQ.2) GO TO 112
000072      111 RSTRS(1)=RESID(N,1)
               1 +RSTRST(N,1)+KN(N)*STRN(N,1)
000075          RSTRS(2)=RESID(N,3)
               1 +RSTRST(N,3)
000100          GO TO 113
000103      112 RSTRS(1)=RESID(N,1)*S2+RESID(N,2)*C2+2.*RESID(N,3)*SC
000110          RSTRS(2)=(RESID(N,2)-RESID(N,1))*SC+RESID(N,3)*(S2-C2)
000115      113 CONTINUE
000115          DO 160 I=1,4
000132          J=2*I-1
000134          PPP(J)=L*RSTRS(1)/2.
000134          J=2*I
000136      160 PPP(J)=-L*RSTRS(2)/2.
000141          DO 161 I=1,4
000145      161 PPP(I)=-PPP(I)
000147          DO 200 II=1,4
000150          IS=2*II-1
000151          IN=2*II
000153          DO 200 JJ=1,4
000163          JS=2*JJ-1
000165          JN=2*JJ
000166          ESTIF(IS,JS)=COMS*A(II,JJ)
000172      200 ESTIF(IN,JN)=COMN*A(II,JJ)
          C***  ROTATE GLOBAL COORDINATES
000207          TR(1,1)=DR/L
000210          TR(1,2)=DZ/L
000211          TR(2,1)=-DZ/L
000211          TR(2,2)=DR/L
000212          IF(TR(1,1).EQ.1.) GO TO 405
000215          DO 400 NN=1,4
000216          DO 410 II=1,8
000221          JJ=2*NN-1
000223          TEMP=ESTIF(II,JJ)
000227          DO 410 KK=1,2
000243          ESTIF(II,JJ)=TEMP*TR(1,KK)+ESTIF(II,2*NN)*TR(2,KK)
000250      410 JJ=JJ+1
000256          DO 420 II=1,8
000262          JJ=2*NN-1
000264          TEMP=ESTIF(JJ,II)
000267          DO 420 KK=1,2
000305          ESTIF(JJ,II)=TR(1,KK)*TEMP+TR(2,KK)*ESTIF(2*NN,II)
000310      420 JJ=JJ+1
000316      400 CONTINUE
000320      405 CONTINUE
000320          DO 401 I=1,4
000330          J=2*I-1
000332          II=2*I
000334          P(J)=PPP(J)*TR(1,2)+PPP(II)*TR(2,2)
000337      401 P(II)=-PPP(J)*TR(2,2)+PPP(II)*TR(1,2)
000345          RETURN
000345      201 WRITE(6,2090) N
000353          RETURN
000354     2000 FORMAT(10E12.3)
000354     2090 FORMAT(14H BAD JOINT,N= I3/)
000354          END

UNUSED COMPILER SPACE
016300
```

```
            SUBROUTINE MODIFY(A,B,NEQ,MBAND,N,U)
000010      DIMENSION A(160,80), B(160)
000010      DO 250 M=2,MBAND
000011      K=N-M+1
000012      IF(K) 235,235,230
000020  230 B(K)=B(K)-A(K,M)*U
000021      A(K,M)=0.0
000026  235 K=N+M-1
000030      IF(NEQ-K) 250,240,240
000036  240 B(K)=B(K)-A(N,M)*U
000040      A(N,M)=0.0
000044  250 CONTINUE
000047      A(N,1)=1.0
000051      B(N)=U
000052      RETURN
000053      END

UNUSED COMPILER SPACE
020100
```

```
            SUBROUTINE BANSOL(NNN)
000002      COMMON /BANARG/     MM,NUM3LK,B(160),A(160,80),NN
000002      NTAPE=9
000003      IF(NNN.EQ.1) NTAPE=8
000006      NL=NN+1
000007      NH=NN+NN
000010      NB=0
000012      REWIND 7
000014      REWIND 8
000016      REWIND 9
          C**** 7 FOR REDUCED B MATRIX
          C**** 8 FOR NEW B MATRIX - A MATRIX ON FIRST RUN
          C**** 9 FOR REDUCED A MATRIX
000020      GO TO 150
          C     REDUCE EQUATIONS BY BLOCKS
          C    1. SHIFT UP BLOCK OF EQUATIONS
000021    100 NB=NB+1
000023      DO 125 N=1,NN
000025      NM=NN+N
000026      B(N)=B(NM)
000027      B(NM)=0.0
000031      DO 125 M=1,MM
000043      A(N,M)=A(NM,M)
000044    125 A(N,M)=0.0
          C    2.  READ NEXT BLOCK INTO CORE
000051      IF(NUMBLK-NB) 150,200,150
000053    150 READ(NTAPE) ((A(N,M),M=1,MM),N=NL,NH)
000073      READ(8) (B(N),N=NL,NH)
000103      IF(NB) 200,100,200
          C     3. REDUCE BLOCK OF EQUATIONS
000105    200 IF(NTAPE-8) 202,202,201
          C**** REDUCE A AND B IN FIRST PASS
000110    202 DO 300 N=1,NN
000112      IF(A(N,1)) 225,300,225
000113    225 DO 275 L=2,MM
000115      IF(A(N,L)) 230,275,230
000124    230 C=A(N,L)/A(N,1)
000125      I=N+L-1
000127      J=0
000130      DO 250 K=L,MM
000142      J=J+1
000143    250 A(I,J)=A(I,J)-C*A(N,K)
000150      A(N,L)=C
000155    275 CONTINUE
000160    300 CONTINUE
000163    375 WRITE(9) ((A(N,M),M=1,MM),N=1,NN)
          C**** REDUCE B ONLY SUBSEQUENT PASSES
000204    201 DO 301 N=1,NN
000206      IF(A(N,1).EQ.0.0) GO TO 301
000207      DO 276 L=2,MM
000221      IF(A(N,L).EQ.0.0) GO TO 276
000222      I=N+L-1
000224      B(I)=B(I)-A(N,L)*B(N)
000226    276 CONTINUE
000231      B(N)=B(N)/A(N,1)
000234    301 CONTINUE
000237      IF(NUMBLK-NB) 376,400,376
000241    376 WRITE(7) (B(N),N=1,NN)
```

```
G1O
000247          GO TO 100
              C***** BACK SUBSTITUTION
000251        400 BACKSPACE 9
000253        402 DO 450 M=1,NN
000255            N=NN+1-M
000257            DO 425 K=2,MM
000270            L=N+K-1
000272        425 B(N)=B(N)-A(N,K)*B(L)
000276            NM=N+NN
000277            B(NM)=B(N)
000304        450 A(NM,NB)=B(N)
000313            NB=NB-1
000314            IF(NB) 475,500,475
000314        475 BACKSPACE 7
000316            BACKSPACE 9
000320            READ(7) (B(N),N=1,NN)
000326            READ(9) ((A(N,M),M=1,MM),N=1,NN)
000347            BACKSPACE 9
000352            BACKSPACE 7
000354            GO TO 402
              C**** ORDER UNKNOWNS IN B ARRAY
000355        500 K=0
000356            DO 600 NB=1,NUMBLK
000360            DO 600 N=1,NN
000370            K=K+1
000371            NM=N+NN
000371            B(K)=A(NM,NB)
000372        600 CONTINUE
              C**** REWIND 8 READY FOR NEW BLOCKS OF B
000401            REWIND 8
000403            RETURN
000404            END

UNUSED COMPILER SPACE
017000
```

```
                  SUBROUTINE STRESS
000001            COMMON NUMNP,NUMEL,NUMMAT,NUMPC,ACELX,ACELY,N,VOL,NRES,MTYPE,
                 1 HED(12),E(8,12),RO(12),XXNN(12),R(500),Z(500),UR(500),UZ(500),
                 2 CODE(500),IBC(200),JBC(200),PR(200),ANGLE(4),LBAD,NNN,NP,
                 3 EPS(400),NSHELL,RSTRST(400,3),KN(400),KS(400)
000001            COMMON /ARG/ RRR(5),ZZZ(5),S(10,10),P(10),TT(4),LM(4),DD(3,3),
                 1 HH(6,10),RR(4),ZZ(4),C(4,4),H(6,10),D(6,6),F(6,10),TP(6),XI(10)
                 2,EE(7),IX(400,5),MTAG(400),RSTRS(4),RESID(400,3)
000001            COMMON /BANARG/ MBAND,NUMBLK,B(160),A(160,80),ND
000001            COMMON /CUM/ BST(1000),STRN(400,4),NS
000001            COMMON /EXC/ NOUT(100),NONEX
000001            DIMENSION HRES(3,10),SIG(10),STR(3)
000001            REWIND 10
              C     COMPUTED ELEMENT STRESSES
              C****
000003            MPRINT=0
000004            DO 300 M=1,NUMEL
000006            N=M
000010            IX(N,5)=IABS(IX(N,5))
000012            MTYPE=IX(N,5)
000014            IF(MTYPE.EQ.NONEX) GO TO 303
000016            IF (MTYPE. GT. NSHELL) GO TO 300
000024            TENS1=E(1,MTYPE)
000025            TENS2=E(1,MTYPE)
000026            ALPHA=(E(5,MTYPE)+90.)*0.0174532925
              C**** READ DATA FROM TAPE 10 (GENERATED IN QUAD
000031            READ(10)  RRR,ZZZ,C,HH,S,P,VOL,HRES
              C**** CURRENT TOTAL INITIAL STRESSES
000054            DO 100 I=1,3
000065        100 RSTRS(I)=RESID(N,I)+RSTRST(N,I)
000070            RSTRS(4)=RSTRS(3)
              C**** CALCULATE NEW P(9),P(10)  FROM PREVIOUS INITIAL STRESSES
000071            IF(IX(N,3).EQ.IX(N,4)) GO TO 102
000074            DO 101 I=9,10
000113        101 P(I)=P(I)+(RSTRST(N,1)*HRES(1,I)+RSTRST(N,2)*HRES(2,I)
                 1           +RSTRST(N,3)*HRES(3,I))
000122        102 CONTINUE
000122            DO 120 I=1,4
000134            II=2*I
000136            JJ=2*IX(N,I)
000140            P(II-1)=B(JJ-1)
000141        120 P(II)=B(JJ)
000146            DO 150 I=1,2
000147            RR(I)=P(I+8)
000151            DO 150 K=1,8
000160        150 RR(I)=RR(I)-S(I+8,K)*P(K)
000165            COMM=S(9,9)*S(10,10)-S(9,10)*S(10,9)
000170            IF (COMM) 155,160,155
000171        155 P(9)=(S(10,10)*RR(1)-S(9,10)*RR(2))/COMM
000175            P(10)=(-S(10,9)*RR(1)+S(9,9)*RR(2))/COMM
000202        160 DO 170 I=1,6
000204            TP(I)=0.0
000205            DO 170 K=1,10
000215        170 TP(I)=TP(I)+HH(I,K)*P(K)
000222            RR(1)=TP(2)
000223            RR(2)=TP(6)
000225            RR(3)=0.0
000225            RR(4)=TP(3)+TP(5)
```

```
000230     176 DO 180 I=1,4
000233         SIG(I)=RSTRS(I)
000234         RSTRS(I)=0.0
000235         DO 180 K=1,4
000244     180 SIG(I)=SIG(I)+C(I,K)*RR(K)
000251         SIG(3)=SIG(4)
           C*****
           C    OUTPUT STRESSES
           C*****
           C    CALCULATE PRINCIPAL STRESS
           C*****
000253         CC=(SIG(1)+SIG(2))/2.0
000255         BB=(SIG(1)-SIG(2))/2.0
000257         CR=SQRT(BB**2+SIG(3)**2)
000264         SIG(4)=CC+CR
000265         SIG(5)=CC-CR
000266         IF(BB.NE.0.) GO TO 195
000270         EPS(N)=77777.
000272         GO TO 196
000272     195 EPS(N)=ATAN2(SIG(3),BB)/2.
000277     196 SIG(6)=57.296*EPS(N)
           C**** TENSILE STRESSES TO BE ELIMINATED
000301         TMIN=0.0
000302         TMAX=0.0
           C**** TENSILE STRENGTH SET TO ZERO AFTER CRACKING
000302         IF(MTAG(N).EQ.2.OR.MTAG(N).EQ.3) TENS1=0.0
000313         IF(MTAG(N).EQ.3) TENS2=0.0
           C**** BOTH PRINCIPAL STRESSES COMPRESSIVE  MTAG=1
000316         MTAG(N)=1
000320         IF(SIG(4)-TENS1) 261,261,260
           C**** MAJOR PRINCIPAL STRESS TENSILE  MTAG=2
000323     260 MTAG(N)=2
000325         TMAX=SIG(4)
000327     261 IF(SIG(5)-TENS2) 263,263,262
           C**** BOTH PRINCIPAL STRESSES TENSILE     MTAG=3
000332     262 MTAG(N)=3
000334         TMIN=SIG(5)
000336     263 CONTINUE
           CCCC ROTATE BACK TO GLOBAL AXES TO FIND INITIAL STRESSES ALTERATIONS
000336         S2=SIN(EPS(N))**2
000341         C2=COS(EPS(N))**2
000344         CS=SIN(EPS(N))*COS(EPS(N))
000353         STR(1)=TMAX*C2+TMIN*S2
000356         STR(2)=TMAX*S2+TMIN*C2
000360         STR(3)=(TMIN-TMAX)*CS
000362         IF(MTAG(N).GT.1) GO TO 284
           C**** ALPHA MEASURED ANTICLOCKWISE FROM R AXIS
000367         S2=SIN(ALPHA)**2
000371         C2=COS(ALPHA)**2
000374         SC=SIN(ALPHA)*COS(ALPHA)
000405         SIGN=SIG(1)*C2+2.*SIG(3)*SC+SIG(2)*S2
000413         TMN=(SIG(2)-SIG(1))*SC+SIG(3)*(C2-S2)
000420         CJ=E(6,MTYPE)
000421         PHIR=E(7,MTYPE)*0.01745329
000423         SHEAR=CJ-SIGN*SIN(PHIR)/COS(PHIR)
           C**** REMOVE ALL SHEAR IF IN TENSION
000432         IF(SIGN.GT.0.0) SHEAR=CJ
000435         IF(SHEAR.GT.ABS(TMN)) GO TO 284
000443         SENSE=TMN/ABS(TMN)
000443         TOR=(ABS(TMN)-SHEAR)*SENSE
000445         STR(1)=-2.0*TOR*SC
000450         STR(2)=-STR(1)
000450         STR(3)=TOR*(C2-S2)
000453         MTAG(N)=4
000456     284 CONTINUE
000456         IF(MTAG(N).EQ.1) GO TO 283
           C**** CALCULATE FORCES EQUIVALENT TO NEW INITIAL STRESSES (CHANGE ONLY)
000461         DO 270 I=1,3
000470     270 RSTRST(N,I)=RSTRST(N,I)-STR(I)
000473         DO 271 I=1,10
000505     271 P(I)= (STR(1)*HRES(1,I)+STR(2)*HRES(2,I)+STR(3)*HRES(3,I))
           C**** REDUCE TO 8 DEGREES OF FREEDOM -FOR QUADRILATERAL AND BAR ELEMENTS
000514         IF(IX(N,3).EQ.IX(N,4)) GO TO 272
000516         DO 280 II=1,9
000525         CC=S(II,10)/S(10,10)
000527         P(II)=P(II)-CC*P(10)
000531     280 S(II,9)=S(II,9)-CC*S(10,9)
000535         DO 281 II=1,8
000545         CC=S(II,9)/S(9,9)
000546     281 P(II)=P(II)-CC*P(9)
           C**** ELIMINATE IF NODES CONSTRAINED
000551     272 DO 282 I=1,4
000556         II=2*I-1
000557         IJ=IX(N,I)
000560         IF(CODE(IJ).EQ.1.0.OR.CODE(IJ).EQ.3.0) P(II)=0.0
000572         IF(CODE(IJ).EQ.2.0.OR.CODE(IJ).EQ.3.0) P(II+1)=0.0
           C**** ADD LOADS TO UR,UZ
000603         UR(IJ)=UR(IJ)+P(II)
000606         UZ(IJ)=UZ(IJ)+P(II+1)
000611         WRITE(6,7000) N,UR(IJ),UZ(IJ)
000622    7000 FORMAT(I5,2E12.4)
000622     282 CONTINUE
000624     283 CONTINUE
000624     104 IF (MPRINT ) 110,105,110
000625     105 WRITE (6,2000)
000631         MPRINT=50
000632     110 MPRINT=MPRINT-1
000634     305 WRITE(6,2001) N,RRR(5),ZZZ(5),(SIG(I),I=1,6),MTAG(N),SIGN,TMN
           C**** UPDATE RESIDUAL STRESSES AT END OF INCREMENT
000656         IF(NNN.LT.NP) GO TO 300
000661         RESID(N,1)=SIG(1)
000663         RESID(N,2)=SIG(2)
000664         RESID(N,3)=SIG(3)
000666     300 CONTINUE
000671     320 RETURN
000672    2000 FORMAT (7H1EL.NO.    7X   1HX 7X 1HY 4X 8HX-STRESS 4X 8HY-STRESS3X
              19HXY-STRESS 2X 10HMAX-STRESS 2X 10HMIN-STRESS 7H  ANGLE
              1 2X,4HMTAG,4X,7HSIGMA N,4X,6HTOR MN )
000672    2001 FORMAT(I7,2F8.2,5E12.4,F7.2,I5,2E12.4)
000672         END

UNUSED COMPILER SPACE
014700
```

```
      SUBROUTINE JSTR
000001  COMMON NUMNP,NUMEL,NUMMAT,NUMPC,ACELX,ACELY,N,VOL,NRES,MTYPE,
     1 HED(12),E(8,12),RO(12),XXNN(12),R(500),Z(500),UR(500),UZ(500),
     2 CODE(500),IBC(200),JBC(200),PR(200),ANGLE(4),LBAD,NP,NAP,
     3 EPS(400),NSHELL,RSTRST(400,3),KN(400),KS(400)
000001  COMMON /ARG/ RRR(5),ZZZ(5),S(10,10),P(10),TT(4),LM(4),DD(3,3),
     1 HH(6,10),RR(4),ZZ(4),C(4,4),H(6,10),D(6,6),F(6,10),TP(6),XI(10)
     2,EE(7),IX(400,5),MTAG(400),RSTRS(4),RESID(400,3)
000001  COMMON /BANARG/ MBAND,NUMBLK,B(160),A(160,30),ND
000001  COMMON /CUM/BCUM(1000),STRN(400,4),INC
000001  COMMON /MAT/ SHEAR(4,10),DRATIO(4,10),DILTN(4,10),DINC(4),FINC(4)
     1 ,SNJNT(4,10)
000001  COMMON /EXC/ NCUT(100),NONEX
000001  DIMENSION U(4),W(4),UCUM(4),VCUM(4),SHR(10),DRAT(10),DIL(10),
     1 FOR(4),SNJT(10)
000001  DATA FOR/+1.0,+1.0,-1.0,-1.0/
000001  REAL KS,KN,L
C**** TOTAL INCREMENTAL DISPLACEMENT METHOD
C***** DISPLACEMENTS  -SHEAR AND NORMAL
000001  WRITE(6,2000)
000005  2000 FORMAT(1H0,*  N     XCEN     YCEN   NORMAL F/A   SHEAR F/A   INC.NOR
     1M.D CUM.NORM.D. INC.SHEAR D. CUM.SHEAR D.   *)
000005  DO 500 N=1,NUMEL
000007  MAT=IABS(IX(N,5))
000011  IF(MAT.EQ.NONEX) GO TO 500
000013  IX(N,5)=IABS(IX(N,5))
000014  IF(MAT.LE.NSHELL) GO TO 500
000030  KN(N)=E(1,MAT)
000033  KS(N)=E(2,MAT)
000037  CON=1.0
000041  PHI=E(4,MAT)*0.01745
000046  DNP=ABS(E(5,MAT))
000051  MAT=MAT-NSHELL
000053  I=IX(N,1)
000055  J=IX(N,2)
000056  IJ=IX(N,3)
000057  JI=IX(N,4)
000061  DR=R(J)-R(I)
000064  DZ=Z(J)-Z(I)
000067  RR(1)=0.5*(R(J)+R(I))
000074  ZZ(1)=0.5*(Z(J)+Z(I))
000102  L=SQRT(DR*DR+DZ*DZ)
000107  DR=DR/L
000110  DZ=DZ/L
C**** CALCULATE INCREMENTAL AND CUMALITIVE DISPLACEMENTS
000111  DO 100 II=1,4
000122  K=IX(N,II)
000123  V(II)=-R(2*K-1)*DZ+R(2*K)*DR
000131  U(II)=R(2*K-1)*DR+R(2*K)*DZ
000137  VCUM(II)=-BCUM(2*K-1)*DZ+BCUM(2*K)*DR
000145  UCUM(II)=BCUM(2*K-1)*DR+BCUM(2*K)*DZ
000152  100 CONTINUE
C*** INCREMENTAL AND CUMULATIVE STRAIN
000154  EPST=0.5*(U(4)-U(1)+U(3)-U(2))
000160  EPSN=0.5*(V(4)-V(1)+V(3)-V(2))
000165  CEPST=0.5*(UCUM(4)-UCUM(1)+UCUM(3)-UCUM(2))+EPST
000173  CEPSN=0.5*(VCUM(4)-VCUM(1)+VCUM(3)-VCUM(2))+EPSN
000201  IF(NRES.EQ.1) GO TO 150
000207  C2=DR**2
000210  S2=DZ**2
000211  SC=DR*DZ
000212  FTRES=RESID(N,2)*SC-RESID(N,1)*SC+RESID(N,3)*(S2-C2)
000217  FNRES=RESID(N,1)*S2+RESID(N,2)*C2+RESID(N,3)*2.0*SC
C**** CALCULATE EFFECTIVE JOINT DISPLACEMENTS-RESIDUAL COMPONENT ELASTIC
000224  STRN(N,3)=FNRES/KN(N)
000225  STRN(N,4)=FTRES/KS(N)
000230  FNRES=FNRES+RSTRST(N,1)
000232  FTRES=FTRES+RSTRST(N,3)
000233  GO TO 160
000236  150 FNRES=RESID(N,1)+RSTRST(N,1)
000237  FTRES=RESID(N,3)+RSTRST(N,3)
000243  160 FN=KN(N)*(EPSN-STRN(N,1))+FNRES
000247  FT=KS(N)*EPST+FTRES
000252  CEPSN=STRN(N,3)+CEPSN
000254  CEPST=STRN(N,4)+CEPST
C**** WRITE COMPUTED STRESSES AND STRAINS
000257  WRITE(6,1000) N,RR(1),ZZ(1),FN,FT,EPSN,CEPSN,EPST,CEPST
000304  1000 FORMAT(1H ,I5,2F8.2,6E12.4)
C**** COLLECT JOINT PROPERTIES ETC
000305  DISP=ABS(CEPST)
000307  DNC=DINC(MAT)
000310  FNC=FINC(MAT)
000312  DO 165 NINC=1,10
000322  SHR(NINC)=SHEAR(MAT,NINC)
000323  DRAT(NINC)=DRATIO(MAT,NINC)
000324  DIL(NINC)=DILTN(MAT,NINC)
000325  SNJT(NINC)=SNJNT(MAT,NINC)
000326  165 CONTINUE
C**** CHECK JOINT NORMAL BEHAVIOUR
000330  SIGT=0.0
000330  SIGN=0.0
000331  IF(FN) 170,170,171
000333  171 SIGN=-FN
000335  WRITE(6,2004)
000340  RSTRST(N,1)=RSTRST(N,1)+SIGN
000343  GO TO 176
000343  170 CONTINUE
C**** CALCULATE INITIAL STRAIN DUE TO DILATION
000343  RSD=ABS(FN)*SIN(PHI)/COS(PHI)
000352  DISP=DISP*KS(N)/RSD
000355  FNLIM=10.0*FNC
000357  IF(ABS(FN).GT.FNLIM) GO TO 172
000364  CALL INTPL (DRAT,ABS(FN),FNC,RATIO)
000370  CALL INTPL (DIL,DISP,1.0,DILAT)
000373  CALL INTPL(SNJT,ABS(FN),FNC,CLOSN)
000400  DILAT=DILAT*RATIO*DNC
000402  CLOSN=DNP*CLOSN
000404  GO TO 173
000405  172 DILAT=0.0
000406  CLOSN=DNP
000411  173 STINT=-CEPSN-CLOSN+DILAT
000414  STRN(N,1)=STRN(N,1)+STINT
000416  WRITE(6,2003) DILAT,CLOSN
C**** CALCULATE SHEAR STRENGTH
000426  IF(FN)175,176,176
000430  175 CONTINUE
```

```
G13
000430          IF(ABS(CEPST).LT.ABS(STRN(N,2))) CON=-1.0
      C**** STRN(N,2) STORES PREVIOUS SHEAR DISPLACEMENT
000437          STRN(N,2)=CEPST
000441          CALL INTPL (SHR,DISP,1.0,STREN)
000444          FTNORM=FT/RSO
000446          WRITE(6,1002) STREN,FTNORM,DISP
000460     1002 FORMAT(30H NORMALIZED SHEAR BEHAVIOUR   ,17HSHEAR STRENGTH=  ,F6.3
               1 ,13H SHEAR F/A=  ,F6.3,9H DISP.=   ,F6.3)
000460          STREN=STREN*RSO
000462          IF(ABS(STREN)-ABS(FT)) 180,200,180
000465      180 SIGT=FT*(STREN/ABS(FT)-1.0)*CON
000473          GO TO 200
000473      176 SIGT=-FT
000475          WRITE(6,2005)
000500      200 RSTRST(N,3)=RSTRST(N,3)+SIGT
      C**** RESET RESIDUAL STRESSES ON LAST APPROXIMATION
000503          IF(NP.LT.NAP) GO TO 230
000505          RESID(N,1)=FN
000507          RESID(N,3)=FT
000510          GO TO 500
000511      230 CONTINUE
      C**** CALCULATE LOADS EQUIVALENT TO INITIAL STRESS AND STRAIN INCREMENTS
000514          FNADJ=(SIGN-KN(N)*STINT)*L/2.0
000517          FTADJ=SIGT*L/2.0
000520          RADJ=FTADJ*DR-FNADJ*DZ
000523          ZADJ=FTADJ*DZ+FNADJ*DR
000525          DO 300 I=1,4
000527          IJ=IX(N,I)
000532          IF(CODE(IJ).EQ.1.0.OR.CODE(IJ).EQ.3.0) GO TO 301
000543          UR(IJ)=UR(IJ)+FOR(I)*RADJ
000547      301 IF(CODE(IJ).EQ.2.0.OR.CODE(IJ).EQ.3.0) GO TO 300
000560          UZ(IJ)=UZ(IJ)+FOR(I)*ZADJ
000564      300 CONTINUE
000566      500 CONTINUE
000571     2003 FORMAT( *  DILATATION= *,E12.4,* PERMITTED NORMAL CLOSURE=*,E12.4)
000571     2004 FORMAT(*  JOINT IN TENSION  *)
000571     2005 FORMAT(*  NO SHEAR STRENGTH  *)
000571          RETURN
000571          END

UNUSED COMPILER SPACE
015000
```

```
                SUBROUTINE INTPL(A,B,BINC,VALUE)
000006          DIMENSION A(10)
      C**** INTERPOLATION SUBROUTINE(A GIVEN AT SPECIFIED INCREMENTS OF B)
000006          BI=B/BINC+1.0
000010          I=IFIX(BI)
000011          IF(I.GT.9) GO TO 10
000014          DEL=B-BINC*(FLOAT(I)-1.0)
000017          VALUE=A(I)+(A(I+1)-A(I))*DEL/BINC
000022          RETURN
000023       10 VALUE=1.0
000024          RETURN
000025          END

UNUSED COMPILER SPACE
020200
```

APPENDIX

C

WEDGE STABILITY ANALYSIS BY VECTOR METHODS

COMPUTER PROGRAM FOR WEDGE STABILITY ANALYSIS

Purpose

The program is designed to calculate the stability against sliding of a wedge defined by two planes of weakness in a rock slope. The rock is assumed to be rigid but the joints may be deformable in both the shear and normal directions.

Comment

The program notation is based on that used by Wittke (A Numerical Method of Calculating the Stability of Slopes in Rock with Systems of Plane Joints. Rock Mech. & Eng. Geology, Supplement I, 1964). Only sliding stability is considered as the program was written to investigate the influence of joint deformability.

Input Data

Slope and Joint Data - One Set for each problem.

Card 1. (3F5.0)

Columns		PROGRAM NOTATION
1 - 5	Slope Angle	SLA
6 - 10	Crest Angle	CRE
11 - 16	Height from Toe to Crest	H

Card 2 (4F5.0)

1 - 5	Strike of Plane 1	STR 1
6 - 10	Dip of Plane 1	DIP 1
11 - 15	Cohesion of Plane 1	COH 1
16 - 20	Angle of friction of Plane 1	THI 1

Card 3 (4F5.0)

1 - 5	Strike of Plane 2	STR 2
6 - 10	Dip of Plane 2	DIP 2
11 - 15	Cohesion of Plane 2	COH 2
16 - 20	Angle of Friction of Plane 2	THI 2

Card 4 (3F5.0)

1 - 5	X-Acceleration	G(1)
6 - 10	Y-Acceleration	G(2)
11 - 15	Z-Acceleration	G(3)

Card 5 (4F5.0)

1 - 5	Normal Stiffness Joint 1	KN1
5 - 10	Shear Stiffness Joint 1	KS1
11 - 15	Normal Stiffness Joint 2	KN2
16 - 20	Shear Stiffness Joint 2	KS2

Note Only the ratios of the shear and normal stiffnesses are important.

Output

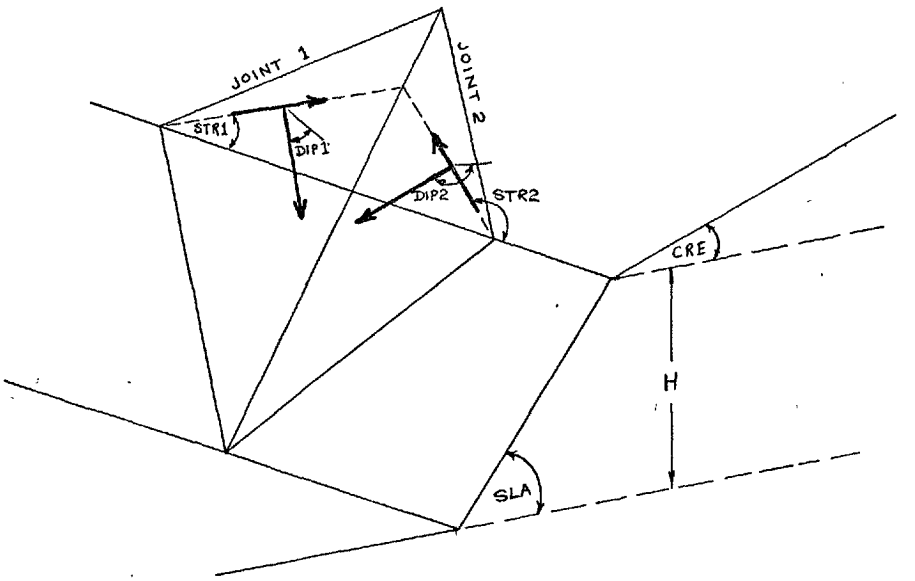
1) Writes out input data

2) a) Writes out if data is invalid
e.g. No wedge defined.

b) Writes out on which plane or planes sliding occurs

c) Writes factor of safety for defined strength

d) Writes out required angle of friction to prevent sliding (cohesion = 0.) taking into account joint deformability.



```
      PROGRAM WDG(INPUT,OUTPUT,TAPE5=INPUT,TAPE6=OUTPUT)
C****** UMGR005  C.M.ST.JOHN  ROCK MECHANICS---IMPERIAL COLLEGE
000002      COMMON/WGD/  U1(3),U2(3),V1(3),V2(3),N1(3),N2(3),X(3),OD(3),OC(3),
     1  TEMP(3),Y1(3),Y2(3),OB(3),G(3),T(3),N(3),
     2 KN1,KN2,KS1,KS2
000002      REAL N,KN1,KN2,KS1,KS2
000002      DO 5000 NREAD=1,10
000004      READ(5,1000) SLA,CRE,H,STR1,DIP1,COH1,THI1,STR2,DIP2,COH2,THI2
000035 1000 FORMAT(3F5.0/4F5.0/4F5.0)
000035      WRITE(6,2000)
000041 2000 FORMAT(1H1,*   WEDGE ANALYSIS DATA   *)
000041      WRITE(6,2001) SLA,CRE,H,STR1,DIP1,COH1,THI1,STR2,DIP2,COH2,THI2
000073 2001 FORMAT(/ * SLOPE ANGLE AND CREST ANGLE *,2F10.2/
     1          * SLOPE HEIGHT TO CREST *,F10.2/
     2          *   DIP AND STRIKE OF JOINTS */
     3 * JOINT 1 *,5X,2F10.4, * COHESION *,F8.2,* FRICTION * F8.2/
     4 * JOINT 2 *,5X,2F10.4, * COHESION *,F8.2,* FRICTION * F8.2/  )
000073      READ(5,1001) G(1),G(2),G(3),KN1,KS1,KN2,KS2
000115 1001 FORMAT(3F5.0/4F5.0)
000115      WRITE(6,1998) (G(I),I=1,3)
000123 1998 FORMAT(  *  GRAVITY VECTOR * ,3F10.2  ,/)
000123      WRITE(6,1999) KN1,KS1,KN2,KS2
000137 1999 FORMAT(  *  STIFFNESS JNT 1 NORM.= * E12.4  * SHEAR= * E12.4,
     1          *  STIFFNESS JNT 2 NORM.= * E12.4  * SHEAR= * E12.4,/)
C**** CHECK DATA
000137      IF(SLA.GT.0.0.AND.SLA.LE.180.) GO TO 1
000150      WRITE(6,2002) SLA
000155 2002 FORMAT(* IMPOSSIBLE SLOPE ANGLE * ,F10.4)
000155      GO TO 5000
000156    1 IF(CRE.GE.0.0.AND.CRE.LT.90.) GO TO 2
000156      WRITE(6,2003) CRE
000173 2003 FORMAT(* IMPOSSIBLE CREST SLOPE * F10.4)
000173      GO TO 5000
000174    2 IF(SLA.GT.CRE) GO TO 3
000200      WRITE(6,2004)
000203 2004 FORMAT(* CREST ANGLE GREATER THAN SLOPE *)
000203      GO TO 5000
000204    3 CONTINUE
C**** WRITE DOWN VECTORS DEFINING THE PROBLEM
000205      ANG=3.1415926/180.0
000206      B1=STR1   *ANG
000207      B2=STR2   *ANG
000210      G1=DIP1   *ANG
000212      G2=DIP2   *ANG
000213      TH1=THI1  *ANG
000215      TH2=THI2  *ANG
000217      U1(1)=COS(B1)
000220      U1(2)=SIN(B1)
000222      U1(3)=0.0
000223      U2(1)=COS(B2)
000225      U2(2)=SIN(B2)
000227      U2(3)=0.0
000230      V1(1)=SIN(B1)*COS(G1)
000235      V1(2)=-COS(B1)*COS(G1)
000243      V1(3)=-SIN(G1)
000246      V2(1)=SIN(B2)*COS(G2)
000253      V2(2)=-COS(B2)*COS(G2)
000261      V2(3)=-SIN(G2)
C**** JOINT NORMALS
000264      CALL VECT(U1,V1,W1,Q,4)
000270      CALL VECT(U2,V2,W2,Q,4)
C**** VECTOR DEFINING INTERSECTION
000274      CALL VECT(W2,W1,X,Q,4)
000300      IF(X(2).LT.0.0) GO TO 31
000302      WRITE(6,2011)
000305 2011 FORMAT(  *      INTERSECTION DOES NOT DEFINE A WEDGE *)
000305      GO TO 5000
000306     31 CONTINUE
C**** CHECK WHETHER ONE PLANE PARALLEL  TO FACE
000306      IF(STR1.EQ.0.0.OR.STR1.EQ.180.0) GO TO 4
000315      IF(STR2.EQ.0.0.OR.STR2.EQ.180.0) GO TO 5
000323      GO TO 6
000323    4 WRITE(6,2005)
000327 2005 FORMAT(* JOINT 1 PARELLEL TO SLOPE*)
000327      PARA=1.0
000330      EV=DIP1
000332      GO TO 7
000333    5 WRITE(6,2006)
000337 2006 FORMAT( * JOINT 2 PARELLEL TO SLOPE*)
000337      PARA=2.0
000340      EV=180.-DIP2
000343      GO TO 7
000343    6 PARA=0.0
000344      EV=ATAN2(X(3),X(2))
000346      EV=180.+EV/ANG
000351      IF(SLA.EQ.180.) GO TO 8
000353    7 IF(EV-SLA) 9,10,10
000356    8 IF(EV-CRE) 9,10,10
000361   10 WRITE(6,2007)
000365 2007 FORMAT(* SLIDING KINEMATICALLY IMPOSSIBLE *)
000365      GO TO 5000
000366    9 CONTINUE
000366      CALL VECT(X,X,TEMP,ABV,1)
000372      CALL VECT(W2,W1,TEMP,ABD,1)
000376      APP=ATAN2(ABV,ABD)/ANG
000402      WRITE(6,4020) APP,EV
000411 4020 FORMAT( *  WEDGE APPERTURE= *,F4.2, *  INTERSECTION DIP =  *,F8.2)
C**** DETERMINE GEOMETRY OF WEDGE
000411      CR=CRE    *ANG
000413      SL=SLA    *ANG
000414      EX=EV     *ANG
000416      TANEX=SIN(EX)/COS(EX)
000423      TANCR=SIN(CR)/COS(CR)
000430      TANSL=SIN(SL)/COS(SL)
000435      TANG1=SIN(G1)/COS(G1)
000442      TANG2=SIN(G2)/COS(G2)
000447      TANB1=SIN(B1)/COS(B1)
000454      TANB2=SIN(B2)/COS(B2)
000461      HS=H*((TANSL-TANEX)*TANCR)/((TANEX-TANCR)*TANSL)
C**** FIND MAGNITUDE AND DIRECTION OF VECTOR APEX TO TOE
000467      CALL VECT(X,TEMP,X,Q,2)
000473      TOTAL=(H+HS)/TEMP(3)
000476      CALL VECT(TEMP,OB,TEMP,TOTAL,3)
C**** FIND VECTORS DEFINING WEDGE LIMITS
C**** OC,OD BECOME VECTOR UP FACE FOR 2 D WEDGE
000504      OD(2)=H/TANSL
```

```
000504          OD(3)=H
000505          OC(2)=H/TANSL
000507          OC(3)=H
000507          IF(PARA.GT.0.0) GO TO 81
000512          OC(1)=-H/(TANG2*SIN(B2))+H/(TANSL*TANB2)
000520          OD(1)=-H/(TANG1*SIN(B1))+H/(TANSL*TANB1)
000530          GO TO 82
000531       81 OC(1)=0.0
000532          OD(1)=0.0
000533       82 CONTINUE
              C**** CALCULATE VOLUMES AND SLIDING AREAS
000533          IF(PARA.EQ.0.0) GO TO 91
000534       92 CALL VECT(OD,OB,TEMP,Q,4)
000540          VOL   =SQRT(TEMP(1)*TEMP(1)+TEMP(2)*TEMP(2)+TEMP(3)*TEMP(3))/2.0
000550       94 AREA=SQRT(OB(1)*OB(1)+OB(2)*OB(2)+OB(3)*OB(3))
000557          GO TO 18
000557       91 CALL VECT(OC,OD,TEMP,Q,4)
000563          OCO   =SQRT(TEMP(1)*TEMP(1)+TEMP(2)*TEMP(2)+TEMP(3)*TEMP(3))
000571          AO=(SL-EX)
000573          VOL=OCO*SIN(AO)*SQRT(OB(2)*OB(2)+OB(3)*OB(3))/6.0
000606          CALL VECT(OD,OB,TEMP,Q,4)
000611          AREA1=SQRT(TEMP(1)*TEMP(1)+TEMP(2)*TEMP(2)+TEMP(3)*TEMP(3))/2.0
000621          CALL VECT(OB,OC,TEMP,Q,4)
000624          AREA2=SQRT(TEMP(1)*TEMP(1)+TEMP(2)*TEMP(2)+TEMP(3)*TEMP(3))/2.0
              C**** TEST FOR DIRECTION OF SLIDING
000634          CALL VECT(V1,X,TEMP,Q,4)
000637          CALL VECT(TEMP,Y1,TEMP,Q,2)
000643          DO 121 I=1,3
000645          C=Y1(I)-W1(I)
000647          IF(ABS(C).LE.0.001) GO TO 121
000652          GO TO 122
000653      121 CONTINUE
000655          GO TO 12
000656      122 PARA=1.0
000660          WRITE(6,2008)
000663     2008 FORMAT(* SLIDING ON PLANE 1 *)
000663          AREA=AREA1
000665          GO TO 18
000665       12 CALL VECT(V2,X,TEMP,Q,4)
000671          CALL VECT(TEMP,Y2,TEMP,Q,2)
000675          DO 141 I=1,3
000677          C=Y2(I)-W2(I)
000701          IF(ABS(C).LE.0.001) GO TO 141
000704          GO TO 142
000705      141 CONTINUE
000707          GO TO 14
000710      142 PARA=2.0
000712          WRITE(6,2009)
000715     2009 FORMAT(* SLIDING ON PLANE 2*)
000715          AREA=AREA2
000717          GO TO 18
000717       14 WRITE(6,2010)
000723     2010 FORMAT(* COMPOSITE SLIDING *)
              C**** VECTOR OF WEDGE WEIGHT
000723       18 VOL=ABS(VOL)
000725          DO 15 IJ=1,3
000731       15 G(IJ)=G(IJ)*VOL
000733          IF(PARA-1.0) 16,17,19
```

```
              C**** CALCULATE SLIDING FORCE,NORMAL FORCE AND SELECT JOINT PROPERTIES
000736       17 CALL VECT(G,V1,TEMP,QT,1)
000742          CALL VECT(G,W1,TEMP,FN,1)
000746          COHES=COH1
000747          TANTH=SIN(TH1)/COS(TH1)
000755          GO TO 20
000755       19 CALL VECT(G,V2,TEMP,QT,1)
000761          CALL VECT(G,W2,TEMP,FN,1)
000765          COHES=COH2
000766          TANTH=SIN(TH2)/COS(TH2)
000773          FN=-FN
              C**** CALCULATE FACTOR OF SAFETY
000775       20 FS=(COHES*AREA+FN*TANTH)/QT
001002          GO TO 100
              C**** STABILITY FOR COMPOSITE SLIDING
001002       16 CALL VECT(X,TEMP,TEMP,QX,2)
001006          CALL VECT(G,X,TEMP,GX,1)
001012          CON=GX/(QX*QX)
001014          CALL VECT(X,T,TEMP,CON,3)
001020          DO 25 I=1,3
001026       25 N(I)=G(I)-T(I)
              C**** T IS VECTOR OF DRIVING FORCE ,N VECTOR OF NORMAL FORCE
001031          C2=(N(1)*W1(2)-N(2)*W1(1))/(W2(2)*W1(1)-W2(1)*W1(2))
001040          C1=(N(1)+C2*W2(1))/W1(1)
001043          C1=ABS(C1)
001044          C2=ABS(C2)
              C**** CALCULATE FACTOR OF SAFETY
001046          SHEAR=SQRT(T(1)*T(1)+T(2)*T(2)+T(3)*T(3))
001053          FS=(COH1*AREA1+COH2*AREA2+(C1*SIN(TH1)/COS(TH1))
                1 +(C2*SIN(TH2)/COS(TH2)))/SHEAR
              C**** WRITE OUT ANSWER
001075          WRITE(6,3000) VOL,AREA1,AREA2
001107     3000 FORMAT( /* VOLUME      AREA PLANE 1  AREA PLANE 2 *,/3E12.4)
001107          GO TO 101
001110       100 WRITE(6,3001) VOL,AREA
001120     3001 FORMAT( /*  VOLUME       AREA * /2E12.4)
001120       101 WRITE(6,3002) FS
001126     3002 FORMAT(/*-----FACTOR OF SAFETY = * E12.4 *-----*)
              C**** CALL SOFT FOR TETRAHEDRAL WEDGE WITH SOFT JOINTS
001126          IF(PARA.EQ.0.0) CALL SOFT(AREA1,AREA2,VOL)
001132      5000 CONTINUE
001134          STOP
001136          END

UNUSED COMPILER SPACE
014000
```

```
                SUBROUTINE VECT(U,V,W,Q,NOPN)
000007          DIMENSION U(3),V(3),W(3)
          C     NOPN=1  Q BECOMES SCALAR PRODUCT OF U AND V
          C     NOPN=2  NORMALISE U INTO V
          C     NOPN=3  MULTIPLY U BY Q,PLACE IN V
          C     NOPN=4  W BECOMES VECTOR PRODUCT OF U AND V
          C     NOPN=5  W BECOMES VECTOR U+ VECTOR V*Q
000007          GO TO (1,2,3,4,5),NOPN
000017        1 Q=0.0
000020          DO 10 I=1,3
000023       10 Q=Q+U(I)*V(I)
000026          IF(Q.NE.0.0) GO TO 15
000032          WRITE(6,17)
000035          STOP
000042        2 Q=0.0
000043          DO 11 I=1,3
000046       11 Q=Q+U(I)*U(I)
000051          IF(Q.NE.0.0) GO TO 16
000055          WRITE(6,17)
000060       17 FORMAT(* NULL VECTOR *)
000063          STOP
000065       16 Q=SQRT(Q)
000073          GO TO 31
000073        3 Q=1.0/Q
000075       31 DO 12 I=1,3
000103       12 V(I)=U(I)/Q
000105          RETURN
000105        4 K=3
000106          DO 13 I=1,3
000114          J=6-I-K
000116          W(I)=U(J)*V(K)-U(K)*V(J)
000121       13 K=I
000127          RETURN
000127        5 DO 14 I=1,3
000133       14 W(I)=U(I)+Q*V(I)
000141       15 RETURN
000142          END

UNUSED COMPILER SPACE
017600
```

```
                SUBROUTINE SET(A,I,J,V,CONST)
000007          DIMENSION A(6,7),B(6,6),V(6)
000007          DO 1 K=1,3
000014          L=I+K-1
000016        1 A(L,J)=V(K)*CONST
000023          RETURN
000023          END

UNUSED COMPILER SPACE
020200
```

```
                SUBROUTINE SOFT(AREA1,AREA2,VOL)
000005          COMMON/WGO/  U1(3),U2(3),V1(3),V2(3),W1(3),W2(3),X(3),OD(3),OC(3),
               1  TEMP(3),Y1(3),Y2(3),O9(3),G(3),T(3),N(3),
               2 KN1,KN2,KS1,KS2
000005          DIMENSION A(6,7),B(6,6)
000005          DIMENSION XN(3),S1(3),S2(3),SH(3),FN(3)
000005          DIMENSION DIV(6)
000005          REAL N,KN1,KN2,KS1,KS2
000005          CALL VECT(X,XN,TEMP,Q,2)
               C**** FORM EQUATIONS TO BE SOLVED
000010          CALL SET(A,1,1,W1,1.0)
000014          CALL SET(A,1,2,W2,-1.0)
000020          CALL VECT(XN,W1,TEMP,Q,4)
000024          CALL VECT(TEMP,S1,TEMP,Q,2)
000030          CALL SET(A,1,3,S1,1.0)
000034          CALL VECT(XN,W2,TEMP,Q,4)
000040          CALL VECT(TEMP,S2,TEMP,Q,2)
000044          CALL SET(A,1,4,S2,1.0)
000050          CALL SET(A,1,5,XN,1.0)
000054          CALL SET(A,1,6,XN,1.0)
000062          DIV(1)=AREA1*KN1
000063          DIV(2)=AREA2*KN2*(-1.0)
000065          DIV(3)=AREA1*KS1
000067          DIV(4)=AREA2*KS2*(-1.0)
000071          DIV(5)=DIV(3)
000072          DIV(6)=DIV(4)
000073          DO 1 J=1,3
000075          K=J+3
000076          DO 1 I=1,6
000107          A(K,I)=A(J,I)/DIV(I)
000110        1 CONTINUE
000116          DO 2 I=1,3
000123          A(I,7)=G(I)
000124          A(I+3,7)=0.0
000124        2 CONTINUE
               C**** SOLVE EQUATIONS- SOLUTION IN LAST COLUMN OF A
               C****    CDC MATRIX INVERSIONLIBRARY PACKAGE
000126          CALL MATRIX(10,6,7,0,A,6,B)
000134          DO 5 K=1,2
000140          DO 3 I=1,3
000144          SH(I)=0.0
000145        3 FN(I)=0.0
000146          IF(K.EQ.2) GO TO 9
000152          DO 7 I=1,3
000160          SH(I)=SH(I)+S1(I)*A(3,7)+XN(I)*A(5,7)
000164        7 FN(I)=W1(I)*A(1,7)
000166          GO TO 8
000170        9 DO 6 I=1,3
000177          SH(I)=SH(I)+S2(I)*A(4,7)+XN(I)*A(6,7)
000203        6 FN(I)=-W2(I)*A(2,7)
000207        8 CONTINUE
000207          WRITE(6,1001) K
000215     1001 FORMAT(/ 15X,* JOINT * ,I5)
               C**** ANGLE OF FRICTION REQUIRED FOR STABILITY
000217          SHEAR=SQRT(SH(1)*SH(1)+SH(2)*SH(2)+SH(3)*SH(3))
000225          FNORM=SQRT(FN(1)*FN(1)+FN(2)*FN(2)+FN(3)*FN(3))
000233          THIR=ATAN2(SHEAR,FNORM)
000236          THIR=THIR/0.01745
000240          WRITE(6,1000) THIR
000250     1000 FORMAT(/*  ANGLE OF FRICTION TO PREVENT SLIDING= * ,E12.4)
000252        5 CONTINUE
000254          RETURN
000255          END

UNUSED COMPILER SPACE
017000
```

APPENDIX

D

THREE DIMENSIONAL ANALYSIS OF JOINTED ROCK MASSES BY FINITE ELEMENTS

COMPUTER PROGRAM FOR JOINTED ROCK MASSES

THREE DIMENSIONAL ANALYSIS

ISOPARAMETRIC ELEMENTS

Purpose

The program is designed to model the behaviour of three dimensional structures in rock containing joints. Joints are ascribed shear and normal stiffnesses and have no tensile strength. The continuum elements are considered to be isotropic, linear, elastic solids.

A failure criterion for the joints in included. Modification of shear stiffness when this criterion is exceeded and modification of normal stiffness as joint closure occurs amount to ascribing non-linear properties to the joints.

Comment

The program was written for the C.D.C.6600 installation at London University.

It is based on the two-dimensional finite element programs developed at the University of California, Berkeley.

Input Data

(1) Title of Problem (12A6

Columns 1 - 72 to contain title which will be printed at the head of output.

(2) Basic Control Information (5I5,3F10.0)

Columns		(PROGRAM NOTATION)
1 - 5	Number of Elements	NUMEL
6 - 10	Number of Nodal Points	NUMNP
11 - 15	Number of Continuum Materials	NUMMAT
16 - 20	Number of Joint Types	NJOINT
21 - 26	Number of Approximations	NAP
26 - 35	Accelration in X direction	ACELX
36 - 45	Acceleration in Y direction	ACELY
46 - 55	Acceleration in Z direction	ACELZ

There can be a total of 10 continuum and joint types

(3) Material Properties (I5,5F10.0)

Solid Material

Columns 1-5	Material Number		MTYPE
5-15	Material Density		RO
16-25	Youngs Modulus		E (1,MTYPE)
26-35	Poissons Ratio		E (2,MTYPE)

Joint Materials

1-5	Joint Number - (must exceed number of Solid Materials)	JTYPE
5-15	Shear Stiffness	E (1,JTYPE)
16-25	Normal Stiffness	E (2,JTYPE)
26-35	Joint Cohesion	E (3,JTYPE)
36-45	Joint Friction	E (4,JTYPE)
46-55	Maximum closure of joint, input as negative amount	E (5,JTYPE)

(4) Nodal Point Data (I5,F5.0, 6F10.0)

Columns 1-5	Nodal Point Number	N
6-10	Nodal Point Load or Displacement Identifier*	CODE
11-20	X-ordinate	X
21-30	Y-ordinate	Y
31-40	Z-ordinate	Z
41-50	X-load or displacement	UX
51-60	Y-load or displacement	UY
61-70	Z-load or displacement	UZ

*Nodal Coding

Loads or displacements are indicated, depending on the Nodal Code.

Code	0	1	2	3	4	5	6	7
X direction	L	D	L	L	D	D	L	D
Y direction	L	L	D	L	D	L	D	D
Z direction	L	L	L	D	L	D	D	D

D. Displacement Specified

L. Load specified

Missing nodal points in the data presented are generated automatically by linear interpolation (i.e. Specify only the first and last nodes in a series equally spaced).

In the event of interpolation the nodal code is assumed to be Zero, and the nodal loadings are also set to Zero.

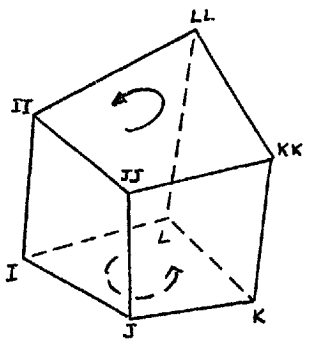
(5) Element Data (11I5)

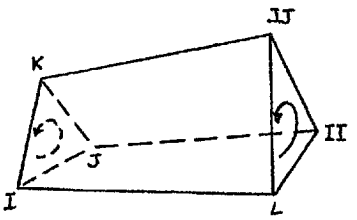
1 - 5	Element Number		M
6 - 10	Material type		NPROP
11 - 15	Number of Nodes		NNOD
16 - 20	I		
21 - 25	J		
26 - 30	K		
31 - 35	L	List of nodes defining	IX(M,8)
36 - 40	II	element	
41 - 45	JJ		
46 - 50	KK	(Max. Difference = 25)	
51 - 55	LL		

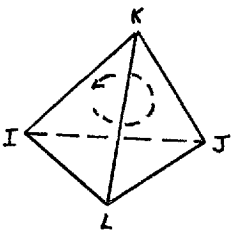
Missing elements will be supplied by successively adding one to each nodal point number of the last specified element. This last element also defines the material type and the number of nodes.

The element with the highest number must appear on the last data card.

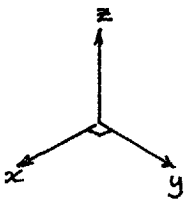
Solid Elements

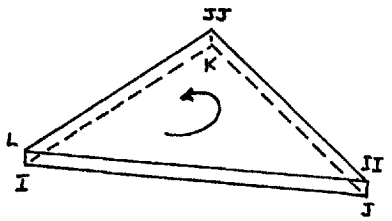


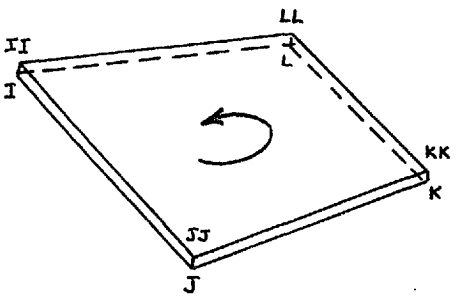




Joint Elements







Note that all elements are labelled anti-clockwise with the further nodes from the viewing point listed first.

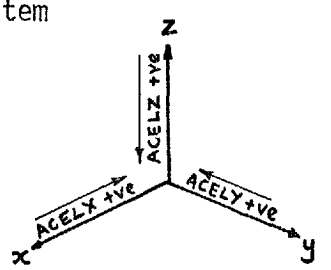
Output

The following output is printed by program instructions:

1) Complete List of Input Data for each approximation
2) Displacements of all Nodes
3) Stresses at the Centroids of all Solid Elements (Not including the Principal Stresses)
4) Stresses and Displacements at the centre of Joint Elements.

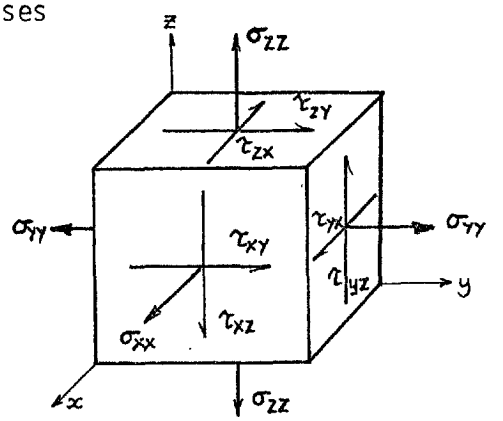
Notes on Output

(a) Co-ordinate System



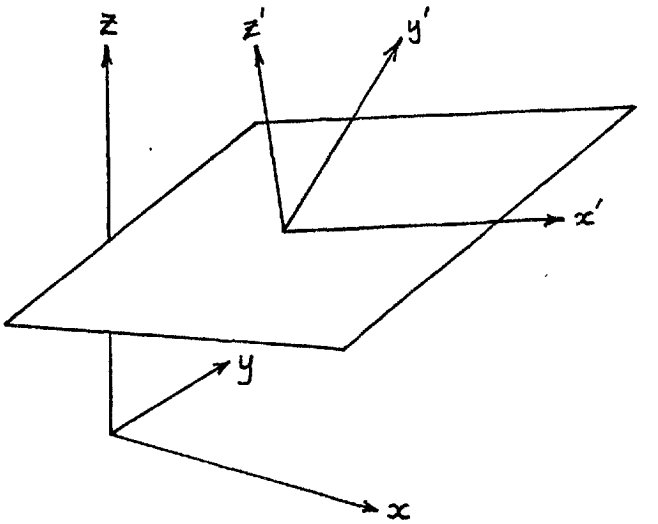
The Right Handed Rectangular xyz Co-ordinate system.

(b) Continuum Stresses



Direct Stresses Sign Convention (Tension +ve)

(c) Joint Element Stresses



The local co-ordinate system for the joint elements is chosen so x' is horizontal and in the plane, and z'normal to the joint plane. Relative displacements of the top face with respect to the bottom are positive if they corespond to this local system. Stresses correspond, with the notation that a normal tensile stress is positive.

Note that the output also gives the maximum shear displacements on the joint surface. The direction of the maximum is measured anti-clockwise from the x' axis.

(d) Non-Linear Joint Properties

(1) A joint in tension is ascribed zero shear and normal stiffness.

(2) The joint normal stiffness (kn) is increased as the closure (zd) approaches the maximum permitted (LIM) according to the following equation:

$$k'_n = \frac{kn \times LIM}{(LIM - zd)}$$

(3) The joint shear stiffness (ks) is modified if the maximum shear stress exceeds the permitted value (STR):

$$k'_s = \frac{STR}{MS} = \frac{c - \sigma_n \tan \phi}{\text{Max. Shear Disp.}}$$

```
                PROGRAM STJN(INPUT,OUTPUT,TAPE5=INPUT,TAPE6=OUTPUT,TAPE8,TAPE9)
C               UMCROOS ST.JOHN  ROCK MECHANICS  IMPERIAL COLLEGE
000002          COMMON /DAT/ NUMEL,NUMNP,NAP,NNN,NUMMAT,MTYPE,ACELX,ACELY,ACELZ,
               1 E(5,10),CODE(104),UX(104),UY(104),UZ(104),IX(70,8),NNOD(70),
               2 NPROP(70),X(104),Y(104),Z(104),LM(8),KX(70),KN(70),RO(10)
000002          COMMON /BANARG/ MBAND,NUMBLK,B(156),A(156,78),ND
000002          DIMENSION HED(12)
000002          REAL KX,KN
                C******  THREE DIMESIONAL STRESS--TETRAHEDRAL ELEMENTS
                C****READ AND PRINT OF CONTROL INFORMATION
000002          READ(5,1000) HED,NUMEL,NUMNP,NUMMAT,NJOINT,NAP,ACELX,ACELY,ACELZ
000030          WRITE(6,2000) HED,NUMEL,NUMNP,ACELX,ACELY,ACELZ
000050          DO 10 I=1,NUMMAT
000052          READ( 5,1001) MTYPE,RO(MTYPE),(E(J,MTYPE),J=1,2)
000065          WRITE(6,2001) MTYPE,RO(MTYPE),(E(J,MTYPE),J=1,2)
000101       10 CONTINUE
000104          IF(NJOINT.EQ.0) GO TO 50
000105          DO 20 J=1,NJOINT
000106          READ(5,1001) JTYPE,(E(I,JTYPE),I=1,5)
000117          WRITE(6,2010)JTYPE,(E(I,JTYPE),I=1,5)
000131       20 CONTINUE
000134       50 CONTINUE
                C**** READ AND PRINT NODAL DATA
000134          WRITE (6,2002)
000140          L9AD=0
000141          L=0
000142       60 READ(5,1002) N,CODE(N),X(N),Y(N),Z(N),UX(N),UY(N),UZ(N)
000170          NL=L+1
000171          ZX=N-L
000173          DX=(X(N)-X(L))/ZX
000175          DY=(Y(N)-Y(L))/ZX
000200          DZ=(Z(N)-Z(L))/ZX
000203       70 L=L+1
000205          IF(N-L) 100,90,80
000210       80 CODE(L)=0.0
000211          X(L)=X(L-1)+DX
000213          Y(L)=Y(L-1)+DY
000215          Z(L)=Z(L-1)+DZ
000217          UX(L)=0.0
000220          UY(L)=0.0
000220          UZ(L)=0.0
000221          GO TO 70
000222       90 WRITE (6,1003)(K,CODE(K),X(K),Y(K),Z(K),UX(K),UY(K),UZ(K),K=NL,N)
000252          IF(NUMNP-N) 100,110,60
000255      100 WRITE(6,2009) N
000263          L9AD=1
000264          GO TO 60
000265      110 CONTINUE
                C**** READ AND PPINT ELEMENT PROPERTIES
000265          WRITE (6,2003)
000271          N=0
                C 130 READ(5,1004) M,NPROP(M),NNOD(M),(IX(M,I),I=1,8)
000272      130 READ(5,1004) M,NPROP(M),NNOD(M),(IX(M,I),I=1,8)
000314      140 N=N+1
000316          IF (M-N) 170,170,150
000330      150 NPROP(N)=NPROP(N-1)
000331          NNOD(N)=NNOD(N-1)
000332          IX(N,1)=IX(N-1,1)+1
000336          IX(N,2)=IX(N-1,2)+1
000341          IX(N,3)=IX(N-1,3)+1
000344          IX(N,4)=IX(N-1,4)+1
000347          IX(N,5)=IX(N-1,5)+1
000351          IX(N,6)=IX(N-1,6)+1
000352          IX(N,7)=IX(N-1,7)+1
000354          IX(N,8)=IX(N-1,8)+1
000355          IX(N,9)=IX(N-1,9)
000357      170 WRITE(6,1005) N,NPROP(N),NNOD(N),(IX(N,I),I=1,8)
000401          IF(M.GT.N) GO TO 140
000405          IF(NUMEL-N) 175,180,130
000406      175 L9AD=L9AD+1
000410          WRITE(6,2004) N
000415      180 IF(NJOINT.EQ.0) GO TO 314
                C********ALLOCATION OF INITIAL JOINT PROPERTIES
000416          DO 30 N=1,NUMEL
000420          MTYPE=NPROP(N)
000421          IF(MTYPE.LE.NUMMAT) GO TO 31
000427          KX(N)=E(1,MTYPE)
000427          KN(N)=E(2,MTYPE)
000431          GO TO 30
000432       31 KX(N)=0.0
000433          KN(N)=0.0
000434       30 CONTINUE
                C***** DETERMINE BAND WIDTH
000437      314 J=0
000440          DO 340 N=1,NUMEL
000442          NODES=NNOD(N)
000444          DO 340 I=1,NODES
000445          DO 325 L=1,NODES
000446          KK=IABS(IX(N,I)-IX(N,L))
000454          IF(KK.LE.25) GO TO 315
000456          WRITE(6,2004) N
000464          L9AD=L9AD+1
000466          GO TO 340
000466      315 IF(KK-J)325,325,320
000471      320 J=KK
000473      325 CONTINUE
000476      340 CONTINUE
000503          MBAND=3*J+3
000506          WRITE (6,2005) MBAND
000513          IF(L9AD.EQ.0) GO TO 501
000514          WRITE(6,2006) L9AD
000522          GO TO 5000
000523      501 DO 500 NNN=1,NAP
                C       FORM STIFFNESS MATRIX
000525          CALL STIFF
000526          IF(L9AD.GT.0) GO TO 5000
                C     SOLVE FOR DISPLACEMENTS
000531          CALL BANSOL
000532          WRITE(6,2007) NNN
000540          WRITE (6,2008)
000544          WRITE(6,1006)(N,B(3*N-2),B(3*N-1),B(3*N),N=1,NUMNP)
                C**** COMPUTE STRESSES
000567          CALL STRESS
000570          IF(NJOINT.GT.0) CALL JSTR
000573      500 CONTINUE
000576     5000 CONTINUE
```

```
000576     1000 FORMAT(12A6/5I5,3F10.0)
000576     1001 FORMAT(I5,6F10.0)
000576     1002 FORMAT (I5,F5.0,6F10.0)
000576     1003 FORMAT(1H ,I5,10X,F5.0,3F10.2,10X,3E12.4)
000576     1004 FORMAT(11I5)
000576     1005 FORMAT(1H ,11I5)
000576     1006 FORMAT(1H ,I5,3E12.4)
000576     2000 FORMAT(1H1,12A6/
               1 27H0 NUMBER OF ELEMENTS------   ,I5 /
               2 27H0 NUMBER OF NODAL POINTS--   ,I5 /
               3 28H0 ACCELERATION -X-DIRECTION-     ,F10.2  /
               4 28H0 ACCELERATION -Y-DIRECTION-     ,F10.2  /
               5 28H0 ACCELERATION -Z-DIRECTION-     ,F10.2  )
000576     2001 FORMAT(1H0,18HMATERIAL NUMBER---  ,I5 ,/ 9H DENSITY=  ,E12.4,
               1 15HYOUNGS MODULUS= ,E12.4 ,15HPOISSONS RATIO= ,E12.4 )
000576     2002 FORMAT(1H1,15HNODAL POINT DATA /
               1 1X,4HNODE,14X,4HCODE,4X,1HX,9X,1HY,9X,1HZ,
               215X,2HUX,10X,2HUY,10X,2HUZ)
000576     2003 FORMAT (1H1,20HELEMENT PROPERTIES  /
               1 8H ELEMENT,1X,4HPROP,1X,5HNODES,3X,20HNODAL POINT LISTING  )
000576     2004 FORMAT(1H0,15HCARD ERROR AT    ,I5)
000576     2005 FORMAT (1H0,10HBANDWIDTH=    I5)
000576     2006 FORMAT(1H0,5HLOAD=    ,I5)
000576     2007 FORMAT(1H1,14HAPPROXIMATION    I5)
000576     2008 FORMAT(1H0,1X,4HNODE,4X,8HX-DISPL.,4X,8HY-DISPL. ,4X,8HZ-DISPL.)
000576     2009 FORMAT(1H0,27HNODAL POINT ERROR CARD NO.    I5)
000576     2010 FORMAT(1H0,10X,12HJOINT NUMBER ,I5,10X,15HSHEAR STIFFNESS ,E12.4,
               1 10X,16HNORMAL STIFFNESS ,E12.4  ,/
               2 10X,8HCOHESION ,E12.4,5X,14HFRICTION ANGLE ,E12.4,
               3 5X,11HMAX.CLOSURE ,E12.4)
000576      600 STOP
000600          END

UNUSED COMPILER SPACE
015300
```

```
          SUBROUTINE STIFF
000001    COMMON /DAT/ NUMEL,NUMNP,NAP,NNN,NUMMAT,MTYPE,ACELX,ACELY,ACELZ,
         1 E(5,10),CODE(104),UX(104),UY(104),UZ(104),IX(70,9),NNOD(70),
         2 NPROP(70),X(104),Y(104),Z(104),LM(8),KX(70),KN(70),RO(10)
000001    COMMON /ESTIF/ NODES,ELBDF(3),YM,PR,ELXYZ(3,9),XI,ETA,ZETA,DETJAC,
         1JAC(3,3),JACINV(3,3),SHAPE(8),DN(3,8),D(6,6),H(3),COORD(3),BB(3,8)
000001    COMMON /STIF/ S(24,24),P(24),LBAD,N,CONST
000001    COMMON /BANARG/ MBAND,NUMBLK,B(156),A(156,78),ND
000001    REWIND 9
000003    NB=26
000004    ND=3*NB
000006    ND2=2*ND
000010    LBAD=0
000011    NUMBLK=0
000012    DO 50 N=1,ND2
000013    B(N)=0.0
000014    DO 50 M=1,ND
000024    A(N,M)=0.0
000025     50 CONTINUE
         C**** FORM STIFFNESS MATRIX IN BLOCKS
000031     60 NUMBLK=NUMBLK+1
000032    NH=NB*(NUMBLK+1)
000034    NM=NH-NB
000035    NL=NM-NB+1
000036    KSHIFT=3*NL-3
000041    DO 210 N=1,NUMEL
000042    IF(NPROP(N)) 210,210,65
000044     65 NODES=NNOD(N)
000046    DO 80 I=1,NODES
000050    IF(IX(N,I)-NL) 80,70,70
000054     70 IF(IX(N,I)-NM) 90,90,80
000061     80 CONTINUE
000064    GO TO 210
000064     90 MTYPE=NPROP(N)
000066    DO 95 I=1,NODES
000102    NEL=IX(N,I)
000103    ELXYZ(1,I)=X(NEL)
000104    ELXYZ(2,I)=Y(NEL)
000106     95 ELXYZ(3,I)=Z(NEL)
000116    IF(MTYPE-NUMMAT) 100,100,110
000124    100 YM=E(1,MTYPE)
000124    PR=E(2,MTYPE)
000125    ELBDF(1)=RO(MTYPE)*ACELX
000127    ELBDF(2)=RO(MTYPE)*ACELY
000131    ELBDF(3)=RO(MTYPE)*ACELZ
000133    CALL ELM4K
000134    GO TO 120
000135    110 CALL ELM3J
000136    120 CONTINUE
000136    NPROP(N)=-NPROP(N)
         C**** ADD ELEMENT STIFFNESS TO TOTAL STIFFNESS
000140     165 DO 166 I=1,NODES
000151     166 LM(I)=3*IX(N,I)-3
000154    DO 200 I=1,NODES
000155    DO 200 K=1,3
000156    II=LM(I)+K-KSHIFT
000160    KK=3*I-3+K
000162    B(II)=B(II)+P(KK)
```

```
000165          DO 200 J=1,NODES
000167          DO 200 L=1,3
000170          JJ=LM(J)+L-II+1-KSHIFT
000174          LL=3*J-3+L
000176          IF (JJ) 200,200,175
000200      175 IF(ND-JJ) 180,195,195
000203      180 WRITE (6,2001) N
000211          LBAD=1
000212          GO TO 210
000213      195 A(II,JJ)=A(II,JJ)+S(KK,LL)
000222      200 CONTINUE
000233      210 CONTINUE
          C**** ADD CONCENTRATED FORCES WITHIN BLOCK
000236          DO 250 N=NL,NM
000247          K=3*N-KSHIFT
000251          B(K  )=B(K  )+UZ(N)
000253          B(K-1)=B(K-1)+UY(N)
000255      250 B(K-2)=B(K-2)+UX(N)
          C**** DISPLACEMENT BOUNDARY CONDITIONS
000260          DO 400 M=NL,NH
000262          IF(M-NUMNP) 315,315,400
000264      315 NC=CODE(M)
000266          IF(NC.EQ.0) GO TO 400
000267          U=UX(M)
000270          N=3*M-2-KSHIFT
000273          IF(NC.EQ.2.OR.NC.EQ.3.OR.NC.EQ.6) GO TO 320
000305          CALL MODIFY(A,B,ND2,MBAND,N,U)
000311      320 U=UY(M)
000313          N=N+1
000315          IF (NC.EQ.1.OR.NC.EQ.3.OR.NC.EQ.5) GO TO 325
000327          CALL MODIFY(A,B,ND2,MBAND,N,U)
000333      325 U=UZ(M)
000335          N=N+1
000337          IF(NC.EQ.1.OR.NC.EQ.2.OR.NC.EQ.4) GO TO 400
000351          CALL MODIFY(A,B,ND2,MBAND,N,U)
000355      400 CONTINUE
          C**** WRITE BLOCK OF EQUATIONS ON TAPE AND SHIFT UP LOWER
000360          WRITE(9) (B(N),(A(N,M),M=1,MBAND),N=1,ND)
000402          DO 420 N=1,ND
000405          K=N+ND
000406          B(N)=B(K)
000407          B(K)=0.0
000411          DO 420 M=1,ND
000423          A(N,M)=A(K,M)
000424      420 A(K,M)=0.0
          C**** CHECK LAST BLOCK
000430          IF (NM-NUMNP) 60,480,480
000433      480 CONTINUE
000433          IF(LBAD.EQ.0) GO TO 500
000434          WRITE(6,2002) LBAD
000442     2000 FORMAT (1H ,27HNEGATIVE VOLUME ELEMENT NO.     I5)
000442     2001 FORMAT(1H ,28HBAND WIDTH EXCEEDS ALLOWABLE     I5)
000442     2002 FORMAT(1H ,5HLBAD=     I5)
000442      500 RETURN
000443          END

UNUSED COMPILER SPACE
016100
```

```
          SUBROUTINE ELMAK
000001    COMMON /ESTIF/ NODES,ELRDF(3),YM,PR,ELXYZ(3,8),XI,ETA,ZETA,DETJAC,
         1JAC(3,3),JACINV(3,3),SHAPE(8),DN(3,8),D(6,6),H(3),COORD(3),B(3,8)
000001    COMMON /STIF/ S(24,24),P(24),NERR,NELEM,CONST
000001    REAL JAC,JACINV
          C
          C  ELEMENT STIFFNESS MATRIX -HEXADEDRAL,TETRAHEDRAL OR PENTAHEDRAL
000001          NDD3=3*NODES
000003          DO 1 I=1,NDD3
000004          P(I)=0.0
000005          DO 1 J=1,NDD3
000014        1 S(I,J)=0.0
000020          IF(NODES.EQ.8) GO TO 6
000022          IF(NODES.EQ.6) GO TO 6
000024          IF(NODES.EQ.4) GO TO 4
000025          WRITE(6,2000) NELEM,NODES
000035   2000 FORMAT(1X,57H***ERROR***THREE DIMENSIONAL ISOPARAMETRIC ELEMENT NU
         AMBER,I4,18H DEFINED AS HAVING,I3,6H NODES )
000035          NERR=NERR+1
000037          RETURN
000037        4 ZETA=0.25
          C     INTEGRATION EXPLICIT FOR TETRAHEDRON
000040          ETA=0.25
000041          XI=0.25
000043          CALL DXYZ(YM,PR,D)
000045          CALL BXYZ
000046          CONST=DETJAC/6.0
000050          CALL STIF3
000051          GO TO 10
000052        6 MESH=3
000053          H(1)=0.555555555555556
000054          H(2)=0.888888888888889
000056          H(3)=0.555555555555556
000056          COORD(1)=-0.774596669241483
000060          COORD(2)= 0.000000000000000
000060          COORD(3)= 0.774596669241483
000062          CALL DXYZ(YM,PR,D)
000065          IF(NODES.EQ.8) GO TO 8
          C***NUMERICAL INTEGRATION ALONG LENGTH OF PENTAHEDRON
000067          DO 61 IXI=1,MESH
000071          XI=COORD(IXI)
000073          CALL BXYZ
000074          CONST=H(IXI)*DETJAC/2.0
000077       61 CALL STIF3
000103          GO TO 10
000103        8 DO 81 KZETA=1,MESH
000105          ZETA=COORD(KZETA)
000107          DO 81  JETA=1,MESH
000110          ETA=COORD(JETA)
000112          DO 81   IXI=1,MESH
000113          XI=COORD(IXI)
000115          CALL BXYZ
000116          CONST=H(KZETA)*H(JETA)*H(IXI)*DETJAC
000123       81 CALL STIF3
000133       10 DO 12 I=2,NDD3
          C**** COMPLETE ELEMENT STIFFNESS MATRIX
000135          K=I-1
000136          DO 12 J=1,K
```

```
000147      12 S(J,I)=S(I,J)
000154         RETURN
000154         END

UNUSED COMPILER SPACE
017400



               SUBROUTINE DXYZ(YM,PR,D)
009005         DIMENSION D(6,6)
000005         REAL JAC,JACINV
          C
          C    ELASTICITY MATRIX D FOR AN ISOTROPIC THREE DIMENSIONAL ELEMENT
          C
000005         DO 1 I=1,6
000006         DO 1 J=I,6
000013       1 D(I,J)=0.0
000025         CONST=YM/((1.0+PR)*(1.0-2.0*PR))
000031         D(1,1)=CONST*(1.0-PR)
000033         D(1,2)=CONST*PR
000034         D(1,3)=CONST*PR
000035         D(2,2)=CONST*(1.0-PR)
000036         D(2,3)=CONST*PR
000037         D(3,3)=CONST*(1.0-PR)
000040         D(4,4)=CONST*(0.5-PR)
000041         D(5,5)=CONST*(0.5-PR)
000042         D(6,6)=CONST*(0.5-PR)
000043         DO 2 I=1,5
000045         K=I+1
000046         DO 2 J=K,6
000055       2 D(J,I)=D(I,J)
000063         RETURN
000064         END

UNUSED COMPILER SPACE
020100
```

```
               SUBROUTINE STIF3
000001         COMMON /ESTIF/ NODES,ELBDF(3),YM,PR,ELXYZ(3,8),XI,ETA,ZETA,DETJAC,
              1JAC(3,3),JACINV(3,3),SHAPE(8),DN(3,8),D(6,6),H(3),COORD(3),B(3,8)
000001         COMMON /STIF/ S(24,24),P(24),NERR,NELEM,CONST
000001         DO 9 JBLOCK=1,3
000003         JD1=JBLOCK
000004         JD2=4
000005         JD3=6
000006         IB1=JBLOCK
000007         IB2=2
000010         IB3=3
000011         IF(JBLOCK.EQ.1) GO TO 6
000013         IF(JBLOCK.EQ.2) GO TO 5
000014         JD2=5
000015         IB3=1
000016         GO TO 6
000017       5 JD3=5
000020         IB2=1
000021       6 DO 9 J=1,NODES
000023         NCOL=(J-1)*3+JBLOCK
000025         K=J
000027         DO 9 IBLOCK=JBLOCK,3
000037         ID1=IBLOCK
000037         ID2=4
000040         ID3=6
000041         IF(IBLOCK.EQ.2) ID3=5
000044         IF(IBLOCK.EQ.3) ID2=5
000047         BD1=D(ID1,JD1)*B(IB1,J)+D(ID1,JD2)*B(IB2,J)+D(ID1,JD3)*B(IB3,J)
000062         BD2=D(ID2,JD1)*B(IB1,J)+D(ID2,JD2)*B(IB2,J)+D(ID2,JD3)*B(IB3,J)
000074         BD3=D(ID3,JD1)*B(IB1,J)+D(ID3,JD2)*B(IB2,J)+D(ID3,JD3)*B(IB3,J)
000107         IB4=IBLOCK
000111         IB5=2
000112         IB6=3
000113         IF(IBLOCK.EQ.2) IB5=1
000116         IF(IBLOCK.EQ.3) IB6=1
000121         DO 8 I=K,NODES
000123         NROW=(I-1)*3+IBLOCK
000125         IF(NCOL.GT.NROW) GO TO 7
000131         NC=NCOL
000131         NR=NROW
000132         GO TO 8
000133       7 NC=NROW
000134         NR=NCOL
000136       8 S(NR,NC)=S(NR,NC)        +CONST*(B(IB4,I)*BD1+B(IB5,I)*BD2+
              1 B(IB6,I)*BD3)
000157       9 K=1
000166         DO 11 I=1,3
000170         DO 11 NODE=1,NODES
000201         K=3*(NODE-1)+I
000204         P(K)=P(K)-CONST*SHAPE(NODE)*ELBDF(I)
000207      11 CONTINUE
000213         RETURN
000213         END

UNUSED COMPILER SPACE
017300
```

```
                SUBROUTINE BXYZ
000001          COMMON /ESTIF/ NODES,ELBDF(3),YM,PR,ELXYZ(3,8),XI,ETA,ZETA,DETJAC,
               1JAC(3,3),JACINV(3,3),SHAPE(8),DN(3,8),D(6,6),H(3),COORD(3),B(3,8)
000001          COMMON /STIFF S(24,24),P(24),NERR,NELEM,CONST
000001          REAL JAC,JACINV
          C
          C     STRAIN MATRIX B FOR A POINT (XI,ETA,ZETA) IN A THREE DIMENSIONAL
          C     ISOPARAMETRIC ELEMENT
          C
000001          IF(NODES.EQ.6) GO TO 60
000003          IF(NODES.EQ.8) GO TO 80
          C*** SHAPE FUNCTION AND DERIVATIVE - TETRAHEDRON
000005          SHAPE(1)=XI
000006          SHAPE(2)=ZETA
000007          SHAPE(3)=ETA
000011          SHAPE(4)=1.0-XI-ETA-ZETA
000014          DO 4 I=1,3
000015          DO 5 J=1,3
000023        5 DN(I,J)=0.0
000025        4 DN(I,4)=-1.0
000031          DN(1,1)=1.0
000031          DN(2,3)=1.0
000032          DN(3,2)=1.0
000034          GO TO 15
          C*** SHAPE FUNCTION AND DERIVATIVE - PENTAHEDRON
000034       60 XII=1.0
000035          ZETA=0.33333333333333333
000037          ETA =0.33333333333333333
000040          DO 61 I=1,4,3
000052          XII=-XII
000053          SHAPE(I)=ZETA*(1.0+XII*XI)/2.0
000057          DN(1,I)=ZETA*XII/2.0
000060          DN(2,I)=0.0
000061       61 DN(3,I)=(1.0+XII*XI)/2.0
000064          DO 62 I=2,5,3
000102          XII=-XII
000103          SHAPE(I)=(1.0-ETA-ZETA)*(1.0+XII*XI)/2.0
000107          DN(1,I)=(1.0-ETA-ZETA)*XII/2.0
000110          DN(2,I)=-1.0*(1.0+XII*XI)/2.0
000113       62 DN(3,I)=-1.0*(1.0+XII*XI)/2.0
000120          DO 63 I=3,6,3
000132          XII=-XII
000133          SHAPE(I)=ETA*(1.0+XII*XI)/2.0
000137          DN(1,I)=ETA*XII/2.0
000140          DN(2,I)=(1.0+XII*XI)/2.0
000142       63 DN(3,I)=0.0
000144          GO TO 15
          C*** SHAPE FUNCTION AND DERIVATIVE - HEXAHEDRON
000145       80 XII=-1.0
000146          ETAI=1.0
000150          ZETAI=-1.0
000151          DO 2 NODE=1,NODES
000163          HOLD=XII
000164          XII=-ETAI
000166          ETAI=HOLD
000166          IF(NODE.EQ.5) ZETAI=1.0
000172          SHAPE(NODE)=(1.0+XII*XI)*(1.0+ETAI*ETA)*(1.0+ZETAI*ZETA)/8.0
000203          DN(1,NODE)=XII*(1.0+ETAI*ETA)*(1.0+ZETAI*ZETA)/8.0
000210          DN(2,NODE)=ETAI*(1.0+XII*XI)*(1.0+ZETAI*ZETA)/8.0
000216        2 DN(3,NODE)=ZETAI*(1.0+XII*XI)*(1.0+ETAI*ETA)/8.0
000225       15 DO 17 I=1,3
000227          DO 16 J=1,3
000235       16 JAC(I,J)=0.0
000237          DO 17 NODE=1,NODES
000240          DO 17 K=1,3
000254       17 JAC(I,K)=JAC(I,K)+DN(I,NODE)*ELXYZ(K,NODE)
000264          DETJAC=JAC(1,1)*(JAC(2,2)*JAC(3,3)-JAC(2,3)*JAC(3,2))+
                A        JAC(1,2)*(JAC(2,3)*JAC(3,1)-JAC(2,1)*JAC(3,3))+
                B        JAC(1,3)*(JAC(2,1)*JAC(3,2)-JAC(2,2)*JAC(3,1))
000301          IF (DETJAC.LE.0.0) GO TO 20
000303          JACINV(1,1)= (JAC(2,2)*JAC(3,3)-JAC(2,3)*JAC(3,2))/DETJAC
000307          JACINV(1,2)=-(JAC(1,2)*JAC(3,3)-JAC(1,3)*JAC(3,2))/DETJAC
000313          JACINV(1,3)= (JAC(1,2)*JAC(2,3)-JAC(1,3)*JAC(2,2))/DETJAC
000320          JACINV(2,1)=-(JAC(2,1)*JAC(3,3)-JAC(2,3)*JAC(3,1))/DETJAC
000324          JACINV(2,2)= (JAC(1,1)*JAC(3,3)-JAC(1,3)*JAC(3,1))/DETJAC
000331          JACINV(2,3)=-(JAC(1,1)*JAC(2,3)-JAC(1,3)*JAC(2,1))/DETJAC
000335          JACINV(3,1)= (JAC(2,1)*JAC(3,2)-JAC(2,2)*JAC(3,1))/DETJAC
000341          JACINV(3,2)=-(JAC(1,1)*JAC(3,2)-JAC(1,2)*JAC(3,1))/DETJAC
000346          JACINV(3,3)= (JAC(1,1)*JAC(2,2)-JAC(1,2)*JAC(2,1))/DETJAC
000352          DO 18 I=1,3
000354          DO 18 NODE=1,NODES
000375       18 B(I,NODE)=JACINV(I,1)*DN(1,NODE)+JACINV(I,2)*DN(2,NODE)+JACINV(I,3
               A)*DN(3,NODE)
000406          RETURN
000406       20 WRITE(6,2000) NELEM
000414     2000 FORMAT(1H0,36HZERO OR NEGATIVE DETERMINATE.ELEMENT   ,I5)
000414          NERR=NERR+1
000416          RETURN
000416          END

UNUSED COMPILER SPACE
016500
```

```
                SUBROUTINE ELM3J
000001          COMMON /DAT/ NUMEL,NUMNP,NAP,NNN,NUMMAT,MTYPE,ACELX,ACELY,ACELZ,
               1 E(5,10),CODE(104),UX(104),UY(104),UZ(104),IX(70,8),NNOD(70),
               2 NPROP(70),X(104),Y(104),Z(104),LM(8),KX(70),KN(70),RO(10)
000001          COMMON /ESTIF/ NODES,ELBDF(3),YM,PR,ELXYZ(3,8),XI,ETA,ZETA,DETJAC,
               1JAC(3,3),JACINV(3,3),SHAPE(8),DN(3,8),D(6,6),H(3),COORD(3),B(3,8)
000001          COMMON /STIF/ S(24,24),P(24),NERR,NELEM,CONST
000001          COMMON /JNT/ KSN(3,3),DC(3,3),TXYZ(3,8),NOD,NOD2
000001          DIMENSION KT(3,3)
000001          REAL JAC,JACINV,KSN,KT,KX,KN
000001          NOD=NODES/2
000002          NOD2=NOD*3
000004          DO 1 I=1,NOD2
000007          P(I)=0.0
000007          P(NOD2+I)=0.0
000012          DO 1 J=1,NOD2
000020        1 S(I,J)=0.0
000024          DO 111 I=1,3
000025          DO 111 J=1,3
000033      111 KSN(I,J)=0.0
000040          KSN(1,1)=KX(NELEM)
000041          KSN(2,2)=KX(NELEM)
000041          KSN(3,3)=KN(NELEM)
000043          CALL TRAN(ELXYZ,DC)
              C**** OBTAIN LOCAL COORDINATES BY TRANSFORMATION (Z(LOCAL)=CONSTANT)
000045      114 DO 4 I=1,NOD
000057          TXYZ(1,I)=DC(1,1)*ELXYZ(1,I)+DC(1,2)*ELXYZ(2,I)+DC(1,3)*ELXYZ(3,I)
000063          TXYZ(2,I)=DC(2,1)*ELXYZ(1,I)+DC(2,2)*ELXYZ(2,I)+DC(2,3)*ELXYZ(3,I)
000070        4 TXYZ(3,I)=DC(3,1)*ELXYZ(1,I)+DC(3,2)*ELXYZ(2,I)+DC(3,3)*ELXYZ(3,I)
              C****TRANSFORM JOINT STIFFNESS TO GLOBAL AXES
000076          DO 2 I=1,3
000100          DO 2 J=1,3
000101          KT(I,J)=0.0
000103          DO 2 K=1,3
000115        2 KT(I,J)=KT(I,J)+KSN(I,K)*DC(K,J)
000124          DO 3 I=1,3
000126          DO 3 J=1,3
000127          KSN(I,J)=0.0
000131          DO 3 K=1,3
000142        3 KSN(I,J)=KSN(I,J)+ DC(K,I)*KT(K,J)
000151          IF(NODES.EQ.6) GO TO 6
000153          IF(NODES.EQ.8) GO TO 8
000155          WRITE(6,2000) NELEM,NODES
000164     2000 FORMAT(1H0,5HJOINT ,I5,2X,3HHAS,I5,2X,5HNODES)
000164          RETURN
000165        6 MESH=1
000166          COORD(1)=0.333333333333333
000167          H(1)=0.0
000170          GO TO 10
000171        8 MESH=3
000172          COORD(1)=-0.774596669241483
000173          COORD(2)=0.000000000000000
000174          COORD(3)=0.774596669241483
000175          H(1)=0.555555555555556
000177          H(2)=0.888888888888889
000200          H(3)=0.555555555555556
000202       10 DO 20 JETA=1,MESH
000204          ETA=COORD(JETA)
000206          DO 20 IXI=1,MESH
000207          XI=COORD(IXI)
000211          CALL JXY7
000212          CONST=H(JETA)*H(IXI)*DETJAC
000216          DO 30 IBLOCK=1,NOD
000217          DO 30 JBLOCK=1,IBLOCK
000220          IF(NODES.EQ.6) GO TO 31
000222          IF(IBLOCK.EQ.JBLOCK) GO TO 32
000224          CONST=0.375*DETJAC
000226          GO TO 31
000226       32 CONST=0.750*DETJAC
000230       31 DO 30 K=1,3
000232          DO 30 L=1,3
000252          I=(IBLOCK-1)*3+K
000253          J=(JBLOCK-1)*3+L
000254          IF(J.GT.I) GO TO 30
000260          S(I,J)=S(I,J)+CONST*SHAPE(IBLOCK)*KSN(K,L)*SHAPE(JBLOCK)
000266       30 CONTINUE
000276       20 CONTINUE
000303          DO 40 I=2,NOD2
000304          K=I-1
000305          DO 40 J=1,K
000315       40 S(J,I)=S(I,J)
000323          DO 50 I=1,NOD2
000324          DO 50 J=1,NOD2
000336          IN=I+NOD2
000337          JN=J+NOD2
000340          S(I,JN)=S(I,J)*(-1.0)
000344          S(IN,J)=S(I,J)*(-1.0)
000345       50 S(IN,JN)=S(I,J)
000350          RETURN
000361          END

UNUSED COMPILER SPACE
016300
```

```
                SUBROUTINE JXYZ
000001          COMMON /ESTIF/ NODES,ELBDF(3),YM,PR,ELXYZ(3,8),XI,ETA,ZETA,DETJAC,
               1JAC(3,3),JACINV(3,3),SHAPE(8),DN(3,8),D(6,6),H(3),COORD(3),B(3,8)
000001          COMMON /STIF/ S(24,24),P(24),NERR,NELEM,CONST
000001          COMMON /JNT/ KSN(3,3),DC(3,3),TXYZ(3,8),NOD,NOD2
000001          REAL JAC,JACINV,KSN,KT
000001          IF(NODES.EQ.8) GO TO 8
000003          SHAPE(1)=ETA
000004          SHAPE(2)=1.0-ETA-XI
000007          SHAPE(3)=XI
000010          DN(2,3)=0.0
000010          DN(2,2)=-1.0
000012          DN(2,1)=1.0
000012          DN(1,3)=1.0
000013          DN(1,2)=-1.0
000014          DN(1,1)=0.0
000015          GO TO 10
000016        8 XII=-1.0
000017          ETAI=1.0
000021          DO 81 I=1,NOD
000033          HOLD=XII
000034          XII=-ETAI
000036          ETAI=HOLD
000036          SHAPE(I)=(1.0+XII*XI)*(1.0+ETAI*ETA)/4.0
000043          DN(1,I)=XII*(1.0+ETAI*ETA)/4.0
000046       81 DN(2,I)=ETAI*(1.0+XII*XI)/4.0
000053       10 DO 21 I=1,2
000055          DO 20 J=1,2
000063       20 JAC(I,J)=0.0
000065          DO 21 NODE=1,NOD
000066          DO 21 K=1,2
000102       21 JAC(I,K)=JAC(I,K)+DN(I,NODE)*TXYZ(K,NODE)
000112          DETJAC=JAC(1,1)*JAC(2,2)-JAC(2,1)*JAC(1,2)
000115          IF(DETJAC.GT.0.0) GO TO 50
000120          WRITE(6,2000) NELEM,DETJAC
000127     2000 FORMAT(1H0,22HDETERMINATE OF ELEMENT,I5,2X,2HIS,E12.4)
000127          NERR=NERR+1
000131       50 RETURN
000132          END

UNUSED COMPILER SPACE
017500
```

```
                SUBROUTINE TRAN(ELXYZ,DC)
000004          DIMENSION ELXYZ(3,8),DC(3,3)
000004          DO 11 I=1,3
000005          DO 11 J=1,3
000012       11 DC(I,J)=0.0
             C*** FORM TRANFORMATION MATRIX FOR PLANE JOINT
000017          A=(ELXYZ(2,2)-ELXYZ(2,1))*(ELXYZ(3,3)-ELXYZ(3,1))
               1 -(ELXYZ(2,3)-ELXYZ(2,1))*(ELXYZ(3,2)-ELXYZ(3,1))
000031          B=(ELXYZ(1,1)-ELXYZ(1,2))*(ELXYZ(3,3)-ELXYZ(3,1))
               1 -(ELXYZ(1,1)-ELXYZ(1,3))*(ELXYZ(3,2)-ELXYZ(3,1))
000043          C=(ELXYZ(1,2)-ELXYZ(1,1))*(ELXYZ(2,3)-ELXYZ(2,1))
               1 -(ELXYZ(1,3)-ELXYZ(1,1))*(ELXYZ(2,2)-ELXYZ(2,1))
000054          AB=(A**2+B**2)**0.5
000061          ABC=(A**2+B**2+C**2)**0.5
000067          DC(3,3)=C/ABC
000071          IF(DC(3,3).EQ.1.0) GO TO 14
000100          DC(1,1)=-B/AB
000101          DC(1,2)=A/AB
000103          DC(1,3)=0.0
000104          DC(2,1)=-A*C/(AB*ABC)
000106          DC(2,2)=-B*C/(AB*ABC)
000107          DC(2,3)=AB/ABC
000111          DC(3,1)=A/ABC
000113          DC(3,2)=B/ABC
000114          RETURN
000114       14 DC(1,1)=1.0
000116          DC(2,2)=1.0
000117          RETURN
000117          END

UNUSED COMPILER SPACE
020000
```

```
                SUBROUTINE STRESS
000001          COMMON /DAT/ NUMEL,NUMNP,NAP,NNN,NUMMAT,MTYPE,ACELX,ACELY,ACELZ,
               1 E(5,10),CODE(104),UX(104),UY(104),UZ(104),IX(70,9),NNOD(70),
               2 NPROP(70),X(104),Y(104),Z(104),LM(8),KX(70),KN(70),RO(10)
000001          COMMON /ESTIF/ NODES,ELMOF(3),YM,PR,ELXYZ(3,9),XI,ETA,ZETA,DETJAC,
               1JAC(3,3),JACINV(3,3),SHAPE(8),DN(3,8),D(6,6),H(3),COORD(3),BB(3,8)
000001          COMMON /STIF/ S(24,24),P(24),LMAD,N,CONST
000001          COMMON /RANARG/ MBAND,NUMBLK,B(156),A(156,74),ND
000001          DIMENSION SIG(6),EPA(6),CEN(3)
000001          WRITE(6,2000)
000005          DO 100 N=1,NUMEL
000007          MTYPE=IABS(NPROP(N))
000011          IF(MTYPE.GT.NUMMAT) GO TO 100
000014          NPROP(N)=MTYPE
000014          NODES=NNOD(N)
000016          DO 1 I=1,NODES
000032          NEL=IX(N,I)
000033          ELXYZ(1,I)=X(NEL)
000034          ELXYZ(2,I)=Y(NEL)
000036        1 ELXYZ(3,I)=Z(NEL)
000051          YM=E(1,MTYPE)
000051          PR=E(2,MTYPE)
000053          DO 2 I=1,6
000057          SIG(I)=0.0
000060        2 EPA(I)=0.0
000061          IF(NODES.EQ.8) GO TO 8
000063          IF(NODES.EQ.6) GO TO 6
000065          ZETA=0.25
000066          ETA=0.25
000066          XI=0.25
000070          GO TO 10
000070        6 ZETA=0.33333333333333333
000071          ETA=0.33333333333333333
000072          XI=0.0
000074          GO TO 10
000074        8 ZETA=0.0
000075          ETA=0.0
000075          XI=0.0
000076       10 DO 20 I=1,NODES
000103          II=3*I-3
000104          JJ=3*IX(N,I)-3
000106          DO 20 J=1,3
000115       20 P(II+J)=B(JJ+J)
000122          CALL BXYZ
000123          CALL DXYZ(YM,PR,D)
             C**** CALCULATE ELEMENT STRAIN AT CENTROID
000126          DO 30 I=1,NODES
000130          NUM=3*(I-1)
000132          DO 40 J=1,3
             C**** CALCULATE ELEMENT STRESSES  -GLOBAL COORDINATES
000142       40 EPA(J)=EPA(J)+BB(J,I)*P(NUM+J)
000153          EPA(4)=EPA(4)+BB(2,I)*P(NUM+1)+BB(1,I)*P(NUM+2)
000157          EPA(5)=EPA(5)+BB(3,I)*P(NUM+2)+BB(2,I)*P(NUM+3)
000164       30 EPA(6)=EPA(6)+BB(1,I)*P(NUM+3)+BB(3,I)*P(NUM+1)
000175          DO 50 I=1,6
000177          DO 50 J=1,6
000206       50 SIG(I)=SIG(I)+D(I,J)*EPA(J)
000213          DO 60 J=1,3
000215          CEN(J)=0.0
000216          DO 60 I=1,NODES
000226       60 CEN(J)=CEN(J)+SHAPE(I)*ELXYZ(J,I)
             C*** WRITE ELEMENT STRESSES
000233          WRITE(6,1000) N,(CEN(I),I=1,3),(SIG(J),J=1,6)
000245       100 CONTINUE
000250      1000 FORMAT(1H ,I5,3F9.2,6E12.4)
000250      2000 FORMAT(1H1,7HELEMENT,5X,2HXC,8X,2HYC,8X,2HZC,6X,
               1 2HXX,10X,2HYY,10X,2HZZ,10X,2HXY,10X,2HYZ,10X,2HZX)
000250          RETURN
000250          END

UNUSED COMPILER SPACE
016700
```

```
                SUBROUTINE JSTP
000001          COMMON /DAT/ NUMEL,NUMNP,NAP,NNN,NUMMAT,MTYPE,ACELX,ACELY,ACELZ,
                1 E(5,10),CODE(104),UX(104),UY(104),UZ(104),IX(70,8),NNOD(70),
                2 NPROP(70),X(104),Y(104),Z(104),LM(8),KX(70),KN(70),RO(10)
000001          COMMON /ESTIF/ NODES,ELBDF(3),YM,PR,ELXYZ(3,8),XI,ETA,ZETA,DETJAC,
                1JAC(3,3),JACINV(3,3),SHAPE(8),DN(3,8),D(6,6),H(3),COORD(3),BB(3,8)
000001          COMMON /STIF/ S(24,24),P(24),LBAD,N,CONST
000001          COMMON /JNT/ KSN(3,3),DC(3,3),TXYZ(3,8),NOD,NOD2
000001          COMMON /BANARG/ MBAND,NUMBLK,B(156),A(156,78),ND
000001          REAL KS,KN,KX,KT,LIM,MS
000001          INTEGER FAIL
000001          WRITE(6,2000)
                C**** OBTAIN NODAL POINT DISPLACEMENTS AND MEAN DISPLACEMENTS
000005          DO 900 N=1,NUMEL
000007          MTYPE=IABS(NPROP(N))
000011          IF(MTYPE.LE.NUMMAT) GO TO 900
000014          NPROP(N)=MTYPE
000014          NOD=NNOD(N)/2
000016          FAIL=0
000017          UM=VM=WM=XC=YC=ZC=0.0
000025          DO 200 I=1,NOD
000050          M=IX(N,I)
000052          ELXYZ(1,I)=X(M)
000053          ELXYZ(2,I)=Y(M)
000056          ELXYZ(3,I)=Z(M)
                C**** CALCULATE CENTROID OF JOINT
000061          NN=3*M-2
000065          XC=XC+X(M)/NOD
000070          YC=YC+Y(M)/NOD
000072          ZC=ZC+Z(M)/NOD
000075          J=I+NOD
000077          ML=IX(N,J)
000101          MN=3*ML-2
000104          UM=UM+(B(MN  )-B(NN  ))/NOD
000110          VM=VM+(B(MN+1)-B(NN+1))/NOD
000115          WM=WM+(B(MN+2)-B(NN+2))/NOD
000121      200 CONTINUE
                C***  FORM TRANSFORMATIONS EQUATIONS
000136          CALL TRAN(ELXYZ,DC)
                C**** TRANSFORMDISPLACEMENTS TO SHEAR AND NORMAL-XD=STRIKE DISPL.
000140          XD=DC(1,1)*UM+DC(1,2)*VM+DC(1,3)*WM
000145          YD=DC(2,1)*UM+DC(2,2)*VM+DC(2,3)*WM
000153          ZD=DC(3,1)*UM+DC(3,2)*VM+DC(3,3)*WM
                C**** MAGNITUDE AND DIRECTION OF MAXIMUM SHEAR DISPLACEMENT
000161          ANG=ATAN2(YD,XD)
000171          ANG=ANG*57.296
000172          MS=(XD**2+YD**2)**0.5
                C**** OBTAIN MEAN SHEAR AND NORMAL FORCES PER UNIT AREA
000200          FN=ZD*KN(N)
000202          FS=MS*KX(N)
                C**** MODIFICATION OF NORMAL STIFFNESS WITH DISPLACEMENT
000203          LIM=E(5,MTYPE)
000204          COH=E(3,MTYPE)
000205          TH=E(4,MTYPE)/57.296
000210          TANTH=SIN(TH)/COS(TH)
000214          IF(ZD.GE.0.0) GO TO 300
000216          IF(ZD.LE.LIM) GO TO 350
000220          KN(N)=KN(N)*LIM/(LIM-ZD)
000223              GO TO 400
000224      300 KN(N)=0.0
000226              GO TO 400
000226      350 KN(N)=KN(N)*10.0**10
000232      400 STR=COH+ABS(FN)*TANTH
000236          IF(FN.GT.0.0) GO TO 499
000240          IF(ABS(FS).LE.STR) GO TO 500
000243          KX(N)=STR/MS
000245          FAIL=1
000246          GO TO 500
000246      499 KX(N)=0.0
000250          FAIL=2
000251      500 CONTINUE
000251          WRITE(6,1000) N,XC,YC,ZC,XD,YD,ZD,MS,ANG,FN,FS,FAIL
000305     1000 FORMAT(1H ,I4,3F8.3,4E13.4,F8.2,2E12.4,I5)
000305     2000 FORMAT(1H1,5HJOINT,5X,2HXC,6X,2HYC,6X,2HZC,3X,12HSTRIKE DISP.,
                1 3X,9HDIP DISP.,2X,10HNORM DISP.,3X,9HMAX.DISP.,1X,
                2 7HDIRECT.,2X,10HNORMAL F/A,3X,9HSHEAR F/A,3X,4HSLIP)
000305      900 CONTINUE
000310          RETURN
000310          END

UNUSED COMPILER SPACE
016500
```

```
                SUBROUTINE BANSOL
000001          COMMON /BANARG/     MM,NUMBLK,B(156),A(156,78),NN
000001          NL=NN+1
000003          NH=NN+NN
000004          REWIND 8
000006          REWIND 9
000010          NB=0
000011          GO TO 150
                C*****
                C     REDUCE EQUATIONS BY BLOCKS
                C*****
                C          1. SHIFT BLOCK OF EQUATIONS
                C*****
000012        100 NB=NB+1
000014          DO 125 N=1,NN
000016          NM=NN+N
000017          B(N)=B(NM)
000020          B(NM)=0.0
000022          DO 125 M=1,MM
000034          A(N,M)=A(NM,M)
000035        125 A(NM,M)=0.0
                C***       2. READ NEXT BLOCK OF EQUATIONS INTO CORE ***
000041          IF (NUMBLK-NB) 150,200,150
000043        150 READ (9) (B(N),(A(N,M),M=1,MM),N=NL,NH)
000065          IF (NB) 200,100,200
                C***       3. REDUCE BLOCK OF EQUATIONS  ***
000066        200 DO 300 N=1,NN
000070          IF (A(N,1)) 225,300,225
000071        225 B(N)=B(N)/A(N,1)
000074          DO 275 L=2,MM
000075          IF (A(N,L)) 230,275,230
000104        230 C=A(N,L)/A(N,1)
000105          I=N+L-1
000107          J=0
000110          DO 250 K=L,MM
000122          J=J+1
000123        250 A(I,J)=A(I,J)-C*A(N,K)
000134          B(I)=B(I)-A(N,L)*B(N)
000136          A(N,L)=C
000137        275 CONTINUE
000142        300 CONTINUE
                C***       4. WRITE BLOCK OF REDUCED EQUATIONS  ON TAPE 8  ***
000145          IF (NUMBLK-NB) 375,400,375
000147        375 WRITE (8) (B(N),(A(N,M),M=2,MM),N=1,NN)
000171          GO TO 100
                C*****
                C     BACK-SUBSTITION
                C*****
000172        400 DO 450 M=1,NN
000174          N=NN+1-M
000175          DO 425 K=2,MM
000207          L=N+K-1
000211        425 B(N)=B(N)-A(N,K)*B(L)
000215          NM=N+NN
000216          B(NM)=B(N)
000221        450 A(NM,NB)=B(N)
000230          NB=NB-1
000231          IF (NB) 475,500,475
000231        475 BACKSPACE 8
000233          READ (8) (B(N),(A(N,M),M=2,MM),N=1,NN)
000255          BACKSPACE 8
000257          GO TO 400
                C*****
                C     ORDER UNKNOWNS IN B ARRAY
                C*****
000260        500 K=0
000261          DO 600 NB=1,NUMBLK
000263          DO 600 N=1,NN
000273          NM=N+NN
000274          K=K+1
000274        600 B(K)=A(NM,NB)
000303          RETURN
000304          END

UNUSED COMPILER SPACE
017200



                SUBROUTINE MODIFY(A,B,NEQ,MBAND,N,U)
000010          DIMENSION A(156,78),B(156)
000010          DO 250 M=2,MBAND
000011          K=N-M+1
000012          IF(K) 235,235,230
000020        230 B(K)=B(K)-A(K,M)*U
000021          A(K,M)=0.0
000026        235 K=N+M-1
000030          IF(NEQ-K) 250,240,240
000036        240 B(K)=B(K)-A(N,M)*U
000040          A(N,M)=0.0
000044        250 CONTINUE
000047          A(N,1)=1.0
000051          B(N)=U
000052          RETURN
000053          END

UNUSED COMPILER SPACE
020100
```